

**Small RNAs and cysteine-rich proteins -
novel molecular weapons
of oomycete plant pathogens**

Dissertation der Fakultät für Biologie
der Ludwig-Maximilians-Universität München

Florian Dunker (M. Sc.)

München, 2021

Diese Dissertation wurde angefertigt
unter der Leitung von PD Dr. Arne Weiberg
am Lehrstuhl für Genetik, Fakultät für Biologie
der Ludwig-Maximilians-Universität München

Erstgutachter:	PD Dr. Arne Weiberg
Zweitgutachter:	Prof. Dr. Wolfgang Frank
Tag der Abgabe:	29.03.2021
Tag der mündlichen Prüfung:	08.10.2021

“An expert is a person, who has made all the mistakes,
that can be made in a very narrow field.”

— Niels Bohr (1885-1962)

Eidesstattliche Erklärung

Ich versichere hiermit an Eides statt, dass die vorgelegte Dissertation von mir selbständig und ohne unerlaubte Hilfe angefertigt ist.

München, den 08.11.2021

Florian Dunker

(Unterschrift)

Erklärung

Hiermit erkläre ich, *

- dass die Dissertation nicht ganz oder in wesentlichen Teilen einer anderen Prüfungskommission vorgelegt worden ist.
- dass ich mich anderweitig einer Doktorprüfung ohne Erfolg **nicht** unterzogen habe.
- ~~dass ich mich mit Erfolg der Doktorprüfung im Hauptfach
und in den Nebenfächern
bei der Fakultät für der
(Hochschule/Universität)
unterzogen habe.~~
- ~~dass ich ohne Erfolg versucht habe, eine Dissertation einzureichen oder mich der Doktorprüfung zu unterziehen.~~

München, den 08.11.2021

Florian Dunker

(Unterschrift)

*) Nichtzutreffendes streichen

Table of Contents

EIDESSTÄTTLICHE ERKLÄRUNG	IV
TABLE OF CONTENTS.....	V
GENERAL ABBREVIATION INDEX	VII
GENE NAME ABBREVIATION INDEX	VIII
LIST OF PUBLICATIONS	X
DECLARATION OF CONTRIBUTION AS CO-AUTHOR.....	XI
LICENSE AND PERMISSION	XIII
SUMMARY.....	1
INTRODUCTION	2
Oomycetes: constant threats to global food resources	2
<i>Hyaloperonospora arabidopsidis</i> as an oomycete model plant pathogen	3
Oomycete effectors with focus on <i>H. arabidopsidis</i>	4
The plant immune response to <i>H. arabidopsidis</i>	6
RNA interference in plants and its role in plant immunity	8
RNA interference in oomycetes	10
Cross-kingdom RNA interference.....	10
Host-induced gene silencing (HIGS) as a genetic tool in basic and applied research	12
AIMS OF THE THESIS	15
RESULTS.....	16
I: Oomycete small RNAs bind to the plant RNA-induced silencing complex for virulence.	16
Supplementary data:	40
II: Plant ARGONAUTE protein immunopurification for pathogen cross kingdom small RNA analysis.....	70
III: An Arabidopsis downy mildew non-RxLR effector suppresses induced plant cell death to promote biotroph infection.....	95
Supplementary data:	110
DISCUSSION	118
<i>Hyaloperonospora arabidopsidis</i> as a new cross-kingdom RNAi model.....	118

B. cinerea and *H. arabidopsidis*: two complementary cross-kingdom RNAi model systems 121

Cross-kingdom RNAi: childhood friend or recurrent affair of life? 122

Host-induced gene silencing as a tool for functional gene studies in *H. arabidopsidis*..... 124

Where do we go from here? Future directions of cross-kingdom RNAi research..... 125

Cysteine-rich proteins: the abandoned child of oomycete effector research..... 127

Who am I? And if so, how many? Comparison of protein and sRNA effectors..... 129

REFERENCES 133

ACKNOWLEDGEMENT 153

General abbreviation index

CFP	Cyan fluorescent protein
CRN	Crinkler effector
DAMP	Damage associated molecular pattern
DNA	Deoxyribonucleic acid
dpi	days post inoculation
ETI	Effector-triggered immunity
ETS	Effector-triggered susceptibility
FITC	Fluorescein isothiocyanate
GFP	Green fluorescent protein
GUS	β -Glucuronidase
HIGS	Host-induced gene silencing
HR	Hypersensitive response
INA	2,6-Dichloroisonicotinic acid
MAMP	Microbe-associated molecular pattern
MAP kinase	Mitogen-activated protein kinase
miRNA	microRNA
milRNA	microRNA-like RNA
MVB	Multi vesicular body
NAD ⁺	Nicotinamide adenine dinucleotide
nat-siRNA	natural antisense RNA
NLP	Necrosis and ethylene-inducing peptide (NEP)-like protein
NLR	Nuclear oligomerization domain (NOD)-like receptor
nt	nucleotide
PAMP	Pathogen-associated molecular pattern
PCD	Programmed cell death
pha-siRNA	phased, small interfering RNA
PPR	Pentatricopeptide repeat
<i>Pst</i>	<i>Pseudomonas syringae</i> pv <i>tomato</i>
PTI	PAMP-triggered immunity
(qRT)-PCR	(quantitative reverse transcription)-Polymerase chain reaction
<i>R</i> gene	Resistance gene
RISC	RNA-induced silencing complex
RNA	Ribonucleic acid

RNAi	RNA interference
SA	Salicylic acid
SNP	Single nucleotide polymorphism
SP	Signal peptide
sRNA	small RNA
(s)RNA-seq	(small) RNA sequencing
WT	Wild type
YFP	Yellow fluorescent protein

Gene name abbreviation index

<i>AtAED3</i>	<i>APOPLASTIC, ENHANCED DISEASE SUSCEPTIBILITY 1-DEPENDENT 3 (AT1G09750)</i>
<i>AtAGO1</i>	<i>ARGONAUTE 1 (AT1G48410)</i>
<i>AtAGO2</i>	<i>ARGONAUTE 2 (AT1G31280)</i>
<i>AtAGO4</i>	<i>ARGONAUTE 4 (AT2G27040)</i>
<i>AtDCL1</i>	<i>DICER-LIKE 1 (AT1G01040)</i>
<i>AtDCL2</i>	<i>DICER-LIKE 2 (AT3G03300)</i>
<i>AtDCL3</i>	<i>DICER-LIKE 3 (AT3G43920)</i>
<i>AtDCL4</i>	<i>DICER-LIKE 4 (AT5G20320)</i>
<i>AtHEN1</i>	<i>HUA ENHANCER 1 (AT4G20910)</i>
<i>AtHYL1</i>	<i>HYPONASTIC LEAVES 1 (AT1G09700)</i>
<i>AtHST</i>	<i>HASTY (AT3G05040)</i>
<i>AtMED19a</i>	<i>MEDIATOR SUBUNIT 19a (AT5G12230)</i>
<i>AtMEMB12</i>	<i>MEMBRIN 12 (AT5G50440)</i>
<i>AtNPR</i>	<i>NON-EXPRESSOR OF PATHOGENESIS-RELATED GENES (several paralogs)</i>
<i>AtPDF1.2</i>	<i>PLANT DEFENSIN 1.2 (AT5G44420)</i>
<i>AtPDLP</i>	<i>PLASMODESMATA-LOCATED PROTEIN 1 (AT5G43980)</i>
<i>AtPR1</i>	<i>PATHOGENESIS-RELATED GENE 1 (AT2G14610)</i>
<i>AtRCD1</i>	<i>RADICAL-INDUCED CELL DEATH 1 (AT1G32230)</i>
<i>AtRDR</i>	<i>RNA-DEPENDENT RNA POLYMERASE (several paralogs)</i>
<i>AtRPP1</i>	<i>RECOGNITION OF PERONOSPORA PARASITICA 1 (AT3G44480)</i>
<i>AtSE</i>	<i>SERRATE (AT2G27100)</i>
<i>AtTPL</i>	<i>TOPLESS (AT1G15750)</i>

<i>AtTPR1</i>	<i>TOPLESS-RELATED 1 (AT1G80490)</i>
<i>AtWNK2</i>	<i>WITH NO LYSINE (K) KINASE (AT3G22420)</i>
<i>HaA1E</i>	<i>Aldose-1-epimerase (HpaG814621)</i>
<i>HaACT A</i>	<i>Actin A (HpaG807716)</i>
<i>HaDCL1</i>	<i>Dicer-like 1 (HpaG808216)</i>
<i>HaCR1</i>	<i>Cystein-rich protein 1 (HpaG806256)</i>
<i>HaNLP3</i>	<i>Necrosis and ethylene-inducing peptide-like protein 1 (HpaG809243)</i>
<i>HaRxL21</i>	<i>RxLR effector 21 (HpaG811507)</i>
<i>HaRxL44</i>	<i>RxLR effector 44 (HpaG808319)</i>
<i>HaRxL62</i>	<i>RxLR effector 62 (HpaG813486)</i>
<i>HaRxL96</i>	<i>RxLR effector 96 (HpaG802236)</i>
<i>HaRxL106</i>	<i>RxLR effector 106 (HpaG811507)</i>
<i>PSR1</i>	<i>Phytophthora Suppressor of RNA Silencing 1 (P. sojae)</i>
<i>PSR2</i>	<i>Phytophthora Suppressor of RNA Silencing 2 (P. sojae)</i>
<i>SID1</i>	<i>Systemic RNAi defective 1 (C. elegans)</i>
<i>SID2</i>	<i>Systemic RNAi defective 2 (C. elegans)</i>

List of publications

I) Dunker, F., Trutzenberg, A., Rothenpieler, J.S., Kuhn, S., Pröls, R., Schreiber, T., Tissier, A., Kemen, A., Kemen, E., Hückelhoven, R., Weiberg, A., 2020. Oomycete small RNAs bind to the plant RNA-induced silencing complex for virulence. *eLife* **9**, e56096.

II) Dunker, F.#, Lederer, B.#, and Weiberg, A., 2021. Plant ARGONAUTE protein immunopurification for pathogen cross kingdom small RNA analysis. *Bio-protocol* **11**, e3911

These authors contributed equally to the work.

III) Dunker, F.#, Oberkofler, L.#, Lederer, B., Trutzenberg, A., Weiberg, A., 2021. An Arabidopsis downy mildew non-RxLR effector suppresses induced plant cell death to promote biotroph infection. *J. Exp. Bot.* **72**, 718–732.

These authors contributed equally to the work.

Declaration of contribution as co-author

Publication I:

Dunker, F., Trutzenberg, A., Rothenpieler, J. S., Kuhn, S., Pröls, R., Schreiber, T., Tissier, A., Kemen, A., Kemen, E., Hückelhoven, R., Weiberg, A. 2020. Oomycete small RNAs bind to the plant RNA-induced silencing complex for virulence. *eLife* **9**, e56096

In this publication, I designed and performed all experiments and contributed all data, if they are not explicitly listed below.

The analysis of next generation sequencing data was jointly performed by Arne Weiberg and me. I provided the figure design and the original draft of the manuscript, that was then substantially revised and edited jointly by Arne Weiberg and me. Adriana Tutzenberg provided data for Figure 1- figure supplement 2 and Figure 4c, Jan S. Rothenpieler provided data for Figure 1- figure supplement 2 and Figure 2- figure supplement 4 b, and Sarah Kuhn provided data for Figure 1- figure supplement 3.

Reinhard Pröls and Ralph Hückelhoven provided data for Figure 2- figure supplement 6, Tom Schreiber and Alain Tisisier provided a plant codon- optimized Csy4 sequence, Ariane Kemen and Eric Kemen provided data for Figure 2- figure supplement 6.

Arne Weiberg conceived the overall aim of the study, contributed to the experimental design, acquired funding and supervised the project.

Publication II:

II) Dunker, F.[#], Lederer, B.[#], and Weiberg, A., 2021. Plant ARGONAUTE protein immunopurification for pathogen cross kingdom small RNA analysis. *Bio-protocol* **11**, e3911

[#] These authors contributed equally to the work.

In this publication, I developed the method and performed all experiments that are displayed. I wrote the initial draft of the paper, that was substantially revised and edited jointly by Arne Weiberg, Bernhard Lederer and me. Bernhard Lederer contributed the figures displaying the schematic overview and the bioinformatic work flow.

Publication III:

Dunker, F.[#], Oberkofler, L.[#], Lederer, B., Trutzenberg, A., Weiberg, A., 2021. An Arabidopsis downy mildew non-RxLR effector suppresses induced plant cell death to promote biotroph infection. *J. Exp. Bot.* **72**, 718–732.

[#] These authors contributed equally to the work.

In this publication, I designed and performed the experiments for Figure 1B-C (*HaCRI^{RNAi} #2* line), Figure 1D, Figure 2B+E, Figure 4A+D, Supplemental Figure S1, Supplemental Figure S4, Supplemental Figure S5 (*HaCRI^{RNAi} #2* line), Supplemental Figure S6, Supplemental Figure S7 (*HaCRI^{RNAi}* lines), Supplemental Figure S8B, Supplemental Figure S9, Supplemental Figure S10, and Supplemental Figure S12. I prepared all figures with suggestions from Lorenz Oberkofler and Arne Weiberg. I wrote the initial draft of the paper, that was substantially revised and edited by Arne Weiberg, Bernhard Lederer and me together.

Lorenz Oberkofler performed the experiments for Figure 1B (*HaCRI^{RNAi} #1* line), Figure 2C-D, Figure 3A, Supplemental Figure S2, Supplemental Figure S3, Supplemental Figure S5 (all but *HaCRI^{RNAi} #2* line), Supplemental Figure S7 (*HaACT^{RNAi}* line), and Supplemental Figure S8A.

Bernhard Lederer performed the experiments for Figure 3B+D, Figure 4B-C, Supplemental Figure S11, the cDNA for Supplemental Figure S12 and prepared the graphical model for Figure 3C.

Adriana Trutzenberg provided the hairpin construct plasmids and the T1 generation of *HaCRI^{RNAi}* plant lines.

Arne Weiberg conceived the overall aim of the study, contributed to the experimental design, acquired funding and supervised the project.

(Dr. Arne Weiberg)

License and permission

Dunker, F., et al. 2020. Oomycete small RNAs bind to the plant RNA-induced silencing complex for virulence. *eLife* **9**, e56096.

Dunker, F.[#], Lederer, B.[#], et al. 2021. Plant ARGONAUTE protein immunopurification for pathogen cross kingdom small RNA analysis. *Bio-protocol* **11**, e3911

[#] These authors contributed equally to the work.

Dunker, F.[#], Oberkofler, L.[#], et al. 2021. An Arabidopsis downy mildew non-RxLR effector suppresses induced plant cell death to promote biotroph infection. *J. Exp. Bot.* **72**, 718–732.

[#] These authors contributed equally to the work.

These articles were published and re-printed under the Creative Commons Attribution license (CC-BY 4.0). For details on the license please refer to <https://creativecommons.org/licenses/>

Summary

Oomycetes comprise infamous plant pathogens that jeopardize global food resources. Effector proteins promote infections of pathogens and are consequently also found in large numbers in the genome of oomycetes. More recently, it was discovered that in fungi also small RNAs (sRNAs) can act as effectors by silencing host immunity genes by cross-kingdom RNA interference (RNAi). The effector diversity results in a highly complex, multilayered host pathogen cross-talk, whereas oomycete effector research has been mainly focused on a single effector class: the RxLR effectors. Consequently, I wanted to investigate two understudied oomycete effector classes: sRNAs and small secreted non-RxLR cysteine-rich (CR) proteins. I adapted an immunopurification-based method for high-throughput sequencing of pathogen sRNAs that were associated with the host ARGONAUTE (AGO) protein forming the RNA-induced silencing complex (RISC). From our first insights into the putative sRNA effectors of *H. arabidopsidis* I selected candidates that revealed target transcript repression. I designed a novel *in situ* reporter that demonstrated both pathogen sRNA translocation into plants and efficient host target silencing. Thereby, I directly visualized the spatial dimension of cross-kingdom RNAi in the host tissue. I validated the crucial contribution of sRNAs to virulence by scavenging three of them with a plant encoded sRNA target mimic array. Hereby, I introduced *H. arabidopsidis* as a complementary cross-kingdom RNAi model to *B. cinerea*. I suggest that pathogen sRNA effectors are not only a widespread virulence mechanism, but also that comparative research can enlighten the evolutionary forces that shape sRNA arsenals in pathogens with distinct lifestyles and host ranges.

As *H. arabidopsidis* remains inaccessible to classical reverse genetics, me and my colleagues established host-induced gene silencing (HIGS) in Arabidopsis as a tool to knock down and study non-RxLR *HaCR1* protein effector function. Isolated Arabidopsis *HaCR1^{RNAi}* lines displayed prominent host cell death upon *H. arabidopsidis* infection suggesting that *HaCR1* inhibits induced plant cell death to promote infection. *HaCR1* seemed to reside in the plant apoplast and its activity was strictly dependent on its signal peptide. We found that *HaCR1* inhibited plant extracellular protease activity, suggesting that *HaCR1* might interfere with plant defensive proteases and protease-dependent programmed cell death (PCD), providing for the first time, insights into the molecular function of a *H. arabidopsidis* apoplastic effector.

Taken together, I provide new insights into the role of sRNAs and cysteine-rich protein effectors for *H. arabidopsidis* host infection. Completing the picture of the pathogen virulence arsenal poses an important prerequisite towards more effective pathogen control.

Introduction

Oomycetes: constant threats to global food resources

Plants are permanently threatened by a plethora of herbivores and pathogens. It is estimated that around 20-40% of global production of major crops is lost due to pests and diseases, severely impacting food availability for the growing world population (Savary et al., 2019). Major agricultural pests comprise highly different organisms such as weeds, bacteria, fungi, nematodes, insects and oomycetes (Oerke, 2006). The latter are filamentous organisms that superficially resemble fungi, but are phylogenetically distinct from them, belonging together with diatoms and brown algae to the phylum straminipila also known as the stramenopiles (Thines, 2014). Oomycetes comprise free living saprophytic species, that fulfill important ecological functions degrading organic matter especially in freshwater ecosystems (Masigol et al., 2019). However, the majority of oomycete species has adapted to a parasitic lifestyle, giving rise to some of the most notorious plant pathogens (Thines and Kamoun, 2010). Outbreaks of oomycete pathogens like *Phytophthora infestans*, causing the potato late blight disease, can lead to devastating crop losses such as the one responsible for the Great Famine in Ireland in the 1840s, and more recently 2008 in South India. Further examples of oomycete pathogens with a high economic impact include the soybean root rot pathogen *Phytophthora sojae*, the oil palm pathogen *Phytophthora palmivora* and the grape downy mildew pathogen *Plasmopara viticola* (Derevnina et al., 2016; Kamoun et al., 2015).

Besides plant pathogens, some oomycetes have evolved into parasites in aquatic ecosystems like the infamous fish pathogen *Saprolegnia parasitica*. Especially after the ban of treatment with Malachite Green due to its high toxicity, it is estimated that around 10% of all cultured salmon worldwide succumb to saprolegniasis (Earle and Hintz, 2014). Finally, oomycetes are among the few pathogens that can also cause enormous damage in natural ecosystems. Examples include the large-scale abolition of oak trees by *Phytophthora ramorum* in California (Grünwald et al., 2008), the devastating dieback disease outbreaks caused by *Phytophthora cinnamomi* wiping out entire ecosystems in Australia (Cahill et al., 2008), and also the eradication of large parts of wild European crayfish populations by the crayfish plague pathogen *Aphanomyces astaci* (Svoboda et al., 2017).

Oomycete control in agriculture has been relying on the extensive application of chemical pesticides and the breeding of resistant crop cultivars. However, oomycetes have displayed a remarkable capability to quickly adapt to plant resistance and withstand pesticide treatments (Delmas et al., 2017; Fry, 2008). In addition, chemical pesticide application bears large

economic costs and can be highly detrimental for ecosystems, consumers, and farmers (Sang and Kim, 2020). A central limiting factor for more specific, durable, and sustainable oomycete pest control is the incomplete knowledge of their molecular weaponry. How oomycetes overcome host immunity and reprogram host physiology for their own benefit remain, despite extensive research efforts, incompletely answered questions.

Hyaloperonospora arabidopsidis as an oomycete model plant pathogen

One central model system to uncover the molecular basis for oomycete virulence as well as plant resistance is the Arabidopsis (*Arabidopsis thaliana*) downy mildew pathogen *Hyaloperonospora arabidopsidis* (Kamoun et al., 2015). *H. arabidopsidis* is one of the few pathogens frequently colonizing wild Arabidopsis plants, being its sole natural host (Agler et al., 2016; McDowell, 2014). It is an obligate biotrophic pathogen that fully relies on nutrients obtained from living host cells and can only complete its life cycle if the host tissue remains alive during the entire interaction (Glazebrook, 2005).

The infection cycle starts with a germinating conidiospore on the host leaf surface that penetrates through the cuticle and forms intercellular hyphae in the leaf (Slusarenko and Schlaich, 2003). The pathogen develops specialized invaginations breaching the host cell wall, called haustoria, which are believed to be the main hub for nutrient delivery as well as signal exchange. The haustoria are separated from the plant cytoplasm by a newly synthesized plant membrane called extrahaustorial membrane and the space between haustorium and plant cell is filled with an amorphous layer: the extrahaustorial matrix (Judelson and Ah-Fong, 2019). This intimate interaction requires extensive communication between the host and the pathogen. In the case of biotrophic pathogens like *H. arabidopsidis*, this communication is required not only to dampen the host immune response, but also to largely subvert host physiology to enable constant nutrient delivery and life cycle completion (Thordal-Christensen et al., 2018).

The asexual life cycle of *H. arabidopsidis* is completed by the formation of aerial, tree-like condiophores that breach out of the stomata and carry the conidiospores. These conidiospores can start a new infection cycle on other leaves or plants. In addition, *H. arabidopsidis* is a homothallic organism and can reproduce sexually by the differentiation of hyphae into oogonia and antheridia, usually followed by self-fertilization. However, crossing of distinct isolates is also possible (Bailey et al., 2011; Koch and Slusarenko, 1990). Fertilization leads to the development of oospores, which represent a permanent form, for example, to over-winter. Germinated oospores can infect the roots of Arabidopsis, followed by systemic growth and conidiospore production, re-starting the asexual reproduction cycle (Slusarenko and Schlaich, 2003).

Oomycete effectors with focus on *H. arabidopsidis*

To obtain nutrients from the host and complete their life cycle, oomycetes like *H. arabidopsidis* and other groups of pathogens and pests, rely on small, secreted peptides to manipulate their hosts: the so-called effectors (Hogenhout et al., 2009). The number of putative effectors in plant pathogenic oomycete genomes ranges from ~80 in the white rust pathogen *Albugo laibachii*, over ~130 in *H. arabidopsidis*, to ~700 in *Phytophthora infestans* (Baxter et al., 2010; Haas et al., 2009; Kemen et al., 2011). Effectors do not only interfere with host immunity but redirect the entire host physiology to provide nutrients. Thus, targets of effectors also include susceptibility genes like cell wall remodeling enzymes (van Schie and Takken, 2014).

The effectors of *H. arabidopsidis* can be classified by sequence features into RxLRs, CRINKLERs (CRNs) with a LFLAK motif, necrosis and ethylene-inducing peptide-like proteins (NLPs) and so called cysteine-rich (CR) proteins (Cabral et al., 2011). Importantly these classes do not represent conventional protein families and show, apart from short translocation motifs or overall amino acid frequencies, little to no sequence homology (Schornack et al., 2009; Win et al., 2007). Most effectors are refined to a single pathogen species or even isolate while conserved protein effectors are an exception. Out of over hundred effectors, only six effectors were shared between *H. arabidopsidis* and the sunflower downy mildew pathogen *Plasmopara halstedii* and only three syntenic effector families were conserved between *H. arabidopsidis* and *P. infestans* (Baxter et al., 2010; Sharma et al., 2015). However, around 30% of effectors share common structural elements in the WY-domain fold without sequence conservation, indicating potential functional conservation (Win et al., 2012). Much research effort has been directed towards effectors containing a RxLR amino acid motif, where x stands for any amino acid, frequently followed by a (d)EER motif (Govers and Bouwmeester, 2008; Rehmany et al., 2005). RxLR effectors were found to be translocated into the host cell during infection and comprise the vast majority of known avirulence genes (Rouxel and Balesdent, 2010; Whisson et al., 2007). Despite being essential for the translocation, the exact molecular role of the RxLR motif itself remains controversial (Ellis and Dodds, 2011; Wawra et al., 2012). RxLR effectors are common and crucial for the virulence of *Phytophthora* and downy mildew species like *H. arabidopsidis*, but do not seem to play a comparable role in other pathogenic oomycete genera like *Albugo*, *Phytium* or *Saprolegnia* (Anderson et al., 2015). The molecular function of an increasing number of RxLR effectors from plant pathogenic oomycetes has been elucidated and host target proteins have been identified (Kanja and Hammond-Kosack, 2020).

A large-scale experiment reported a bacterial growth promotion of 70% of the tested 64 RxLR effectors of *H. arabidopsidis* in at least one Arabidopsis accessions, when the effector was delivered by modified *Pseudomonas syringae* bacteria. Out of these effectors promoting bacterial growth, 77% could also reduce plant callose deposition, a hallmark of plant immunity. The expression of nine candidate effectors in Arabidopsis resulted, in seven cases, in higher *H. arabidopsidis* proliferation, but no further interactors or molecular functions were suggested (Fabro et al., 2011). In another study, overexpression of 13 RxLR effectors *in planta* led, in all but one case, to increased susceptibility towards *Pseudomonas syringae* infection, however it suppressed the growth of the oomycete *P. capsici*. The growth of *H. arabidopsidis* itself was not influenced, indicating sufficient endogenous effector production or small contribution of individual effectors (Pel et al., 2014). The effectors *HaRxL62* and *HaRxL96* reduced SA dependent defense marker gene induction and interfered with basal immune responses like callose deposition, however no molecular mechanism was suggested (Anderson et al., 2012; Asai et al., 2014).

Compared to *Phytophthora* species, the amount of *H. arabidopsidis* effectors with an elucidated molecular function remains low. The effector *HaRxL44* weakened the salicylic acid dependent immune response by destabilizing the Arabidopsis mediator complex component *MED19a* (Caillaud et al., 2013). Also the second characterized effector, *HaRxL106*, targeted salicylic acid-dependent immune responses, directly binding RADICAL-INDUCED CELL DEATH 1 (RCD1) and perturbing its capacity to activate immune response factors (Wirthmueller et al., 2018). The effector *HaRxL21* recruits the Arabidopsis transcription repressors TOPLESS (TPL) and TOPLESS-RELATED (TPR) 1 to interfere with the defense gene induction and thereby promotes the infection with *H. arabidopsidis*, but also with the necrotrophic pathogen *B. cinerea* (Harvey et al., 2020).

Molecular effector functions have been predominantly investigated by heterologous effector expression *in planta* and *in vitro* assays, as the obligate biotrophic *H. arabidopsidis* can be neither cultured nor transformed (McDowell, 2014). A study investigating the function of the *H. arabidopsidis* NLPs came to the conclusion that, despite their homology, those effectors have lost the ability to trigger host cell death (Cabral et al., 2012). A structural analysis revealed that *HaNLP3* has lost the molecular flexibility to bind plant sphingolipid glycosylinositol phosphorylceramides and thereby promote phytotoxicity (Lenarčič et al., 2019). However, this special feature is in line with their occurrence in a biotrophic pathogen.

Functional data on other *H. arabidopsidis* effector classes are limited and do not expand further as their role of avirulence genes in race-specific resistance, like the only known non-RxLR

avirulence gene ATR5. ATR5 however does contain a conventional EER motif and the RXLR motif might be replaced by a functionally redundant GRVR motif (Bailey et al., 2011). Especially little is known about the class of cysteine-rich proteins, even if those contain the most highly expressed effectors of *H. arabidopsidis* (Asai et al., 2014). The most abundant effector transcript of *H. arabidopsidis* encodes *Cystein-rich protein (HaCR) 1*, also known as *Ppat14*, which function remains so far largely enigmatic (Bittner-Eddy et al., 2003; Cabral et al., 2011). Effectors frequently display a large number of cysteines, that are believed to aid protein stability by the formation of disulfide bridges. This is believed to be especially essential to withstand the harsh, protease-rich environment in the plant apoplast (Rocafort et al., 2020). In recent years, sRNAs triggering gene silencing by RNA interference (RNAi) have emerged as an entirely new class of fungal pathogen effectors besides the extensively studied proteinaceous effectors (Weiberg et al., 2014).

The plant immune response to *H. arabidopsidis*

To enable successful infection, plant pathogens like *H. arabidopsidis* have to overcome a multi-layered and complex plant immune system. Unlike vertebrates, plants do not possess specialized mobile immune cells, but every cell provides a cell-autonomous immune response (Spoel and Dong, 2012). The concept of plant immunity/susceptibility is classically described by the zig-zag model introduced around 15 years ago and outlined in the following paragraph (Jones and Dangl, 2006).

Plants achieve basic immunity by membrane bound receptors that recognize conserved pathogen/microbe- or damage-associated molecular patterns (PAMPs/MAMPs/DAMPs) like bacterial flagellin, chitin or plant cell wall fragments. The perception of PAMPs triggers a signaling cascade, that ultimately provides immunity towards a wide variety of pathogens known as PAMP-triggered immunity (PTI). Classic oomycete PAMPs include β -glucans and eicosapolyenoic acids, although their detection mechanism remains to be determined (Robinson and Bostock, 2014). A well described PTI response that limits the spread of *H. arabidopsidis* is the induction of salicylic acid (SA) dependent defense genes *PATHOGENESIS-RELATED GENE 1 (AtPRI)*. *AtPRI* encodes for a secreted sterol binding protein, that efficiently limits the growth of sterol auxotrophic oomycetes like *H. arabidopsidis* (Alexander et al., 1993; Gamir et al., 2017). Another classic PTI response is the deposition of callose, that in the case of *H. arabidopsidis* first accumulates at the haustorial neck and later encases the entire haustorium. This process is regulated by the plasmodesmal protein PLASMODESMATA-LOCATED PROTEIN 1 (PDLP1), which accordingly limits *H. arabidopsidis* proliferation (Caillaud et al., 2014).

However, adapted, virulent pathogens have evolved strategies to overcome PTI and enable successful infection. A striking similarity between highly diverse pathogens like bacteria, oomycetes, and fungi is the subversion of the plant PTI by effectors that were described in the previous chapter, resulting in effector-triggered susceptibility (ETS). In a next layer of immunity, specific effectors, in this context also named avirulence genes, can be recognized by host nucleotide-binding oligomerization domain-like receptors (NOD-like receptors, NLRs), leading to a strong immune response and plant resistance. Therefore, receptors mediating this effector-triggered immunity (ETI) are also called resistance genes (*R* genes). ETI is frequently marked by an programmed, localized host cell death, called the hypersensitive response (HR), that is especially efficient against biotrophic pathogens like *H. arabidopsidis*. *R* gene mediated resistance of Arabidopsis against *H. arabidopsidis* largely follows Henry Flor's gene-for-gene concept (Flor, 1971) also known as race specific resistance. So far 47 *R* genes, called *RECOGNITION OF PERONOSPORA PARASITICA (RPP)*, providing resistance against at least one isolate of *H. arabidopsidis* were described, however are large number of them represents only different alleles and they are predominantly encoded by six genomic loci (Nemri et al., 2010). Extensive research efforts have led to the molecular identification of seven Arabidopsis *RPP* genes together with the three corresponding *H. arabidopsidis* avirulence genes (Woods-Tör et al., 2018). Recently, it was demonstrated that upon direct binding of the *H. arabidopsidis* effector ATR1, the resistance gene *AtRPP1* becomes oligomerized and then catalyzes the hydrolysis of NAD⁺ (S. Ma et al., 2020), a known cell death trigger in animals and plants (Horsefield et al., 2019). However, some *H. arabidopsidis* effectors like *HaRxL103* evade recognition by resistance genes through polymorphisms in expression and localization (Asai et al., 2018).

In addition to full resistance, there are various degrees of intermediate resistance phenotypes termed flecking necrosis, pitting necrosis and trailing necrosis. In addition, host resistance is developmental stage specific, with the cotyledons usually being more susceptible than true leaves (Coates and Beynon, 2010; Krasileva et al., 2011).

Plant hormones play paramount roles to integrate pathogen stimuli and mediate immune responses. The defense response against biotrophic pathogens like *H. arabidopsidis* is mainly mediated by SA (Glazebrook, 2005) and pre-treatment of plants with either SA or the synthetic analog 2,6-dichloroisonicotinic acid (INA) primes the plants for a strong immune response against *H. arabidopsidis* leading to trailing necrosis and enhanced resistance (Lawton et al., 1995). The paramount role of SA is also highlighted by the large number downy mildew

effectors interfering with hormone signaling (Asai et al., 2014; Caillaud et al., 2013; Wirthmueller et al., 2018).

Over the last decade it has become more apparent that the signaling pathways between PTI and ETI are highly interconnected, overlapping and potentially continuous, rather than distinct processes (Thomma et al., 2011). Importantly, major plant defense hormones like SA are crucial to achieve both PTI and ETI (Zhang and Li, 2019). Therefore, some researchers proposed a refined model for plant immunity/susceptibility focusing on immunity layers instead of the immunity trigger molecule (Wang et al., 2019). Hence, the plant immune response consists of three layers: the recognition layer (i.e., the receptors), the signal integration layer (e.g. kinase cascades and hormone production) and the defense-action layer (e.g. anti-microbial protein secretion or PCD and HR). This complex immune system has to be tightly regulated to ensure both prevention of auto-immunity and rapid activation upon pathogen infection (Spoel and Dong, 2012). In recent years, it was discovered that among the major regulators of plant immunity are plant sRNAs, which suppress complementary immunity genes or susceptibility genes after infection via RNAi.

RNA interference in plants and its role in plant immunity

In eukaryotes, sRNAs can trigger the repression of complementary transcripts, a phenomenon known as RNAi. RNAi has crucial functions such as transposon control, antiviral defense and endogenous gene regulation for development, physiology and stress response (Alberts, 2015). Small RNAs in plants are classified according to their biogenesis pathways into microRNAs (miRNAs), natural antisense small interfering RNAs (nat-siRNAs), phased secondary small interfering small RNAs (pha-siRNA) and other classes involved in RNA directed DNA methylation termed heterochromatic small interfering RNAs (hc-siRNAs). While miRNAs are derived from hairpin folding primary microRNAs (pri-miRNAs) transcribed by RNA-Polymerase II, siRNAs derive from perfectly complementary double stranded RNAs and typically depend on a RNA dependent RNA polymerase (RDR) (Bologna and Voinnet, 2014). These double stranded RNA precursors are processed by the Dicer complex (consisting of a Dicer-like endonuclease (DCL) and several co-factors) into short 21-24 nt long sRNAs (Khraiweh et al., 2012). These sRNAs then bind to an Argonaute (AGO) protein to form the plant RNA-induced silencing complex (RISC) (Baumberger and Baulcombe, 2005). After the star strand is dismissed, the guide strand of the sRNA then binds complementary mRNAs and mediates to their cleavage via the Argonaute slicer function or translational repression (Fang and Qi, 2016). The genome of Arabidopsis encodes for ten Argonaute proteins, with *AtAGO1* as the major Argonaute protein in post-transcriptional gene silencing (Vaucheret, 2008). The

sorting of plant sRNAs into the diverse Argonaute proteins depends on the sRNA size and the 5' nucleotide. Immunopurification of Argonaute proteins, coupled to sequencing of the associated sRNAs, revealed that Arabidopsis AGO1 preferentially binds to 21 nt long sRNAs with 5' terminal uracil, two central features of plant miRNAs (Mi et al., 2008; Montgomery et al., 2008). Similar approaches were used to gain insights into changes of the sRNAs associated with the host AGO1 and AGO2 during bacterial infection (X. Zhang et al., 2011) and several method reports with protocol details on co-immunopurification of plant RISC with associated plant sRNAs are published (Carbonell, 2017; Zhao et al., 2012).

Besides its role in development and physiology, RNAi can regulate the plant immune system. Some sRNAs are positive regulators of immunity, they become induced upon infection and silence susceptibility genes. The Arabidopsis miR393 was the first discovered plant miRNA that confers immunity against bacterial infection. After bacterial infection, it is induced and represses auxin signaling, and thereby potentially shifts the growth-defense equilibrium (Navarro et al., 2006). Interestingly, the star strand of the same miRNA miR393* can bind to *AtAGO2* and silences the negative regulator of plant immunity *MEMBRIN (AtMEMB) 12* to prevent secretion of *AtPR1* (X. Zhang et al., 2011).

In the absence of pathogens, the miR472/miR482 family suppresses *R* gene expression by post-transcriptional silencing. However, *NLR* transcripts are not only a direct target of this miRNA family, but also trigger the production of secondary siRNAs that enhance the silencing effect and can also silence *NLR* genes in *trans* that are not directly targeted by miR482 itself (Li et al., 2012; Shivaprasad et al., 2012). Thus, plants prevent auto-immunity risks, but still remain capable of retaining large *NLR* sets to confer a robust immune against most pathogens (Lai and Eulgem, 2018).

Besides post-transcriptional silencing, sRNAs do also mediate transcriptional gene silencing of immune genes by the RNA-directed DNA methylation (RdDM) pathway using AGO4 as the main hub (Bologna and Voinnet, 2014). Arabidopsis mutants impaired in RdDM revealed enhanced resistance against *H. arabidopsidis* infection, whereas hypermethylation mutants displayed increased susceptibility. This methylation status dependent resistance was associated with increased callose deposition and enhanced salicylic acid dependent defense gene expression (López Sánchez et al., 2016).

The crucial importance of sRNAs for defense against oomycetes is furthermore underscored by the evolution of oomycete effectors that suppress silencing. *Phytophthora sojae* encodes for two silencing suppressors, *Phytophthora Suppressor of RNA silencing (PSR) 1* that suppresses biosynthesis of diverse sRNAs like miRNAs and siRNAs, and *PSR2* that is specifically

repressing phased siRNAs (Hou et al., 2019; Qiao et al., 2013). While *PSR1* is restricted to *P. sojae*, *PSR2* is a conserved effector of various *Phytophthora* species and homolog of *PSR2* is also encoded in the *H. arabidopsidis* genome. However, unlike the *Phytophthora PSR2* effectors it is missing the RxLR translocation motif and only contains a dEER-like motif, so its activity remains unclear (Xiong et al., 2014). Intriguingly, the suppression of silencing by pathogen effectors automatically releases silencing of plant NLRs, providing a plant counter-defense, another advantage of *R* gene control via RNAi (Lai and Eulgem, 2018).

RNA interference in oomycetes

While extensive studies have elucidated the RNAi machinery and function in plants, relatively little is known about the role of RNAi in oomycetes. Small RNA-seq of *P. infestans* revealed two distinct classes of 21 nt and 25-26 nt which are mainly encoded by gene sparse, but transposon and effector-rich genomic regions, and are associated with oomycete Argonaute proteins (Åsman et al., 2016; Fahlgren et al., 2013; Vetukuri et al., 2012). Though it has been suggested that sRNAs mediate large-scale transposon control and co-repression of nearby effector genes (Vetukuri et al., 2013; Whisson et al., 2012), no direct experimental evidence for this hypothesis has been reported.

Recently, a combined sRNA-seq and mRNA-seq study on *P. parasitica* reported widespread efficient silencing of homologous genes by 25-26 nt sRNAs, while 21 nt sRNAs failed to repress gene expression (Jia et al., 2017). This report however investigated only silencing in *cis*, that means of the locus from which the sRNAs were produced. Conversely, any silencing in *trans* as well as the role of the single *bona fide Phytophthora* miRNA miR8788 remain largely unknown and controversial (Fahlgren et al., 2013). One demonstrated role of RNAi in *P. sojae* pathogenicity is trans-generational silencing of the avirulence gene *PsAVR3a* by cis-regulatory sRNAs. Silencing of *AvR3a* might be an advantage for *P. sojae* to escape *RPS3a* gene mediated resistance (Qutob et al., 2013). Like *Phytophthora*, the genome of *H. arabidopsidis* encodes all canonical RNAi components: two DCL genes, one RDR gene and two AGO genes (Bollmann et al., 2018, 2016), suggesting production of small regulatory RNAs. However, any role of RNAi or small RNAs has not so far been investigated.

Cross-kingdom RNA interference

The role of pathogen sRNAs as direct regulators of host genes was firstly observed in the fungal plant pathogen *Botrytis cinerea*. Upon infection, sRNAs of this broad host, necrotrophic pathogen invaded the host RISC. This resulted in a repression of complementary immunity genes, such as mitogen-activated protein (MAP) kinases in both tomato (*Solanum*

lycopersicum) and *Arabidopsis* (Weiberg et al., 2013). These secreted sRNAs were crucial for *Botrytis* virulence, and thus the term small RNA effector was coined in analogy to protein effectors (Wang et al., 2015). The direct communication between two phylogenetically distinct organisms via sRNAs was termed cross-kingdom RNA interference (Weiberg et al., 2015). *Botrytis* cross-kingdom sRNAs exhibited key characteristics of plant miRNAs enabling them to bind to the host AGO1 and direct silencing of complementary host mRNA sequences. Consequently, hypomorphic *atago1-27* mutants resisted infection by *Botrytis cinerea*, while *atdcl1-7* mutants revealed no such resistance, suggesting the mobile entity are ready processed sRNAs rather than longer precursors (Weiberg et al., 2013).

In the last couple of years several other fungal pathogens like *Sclerotinia sclerotium*, *Puccinia striiformis* f. sp. *tritici*, *Verticillium dahliae*, *Fusarium graminearum* and the insect pathogen *Beauveria bassiana* were demonstrated to use comparable virulence strategies (Cui et al., 2019; Derbyshire et al., 2019; Jian and Liang, 2019; B. Wang et al., 2017; Wang et al., 2016). Several additional studies suggested the possibility of cross-kingdom RNAi in fungal pathogens and mutualists based on sequence homology and in silico target predictions, however without experimental evidence (Kusch et al., 2018; Silvestri et al., 2020, 2019). The employment of sRNAs as a new class of effectors is not restricted to fungi, but was also discovered in parasitic plants of the genus *Cuscuta*, the mammalian gastrointestinal nematode *Heligmosomoides polygyrus* and the mutualistic root nodule bacterium *Bradyrhizobium japonicum* (Buck et al., 2014; Johnson et al., 2019; Ren et al., 2019; Shahid et al., 2018).

Interestingly, plants also use sRNAs to counteract pathogens, downregulating their virulence genes, making cross-kingdom RNAi a bidirectional phenomenon. A first incidence of this natural host-induced gene silencing was reported in cotton plants defending against the fungus *Verticillium dahliae* (Zhang et al., 2016). Afterwards, defensive sRNAs were also discovered in *Arabidopsis* when under attack by the fungus *Botrytis cinerea*, making sRNA crosstalk truly bi-directional in this interaction (Cai et al., 2018b; Wang et al., 2016 and Figure 1).

Recent research has been focused on the means of transport of sRNAs between host and pathogen, with extracellular vesicles (EVs) garnering a lot of attention. These are small membrane-enclosed compartments produced by all domains of life with very diverse cargos such as DNA, proteins, toxins and RNAs of various lengths, including sRNAs (van Niel et al., 2018). Though their involvement in cross-kingdom sRNA transport has been suggested in *Arabidopsis* and nematodes (Cai et al., 2018b; Chow et al., 2019 and Figure 1), convincing direct *in vivo* evidence is missing and especially plant EV research remains in its absolute infancy (Rutter and Innes, 2020).

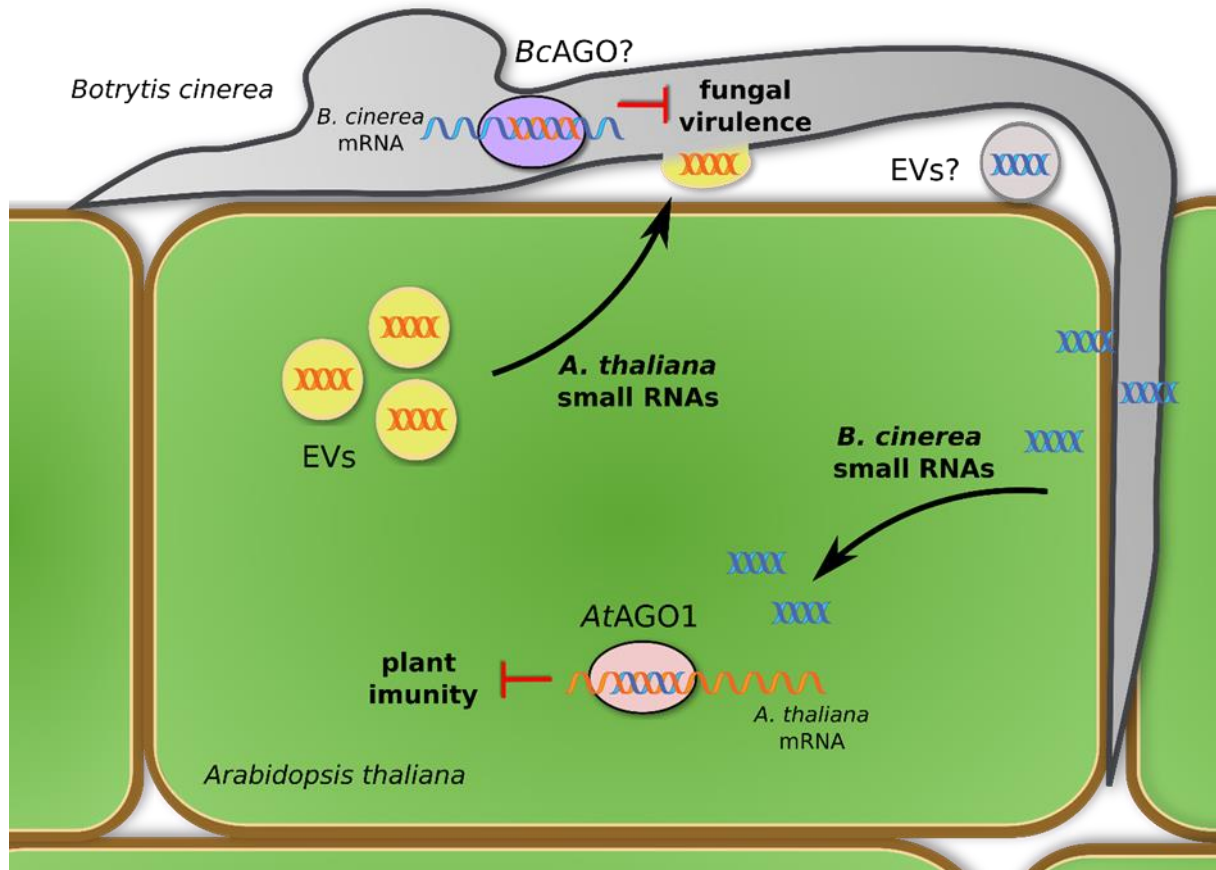


Figure 1: Schematic overview of *B. cinerea*-*Arabidopsis* bidirectional cross kingdom RNAi. Small RNAs of *B. cinerea* load into the host AGO1 protein to confer silencing of immunity genes in *Arabidopsis* and tomato. Equivalently, *Arabidopsis* uses sRNAs to silence fungal virulence genes, some of them involved in vesicle trafficking. The figure also displays the transport of sRNAs via extracellular vesicles (EVs), though *in vivo* a proof of their function in RNA delivery is still missing and thereby remains a tempting speculation.

A fascinating example illustrating the role of sRNAs and protein effectors in the plant-pathogen arms race was suggested for *Phytophthora*: *Arabidopsis* might use phased siRNA from pentatricopeptide-repeat (PPR) protein encoding loci to suppress *Phytophthora capsici* genes, limiting pathogen growth (Hou et al., 2019). To counteract this oomycete pathogens like *P. sojae* and *P. infestans* may employ the RxLR protein effector PSR2 that impairs phased siRNA biogenesis during infection of their respective hosts (Qiao et al., 2013; Xiong et al., 2014).

Host-induced gene silencing (HIGS) as a genetic tool in basic and applied research
 Transgenic expression of dsRNAs in a host plant can lead to the repression of complementary transcripts in pests and pathogens. This somewhat surprising observation was first discovered in insect larvae feeding on maize and cotton (Baum et al., 2007; Mao et al., 2007). This so-called host-induced gene silencing represented the first clear evidence for cross-kingdom RNA

silencing and was later also observed in a plethora of fungal pathogens including *Blumeria graminis* f. sp. *hordei*, *Fusarium graminearum*, *Magnaporthe oryzae* and *Botrytis cinerea* (Guo et al., 2019; Koch et al., 2013; Nowara et al., 2010; Wang et al., 2016). Thanks to its broad applicability HIGS can have a major impact in future crop protection measures, as the targeting of genes required for pathogen survival or virulence can confer highly specific, durable resistance with minimized environmental effects (Koch and Kogel, 2014). The first HIGS based transgenic maize plant, called SmartStax PRO, was approved by the US Environmental Protection Agency in 2017. It expresses a dsRNA targeting *Snf7* of the western corn rootworm besides several insecticidal proteins of *Bacillus thuringiensis* and its commercial introduction by Monsanto (now part of Bayer) and DowAgroSciences is expected in the next years (Head et al., 2017). However, as with all pest control strategies, careful crop management is paramount, as by selection under laboratory conditions a western corn rootworm population could be obtained, which greatly resisted gene repression by HIGS (Khajuria et al., 2018).

Next to its use as an innovative tool in crop protection, HIGS has also become a powerful reverse genetics method to unravel gene functions in obligate biotrophic organisms such as nematodes, powdery mildews, arbuscular mycorrhizal fungi and rust fungi, that are inaccessible by classical genetical modification methods (Helber et al., 2011; Huang et al., 2006; Pliego et al., 2013; Qi et al., 2018). Compared to the high number of fungal examples, the sample size for successful HIGS application in oomycetes is rather limited. An initial trial in *Phytophthora parasitica* did not lead to silencing of the endogenous target gene, despite expression of the hairpin (M. Zhang et al., 2011). Since then, however, successful application of HIGS restricting pathogen growth was reported from the lettuce downy mildew pathogen *Bremia lactuae* and the potato late blight pathogen *P. infestans* (Govindarajulu et al., 2015; Jahan et al., 2015; Sanju et al., 2015). Another elegant validation of the efficacy of HIGS in oomycetes was the silencing of an avirulence gene, thereby enabling growth of *P. capsici* in an otherwise resistant *Nicotiana* species (Vega-Arreguín et al., 2014). These studies however evaluated HIGS rather as a tool for plant protection and did not target pathogen genes with unknown function, but well described housekeeping or effector genes.

As an alternative approach to HIGS, exogenous application of RNA can also lead to target gene repression: a phenomenon termed environmental RNAi or spray-induced gene silencing (SIGS) (Koch et al., 2016; Wang et al., 2016). SIGS bears the advantage of not requiring genetic modification, and thereby prevent associated extensive regulation and consumer reservation (Cai et al., 2018a). However, to this day, there has been no thorough investigation of the applicability of SIGS outside of controlled laboratory environments, and stability and storage

of RNA pesticides remain an issue to be solved prior to wide market introduction. Recently, a possible approach was proposed by the administration of dsRNAs in layered double hydroxide clay nanosheets to increase their stability. Under such conditions, the plant protective effect of RNAs against viral infection could be expanded to 20 days (Mitter et al., 2017).

Aims of the thesis

An incomplete understanding of the diverse effector arsenal and its molecular function is a central obstacle towards more specific and durable pathogen control management. The sRNAs of *B. cinerea* were reported to promote infection by binding to the host RISC complex in a process called cross-kingdom RNAi. However, it remained unclear if phylogenetically distinct plant pathogens like oomycetes employ sRNA effectors as well.

Therefore, in the first part of this study, I wanted to investigate the role of sRNAs in the virulence of the downy mildew pathogen *Hyaloperonospora arabidopsidis*. In order to gain insights into the *H. arabidopsidis* sRNA effector arsenal, my goal was to establish a protocol for the immunopurification of RISC-associated sRNAs, their high-throughput sequencing, and subsequent bioinformatic analysis.

I wanted to clarify if and how these sRNAs convey virulence and investigate the largely unknown spatial and temporal dimensions of cross-kingdom RNAi. Therefore, a central aim was to establish an *in situ* silencing reporter system that can indicate cross-kingdom RNAi in the native host-pathogen system. Another central aim was to evaluate the importance of sRNA effectors for the virulence, also in comparison to previously investigated protein effectors.

In case *H. arabidopsidis* performs cross-kingdom RNAi, I seek to analyze the target genes and compare them with known *B. cinerea* target genes. Are common pathways or even the same genes targeted by distinct plant pathogens? Can I identify novel host immunity factors by research on cross-kingdom RNAi targets?

The target of the second part of this work was to complement the functional insights on sRNA effectors with an investigation of the highest expressed, but molecularly completely uncharacterized, protein effector class: the cysteine-rich proteins. As *H. arabidopsidis* can neither be cultured nor transformed, my aim was to establish HIGS as a reverse genetics tool and elucidate the function of the cysteine-rich protein effector *HaCR1*. I wanted to achieve a functional *HaCR1* knock-down to enable research on its role during the plant-pathogen interaction. By *in silico* analysis and *in planta* expression of the effector, I wanted to gather further insights into the localization and the molecular function of *HaCR1*.

Taken together, I aimed to provide first evidence of the virulence function of two classes of non-RxLR effectors: sRNAs and cysteine-rich proteins. Thus, I sought to lay the foundation for future research on these highly relevant, though understudied effector classes.

Results

I: Oomycete small RNAs bind to the plant RNA-induced silencing complex for virulence.

Oomycete small RNAs bind to the plant RNA-induced silencing complex for virulence

Florian Dunker¹, Adriana Trutzenberg¹, Jan S Rothenpieler¹, Sarah Kuhn¹, Reinhard Pröls², Tom Schreiber³, Alain Tissier³, Ariane Kemen⁴, Eric Kemen⁴, Ralph Hückelhoven², Arne Weiberg^{1*}

¹Faculty of Biology, Genetics, Biocenter Martinsried, LMU Munich, Martinsried, Germany; ²Phytopathology, School of Life Sciences Weihenstephan, Technical University of Munich, Freising, Germany; ³Department of Cell and Metabolic Biology, Leibniz Institute of Plant Biochemistry, Halle, Germany; ⁴Center for Plant Molecular Biology, Interfaculty Institute of Microbiology and Infection Medicine Tübingen, University of Tübingen, Tübingen, Germany

Abstract The exchange of small RNAs (sRNAs) between hosts and pathogens can lead to gene silencing in the recipient organism, a mechanism termed cross-kingdom RNAi (ck-RNAi). While fungal sRNAs promoting virulence are established, the significance of ck-RNAi in distinct plant pathogens is not clear. Here, we describe that sRNAs of the pathogen *Hyaloperonospora arabidopsidis*, which represents the kingdom of oomycetes and is phylogenetically distant from fungi, employ the host plant's Argonaute (AGO)/RNA-induced silencing complex for virulence. To demonstrate *H. arabidopsidis* sRNA (*HpasRNA*) functionality in ck-RNAi, we designed a novel CRISPR endoribonuclease Csy4/GUS reporter that enabled in situ visualization of *HpasRNA*-induced target suppression in Arabidopsis. The significant role of *HpasRNAs* together with AtAGO1 in virulence was revealed in plant *atago1* mutants and by transgenic Arabidopsis expressing a short-tandem-target-mimic to block *HpasRNAs*, that both exhibited enhanced resistance. *HpasRNA*-targeted plant genes contributed to host immunity, as Arabidopsis gene knockout mutants displayed quantitatively enhanced susceptibility.

*For correspondence:
a.weiberg@lmu.de

Competing interests: The authors declare that no competing interests exist.

Funding: See page 19

Received: 17 February 2020

Accepted: 21 May 2020

Published: 22 May 2020

Reviewing editor: Axel A Brakhage, Hans Knöll Institute, Germany

© Copyright Dunker et al. This article is distributed under the terms of the [Creative Commons Attribution License](https://creativecommons.org/licenses/by/4.0/), which permits unrestricted use and redistribution provided that the original author and source are credited.

Introduction

Plant small RNAs (sRNAs) regulate gene expression via the Argonaute (AGO)/RNA-induced silencing complex (RISC), which is crucial for tissue development, stress physiology and activating immunity (Chen, 2009; Huang et al., 2016; Khraiwesh et al., 2012). The fungal plant pathogen *Botrytis cinerea*, secretes sRNAs that hijack the plant AGO/RISC in Arabidopsis, and *B. cinerea* sRNAs induce host gene silencing to support virulence (Weiberg et al., 2013), a mechanism known as cross-kingdom RNA interference (ck-RNAi) (Weiberg et al., 2015). In fungal-plant interactions, ck-RNAi is bidirectional, as plant-originated sRNAs are secreted into fungal pathogens and trigger gene silencing of virulence genes (Cai et al., 2018; Zhang et al., 2016). It is currently not known, how important ck-RNAi is for pathogen virulence in general and whether other kingdoms of microbial pathogens, such as oomycetes, transfer sRNAs into hosts to support virulence.

Oomycetes comprise some of the most notorious plant pathogens and belong to the eukaryotic phylum stramenopiles, which diverged from animals, plants and fungi over 1.5 billion years ago (Parfrey et al., 2011). Here, we demonstrate that sRNAs of the downy mildew causing oomycete *Hyaloperonospora arabidopsidis* are associated with the host plant's Arabidopsis thaliana AGO1/

RISC and that these mobile oomycete sRNAs are crucial for virulence by silencing plant host defence genes.

Results

Oomycete sRNAs associate with the plant AGO1

We used the oomycete *Hyaloperonospora arabidopsidis* isolate Noco2 as an inoculum that is virulent on the host plant *A. thaliana* ecotype Col-0 (Knoth et al., 2007). We presumed that *H. arabidopsidis* can produce sRNAs, as sRNA biogenesis genes like RNA-dependent RNA polymerases (RDRs) and Dicer-like (DCL) were discovered in the genome (Bollmann et al., 2016). In order to identify oomycete sRNAs that were expressed during infection and might be transferred into plant cells, we performed two types of sRNA-seq experiments. First, we sequenced sRNAs isolated from total RNA extracts at 4 and 7 days post inoculation (dpi) together with mock-treated plants. Second, we sequenced sRNAs isolated from AtAGO1 immunoprecipitation (AtAGO1-IP) samples to seek for translocated oomycete sRNAs. We chose AtAGO1-IP for sequencing, because AtAGO1 is constitutively expressed and forms the major RISC in Arabidopsis (Vaucheret, 2008), and sRNAs of fungal pathogens were previously found to be associated with AtAGO1 during infection (Wang et al., 2016; Weiberg et al., 2013). An overview of *A. thaliana* and *H. arabidopsidis* sRNA (*HpasRNA*) read numbers identified in all sRNA-seq experiments is given in **Supplementary file 1**. Size profiles of *HpasRNA* reads in total sRNA samples depicted two major peaks of 21 nucleotides (nt) and 25 nt (**Figure 1a**), suggesting that at least two categories of sRNAs occurred in this oomycete species. Similar sRNA size profiles were previously reported for plant pathogenic *Phytophthora* species (Fahlgren et al., 2013; Jia et al., 2017). The identified *HpasRNAs* mapped in different amounts to distinct regions of a *H. arabidopsidis* reference genome including ribosomal RNA (rRNA), transfer RNA (tRNA), small nuclear/nucleolar RNA (snRNA/snoRNA), protein-coding messenger RNA (mRNA, cDNA) and non-annotated regions (**Figure 1—figure supplement 1a**). After filtering out rRNA, tRNA and snRNA/snoRNA reads, *HpasRNAs* mapping to protein-coding genes and non-annotated regions still displayed 21 nt as well as 25 nt size enrichment (**Figure 1—figure supplement 1b**) with 5' terminal uracil (U) enrichment (**Figure 1b**). We also identified *HpasRNA* reads in the AtAGO1-IP sRNA-seq data providing evidence that *HpasRNAs* associated with this host AGO-RISC. The AtAGO1-associated *HpasRNAs* revealed a strong enrichment for 21 nt reads with 5' terminal U preference (**Figure 1c**). AtAGO1 is known to bind preferentially endogenous 21 nt sRNAs with 5' terminal U (Mi et al., 2008), and we confirmed such AtAGO1-binding preference to endogenous Arabidopsis sRNAs in our dataset (**Figure 1—figure supplement 1c**). Therefore, we suspected that *HpasRNAs* bound to AtAGO1 during infection might have the potential to silence plant genes. To follow this line, we focussed on 133 unique *HpasRNA* reads that were present in the sRNA-seq data of total RNAs from infected samples with read counts > 5 reads per million and in at least one read in the AtAGO1-IP sRNA-seq dataset. Among those, 34 *HpasRNAs* were predicted to target as a minimum one *A. thaliana* mRNA with stringent cut-off criteria. Most of the AtAGO1-bound *HpasRNAs* with predicted Arabidopsis target genes mapped to non-annotated, intergenic regions in the *H. arabidopsidis* genome (**Supplementary file 2**). These *HpasRNAs* were found to be enriched in AtAGO1-IP data compared to AtAGO2-IP in an additional comparative AGO-IP sRNA-seq experiment (**Supplementary file 2**).

Two predicted Arabidopsis mRNAs targets of *HpasRNAs* are down-regulated upon infection

In the following assays to investigate the function of *HpasRNAs* in ck-RNAi, we chose the AtAGO1-enriched sRNA candidates *HpasRNA2* and *HpasRNA90*. These two *HpasRNAs* were predicted to target the Arabidopsis *WITH NO LYSINE (K) KINASE (AtWNK)2* and the extracellular protease *APOPLASTIC, ENHANCED DISEASE SUSCEPTIBILITY1-DEPENDENT (AtAED)3*, respectively (**Supplementary file 2**). We focussed on these two *HpasRNAs* and target genes, because *AtWNK2* and *AtAED3* mRNA levels were lower in leaves infected with a virulent *H. arabidopsidis* strain compared to an avirulent in a previous RNA-seq study (Asai et al., 2014), suggesting a negative impact of *H. arabidopsidis* proliferation on target transcript accumulation. Further on, members of the WNK protein family as well as *AtAED3* have been previously linked to plant stress response and immunity,

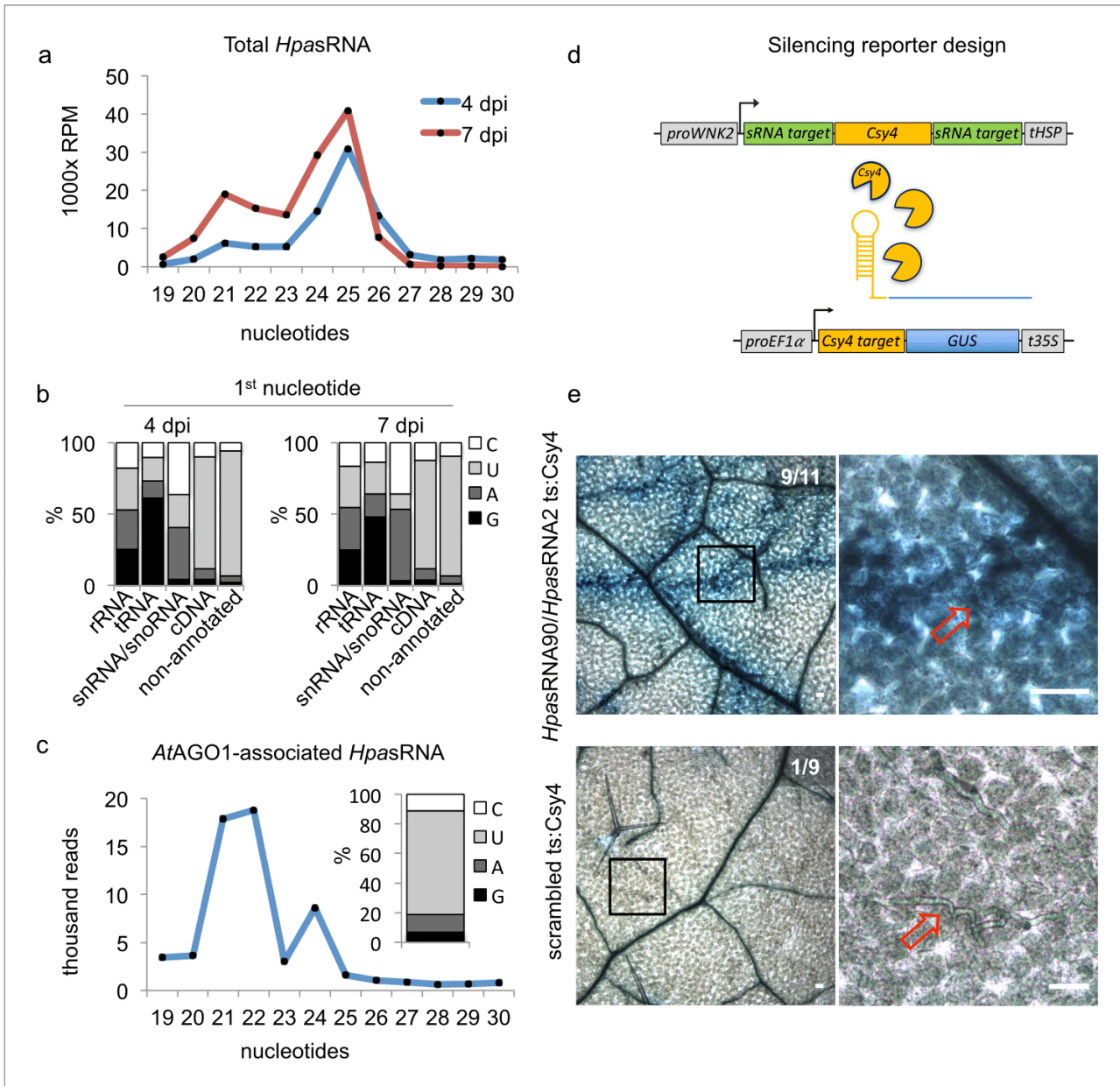


Figure 1. *HpasRNAs* translocated into the plant *AtAGO1* and induced host target silencing in infected plant cells. (a) Size profile of *HpasRNAs* revealed two size peaks at 21 nt and 25 nt at 4 and 7 dpi. (b) The frequency of the first nucleotide at 5' terminal positions of *HpasRNAs* mapping to cDNAs or non-annotated regions revealed bias towards uracil. (c) Size distribution and first nucleotide analysis of *AtAGO1*-associated *HpasRNAs* showed size preference at 21 nt with 5' terminal uracil. (d) A novel *Csy4*/*GUS* reporter construct was assembled to detect *HpasRNA*-directed gene silencing, reporting *GUS* activity if *HpasRNAs* were functional to suppress *Csy4* expression sequence-specificly. (e) *GUS* staining of infected leaves at two magnifications revealed sequence-specific reporter silencing at 4 dpi. *Csy4* with *HpasRNA2* and *HpasRNA90* target sequences (ts) is depicted on the top and with random scrambled ts on the bottom. Red arrows indicate *H. arabidopsidis* hyphae in the higher magnification images. Scale bars indicate 50 μ m. Numbers in the micrographs indicate number of leaves showing *GUS* activity per total leaves inspected.

The online version of this article includes the following figure supplement(s) for figure 1:

Figure supplement 1. Insights into the small RNAome of *H. arabidopsidis* and *Arabidopsis*.

Figure supplement 2. Stem-loop RT-PCR revealed *HpasRNA2*, *HpasRNA30* and *HpasRNA90* expression at 4 and 7 dpi in three biological replicates. *Figure 1 continued on next page*

Figure 1 continued

Figure supplement 3. Relative expression of AtAED3 and AtWNK2 was measured in mock-treated or *H. arabidopsidis* inoculated plants.

Figure supplement 4. 5' RACE PCR did not provide evidence for pathogen sRNA mediated target cleavage.

Figure supplement 5. The reporter was neither activated by an endogenous miRNA target site nor by a distinct pathogen.

respectively (Balakireva and Zamyatnin, 2018; Cao-Pham et al., 2018). We confirmed expression of HpasRNA2 and HpasRNA90 in infected plants at 4 and 7 dpi by stem-loop reverse transcriptase (RT)-PCR (Figure 1—figure supplement 2). We then performed quantitative (q)RT-PCR to measure AtWNK2 and AtAED3 mRNAs expressed in whole seedling leaves of wild type (WT) plants upon *H. arabidopsidis* infection or mock treatment. We used the *atago1-27* mutant as a control line, because we anticipated that target suppression should fail in this mutant. Indeed, AtAED3 was significantly down-regulated upon *H. arabidopsidis* inoculation at 7 dpi, and AtWNK2 expression indicated moderate suppression at 4 dpi in WT plants, when compared to mock-treated plants (Figure 1—figure supplement 3a). Because the down-regulation effects were rather moderate, we repeated this experiment with a second independent *H. arabidopsidis* inoculation that validated the qRT-PCR results (Figure 1—figure supplement 3b). In support of AtAGO1-mediated target silencing through HpasRNAs, WT-like suppression of AtWNK2 and AtAED3 was not observed in the *atago1-27* background (Figure 1—figure supplement 3). However, AtAED3 expression data also indicated down-regulation upon mock treatment during the course of the experiment that might have been caused by the almost 100% relative air humidity during the assay. Moreover, higher transcript levels were measured in *atago1-27* before infection when compared to WT plants.

As Arabidopsis target transcripts displayed expressional down-regulation upon *H. arabidopsidis* infection in WT plants, we wanted to explore, if HpasRNAs guided mRNA slicing of AtWNK2 and AtAED3 through the host AtAGO1/RISC during infection. AtAGO1 possesses RNA cleavage activity on AtmiRNA-guided target mRNAs at the position 10/11 counted from the 5' end of the miRNA (Mallory and Bouché, 2008). We performed 5' rapid amplification of cDNA-ends (RACE)-PCR analysis to determine the 5' ends of target transcripts in RNAs isolated from infected plants pooled from 4 and 7 dpi. We isolated PCR products at the predicted cleavage sizes (Figure 1—figure supplement 4a) for next generation sequencing analysis. In total, we obtained 58,954 and 88,697 reads mapping to AtWNK2 and AtAED3, respectively. However, only a small fraction of reads (639 for AtWNK2 and 17 for AtAED3) mapped at the predicted target sites, while most reads aligned to further 3' downstream regions indicating rapid RNA degradation (Figure 1—figure supplement 4b). The 5' ends that matched to the predicted target sites did not display any predominant peak at the expected cleavage position 10/11, but were rather scattered over the entire target sites (Figure 1—figure supplement 4c). Therefore, RACE-PCR did not support HpasRNA-guided cleavage of the Arabidopsis target mRNAs.

HpasRNAs translocate into Arabidopsis and induce host gene silencing in infected plant cells

To further examine if translocation of HpasRNAs into Arabidopsis was sufficient to induce plant gene silencing during infection, we designed a novel *in situ* silencing reporter. This reporter is based on the CRISPR endonuclease Csy4 that specifically binds to and cleaves a short RNA sequence motif (Haurwitz et al., 2010). We fused this cleavage motif to a β -glucuronidase (GUS) reporter gene to mark it for degradation by Csy4 (Figure 1d). Further on, we cloned the native AtWNK2 and AtAED3 target sequences of HpasRNA2 and HpasRNA90 as flanking tags to the Csy4 coding sequence that turned Csy4 into a target of these HpasRNAs. If HpasRNAs would be capable of silencing effectively the Csy4 transgene, we expected an activation of GUS. Moreover, we constructed control reporters with either a scrambled target sequence or with the binding sequence taken from the endogenous AtmiRNA164 target gene AtCUC2 (Nikovics et al., 2006) instead of the HpasRNA2/HpasRNA90 target sequences. With these control reporters, we intended to test if any HpasRNA2/HpasRNA90-independent suppression of Csy4 or any ck-RNAi-unrelated effect could result in GUS activation. Using the AtmiR164 target site, we anticipated to induce infection-independent local Csy4 silencing, because AtmiR164 expression in young, developing leaves was previously described to be locally restricted to defined regions at the leaf teeth and in the apical meristem (Nikovics et al., 2006). To

simulate *AtWNK2* target mRNA expression level of the *Csy4* reporter transgene, we used a 2 kb-DNA fragment upstream of the *AtWNK2* start codon as a promoter sequence for all reporter constructs.

We transformed the reporter variants into *Arabidopsis* to examine the silencing efficiency of *HpasRNAs* on predicted plant targets upon infection. In each experiment, we tested at least three individual T1 lines per construct, and all plants appeared to be fully compatible with *H. arabidopsidis*. *Csy4* successfully blocked GUS activity in plant cells that were not close to *H. arabidopsidis* infection sites (Figure 1e), providing evidence for functional GUS repression by *Csy4*. Plants expressing *Csy4* transcripts fused to *HpasRNA2* and *HpasRNA90* target sequences highlighted GUS activation along the *H. arabidopsidis* hyphal infection front (Figure 1e). This experiment provided visual insights into the effective plant gene silencing by pathogen sRNAs, and thus let us assume that efficient sRNA translocation from the pathogen into the host cell occurred. GUS activity emerged only around the pathogen hyphae indicating that ck-RNAi did not spread further into distal regions away from primary infection sites. In contrast, *Csy4* linked to a randomly scrambled or *AtmiRNA164* target sequence did not express GUS activation around the *H. arabidopsidis* hyphae (Figure 1e, Figure 1—figure supplement 5a). We concluded that GUS activity induced by *H. arabidopsidis* in plants expressing *Csy4* fused to *HpasRNA2/HpasRNA90* target sites was neither due to target sequence-unspecific regulation of *Csy4* or GUS nor due to pathogen-triggered regulation of the *AtWNK2* promoter. Moreover, reporter plants did also not display any local GUS activity at infection sites when inoculated with the unrelated oomycete pathogen *Phytophthora capsici* (Figure 1—figure supplement 5b). This result further supported that the GUS reporter was activated specifically by *HpasRNAs* and not by infection stress.

Arabidopsis atago1 exhibited enhanced disease resistance against downy mildew

Over one hundred *HpasRNAs* were detected to associate with the plant AGO1/RISC during infection, with 34 *HpasRNAs* being predicted to silence 49 plant targets including stress-related genes (Supplementary file 2). Such *HpasRNAs* can induce host target gene silencing at the infection site (Figure 1e). Based on these observations, we hypothesized that *AtAGO1* was relevant for *H. arabidopsidis* to suppress plant defence genes for infection. To test this hypothesis, we compared the disease outcome of *atago1-27* with WT plants. The *atago1-27* line represents a hypomorphic mutant, and developmental alterations are relatively mild compared to other *atago1* mutant alleles (Morel et al., 2002). Therefore, this *atago1* mutant line was suitable to perform pathogen infection assays. We stained infected leaves with Trypan Blue that visualized *H. arabidopsidis* infection structures and indicated plant cell death using a bright-field light microscope. The *atago1-27* plants exhibited a remarkable change of the disease phenotype by exhibiting dark Trypan Blue-stained host cells around hyphae instead of unstained plant cells colonized with *H. arabidopsidis* haustoria in WT plants (Figure 2a). We interpreted this disease phenotype in *atago1-27* plants as trailing necrosis of plant cells, which has been described for sub-compatible *A. thaliana/H. arabidopsidis* interactions (Coates and Beynon, 2010). Indeed, the trailing necrosis co-occurred with enhanced disease resistance, because *H. arabidopsidis* DNA content was strongly reduced (Figure 2b) and the number of *H. arabidopsidis* conidiospores was significantly lower in *atago1-27* (Figure 2c). Pathogen DNA content was also reduced in *atago1-27* cotyledons (Figure 2—figure supplement 1a) without displaying the trailing necrosis (Figure 2—figure supplement 1b). This reduced disease phenotype was linked to *atago1* mutations, as independent hypomorphic mutant alleles of *atago1-45* and *atago1-46* also displayed trailing necrosis after *H. arabidopsidis* inoculation, albeit to a smaller extent (Figure 2—figure supplement 1c). On the contrary, *atago2-1* and *atago4-2* did neither exhibit trailing necrosis nor reduced oomycete biomass (Figure 2—figure supplement 1d–e). We confirmed that *HpasRNA2* and *HpasRNA90* preferably bound to *AtAGO1* compared to *AtAGO2* by *AtAGO*-IP coupled to stem-loop RT-PCR (Figure 2—figure supplement 2). This result was consistent with the observed reduced disease level in the *atago1* mutant lines in contrast to *atago2-1*.

Taken together, these data strongly suggested that translocated *HpasRNAs* act mainly through *AtAGO1* to suppress plant genes for infection. Nevertheless, increased disease resistance of *atago1* plants could have been caused by impaired function of plant endogenous sRNAs. For instance, *atago1* mutant plants as well as other miRNA pathway mutants, such as *atdcl1*, *athua enhancer(hen) 1 athasty(hst)* or *atserrate(se)* show pleiotropic developmental defects because of impaired plant

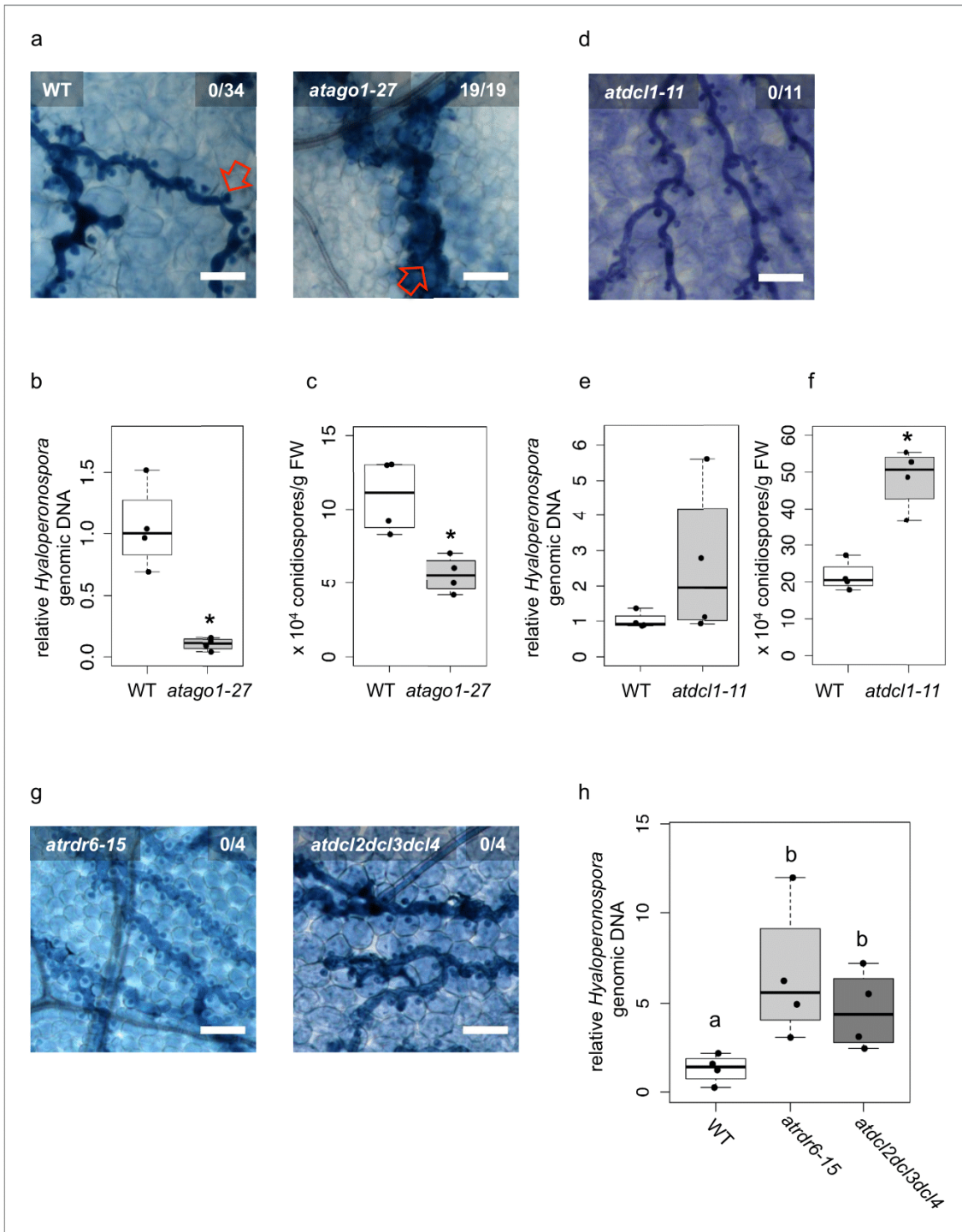


Figure 2. *Arabidopsis atago1* exhibited enhanced disease resistance against *H. arabidopsidis*. (a) Trypan Blue-stained microscopy images showed trailing necrosis around hyphae in *atago1-27*, but no necrosis on WT seedling leaves at 7 dpi. Red arrow in WT marks *H. arabidopsidis* haustorium, red arrow in *atago1-27* indicates trailing necrosis. (b) *H. arabidopsidis* genomic DNA was quantified in *atago1-27* and WT plants by qPCR at 4 dpi relative to plant genomic DNA represented by $n \geq$ four biological replicates. (c) Numbers of conidiospores per gram leaf fresh weight (FW) in *atago1-27* and Figure 2 continued on next page

Figure 2 continued

WT plants at 7 dpi are represented by four biological replicates. (d) Trypan Blue-stained microscopy images of *atdcl1-11* did not show any trailing necrosis at 7 dpi. (e) *H. arabidopsidis* genomic DNA in *atdcl1-11* and WT plants at 4 dpi were in tendency enhanced with $n \geq$ four biological replicates. (f) Number of conidiospores per gram leaf fresh weight (FW) in *atdcl1-11* at 7 dpi was significantly elevated compared to WT plants. (g) Trypan Blue-stained microscopy images of *atrdr6-15* and *atdcl2dcl3dcl4* showed no plant cell necrosis after inoculation with *H. arabidopsidis* at 7 dpi. (h) *H. arabidopsidis* genomic DNA content in leaves was elevated in *atrdr6-15* and *atdcl2dcl3dcl4* compared to WT at 4 dpi with $n \geq$ four biological replicates. Asterisk indicates statistically significant difference by one tailed Student's t-test with $p \leq 0.05$. Letters indicate groups of statistically significant difference by ANOVA followed by TukeyHSD with $p \leq 0.05$. Scale bars in all microscopy images indicate 50 μm and numbers in the micrographs represent observed leaves with necrosis per total inspected leaves.

The online version of this article includes the following figure supplement(s) for figure 2:

Figure supplement 1. Enhanced resistance against infection was restricted to *atago1* mutants.

Figure supplement 2. Stem-loop RT-PCR of *HpasRNAs* from AtAGO1-IP or AtAGO2-IP of mock-treated or *H. arabidopsidis* infected leaf tissue.

Figure supplement 3. Trypan Blue-stained microscopy images presenting the AtmiRNA biogenesis mutants *athst-6*, *athen1-5* and *atse-2* did not show any trailing necrosis at 7 dpi.

Figure supplement 4. Common defence-related marker gene induction was not enhanced in *atago1-27* mutants.

Figure supplement 5. Relative mRNA expression of *AtRBOHD* and *AtRBOHF* determined by qRT-PCR using *AtActin* as reference in WT and *atago1-27* in *H. arabidopsidis* and mock treated plants.

Figure supplement 6. Susceptibility of *atago1* mutants to infection with the biotrophic fungus *E. cruciferarum* and the oomycete *A. laibachii* remained unaltered.

sRNA function (Li and Zhang, 2016; Vaucheret, 2008). To test whether other miRNA pathway mutants also revealed enhanced disease resistance similar to *atago1* plants, we inoculated the *atdcl1-11* mutant line with *H. arabidopsidis*. We did not detect any trailing necrosis or reduced pathogen biomass, but in contrast a significantly increased number of conidiospores (Figure 2d–f) indicating a positive role of *A. thaliana* miRNAs in immune response against *H. arabidopsidis*. These results provided evidence that necrotic trailing and reduced pathogen susceptibility found in *atago1* was not due to the loss of a functional plant miRNA pathway. In support, we did also not observe trailing necrosis upon infection in the *atse-2*, *athen1-5* and *athst-6* mutants (Figure 2—figure supplement 3).

Since *atago1* exhibited trailing necrosis and reduced susceptibility to *H. arabidopsidis*, we wanted to examine if constant activation of defence-related marker genes corresponded with enhanced disease resistance. We profiled gene expression of the *A. thaliana* immunity marker gene *AtPATHOGENESIS-RELATED (PR)1*. *AtPR1* was neither faster nor stronger induced at 6, 12 or 18 h post inoculation in *atago1-27* compared to WT (Figure 2—figure supplement 4a). *AtPR1* and another immunity marker *AtPLANT-DEFENSIN (PDF)1.2* were not higher expressed in *atago1-27* at 1, 4 or 7 dpi compared to WT before or after infection (Figure 2—figure supplement 4b–c). To examine plant gene expression related to induced plant cell death, as observed in *ago1* mutants, we measured transcript levels of the two NADPH oxidases *At REACTIVE BURST OXIDASE HOMOLOG (AtRBOHD)* and *AtRBOHF*. Both genes are required for accumulation of reactive oxygen intermediates to suppress spread of cell death during plant defence (Torres et al., 2005). Moreover, the *atrboh*d and *atrboh*f knockout mutant plants previously revealed increased plant cell death after *H. arabidopsidis* infection and were more resistant against this pathogen (Torres et al., 2002). In consistence, we found that *AtRBOHD* and *AtRBOHF* were induced in WT plants at 7 dpi and were significantly higher expressed than in *atago1-27* (Figure 2—figure supplement 5). These results gave a first hint of a host defence pathway that might be affected due to AtAGO1-associated *HpasRNAs*.

Plant miRNAs can initiate the production of secondary phased siRNAs (phasiRNAs), which negatively control the expression of NLR (NOD-like receptor) class Resistance (R) genes (Li et al., 2012; Shivaprasad et al., 2012). Constitutive expression of NLR genes promotes immune responses such as spontaneous plant cell death resembling a hypersensitive response (Lai and Eulgem, 2018). Therefore, lack of phasiRNAs in *atago1* could cause enhanced expression of NLRs leading to resistance against *H. arabidopsidis*. To examine R gene-based enhanced resistance due to lack of phasiRNAs, we inoculated the *atrdr6-15* and *atdcl2dcl3dcl4* mutants with *H. arabidopsidis* Noco2. The production of phasiRNAs depends on *AtRDR6* and *AtDCL2/AtDCL3/AtDCL4* (Fei et al., 2013). Both mutants did not exhibit trailing necrosis (Figure 2g), but in contrast highlighted increased pathogen biomass upon inoculation with *H. arabidopsidis* (Figure 2h). Higher susceptibility of *atrdr6-15* and

atdcl2dcl3dcl4 to *H. arabidopsis* was also in line with a previous report suggesting a role of Arabidopsis phasiRNAs in silencing of *Phytophthora* genes for host plant defence (Hou et al., 2019).

In order to further explore whether *atago1-27* was more resistant to other biotrophic fungi or oomycetes, we performed infection assays with the powdery mildew fungus *Erysiphe cruciferarum* and the white rust oomycete *Albugo laibachii*. We did not observe any plant cell necrosis in neither pathogen. Moreover, there was neither a reduction in the pustules for *A. laibachii* nor in pathogen biomass of *E. cruciferarum* (Figure 2—figure supplement 6a–d). Taken together, the observed disease resistance of *atago1* plants against *H. arabidopsis* was probably neither based on increased basal plant immunity nor on *R* gene-mediated resistance.

HpasRNAs are crucial for virulence

As we realized that *HpasRNAs* were associated with the host AtAGO1-RISC, silenced plant target genes, and that Arabidopsis *atago1* mutants displayed reduced susceptibility towards *H. arabidopsis* infection, we wanted to understand how important *HpasRNAs* were for *H. arabidopsis* virulence. To shed light on the relevance of *HpasRNAs* for infection, we cloned and expressed a short-tandem-target-mimic (STTM) RNA in Arabidopsis to sequester *HpasRNAs*. The STTM strategy has been previously used to scavenge endogenous plant sRNAs and to prevent gene silencing of native target genes (Tang et al., 2012). We designed a triple STTM transgene to simultaneously bind the pathogen sRNAs *HpasRNA2*, *HpasRNA30*, and *HpasRNA90* by RNA base-pairing. A non-complementary 3-base loop structure at the position 10/11 counted from the 5' end of the *HpasRNAs* was deliberately incorporated to block potential cleavage by plant AGO/RISCs, as previously described (Tang et al., 2012; Figure 3a). We included the AtAGO1-associated *HpasRNA30* in the triple STTM, because it was predicted to silence AtWNK5 (Supplementary file 2), a homolog of AtWNK2, thus we presumed that *HpasRNA30*-induced AtWNK5 suppression might also be important for virulence. The *HpasRNA30* sequence mapped only to the *H. arabidopsis*, but not the Arabidopsis genome, and we detected this *HpasRNA* in infected plants at 4 and 7 dpi by sRNA-seq and stem-loop RT-PCR (Figure 1—figure supplement 2, Supplementary file 2). Remarkably, seven out of eleven individual STTM T1 transgenic lines resembled partially the trailing necrosis phenotype of *atago1* (Figure 3b). We isolated two stable STTM T2 lines (#4, #5). The STTM #4 line showed target de-repression of AtAED3 at 7 dpi and of AtWNK2 at 4 dpi upon *H. arabidopsis* inoculation when compared to plants expressing an empty vector control (Figure 3—figure supplement 1a). These time points corresponded to target gene suppression as found by qRT-PCR analysis before (Figure 1—figure supplement 3). Moreover, both STTM T2 lines exhibited reduced pathogen biomass (Figure 3—figure supplement 1b) and allowed significantly lower production of pathogen conidiospores (Figure 3c). We also cloned STTMs against an rRNA-derived *HpasRNA* as well as against a random scrambled sequence for expression in Arabidopsis. These two types of control STTMs did not exhibit trailing necrosis in at least five independent T1 transgenic lines upon *H. arabidopsis* inoculation (Figure 3d). Furthermore, we also did not observe disease resistance in transgenic plants expressing the STTM against *HpasRNA2/HpasRNA30/HpasRNA90* when inoculated with the unrelated bacterial pathogen *Pseudomonas syringae* DC3000 (Figure 3—figure supplement 1c). These experiments provided evidence that the expression of anti-*HpasRNA* STTMs in Arabidopsis blocked *HpasRNAs* activity that resulted in reduced virulence of *H. arabidopsis*.

Arabidopsis target genes of HpasRNAs contribute to plant defence

Upon uncovering the importance of *HpasRNAs* for virulence, we wanted to assess the contribution of Arabidopsis target genes to plant defence. We obtained three T-DNA insertion lines for the identified target genes AtWNK2 and AtAED3, namely *atwnk2-2*, *atwnk2-3*, and *ataed3-1* (Figure 4—figure supplement 1a). While *atwnk2-2* and *ataed3-1* are two SALK/SAIL lines (Alonso et al., 2003; Sessions et al., 2002) that carry a T-DNA insertion in their coding sequence, respectively, we now re-located the T-DNA insertion of the *atwnk2-3* plant line from the last exon into the 3' UTR, based on sequencing the T-DNA flanking sites (Figure 4—figure supplement 1a). To study infection phenotypes, we stained *H. arabidopsis*-infected leaves with Trypan Blue, and all T-DNA insertion lines resembled pathogen infection structures like in WT plants. However, haustorial density, indicated by the number of haustoria formed per intercellular hyphal distance, was significantly increased in *atwnk2-2* (Figure 4—figure supplement 1b). Intensified haustoria formation was previously

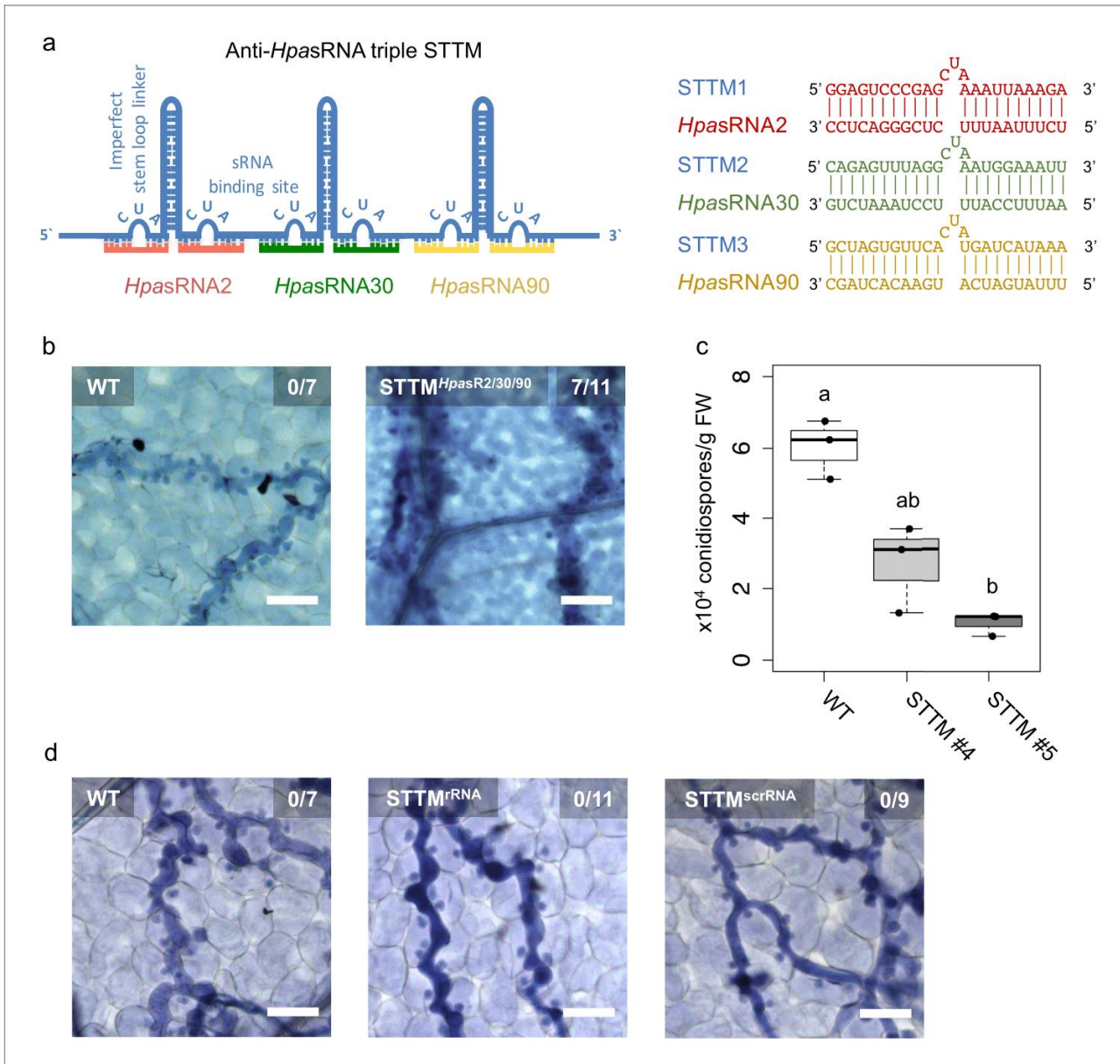


Figure 3. Translocated *HpasRNAs* were crucial for virulence. (a) A triple STTM construct was designed to target the three *HpasRNAs* *HpasRNA2*, *HpasRNA30* and *HpasRNA90* in *Arabidopsis*. (b) *A. thaliana* T1 plants expressing the triple STTM to scavenge *HpasRNA2*, *HpasRNA30* and *HpasRNA90* exhibited trailing necrosis at 7 dpi. (c) Number of conidiospores per gram FW was significantly reduced in two independent STTM-expressing *Arabidopsis* T2 lines (#4, #5) compared to WT. (d) Transgenic *Arabidopsis* plants in T1 expressing a STTM complementary to a rRNA-derived *HpasRNA* (STTM^{RNA}) or to a random scrambled (STTM^{scrRNA}) sequence did not exhibit trailing necrosis at 7 dpi. The scale bars indicate 50 μ m and numbers represent observed leaves with necrosis per total inspected leaves.

The online version of this article includes the following figure supplement(s) for figure 3:

Figure supplement 1. STTM plants revealed higher expression of target genes and lower *H. arabidopsidis* abundance.

interpreted as a sign of enhanced susceptibility in other plant/downy mildew pathogen interactions (Hooftman *et al.*, 2007; Unger *et al.*, 2007). Moreover, the pathogen DNA content was slightly but not significantly increased in *atwnk2-2* and *ataed3-1* compared to WT plants, but this was not the case for *atwnk2-3* (Figure 4a). Nevertheless, a significantly increased number of conidiospores (Figure 4b) and sporangiophores (Figure 4c) was observed in all the tested *atwnk2* and *ataed3* mutant lines upon *H. arabidopsidis* infection compared to WT plants.

We wanted to investigate in more detail the effect of target gene silencing by *HpasRNAs* on plant defence. For this, we cloned *AtWnk2* and *AtAed3* target genes either as native versions or artificially introduced synonymous point mutations in the target sites of *HpasRNAs* to generate the target gene-resistant versions *AtAED3r* and *AtWnk2r* (Figure 4—figure supplement 2). We transformed these gene versions into the respective mutant background *ataed3-1* and *atwnk2-2* expressing them under the control of their native promoters. Transgenic *AtWnk2* and *AtWnk2r* expressing plants reverted from previously described early flowering of *atwnk2-2* (Wang *et al.*, 2008) into the WT phenotype validating successful complementation of *atwnk2-2* (Figure 4—figure supplement 3). If *AtWnk2* and *AtAed3* silencing through *HpasRNA2* or *HpasRNA90* was relevant to plant defence, we would expect that *AtWnk2r* and *AtAed3r* expressing plants become more resistant against *H. arabidopsidis*. Both, the native gene versions and the target site resistant versions, exhibited reduced number of conidiospores compared to T-DNA mutant plants transformed with an empty expression vector, respectively (Figure 4d). To further explore the role of target genes in plant immunity, we attempted to generate overexpression lines of resistant target gene versions by using the strong *Lotus japonicus* *Ubiquitin1* promoter (*proLjUbi1*) (Maekawa *et al.*, 2008). We obtained an overexpressor line of the *AtWnk2r* version (*AtWnk2r-OE*) in the *atwnk2-2* background. These *AtWnk2r-OE* plants showed ectopic cell death in distance from infection sites (Figure 4—figure supplement 4a), as previously described for overexpression lines of other immunity factors, such as *AtBAK1* (Domínguez-Ferreras *et al.*, 2015). Moreover, infection structures frequently displayed aberrant swelling-like structures and extensive branching of hyphae instead of the regular pyriform haustoria formed in *atwnk2-2* (Figure 4—figure supplement 4b), further indicating a role for *AtWnk2* in immune reaction.

To gain more information on the conservation of the 34 identified *AtAGO1*-associated *HpasRNAs* (Supplementary file 2), we analysed RNA sequence diversity using the *H. arabidopsidis* sequenced genomes of the Noco2, Cala2 and Emoy2 isolates (NCBI BioProject IDs: PRJNA298674; PRJNA297499, PRJNA30969). In a complementary approach, we investigated the variation of the 49 predicted plant target sites among 1135 *A. thaliana* genome sequenced accessions published by the 1001 genome project (1001 Genomes Consortium, 2016). Interestingly, all *HpasRNA* were found by BLASTn search in the three *H. arabidopsidis* isolates with only three allelic variations identified in Emoy2 (Figure 4—figure supplement 5a). On the *Arabidopsis* target site, we found single nucleotide polymorphisms (SNPs) and indels in 70% of all target genes (Supplementary file 2), many of those might impair in the predicted *HpasRNA*-induced silencing (Figure 4—figure supplement 5b). Of note, the *HpasRNA2* sequence was deeper conserved in other pathogenic oomycete species, compared to other *HpasRNAs* described in this study (Figure 4—figure supplement 6a). Moreover, the predicted target sites of the pathogen *siR2* homologs lie within a conserved region of other plant *Wnk2* orthologs, with the lowest number of base pair mismatches occurring in the highly-adapted *A. thaliana/H. arabidopsidis* interaction (Figure 4—figure supplement 6b). Whether RNA sequence diversity in *HpasRNAs* and *A. thaliana* target mRNAs drives co-evolution in this co-adapted plant-pathogen system, remains to be further investigated.

Discussion

In this study, we discovered that ck-RNAi happened during *H. arabidopsidis* host infection and contributed to the virulence of this pathogen. Sequencing sRNAs associated with *Arabidopsis* AGO1 revealed at least 34 *HpasRNAs* that entered the host RNAi machinery and potentially targeted multiple plant genes for silencing. These deep sequencing data offered first insights into the *H. arabidopsidis* sRNA transcriptome during host infection. Total read numbers of *AtAGO1*-bound *HpasRNAs* were in the ratio of around 1/1000 compared to *AtAGO1*-bound *Arabidopsis* sRNAs, raising the concern that concentration of pathogen sRNAs might not be sufficient to be functional. Nevertheless, our and other studies found genetic and phenotypic evidence for pathogen oomycete sRNA

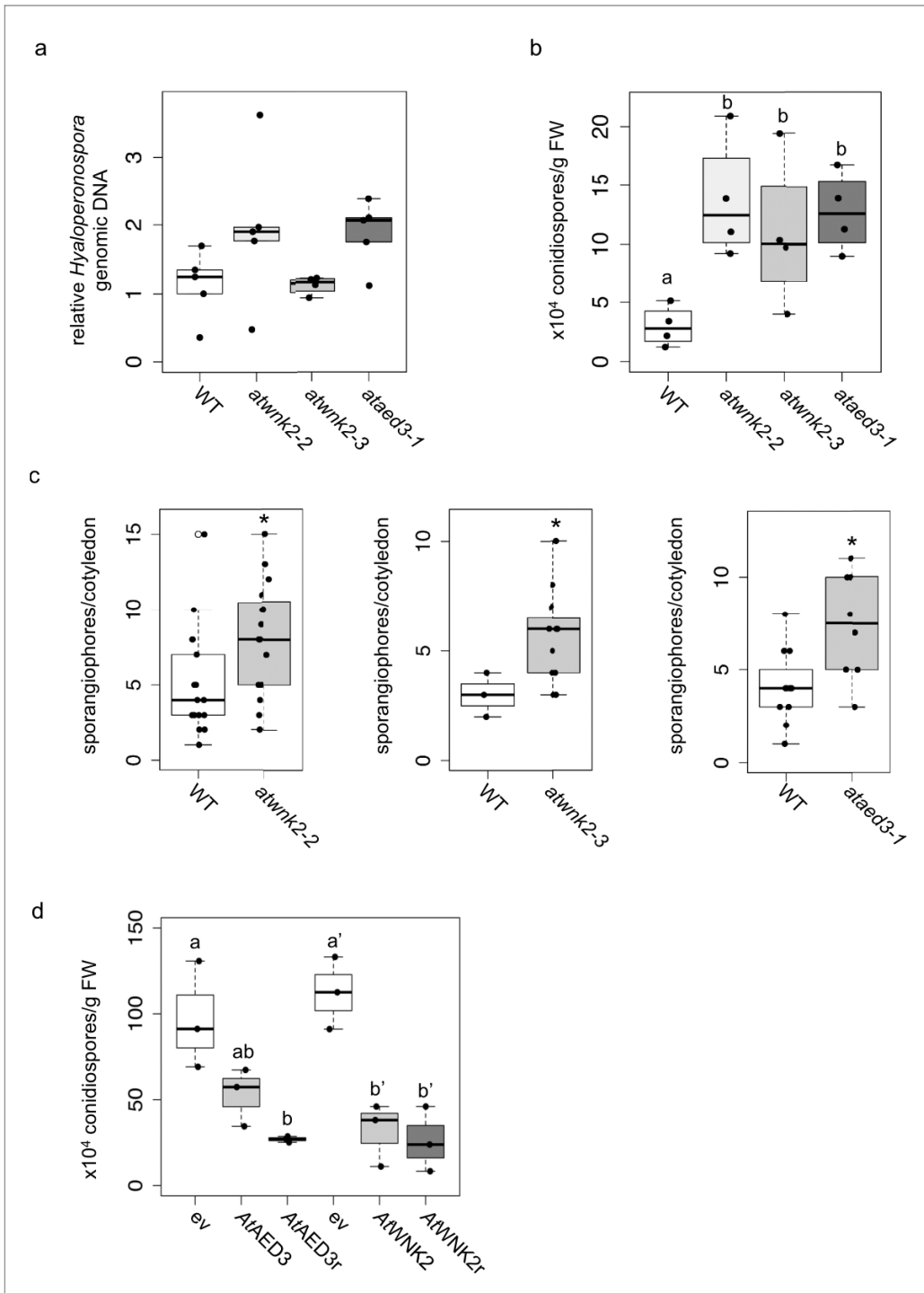


Figure 4. Arabidopsis target genes of *HpasRNAs* contributed to plant defence. (a) *H. arabidopsidis* genomic DNA content in leaves was slightly but not significantly enhanced in *atwnk2-2* and *ataed3-1* compared to WT, but not in *atwnk2-3*, at 4 dpi with $n \geq 4$ biological replicates. (b) T-DNA insertion lines of *HpasRNA* target genes *ataed3-1*, *atwnk2-2*, and *atwnk2-3* showed significantly higher number of sporangiophores per cotyledon upon infection compared to WT at 5 dpi. (c) *ataed3-1*, *atwnk2-2*, and *atwnk2-3* showed significantly higher numbers of conidiospores per gram leaf FW upon infection compared to WT at 5 dpi. (d) *AAWNK2r* showed significantly lower number of conidiospores per gram leaf FW upon infection compared to WT at 5 dpi. *Figure 4 continued on next page*

Figure 4 continued

infection compared to WT at 5 dpi. (d) Number of conidiospores was significantly reduced in gene-complemented mutant lines using the corresponding native promoters *proAtEWNK2* or *proAtAED3* with native gene sequence, *AtAED3* and *AtWNK2*, or with target site resistant versions, *AtAED3r* and *AtWNK2r* compared to the knockout mutant background expressing an empty vector (ev), respectively. Asterisks indicate significant difference by one tailed Student's t-test with $p \leq 0.05$. Letters indicate significant difference by one-site ANOVA test.

The online version of this article includes the following figure supplement(s) for figure 4:

Figure supplement 1. Further details on sRNA target gene mutants.

Figure supplement 2. Target sequence-resistant versions of *AtAED3* (*AtAED3r*) and *AtWNK2* (*AtWNK2r*) were created by introducing synonymous nucleotide substitutions indicated by red letters.

Figure supplement 3. Transgenic *A. thaliana atwnk2-2* was complemented with *proWnk2:Wnk2* or *proWnk2:Wnk2r* that resulted in a WT-like flowering time point, while empty vector (ev) exhibited early flowering phenotype, as reported for *atwnk2-2* (Wang et al., 2008).

Figure supplement 4. *A. thaliana* plants overexpressing *proLjUB1:AtWnk2r* in the *atwnk2-2* background revealed local necrosis without pathogen infection (a) and aberrant hyphae and haustoria swellings (b).

Figure supplement 5. Sequence diversity of *HpasRNAs* and their predicted Arabidopsis target mRNAs.

Figure supplement 6. The pathogen sRNA2 and its target are conserved across different plant pathogenic oomycetes and hosts.

function despite read numbers being in the range of ten per million or lower (Jahan et al., 2015; Qutob et al., 2013). By designing a novel Csy4/GUS repressor reporter system, we demonstrated that *HpasRNAs* have the capacity to translocate into plant cells and suppress host target genes. This new reporter system was capable of visualizing local gene silencing alongside the *H. arabidopsidis* hyphae. Therefore, the relatively small proportion of *HpasRNAs* counted in *AtAGO1* sRNA-seq experiment could be explained by strong dilution with *AtAGO1* molecules purified from non-colonized tissue. For the same reason, we measured moderate *AtWnk2* and *AtAed3* target gene suppression due to dilution effects coming from non-infected leaf lamina.

We assumed that diverse *HpasRNAs* were translocated into Arabidopsis during infection and *AtAGO1* was a major hub of *HpasRNAs*, as detected by *AtAGO1* pull down and sRNA-seq analysis. By which pathways and mechanisms *HpasRNAs* move into plant cells remains an open question. Transport via the extrahaustorial matrix could be a realistic cross-point, as many other biomolecules are exchanged via this route from pathogen to plant cells and vice versa (Judelson and Ah-Fong, 2019). It is noteworthy that accumulation of vesicle-like structures was visualized by electron microscopy at the perahaustorial matrix (Mims et al., 2004). In this regard, transfer of plant sRNAs into pathogen cells via exosomal vesicles was reported to induce ck-RNAi (Cai et al., 2018; Hou et al., 2019), making extracellular vesicles a prime suspect for *HpasRNA* transport into plant cells.

Plant RISC-associated *HpasRNAs* were crucial for successful infection, because transgenic Arabidopsis generated to block the suppressive function of the three candidate *HpasRNA2*, *HpasRNA30* and *HpasRNA90* via STTM target mimics diminished *H. arabidopsidis* virulence. As we identified 34 *AtAGO1*-associated *HpasRNAs* with 49 predicted plant target genes, we suggest that many *HpasRNAs* collaboratively sabotage gene expression of the plant immune response. Such a collaborative function was also suggested for proteinaceous pathogen effectors (Cunnac et al., 2011).

Regarding the role of identified *HpasRNA* target genes in host defence, our data supported quantitative contributions of *AtAed3* and *AtWnk2* to plant immunity. *AtAed3* encodes a putative apoplastic aspartyl protease and has been suggested to be involved in systemic immunity (Breitenbach et al., 2014). *AtWnk2* contributes to flowering time regulation in *A. thaliana*, while other members of the plant WNK family have been linked to the abiotic stress response (Cao-Pham et al., 2018). What is the particular function of these target genes against *H. arabidopsidis* infection and whether these also play a role against other pathogens, still needs to be explored.

The fact that Arabidopsis siRNA biogenesis mutants like *atrd6-15* and *atdcl2dcl3dcl4* displayed increased *H. arabidopsidis* growth is an indication for the important role of secondary phasiRNAs in plant immunity, that was already observed against fungal pathogens like *Verticillium dahliae* and *Magnaporthe oryzae* (Ellendorff et al., 2009; Wagh et al., 2016). This is likely due to the regulatory function of phasiRNAs on endogenous plant immunity genes including the NLRs (Li et al., 2012; Shivaprasad et al., 2012). Two recent studies suggested suppressive roles of secreted plant phasiRNAs in ck-RNAi by silencing fungal *B. cinerea* and oomycete *P. capsici* virulence genes (Cai et al., 2018; Hou et al., 2019). Interestingly, exogenously applied sRNAs targeting the Cellulose synthase 3A gene of *H. arabidopsidis* can lead to pathogen developmental changes and spore germination

inhibition, suggesting functional RNA uptake by this pathogen (Bilir et al., 2019). Together with our data, we think that ck-RNAi in *H. arabidopsidis*/Arabidopsis interaction is bidirectional, as already described in fungal-plant interactions (Cai et al., 2018; Wang et al., 2016).

This study provides evidence that ck-RNAi, originally discovered in the fungal plant pathogen *B. cinerea* (Weiberg et al., 2013), is part of virulence in the oomycete biotrophic pathogen *H. arabidopsidis*. The phenomenon of plant-pathogen ck-RNAi is further proposed in the cereal fungal pathogens *Puccinia striiformis* (Wang et al., 2017) and *Blumeria graminis* (Kusch et al., 2018). We did not notice any enhanced resistance in an Arabidopsis *atago1* mutant against the biotrophic fungus *E. cruciferarum* and the oomycete *A. laibachii*, making ck-RNAi via AtAGO1 unlikely. Further experiments are needed to rule out any importance of ck-RNAi for virulence of these two pathogens via alternative plant AGO-RISCs. The fungal wheat pathogen *Zymoseptoria tritici* was reported to not induce ck-RNAi (Kettles et al., 2019; Ma et al., 2020), while the corn smut pathogen *Ustilago maydis* has lost its canonical RNAi machinery (Kämper et al., 2006; Laurie et al., 2008). It will be interesting to elucidate why some pathogens have evolved ck-RNAi, while some others not.

Materials and methods

Key resources table

Reagent type (species) or resource	Designation	Source or reference	Identifiers	Additional information
Gene (<i>Arabidopsis thaliana</i>)	AtWNK2	arabidopsis.org	AT3G22420	
Gene (<i>Arabidopsis thaliana</i>)	AtAED3	arabidopsis.org	AT1G09750	
Gene (<i>Arabidopsis thaliana</i>)	AtPR1	arabidopsis.org	AT2G14610	
Gene (<i>Arabidopsis thaliana</i>)	AtPDF1.2	arabidopsis.org	AT5G44420	
Gene (<i>Arabidopsis thaliana</i>)	AtAGO1	arabidopsis.org	AT1G48410	
Gene (<i>Arabidopsis thaliana</i>)	AtAGO2	arabidopsis.org	AT1G31280	
Strain, strain background (<i>Hyaloperonospora arabidopsidis</i>)	Noco2	isolated originally in Norwich, UK		
Strain, strain background (<i>Albugo laibachii</i>)	Nc14	Kemen et al., 2011 DOI: 10.1371/journal.pbio.1001094		
Strain, strain background (<i>Pseudomonas syringae</i> pv <i>tomato</i>)	DC3000	Whalen et al., 1991 DOI: 10.1105/tpc.3.1.49		
Strain, strain background (<i>Phytophthora capsici</i>)	LT263	Hurtado-Gonzales and Lamour, 2009 DOI: 10.1111/j.1365-3059.2009.02059.x		
Genetic reagent (<i>Arabidopsis thaliana</i>)	<i>atago1-27</i>	Morel et al., 2002 PMID:11910010		
Genetic reagent (<i>Arabidopsis thaliana</i>)	<i>atago1-45</i>	Nottingham Arabidopsis stock center (NASC)	N67861	
Genetic reagent (<i>Arabidopsis thaliana</i>)	<i>atago1-46</i>	(Nottingham Arabidopsis stock center (NASC)	N67862	
Genetic reagent (<i>Arabidopsis thaliana</i>)	<i>atago2-1</i>	Takeda et al., 2008 DOI: 10.1093/pcp/pcn043		
Genetic reagent (<i>Arabidopsis thaliana</i>)	<i>atago4-2</i>	Agorio and Vera, 2007 DOI: 10.1093/pcp/pcn043		

Continued on next page

Continued

Reagent type (species) or resource	Designation	Source or reference	Identifiers	Additional information
Genetic reagent (<i>Arabidopsis thaliana</i>)	<i>atdcl1-11</i>	Zhang et al., 2008 DOI: 10.1111/j.1365-3040.2008.01786.x		
Genetic reagent (<i>Arabidopsis thaliana</i>)	<i>atdcl2dcl3dcl4</i>	Deleris et al., 2006 DOI: 10.1126/science.1128214		triple mutant
Genetic reagent (<i>Arabidopsis thaliana</i>)	<i>athen1-5</i>	Vazquez et al., 2004 DOI: 10.1016/j.cub.2004.01.035		
Genetic reagent (<i>Arabidopsis thaliana</i>)	<i>athst-6</i>	Bollman et al., 2003 PMID:12620976		
Genetic reagent (<i>Arabidopsis thaliana</i>)	<i>atrdr6-15</i>	Allen et al., 2004 DOI: 10.1038/ng1478		
Genetic reagent (<i>Arabidopsis thaliana</i>)	<i>atse-2</i>	Grigg et al., 2005 DOI: 10.1038/nature04052		
Genetic reagent (<i>Arabidopsis thaliana</i>)	<i>proAGO2:HA-AGO2</i>	Montgomery et al., 2008 DOI: 10.1016/j.cell.2008.02.033		
Genetic reagent (<i>Arabidopsis thaliana</i>)	<i>atwnk2-2</i> (SALK_121042)	Nottingham Arabidopsis stock center (NASC)	N663846	
Genetic reagent (<i>Arabidopsis thaliana</i>)	<i>atwnk2-3</i> (SALK_206118)	Nottingham Arabidopsis stock center (NASC)	N695550	
Genetic reagent (<i>Arabidopsis thaliana</i>)	<i>ataed3-1</i> (SAIL_722_G02C1)	Nottingham Arabidopsis stock center (NASC)	N867202	
Genetic reagent (<i>Arabidopsis thaliana</i>)	<i>proLjUBI:STTMHasR2:STTMHasR30:STTMHasR90</i>	this study		stable triple STTM overexpressor line (maintained in the Weiberg lab)
Genetic reagent (<i>Arabidopsis thaliana</i>)	<i>proAtWNK2:HasRNA2/90ts:Csy4:HasRNA2/90ts; proEF1:Csy4ts:GUS</i>	this study		stable silencing reporter line (maintained in the Weiberg lab)
Genetic reagent (<i>Arabidopsis thaliana</i>)	<i>proAtWNK2:AtmiR164ts:Csy4:AtmiR164ts; proEF1:Csy4ts:GUS</i>	this study		stable silencing reporter line (maintained in the Weiberg lab)
Genetic reagent (<i>Arabidopsis thaliana</i>)	<i>proAtWNK2:scrambled:Csy4:scrambled; proEF1:Csy4ts:GUS</i>	this study		stable silencing reporter line (maintained in the Weiberg lab)
Genetic reagent (<i>Arabidopsis thaliana</i>)	<i>atwnk2-2</i> (<i>proAtWNK2:AtWNK2-GFP</i>)	this study		stable <i>WNK2</i> complementation line (maintained in the Weiberg lab)
Genetic reagent (<i>Arabidopsis thaliana</i>)	<i>atwnk2-2</i> (<i>proAtWNK2:AtWNK2r-GFP</i>)	this study		stable, sRNA resistant <i>WNK2</i> complementation line (maintained in the Weiberg lab)
Genetic reagent (<i>Arabidopsis thaliana</i>)	<i>atwnk2-2</i> (<i>proAtWNK2:GFP</i>)	this study		stable plant line as empty vector control (maintained in the Weiberg lab)
Genetic reagent (<i>Arabidopsis thaliana</i>)	<i>ataed3-1</i> (<i>proAtAED3:AtAED3-GFP</i>)	this study		stable <i>AED3</i> complementation line (maintained in the Weiberg lab)
Genetic reagent (<i>Arabidopsis thaliana</i>)	<i>ataed3-1</i> (<i>proAtAED3:AtAED3r-GFP</i>)	this study		stable, sRNA resistant <i>AED3</i> complementation line (maintained in the Weiberg lab)
Genetic reagent (<i>Arabidopsis thaliana</i>)	<i>ataed3-1</i> (<i>proAtAED3:GFP</i>)	this study		stable plant line as empty vector control (maintained in the Weiberg lab)

Continued on next page

Continued

Reagent type (species) or resource	Designation	Source or reference	Identifiers	Additional information
Antibody	anti-AtAGO1 (rabbit polyclonal)	Agrisera	AS09 527; RRID:AB_2224930	IP(1 µg antibody/g tissue), WB (1:4000)
Antibody	anti-HA (3F10; rat monoclonal)	Roche Diagnostics	Sigma-Aldrich (11867423001); RRID:AB_2314622	IP(0.1 µg antibody/g tissue), WB (1:1000)
Antibody	anti-HA (12CA5; mouse monoclonal)	provided by Dr. Michael Boshart		IP(0.1 µg antibody/g tissue), WB (1:1000), available in the Boshart lab (LMU Munich)
Antibody	anti-mouse IRdye800 (goat polyclonal)	Li-Cor	926-32210; RRID:AB_2782998	secondary antibody WB (1:15000)
Antibody	anti-rat IRdye800 (goat polyclonal)	Li-Cor	926-32219; RRID:AB_1850025	secondary antibody WB (1:15000)
Antibody	anti-rabbit IRdye800 (goat polyclonal)	Li-Cor	926-32211; RRID:AB_621843	secondary antibody WB (1:3000)
Commercial assay or kit	NEBNext Multiplex Small RNA Library Prep Set for Illumina	New England Biolabs (NEB)	NEB: E7300	
Commercial assay or kit	5'/3' RACE Kit, 2nd Generation	Roche Diagnostics	Sigma-Aldrich: 03353621001	
Commercial assay or kit	sparQ DNA Library Prep Kit	Quantabio	vwr.com (95191-024)	
Software, algorithm	Galaxy Server	<i>Giardine et al., 2005</i>		hosted by the Gene Center Munich

Plant material

Arabidopsis thaliana (L.) seedlings were grown on soil under long day conditions (16 hr light/8 hr dark, 22°C, 60% relative humidity). The *atago1-27*, *atago1-45*, *atago1-46*, *atago2-1*, *atago4-2*, *athst-6*, *athen1-5*, *atse-2*, *atdcl1-11*, *atdcl2dcl3dcl4*, *atrd6-15*, and *proAGO2:HA-AGO2* mutant lines (all in the Col-0 background) were described previously (Agorio and Vera, 2007; Allen et al., 2004; Bollman et al., 2003; Deleris et al., 2006; Grigg et al., 2005; Morel et al., 2002; Smith et al., 2009; Takeda et al., 2008; Vazquez et al., 2004; Zhang et al., 2008; Montgomery et al., 2008). The *atwnk2-2* (SALK_121042, [Wang et al., 2008]), *atwnk2-3* (SALK_206118) and *ataed3-1* (SAIL_722_G02C1) lines were verified for the T-DNA insertion by PCR on genomic DNA.

Hyaloperonospora arabidopsidis inoculation

Hyaloperonospora arabidopsidis (GÄUM.) isolate Noco2 was maintained on Col-0 plants. Plant inoculation was performed using $2\text{--}2.5 \times 10^4$ spores/ml and inoculated plants were incubated as described previously (Ried et al., 2019). For *atwnk2-2*, *atwnk2-3*, and *ataed3-1* pathogen assays inoculum strength was reduced to 1×10^4 spores/ml.

Albugo laibachii (THINES and Y.J. CHOI) inoculation

Plants were grown in short-day conditions (10 hr light, 22°C, 65% humidity/14 hr dark, 16°C, 60% humidity, photon flux density $40 \mu\text{mol m}^{-2} \text{s}^{-1}$) and inoculated at the age of six weeks. *A. laibachii* (isolate Nc14; [Kemen et al., 2011]) zoospores obtained from propagation on *Arabidopsis* accession Ws-0 were suspended in water (10^5 spores ml^{-1}) and incubated on ice for 30 min. The spore suspension was filtered through Miracloth (Calbiochem, San Diego, CA, USA) and sprayed onto the plants using a spray gun (~700 µl/plant). Plants were incubated at 8°C in a cold room in the dark overnight. Inoculated plants were kept under 10 hr light/14 hr dark cycles with a 20°C day and 16°C night temperature. Infection rates were determined at 21 dpi for 12 individuals per WT and mutants by visual infection intensity.

Powdery mildew inoculation

Erysiphe cruciferarum (OPIZ EX L. JUNELL) was maintained on highly susceptible Col-0 *phytoalexin deficient (pad)4* mutants in a growth chamber at 22°C, a 10 hr photoperiod with 150 $\mu\text{mol m}^{-2}\text{s}^{-1}$, and 60% relative humidity. For pathogen assays 6 week-old Arabidopsis plants were inoculated with *E. cruciferarum* in a density of 3–5 spores mm^{-2} and replaced under the same conditions.

Pseudomonas pathogen assay

Pseudomonas syringae pv. *tomato* DC3000 was streaked from a freezer stock onto LB agar plates with Rifampicin. A single colony was used for inoculation of an overnight culture in liquid LB with Rifampicin. *Pseudomonas* was resuspended in 10 mM MgCl_2 and bacteria concentration was adjusted to $\text{OD}_{600} = 0.0002$. 5–6 week-old Arabidopsis grown under short day conditions were leaf infiltrated using a needleless syringe, dried for 2 h and incubated under long day conditions. At 3 dpi, three leaf discs per plant ($\text{Ø}=0.6$ cm) were harvested and homogenized in 10 mM MgCl_2 for one biological replicate. Bacteria populations were counted as colony forming units using a serial dilution spotted on LB agar plates with Rifampicin.

Phytophthora capsici (LEONIAN) inoculation

Phytophthora capsici LT263 (Hurtado-Gonzales and Lamour, 2009) was maintained on rye agar plates (Caten and Jinks, 1968). Agar plugs from fresh mycelium ($\text{Ø}=0.4$ cm) were placed on leaves of 5–6 week-old Arabidopsis plants grown under short day conditions. After 24 hr, plugs were removed and leaves were taken for GUS staining at 48 and 72 hpi.

Trypan Blue staining

Infected leaves were stained with Trypan Blue as described previously (Koch and Slusarenko, 1990). Microscopic images were taken with a DFC450 CCD-Camera (Leica) on a CTR 6000 microscope (Leica Microsystems).

GUS staining

Infected leaves were vacuum-infiltrated with GUS staining solution (0.625 mg ml^{-1} X-Gluc, 100 mM phosphate buffer pH 7.0, 5 mM EDTA pH 7.0, 0.5 mM $\text{K}_3[\text{Fe}(\text{CN})_6]$, 0.5 mM $\text{K}_4[\text{Fe}(\text{CN})_6]$, 0.1% Triton X-100) and incubated overnight at 37°C. Leaves were de-stained with 70% ethanol overnight and microscopic images were taken with the same microscopy set up as Trypan Blue stained samples.

Pathogen quantification

H. arabidopsidis spores were harvested at 7 dpi into 2 ml of water. The spore concentration was determined using a haemocytometer (Neubauer improved, Marienfeld). The sporangioaphore number was counted on detached cotyledons using a binocular. For biomass estimation, genomic DNA was isolated using the CTAB method followed by chloroform extraction and isopropanol precipitation (Chen and Ronald, 1999). Four leaves were pooled for one biological replicate and isolated DNA was diluted to a concentration of 5 $\text{ng } \mu\text{l}^{-1}$. *H. arabidopsidis* and *A. thaliana* genomic DNA was quantified by qPCR on a qPCR cycler (CFX96, Bio-Rad) using SYBR Green (Invitrogen, Thermo Fischer Scientific) and GoTaq G2 Polymerase (Promega) using species-specific primers (Supplementary file 3). Relative DNA content was calculated using the $2^{-\Delta\Delta\text{Ct}}$ method (Livak and Schmittgen, 2001).

A. thaliana gene expression analysis

Total RNA was isolated using a CTAB-based method (Bemm et al., 2016). Genomic DNA was removed using DNase I (Sigma-Aldrich) and cDNA synthesis was performed with 1 μg total RNA using SuperScriptIII RT or Maxima H⁻ RT (Thermo Fisher Scientific). Gene expression was measured by qPCR using a qPCR cycler (Quantstudio5, Thermo Fisher Scientific) and Prismaquant low ROX qPCR master mix (Steinbrenner Laborsysteme). Differential expression was calculated using the $2^{-\Delta\Delta\text{Ct}}$ method (Livak and Schmittgen, 2001).

Generation of transgene expression vectors

Plasmids for Arabidopsis transformation were constructed using the plant Golden Gate based toolkit (Binder *et al.*, 2014). The coding sequences of AtWNK2 and AtAED3 were amplified by PCR from Arabidopsis cDNA, and silent mutations were introduced by PCR in the target sequence of HpasRNA2 and HpasRNA90, respectively. For overexpression, AtWNK2r was ligated into a binary expression vector with a C-terminal GFP tag under the control of the LjUBQ1 promoter. AtWNK2r and AtAED3r were also ligated into a binary expression vector with a C-terminal GFP tag under the control of their native promoters (~2 kb upstream of the translation start site). Promoter function was tested by fusion to 2xGFP-NLS and fluorescence microscopy of transiently transformed *Nicotiana benthamiana* leaves. STTM sequences were designed as described previously (Tang *et al.*, 2012), and flanks with BsaI recognition sites were introduced. STTM sequences were synthesized as single stranded DNA oligonucleotides (Sigma Aldrich). The strands were end phosphorylated by T4 polynucleotide kinase (NEB), annealed, and cloned into an expression vector under the control of the pro35S. The final vector with STTMs for HpasRNA2, HpasRNA30, and HpasRNA90 in a row after each other, a rRNA-derived HpasRNA, or a scrambled sequence was assembled, respectively. The coding sequence of Csy4 was synthesized (MWG Eurofins) with codon optimization for expression in plants. Cloned Csy4 was flanked with new overhangs for integration in the Golden Gate toolkit by PCR. A fusion of the target sequences of HpasRNA2 and HpasRNA90, the target sequence of AtmiRNA164a, a scrambled target site, and the target sequence of Csy4 were synthesized as single strands (Sigma Aldrich). The strands were end phosphorylated by T4 polynucleotide kinase (NEB) and annealed. Csy4 was flanked with the respective target sequences and ligated into a vector under the control of the AtWNK2 promoter by BsaI cut ligation. For the reporter, a Csy4 target sequence was inserted between the Kozak sequence and the start codon of the GUS gene and ligated into a vector under the control of the AtEF1 α promoter. The final binary expression vector was assembled by combination of the Csy4 and the GUS vectors by BpiI cut ligation. All cloning primers are listed in [Supplementary file 3](#).

Generation of transgenic Arabidopsis plants

Arabidopsis plants of Col-0 (WT), *atwnk2-2*, and *ataed3-1* were transformed with the respective construct using the *Agrobacterium tumefaciens* strain AGL1 by the floral dip method (Clough and Bent, 1998). Transformed plants were selected on 1/2 MS + 1% sucrose agar plates containing 50 μ g/ml kanamycin, and were subsequently transferred to soil. Experiments were carried out on T1 generation plants representing independent transformants, unless a transformation line number is indicated (e.g. STTM #4). These experiments were carried out using T2 plants.

AGO Western blot analysis and sRNA co-immunopurification

SRNAs bound to *A. thaliana* AGO1 or HA-tagged AtAGO2 were co-immunopurified (co-IPed) from native proteins without any cross-linking agent and isolated as described previously, with minor modifications (Zhao *et al.*, 2012). In brief, 5 g infected leaf tissue were ground in liquid N₂ to fine powder and thawed in 20 ml IP extraction buffer (20 mM Tris-HCl, 300 mM NaCl, 5 mM MgCl₂, 0.5% (v/v) NP40, 5 mM, one tablet/50 ml protease inhibitor (Roche Diagnostics), 200 U RNase inhibitor (RiboLock, Thermo Fisher Scientific)). The cellular debris was removed by centrifugation at 4000 g and 4°C and the supernatant was filtered with two layers of Miracloth (Merck Millipore). 1 μ g α -AGO1 antibody (Agrisera)/g leaf tissue or 0.1 μ g α -HA antibody (3F10, Roche or 12CA5)/g leaf tissue was incubated on a wheel at 4°C for 30 min. Protein pull down and washing was performed using 400 μ l Protein A agarose beads (Roche) as described by Zhao *et al.*, 2012. For Western blot analysis 30% of the co-IP fraction were used, and protein was detected using α -AGO1 antibody (Agrisera) in 1:4000 dilution or α -HA antibody (3F10, Roche or 12CA5) in 1:1000 dilution, respectively. This was followed by an incubation with adequate secondary antibody (α -rabbit IRdye800 (LI-COR, 1:3000 dilution), α -mouse IRdye800 (LI-COR, 1:15000 dilution), and α -rat IRdye800 (LI-COR, 1:15000 dilution)), and protein detection was performed with the Odyssey imaging system (LI-COR). Recovery of the co-IPed sRNAs was achieved as previously described (Carbonell *et al.*, 2012), and was directly used for stem-loop RT-PCR analysis or sRNA library preparation.

Stem-loop RT PCR

SRNAs were detected by stem-loop RT-PCR from 1 µg of total RNA or 5% of the AtAGO co-IPed RNA, as described previously (Varkonyi-Gasic *et al.*, 2007).

5' RACE-PCR

5' RACE-PCR was performed on 1 µg of total RNA isolated from *Hyaloperonospora*-infected Arabidopsis leaves pooled from equal amounts isolated at 4 and 7 dpi, using the 5'/3' RACE Kit, 2nd Generation (Roche Diagnostics). After the first round of PCR, a gel fraction of the expected size was cut out and a nested PCR was carried out on the eluted DNA. Bands were cut out and DNA was eluted using GeneJet Gel Extraction Kit (Thermo Fisher Scientific). A library was constructed from the eluted PCR fragments using the sparQ DNA Library Prep Kit (Quantabio) and sequenced on an Illumina MiSeq platform.

sRNA cloning, sequencing and target gene prediction

SRNAs were isolated from total RNA for high throughput sequencing as previously described (Weiberg *et al.*, 2013). SRNAs were cloned for Illumina sequencing using the Next Small RNA Prep kit (NEB) and sequenced on an Illumina HiSeq1500 platform. The Illumina sequencing data were analysed using the GALAXY Biostar server (Giardine *et al.*, 2005). Raw data were de-multiplexed (Illumina Demultiplex, Galaxy Version 1.0.0) and adapter sequences were removed (Clip adaptor sequence, Galaxy Version 1.0.0). Sequence raw data are deposited at the NCBI SRA server (BioProject accession: PRJNA395139). Reads were then mapped to a master genome of *Hyaloperonospora arabidopsidis* comprising the isolates Emoy2 (BioProject PRJNA30969), Cala2 (BioProject PRJNA297499), Noks1 (BioProject PRJNA298674) using the BOWTIE algorithm (Galaxy Version 1.1.0) allowing zero mismatches (-v 0). Subsequently, reads were cleaned from *Arabidopsis thaliana* sequences (TAIR10 release) with maximal one mismatch. For normalization, ribosomal RNA (rRNA), transfer RNA (tRNA), small nuclear RNAs (snRNAs), and small nucleolar RNA (snoRNA) reads were filtered out using the SortMeRNA program (Galaxy Version 2.1b.1). The remaining reads were counted and normalized on total *H. arabidopsidis* reads per million (RPM). The *Hpas*RNAs were clustered if their 5' end position or 3' end position were within the range of three nucleotides referring to the genomic loci (Weiberg *et al.*, 2013). Target gene prediction of sRNAs was performed with the TAPIR program using a maximal score of 4.5 and a free energy ratio of 0.7 as thresholds (Bonnet *et al.*, 2010). Allelic variation analysis of *Hpas*RNA target sites in *A. thaliana* mRNAs was done at the 1001Polymorph browser (<https://tools.1001genomes.org/polymorph/>).

DNA alignment

Search for homologous sequences of *Hpas*RNA was performed by BLASTn search using the genomes of Noco2 (PRJNA298674), Cala2 (PRJNA297499) and Emoy2 (PRJNA30969), or the Ensembl Protists database (<http://protists.ensembl.org>). Homolog DNA sequences of 100 nucleotides up- and downstream of *SRNA2* homologs were aligned using the CLC Main Workbench package.

Statistical analysis

All statistical tests were carried out using R studio (version 1.0.136, rstudio.com). ANOVA tests were performed on log-transformed data. Letters indicate groups of statistically significant difference by ANOVA followed by TukeyHSD with $p \leq 0.05$. The dashes on the letters imply an independent ANOVA with TukeyHSD per time point.

Acknowledgements

The authors thank Michaela Pagliara for excellent technical assistance, Alexandra Corduneanu for help with data collection of *P. capsici* inoculations, Dr. Martin Parniske for critical reading of the manuscript, inspiring scientific discussions, and support, as well as Christopher Alford for reviewing the manuscript as a native English speaker. We want to thank Dr. Aline Banhara and Fang-Yu Hwu for introducing us into the *H. arabidopsidis*/Arabidopsis pathosystem. We want to thank the Gene Center Munich for Illumina HiSeq sequencing, as well as Gisela Brinkmann and the Genomics Service

Unit of the LMU for Illumina MiSeq service. Seeds used in this study were provided by the Nottingham Arabidopsis Stock Centre (NASC) unless otherwise specified. We thank Dr. Hervé Vaucheret, Dr. James Carrington, and Dr. Steven Jacobsen for kindly providing us seeds of the *atago1-27*, *atdcl2dcl3dcl4*, *atdr6-15*, *atse-2*, and *proHA:HA-AGO2* mutants and Dr. Tino Köster for the *atdcl1-11* mutant. We thank Dr. Michael Boshart for providing us α HA (12CA5) antibody. We thank Dr. David Chiasson and Martin Bircheneder for providing Golden Gate entry plasmids and Dr. Dagmar Hann for providing the *Pst* DC3000 strain. This work was supported by the German Research Foundation (DFG; Grant-ID WE 5707/1–1). The funders had no role in study design, data collection and analysis, decision to publish or in preparation of the manuscript.

Additional information

Funding

Funder	Grant reference number	Author
Deutsche Forschungsgemeinschaft	WE 5707/1-1	Arne Weiberg

The funders had no role in study design, data collection and interpretation, or the decision to submit the work for publication.

Author contributions

Florian Dunker, Conceptualization, Data curation, Formal analysis, Validation, Investigation, Methodology, Writing - original draft, Writing - review and editing; Adriana Trutzenberg, Jan S Rothenpieler, Sarah Kuhn, Formal analysis, Investigation; Reinhard Pröls, Methodology; Tom Schreiber, Alain Tissier, Eric Kemen, Ralph Hüchelhoven, Resources; Ariane Kemen, Formal analysis, Methodology; Arne Weiberg, Conceptualization, Resources, Data curation, Supervision, Funding acquisition, Validation, Investigation, Methodology, Writing - original draft, Project administration, Writing - review and editing

Author ORCIDs

Florian Dunker  <https://orcid.org/0000-0003-1586-412X>
 Jan S Rothenpieler  <http://orcid.org/0000-0001-8892-8230>
 Arne Weiberg  <https://orcid.org/0000-0003-4300-4864>

Decision letter and Author response

Decision letter <https://doi.org/10.7554/eLife.56096.sa1>
 Author response <https://doi.org/10.7554/eLife.56096.sa2>

Additional files

Supplementary files

- Supplementary file 1. sRNA read numbers.
- Supplementary file 2. Predicted *A. thaliana* target genes of *Hpas*RNAs.
- Supplementary file 3. List of oligonucleotides used in this study.
- Transparent reporting form

Data availability

Sequencing data have been deposited in NCBI SRA (PRJNA395139).

The following dataset was generated:

Author(s)	Year	Dataset title	Dataset URL	Database and Identifier
Weiberg A	2017	Arabidopsis thaliana Col-0 infected	https://www.ncbi.nlm.nih.gov/sra/PRJNA395139	NCBI Sequence Read

References

- 1001 Genomes Consortium.** 2016. 1,135 genomes reveal the global pattern of polymorphism in *Arabidopsis thaliana*. *Cell* **166**:481–491. DOI: <https://doi.org/10.1016/j.cell.2016.05.063>, PMID: 27293186
- Agorio A, Vera P.** 2007. ARGONAUTE4 is required for resistance to *Pseudomonas syringae* in *Arabidopsis*. *The Plant Cell* **19**:3778–3790. DOI: <https://doi.org/10.1105/tpc.107.054494>, PMID: 17993621
- Allen E, Xie Z, Gustafson AM, Sung GH, Spatafora JW, Carrington JC.** 2004. Evolution of microRNA genes by inverted duplication of target gene sequences in *Arabidopsis thaliana*. *Nature Genetics* **36**:1282–1290. DOI: <https://doi.org/10.1038/ng1478>, PMID: 15565108
- Alonso JM, Stepanova AN, Leisse TJ, Kim CJ, Chen H, Shinn P, Stevenson DK, Zimmerman J, Barajas P, Cheuk R, Gadrinab C, Heller C, Jeske A, Koesema E, Meyers CC, Parker H, Prednis L, Ansari Y, Choy N, Deen H, et al.** 2003. Genome-wide insertional mutagenesis of *Arabidopsis thaliana*. *Science* **301**:653–657. DOI: <https://doi.org/10.1126/science.1086391>, PMID: 12893945
- Asai S, Rallapalli G, Piquerez SJ, Caillaud MC, Furzer OJ, Ishaque N, Wirthmueller L, Fabro G, Shirasu K, Jones JD.** 2014. Expression profiling during *Arabidopsis*/downy mildew interaction reveals a highly-expressed effector that attenuates responses to salicylic acid. *PLOS Pathog* **10**:e1004443. DOI: <https://doi.org/10.1371/journal.ppat.1004443>, PMID: 25329884
- Balakireva A, Zamyatin A.** 2018. Indispensable role of proteases in plant innate immunity. *International Journal of Molecular Sciences* **19**:629. DOI: <https://doi.org/10.3390/ijms19020629>
- Bemm F, Becker D, Larisch C, Kreuzer I, Escalante-Perez M, Schulze WX, Ankenbrand M, Van de Weyer AL, Krol E, Al-Rasheid KA, Mithöfer A, Weber AP, Schultz J, Hedrich R.** 2016. Venus flytrap carnivorous lifestyle builds on herbivore defense strategies. *Genome Research* **26**:812–825. DOI: <https://doi.org/10.1101/gr.202200.115>, PMID: 27197216
- Bilir Ö, Telli O, Norman C, Budak H, Hong Y, Tör M.** 2019. Small RNA inhibits infection by downy mildew pathogen *Hyaloperonospora arabidopsidis*. *Molecular Plant Pathology* **20**:1523–1534. DOI: <https://doi.org/10.1111/mpp.12863>, PMID: 31557400
- Binder A, Lambert J, Morbitzer R, Popp C, Ott T, Lahaye T, Parniske M.** 2014. A modular plasmid assembly kit for multigene expression, gene silencing and silencing rescue in plants. *PLOS ONE* **9**:e88218. DOI: <https://doi.org/10.1371/journal.pone.0088218>, PMID: 24551083
- Bollman KM, Aukerman MJ, Park MY, Hunter C, Berardini TZ, Poethig RS.** 2003. HASTY, the *Arabidopsis* ortholog of exportin 5/MSN5, regulates phase change and morphogenesis. *Development* **130**:1493–1504. DOI: <https://doi.org/10.1242/dev.00362>, PMID: 12620976
- Bollmann SR, Fang Y, Press CM, Tyler BM, Grünwald NJ.** 2016. Diverse evolutionary trajectories for small RNA biogenesis genes in the oomycete genus *Phytophthora*. *Frontiers in Plant Science* **7**:284. DOI: <https://doi.org/10.3389/fpls.2016.00284>, PMID: 27014308
- Bonnet E, He Y, Billiau K, Van de Peer Y.** 2010. TAPIR, a web server for the prediction of plant microRNA targets, including target mimics. *Bioinformatics* **26**:1566–1568. DOI: <https://doi.org/10.1093/bioinformatics/btq233>, PMID: 20430753
- Breitenbach HH, Wenig M, Wittek F, Jordá L, Maldonado-Alconada AM, Sarioglu H, Colby T, Knappe C, Bichlmeier M, Pabst E, Mackey D, Parker JE, Vlot AC.** 2014. Contrasting roles of the apoplast aspartyl protease APOPLASTIC, ENHANCED DISEASE SUSCEPTIBILITY1-DEPENDENT1 and LEGUME LECTIN-LIKE PROTEIN1 in *Arabidopsis* systemic acquired resistance. *Plant Physiology* **165**:791–809. DOI: <https://doi.org/10.1104/pp.114.239665>, PMID: 24755512
- Cai Q, Qiao L, Wang M, He B, Lin FM, Palmquist J, Huang SD, Jin H.** 2018. Plants send small RNAs in extracellular vesicles to fungal pathogen to silence virulence genes. *Science* **360**:1126–1129. DOI: <https://doi.org/10.1126/science.aar4142>, PMID: 29773668
- Cao-Pham AH, Urano D, Ross-Elliott TJ, Jones AM.** 2018. Nudge-nudge, WNK-WNK (kinases), say no more? *New Phytologist* **220**:35–48. DOI: <https://doi.org/10.1111/nph.15276>, PMID: 29949669
- Carbonell A, Fahlgren N, Garcia-Ruiz H, Gilbert KB, Montgomery TA, Nguyen T, Cuperus JT, Carrington JC.** 2012. Functional analysis of three *Arabidopsis* ARGONAUTES using slicer-defective mutants. *The Plant Cell* **24**:3613–3629. DOI: <https://doi.org/10.1105/tpc.112.099945>, PMID: 23023169
- Caten CE, Jinks JL.** 1968. Spontaneous variability of single isolates of *Phytophthora infestans*. I. Cultural variation. *Canadian Journal of Botany* **46**:329–348. DOI: <https://doi.org/10.1139/b68-055>
- Chen X.** 2009. Small RNAs and their roles in plant development. *Annual Review of Cell and Developmental Biology* **25**:21–44. DOI: <https://doi.org/10.1146/annurev.cellbio.042308.113417>, PMID: 19575669
- Chen D-H, Ronald PC.** 1999. A rapid DNA miniprep method suitable for AFLP and other PCR applications. *Plant Molecular Biology Reporter* **17**:53–57. DOI: <https://doi.org/10.1023/A:1007585532036>
- Clough SJ, Bent AF.** 1998. Floral dip: a simplified method for *Agrobacterium*-mediated transformation of *Arabidopsis thaliana*. *The Plant Journal* **16**:735–743. DOI: <https://doi.org/10.1046/j.1365-313x.1998.00343.x>, PMID: 10069079
- Coates ME, Beynon JL.** 2010. *Hyaloperonospora arabidopsidis* as a pathogen model. *Annual Review of Phytopathology* **48**:329–345. DOI: <https://doi.org/10.1146/annurev-phyto-080508-094422>, PMID: 19400636

- Cunnac S, Chakravarthy S, Kvitko BH, Russell AB, Martin GB, Collmer A. 2011. Genetic disassembly and combinatorial reassembly identify a minimal functional repertoire of type III effectors in *Pseudomonas syringae*. *PNAS* **108**:2975–2980. DOI: <https://doi.org/10.1073/pnas.1013031108>
- Deleris A, Gallego-Bartolome J, Bao J, Kasschau KD, Carrington JC, Voinnet O. 2006. Hierarchical action and inhibition of plant Dicer-like proteins in antiviral defense. *Science* **313**:68–71. DOI: <https://doi.org/10.1126/science.1128214>, PMID: 16741077
- Domínguez-Ferreras A, Kiss-Papp M, Jehle AK, Felix G, Chinchilla D. 2015. An overdose of the Arabidopsis coreceptor BRASSINOSTEROID INSENSITIVE1-ASSOCIATED RECEPTOR KINASE1 or its ectodomain causes autoimmunity in a SUPPRESSOR OF BIR1-1-Dependent manner. *Plant Physiology* **168**:1106–1121. DOI: <https://doi.org/10.1104/pp.15.00537>, PMID: 25944825
- Ellendorff U, Fradin EF, de Jonge R, Thomma BP. 2009. RNA silencing is required for Arabidopsis defence against verticillium wilt disease. *Journal of Experimental Botany* **60**:591–602. DOI: <https://doi.org/10.1093/jxb/ern306>, PMID: 19098131
- Fahlgren N, Bollmann SR, Kasschau KD, Cuperus JT, Press CM, Sullivan CM, Chapman EJ, Hoyer JS, Gilbert KB, Grünwald NJ, Carrington JC. 2013. *Phytophthora* have distinct endogenous small RNA populations that include short interfering and microRNAs. *PLOS ONE* **8**:e77181. DOI: <https://doi.org/10.1371/journal.pone.0077181>, PMID: 24204767
- Fei Q, Xia R, Meyers BC. 2013. Phased, secondary, small interfering RNAs in posttranscriptional regulatory networks. *The Plant Cell* **25**:2400–2415. DOI: <https://doi.org/10.1105/tpc.113.114652>, PMID: 23881411
- Giardine B, Riemer C, Hardison RC, Burhans R, Elnitski L, Shah P, Zhang Y, Blankenberg D, Albert I, Taylor J, Miller W, Kent WJ, Nekrutenko A. 2005. Galaxy: a platform for interactive large-scale genome analysis. *Genome Research* **15**:1451–1455. DOI: <https://doi.org/10.1101/gr.4086505>, PMID: 16169926
- Grigg SP, Canales C, Hay A, Tsiantis M. 2005. SERRATE coordinates shoot meristem function and leaf axial patterning in Arabidopsis. *Nature* **437**:1022–1026. DOI: <https://doi.org/10.1038/nature04052>, PMID: 16222298
- Haurwitz RE, Jinek M, Wiedenheft B, Zhou K, Doudna JA. 2010. Sequence- and structure-specific RNA processing by a CRISPR endonuclease. *Science* **329**:1355–1358. DOI: <https://doi.org/10.1126/science.1192272>, PMID: 20829488
- Hooftman DAP, Nieuwenhuis BPS, Posthuma KI, Oostermeijer JGB, den Nijs HCM. 2007. Introgression potential of downy mildew resistance from lettuce to *Lactuca serriola* and its relevance for plant fitness. *Basic and Applied Ecology* **8**:135–146. DOI: <https://doi.org/10.1016/j.baae.2006.03.008>
- Hou Y, Zhai Y, Feng L, Karimi HZ, Rutter BD, Zeng L, Choi DS, Zhang B, Gu W, Chen X, Ye W, Innes RW, Zhai J, Ma W. 2019. A *Phytophthora* effector suppresses trans-kingdom RNAi to promote disease susceptibility. *Cell Host & Microbe* **25**:153–165. DOI: <https://doi.org/10.1016/j.chom.2018.11.007>, PMID: 30595554
- Huang J, Yang M, Zhang X. 2016. The function of small RNAs in plant biotic stress response. *Journal of Integrative Plant Biology* **58**:312–327. DOI: <https://doi.org/10.1111/jipb.12463>, PMID: 26748943
- Hurtado-Gonzales OP, Lamour KH. 2009. Evidence for inbreeding and apomixis in close crosses of *Phytophthora capsici*. *Plant Pathology* **58**:715–722. DOI: <https://doi.org/10.1111/j.1365-3059.2009.02059.x>
- Jahan SN, Åsman AK, Corcoran P, Fogelqvist J, Vetukuri RR, Dixelius C. 2015. Plant-mediated gene silencing restricts growth of the potato late blight pathogen *Phytophthora infestans*. *Journal of Experimental Botany* **66**:2785–2794. DOI: <https://doi.org/10.1093/jxb/erv094>, PMID: 25788734
- Jia J, Lu W, Zhong C, Zhou R, Xu J, Liu W, Gou X, Wang Q, Yin J, Xu C, Shan W. 2017. The 25–26 nt small RNAs in *Phytophthora parasitica* are associated with efficient silencing of homologous endogenous genes. *Frontiers in Microbiology* **8**:773. DOI: <https://doi.org/10.3389/fmicb.2017.00773>, PMID: 28512457
- Judelson HS, Ah-Fong AMV. 2019. Exchanges at the plant-oomycete interface that influence disease. *Plant Physiology* **179**:1198–1211. DOI: <https://doi.org/10.1104/pp.18.00979>, PMID: 30538168
- Kämper J, Kahmann R, Bölker M, Ma LJ, Brefort T, Saville BJ, Banuett F, Kronstad JW, Gold SE, Müller O, Perlin MH, Wösten HA, de Vries R, Ruiz-Herrera J, Reynaga-Peña CG, Sneltselaar K, McCann M, Pérez-Martín J, Feldbrügge M, Basse CW, et al. 2006. Insights from the genome of the biotrophic fungal plant pathogen *Ustilago maydis*. *Nature* **444**:97–101. DOI: <https://doi.org/10.1038/nature05248>, PMID: 17080091
- Kemen E, Gardiner A, Schultz-Larsen T, Kemen AC, Balmuth AL, Robert-Seilaniantz A, Bailey K, Holub E, Studholme DJ, Maclean D, Jones JD. 2011. Gene gain and loss during evolution of obligate parasitism in the white rust pathogen of *Arabidopsis thaliana*. *PLOS Biology* **9**:e1001094. DOI: <https://doi.org/10.1371/journal.pbio.1001094>, PMID: 21750662
- Kettles GJ, Hofinger BJ, Hu P, Bayon C, Rudd JJ, Balmer D, Courbot M, Hammond-Kosack KE, Scalliet G, Kanyuka K. 2019. sRNA profiling combined with gene function analysis reveals a lack of evidence for cross-kingdom RNAi in the wheat - *Zymoseptoria tritici* pathosystem. *Frontiers in Plant Science* **10**:892. DOI: <https://doi.org/10.3389/fpls.2019.00892>, PMID: 31333714
- Khraiwesh B, Zhu J-K, Zhu J. 2012. Role of miRNAs and siRNAs in biotic and abiotic stress responses of plants. *Biochimica et Biophysica Acta (BBA) - Gene Regulatory Mechanisms* **1819**:137–148. DOI: <https://doi.org/10.1016/j.bbagrm.2011.05.001>
- Knott C, Ringler J, Dangl JL, Eulgem T. 2007. Arabidopsis WRKY70 is required for full RPP4-mediated disease resistance and basal defense against *Hyaloperonospora parasitica*. *Molecular Plant-Microbe Interactions* **20**:120–128. DOI: <https://doi.org/10.1094/MPMI-20-2-0120>, PMID: 17313163
- Koch E, Slusarenko A. 1990. Arabidopsis is susceptible to infection by a downy mildew fungus. *The Plant Cell* **2**:437–445. DOI: <https://doi.org/10.1105/tpc.2.5.437>, PMID: 2152169

- Kusch S, Frantzeskakis L, Thieron H, Panstruga R. 2018. Small RNAs from cereal powdery mildew pathogens may target host plant genes. *Fungal Biology* **122**:1050–1063. DOI: <https://doi.org/10.1016/j.funbio.2018.08.008>, PMID: 30342621
- Lai Y, Eulgem T. 2018. Transcript-level expression control of plant NLR genes. *Molecular Plant Pathology* **19**:1267–1281. DOI: <https://doi.org/10.1111/mpp.12607>, PMID: 28834153
- Laurie JD, Linning R, Bakkeren G. 2008. Hallmarks of RNA silencing are found in the smut fungus *Ustilago hordei* but not in its close relative *Ustilago maydis*. *Current Genetics* **53**:49–58. DOI: <https://doi.org/10.1007/s00294-007-0165-7>, PMID: 18060405
- Li F, Pignatta D, Bendix C, Brunkard JO, Cohn MM, Tung J, Sun H, Kumar P, Baker B. 2012. MicroRNA regulation of plant innate immune receptors. *PNAS* **109**:1790–1795. DOI: <https://doi.org/10.1073/pnas.1118282109>, PMID: 22307647
- Li C, Zhang B. 2016. MicroRNAs in control of plant development. *Journal of Cellular Physiology* **231**:303–313. DOI: <https://doi.org/10.1002/jcp.25125>, PMID: 26248304
- Livak KJ, Schmittgen TD. 2001. Analysis of relative gene expression data using real-time quantitative PCR and the $2^{-\Delta\Delta C_T}$ Method. *Methods* **25**:402–408. DOI: <https://doi.org/10.1006/meth.2001.1262>, PMID: 11846609
- Ma X, Wiedmer J, Palma-Guerrero J. 2020. Small RNA bidirectional crosstalk during the interaction between wheat and *Zymoseptoria tritici*. *Frontiers in Plant Science* **10**:1669. DOI: <https://doi.org/10.3389/fpls.2019.01669>, PMID: 31969895
- Maekawa T, Kusakabe M, Shimoda Y, Sato S, Tabata S, Murooka Y, Hayashi M. 2008. Polyubiquitin promoter-based binary vectors for overexpression and gene silencing in *Lotus japonicus*. *Molecular Plant-Microbe Interactions* **21**:375–382. DOI: <https://doi.org/10.1094/MPMI-21-4-0375>, PMID: 18321183
- Mallory AC, Bouché N. 2008. MicroRNA-directed regulation: to cleave or not to cleave. *Trends in Plant Science* **13**:359–367. DOI: <https://doi.org/10.1016/j.tplants.2008.03.007>, PMID: 18501664
- Mi S, Cai T, Hu Y, Chen Y, Hodges E, Ni F, Wu L, Li S, Zhou H, Long C, Chen S, Hannon GJ, Qi Y. 2008. Sorting of small RNAs into Arabidopsis argonaute complexes is directed by the 5' terminal nucleotide. *Cell* **133**:116–127. DOI: <https://doi.org/10.1016/j.cell.2008.02.034>, PMID: 18342361
- Mims CW, Richardson EA, Holt III BF, Dangl JL. 2004. Ultrastructure of the host–pathogen interface in *Arabidopsis thaliana* leaves infected by the downy mildew *Hyaloperonospora parasitica*. *Canadian Journal of Botany* **82**:1001–1008. DOI: <https://doi.org/10.1139/b04-073>
- Montgomery TA, Howell MD, Cuperus JT, Li D, Hansen JE, Alexander AL, Chapman EJ, Fahlgren N, Allen E, Carrington JC. 2008. Specificity of ARGONAUTE7-miR390 interaction and dual functionality in TAS3 transacting siRNA formation. *Cell* **133**:128–141. DOI: <https://doi.org/10.1016/j.cell.2008.02.033>, PMID: 18342362
- Morel JB, Godon C, Mourrain P, Béclin C, Boutet S, Feuerbach F, Proux F, Vaucheret H. 2002. Fertile hypomorphic ARGONAUTE (*ago1*) mutants impaired in post-transcriptional gene silencing and virus resistance. *The Plant Cell* **14**:629–639. DOI: <https://doi.org/10.1105/tpc.010358>, PMID: 11910010
- Nikovics K, Blein T, Peaucelle A, Ishida T, Morin H, Aida M, Laufs P. 2006. The balance between the MIR164A and CUC2 genes controls leaf margin serration in Arabidopsis. *The Plant Cell* **18**:2929–2945. DOI: <https://doi.org/10.1105/tpc.106.045617>, PMID: 17098808
- Parfrey LW, Lahr DJ, Knoll AH, Katz LA. 2011. Estimating the timing of early eukaryotic diversification with multigene molecular clocks. *PNAS* **108**:13624–13629. DOI: <https://doi.org/10.1073/pnas.1110633108>, PMID: 21810989
- Qutob D, Chapman BP, Gijzen M. 2013. Transgenerational gene silencing causes gain of virulence in a plant pathogen. *Nature Communications* **4**:2354. DOI: <https://doi.org/10.1038/ncomms2354>, PMID: 23322037
- Ried MK, Banhara A, Hwu FY, Binder A, Gust AA, Höfle C, Hükelhoven R, Nürnberger T, Parniske M. 2019. A set of Arabidopsis genes involved in the accommodation of the downy mildew pathogen *Hyaloperonospora arabidopsidis*. *PLOS Pathogens* **15**:e1007747. DOI: <https://doi.org/10.1371/journal.ppat.1007747>, PMID: 31299058
- Sessions A, Burke E, Presting G, Aux G, McElver J, Patton D, Dietrich B, Ho P, Bacwaden J, Ko C, Clarke JD, Cotton D, Bullis D, Snell J, Miguel T, Hutchison D, Kimmerly B, Mitzel T, Katagiri F, Glazebrook J, et al. 2002. A high-throughput Arabidopsis reverse genetics system. *The Plant Cell* **14**:2985–2994. DOI: <https://doi.org/10.1105/tpc.004630>, PMID: 12468722
- Shivaprasad PV, Chen HM, Patel K, Bond DM, Santos BA, Baulcombe DC. 2012. A microRNA superfamily regulates nucleotide binding site-leucine-rich repeats and other mRNAs. *The Plant Cell* **24**:859–874. DOI: <https://doi.org/10.1105/tpc.111.095380>, PMID: 22408077
- Smith MR, Willmann MR, Wu G, Berardini TZ, Möller B, Weijers D, Poethig RS. 2009. Cyclophilin 40 is required for microRNA activity in Arabidopsis. *PNAS* **106**:5424–5429. DOI: <https://doi.org/10.1073/pnas.0812729106>, PMID: 19289849
- Takeda A, Iwasaki S, Watanabe T, Utsumi M, Watanabe Y. 2008. The mechanism selecting the guide strand from small RNA duplexes is different among argonaute proteins. *Plant and Cell Physiology* **49**:493–500. DOI: <https://doi.org/10.1093/pcp/pcn043>, PMID: 18344228
- Tang G, Yan J, Gu Y, Qiao M, Fan R, Mao Y, Tang X. 2012. Construction of short tandem target mimic (STTM) to block the functions of plant and animal microRNAs. *Methods* **58**:118–125. DOI: <https://doi.org/10.1016/j.ymeth.2012.10.006>, PMID: 23098881
- Torres MA, Dangl JL, Jones JD. 2002. Arabidopsis gp91phox homologues *AtrbohD* and *AtrbohF* are required for accumulation of reactive oxygen intermediates in the plant defense response. *PNAS* **99**:517–522. DOI: <https://doi.org/10.1073/pnas.012452499>, PMID: 11756663

- Torres MA, Jones JD, Dangl JL. 2005. Pathogen-induced, NADPH oxidase-derived reactive oxygen intermediates suppress spread of cell death in *Arabidopsis thaliana*. *Nature Genetics* **37**:1130–1134. DOI: <https://doi.org/10.1038/ng1639>, PMID: 16170317
- Unger S, Büche C, Boso S, Kassemeyer HH. 2007. The course of colonization of two different *Vitis* genotypes by *Plasmopara viticola* indicates compatible and incompatible host-pathogen interactions. *Phytopathology* **97**: 780–786. DOI: <https://doi.org/10.1094/PHYTO-97-7-0780>, PMID: 18943926
- Varkonyi-Gasic E, Wu R, Wood M, Walton EF, Hellens RP. 2007. Protocol: a highly sensitive RT-PCR method for detection and quantification of microRNAs. *Plant Methods* **3**:12. DOI: <https://doi.org/10.1186/1746-4811-3-12>, PMID: 17931426
- Vaucheret H. 2008. Plant ARGONAUTES. *Trends in Plant Science* **13**:350–358. DOI: <https://doi.org/10.1016/j.tplants.2008.04.007>, PMID: 18508405
- Vazquez F, Gascioli V, Crété P, Vaucheret H. 2004. The nuclear dsRNA binding protein HYL1 is required for microRNA accumulation and plant development, but not posttranscriptional transgene silencing. *Current Biology* **14**:346–351. DOI: <https://doi.org/10.1016/j.cub.2004.01.035>, PMID: 14972688
- Wagh SG, Alam MM, Kobayashi K, Yaeno T, Yamaoka N, Toriba T, Hirano H-Y, Nishiguchi M. 2016. Analysis of rice RNA-dependent RNA polymerase 6 (OsRDR6) gene in response to viral, bacterial and fungal pathogens. *Journal of General Plant Pathology* **82**:12–17. DOI: <https://doi.org/10.1007/s10327-015-0630-y>
- Wang Y, Liu K, Liao H, Zhuang C, Ma H, Yan X. 2008. The plant WNK gene family and regulation of flowering time in *Arabidopsis*. *Plant Biology* **10**:548–562. DOI: <https://doi.org/10.1111/j.1438-8677.2008.00072.x>, PMID: 18761494
- Wang M, Weiberg A, Lin FM, Thomma BP, Huang HD, Jin H. 2016. Bidirectional cross-kingdom RNAi and fungal uptake of external RNAs confer plant protection. *Nature Plants* **2**:16151. DOI: <https://doi.org/10.1038/nplants.2016.151>, PMID: 27643635
- Wang B, Sun Y, Song N, Zhao M, Liu R, Feng H, Wang X, Kang Z. 2017. Puccinia striiformis f. sp. tritici microRNA-like RNA 1 (Pst-milR1), an important pathogenicity factor of pst, impairs wheat resistance to pst by suppressing the wheat pathogenesis-related 2 gene. *The New Phytologist* **215**:338–350. DOI: <https://doi.org/10.1111/nph.14577>, PMID: 28464281
- Weiberg A, Wang M, Lin FM, Zhao H, Zhang Z, Kaloshian I, Huang HD, Jin H. 2013. Fungal small RNAs suppress plant immunity by hijacking host RNA interference pathways. *Science* **342**:118–123. DOI: <https://doi.org/10.1126/science.1239705>, PMID: 24092744
- Weiberg A, Bellinger M, Jin H. 2015. Conversations between kingdoms: small RNAs. *Current Opinion in Biotechnology* **32**:207–215. DOI: <https://doi.org/10.1016/j.copbio.2014.12.025>, PMID: 25622136
- Whalen MC, Innes RW, Bent AF, Staskawicz BJ. 1991. Identification of *Pseudomonas syringae* pathogens of *Arabidopsis* and a bacterial locus determining avirulence on both *Arabidopsis* and soybean. *The Plant Cell* **3**:49–59. DOI: <https://doi.org/10.1105/tpc.3.1.49>, PMID: 1824334
- Zhang JF, Yuan LJ, Shao Y, Du W, Yan DW, Lu YT. 2008. The disturbance of small RNA pathways enhanced abscisic acid response and multiple stress responses in *Arabidopsis*. *Plant, Cell & Environment* **31**:562–574. DOI: <https://doi.org/10.1111/j.1365-3040.2008.01786.x>, PMID: 18208512
- Zhang T, Zhao YL, Zhao JH, Wang S, Jin Y, Chen ZQ, Fang YY, Hua CL, Ding SW, Guo HS. 2016. Cotton plants export microRNAs to inhibit virulence gene expression in a fungal pathogen. *Nature Plants* **2**:16153. DOI: <https://doi.org/10.1038/nplants.2016.153>, PMID: 27668926
- Zhao H, Lii Y, Zhu P, Jin H. 2012. Isolation and profiling of protein-associated small RNAs. *Methods in Molecular Biology* **883**:165–176. DOI: https://doi.org/10.1007/978-1-61779-839-9_13, PMID: 22589133

Supplementary data:

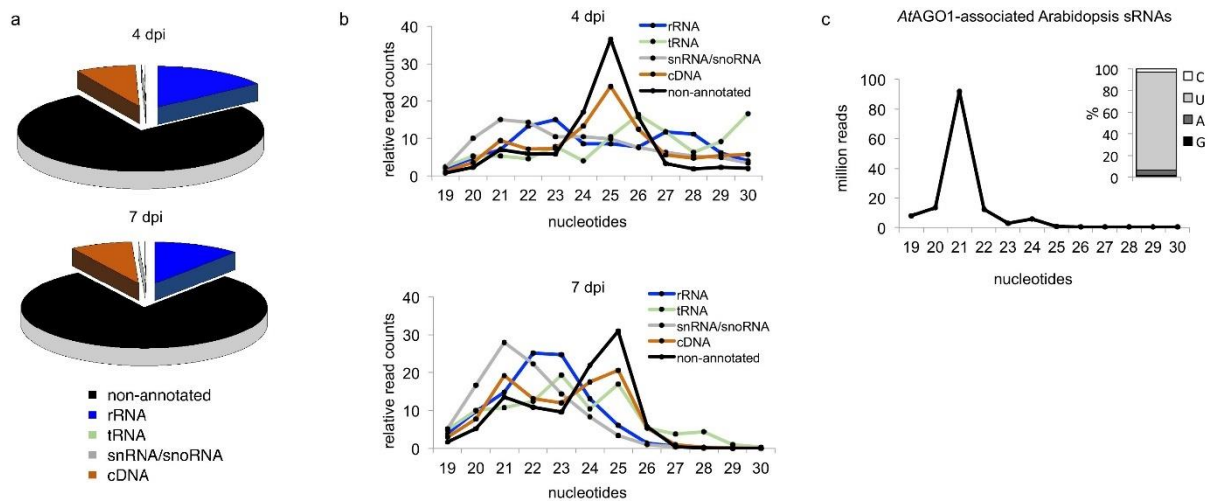


Figure 1 – figure supplement 1

Insights into the small RNAome of *H. arabidopsidis* and *Arabidopsis*.

(a) *HpasRNAs* mapped to distinct coding and to non-coding genomic regions. (b) Relative read counts and size distribution of *HpasRNAs* mapped to different genomic regions at 4 and 7 dpi. (c) Size distribution and first nucleotide analysis of *AtAGO1*-associated sRNAs of *A. thaliana*.

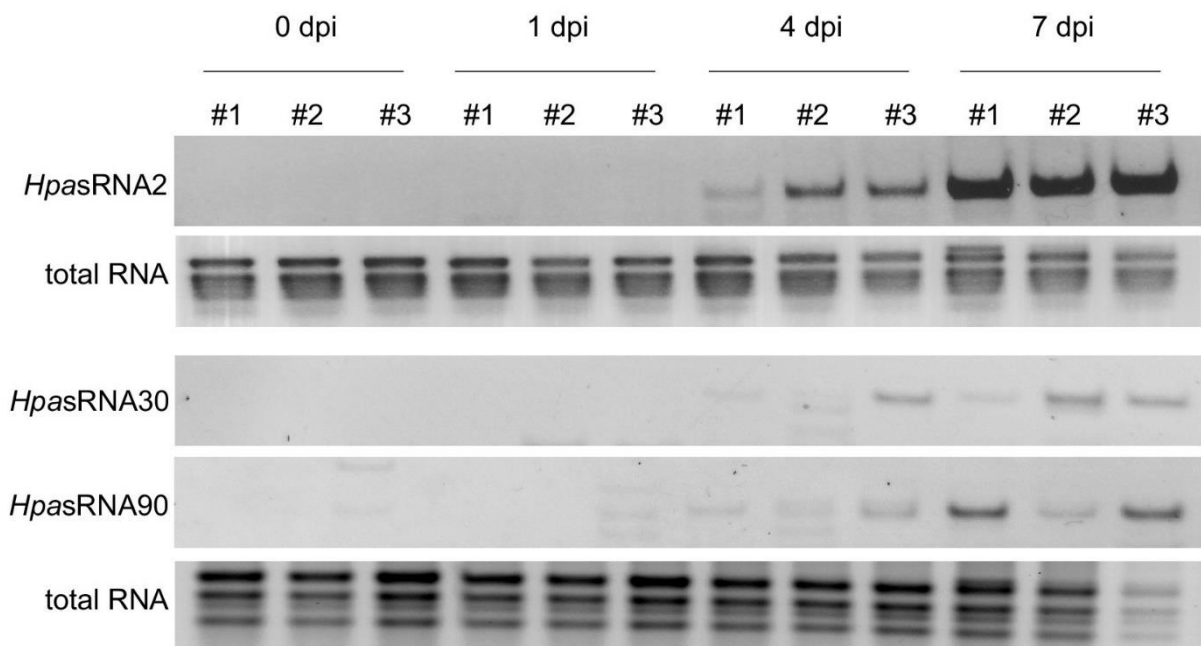


Figure 1 – figure supplement 2

Stem-loop RT-PCR revealed *HpasRNA2*, *HpasRNA30* and *HpasRNA90* expression at 4 and 7 dpi in three biological replicates.

Total RNA served as loading control.

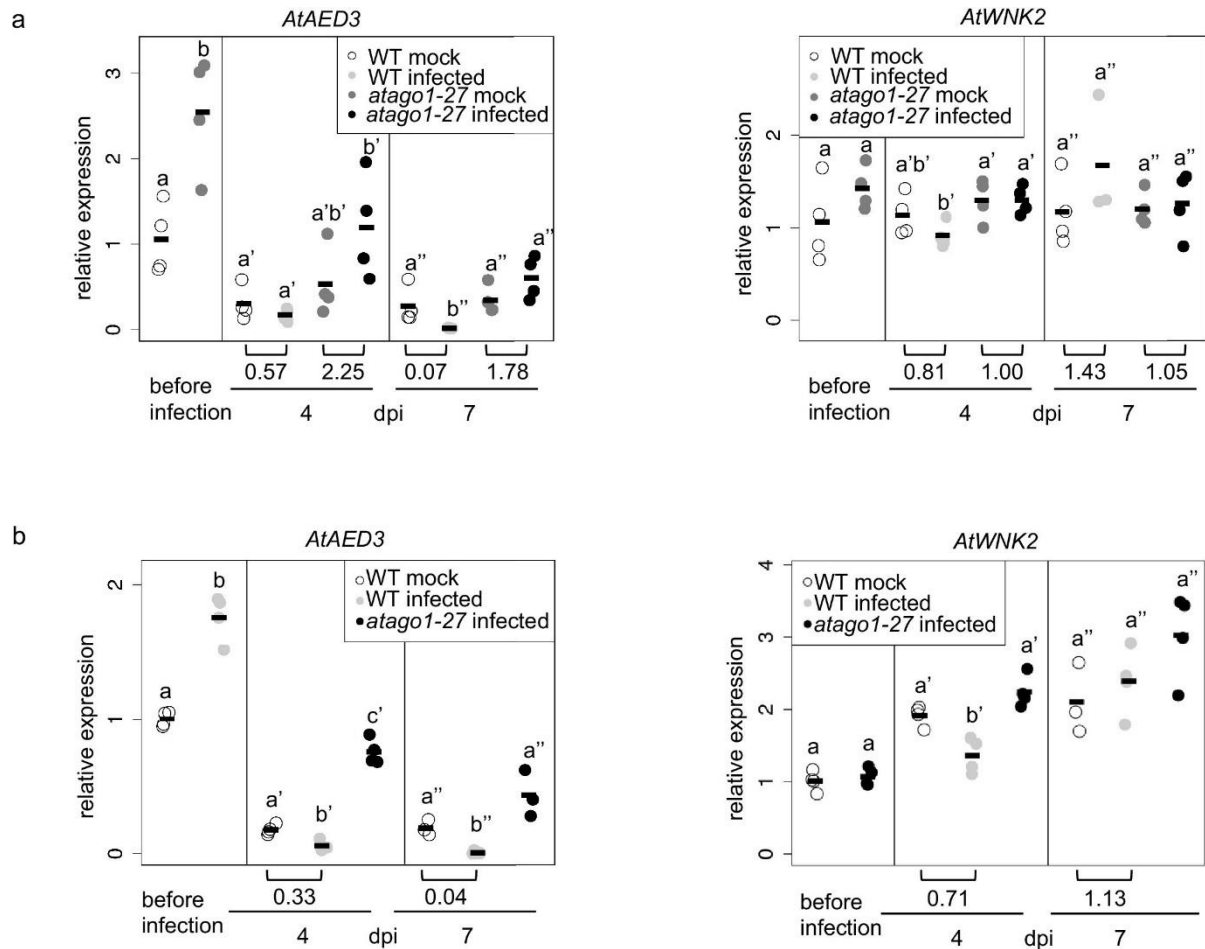


Figure 1 – figure supplement 3

Relative expression of *AtAED3* and *AtWNK2* was measured in mock-treated or *H. arabidopsidis* inoculated plants.

H. arabidopsidis-infected WT and *atago1-27* seedlings before and at 4 and 7 dpi by qRT-PCR using *AtActin* as a reference in two independent infection experiments (a, b). The bars within the graphs represent the average of $n \geq$ three biological replicates, and letters indicate groups of statistically significant difference within one time point by ANOVA followed by TukeyHSD with $p \leq 0.05$. Numbers below the graphs give change-fold factors of *H. arabidopsidis*-infected versus mock-treated samples.

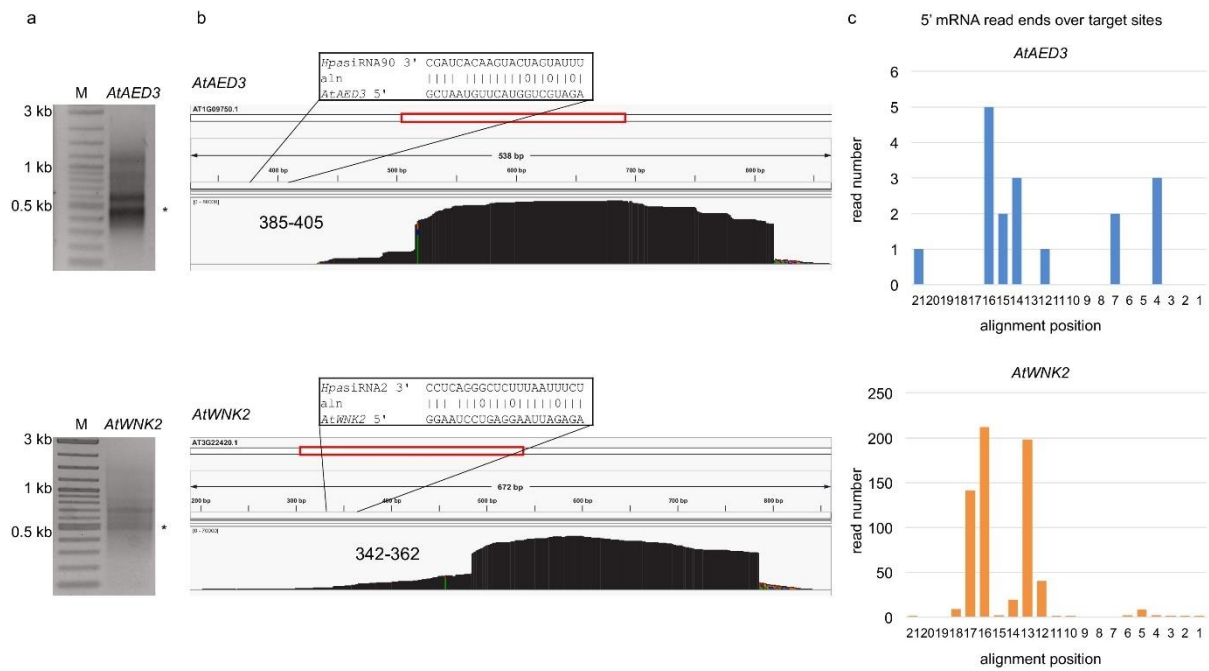
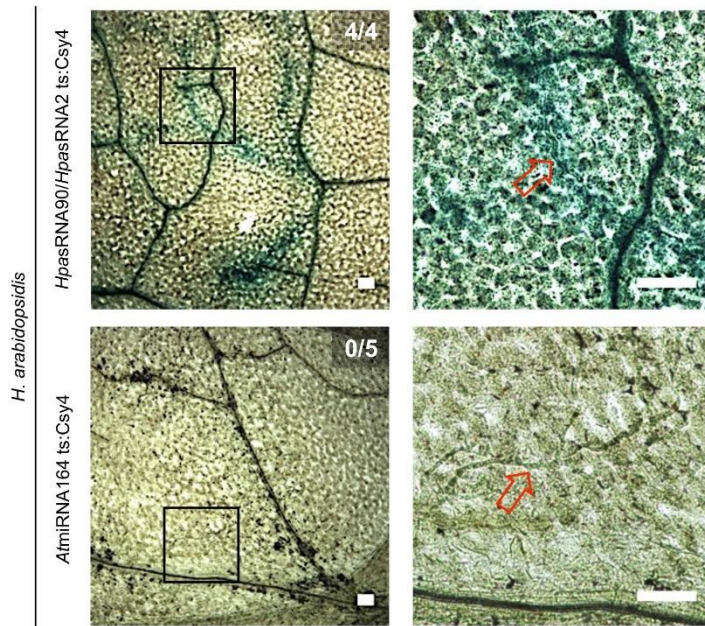


Figure 1 – figure supplement 4

5' RACE PCR did not provide evidence for pathogen sRNA mediated target cleavage.

(a) Agarose gel images show RACE-PCR bands amplified at the predicted cleavage size of 440 bp for *AtAED3* and 530 bp for *AtWNK2*, marked with asterisks. (b) Mapping schemes of *AtWNK2* and *AtAED3* mRNA reads indicated the ends of RACE-PCR fragments corresponding to a as revealed by next generation sequencing. (c) Numbers of 5' end position of *AtWNK2* and *AtAED3* mRNAs at the predicted *HpasRNA2* or *HpasRNA90* target sites.

a



b

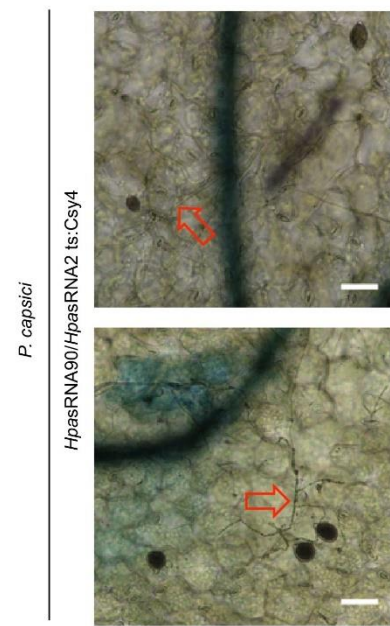


Figure 1 – figure supplement 5

The reporter was neither activated by an endogenous miRNA target site nor by a distinct pathogen.

(a) Csy4 repressor reporter with *HpasRNA2* and *HpasRNA90* target sequence (ts) is depicted on the top and with *AtmiRNA164* ts of the *AtCUC2* target gene on the bottom. GUS staining of infected leaves at two magnifications revealed sequence-specific reporter silencing at 4 dpi in *HpasRNA2/HpasRNA90* ts construct but not in *AtmiRNA164* ts. (b) The Csy4 reporter was not activated by the oomycete pathogen *Phytophthora capsici*. At 2 dpi, *P. capsici* formed a dense hyphal network, but no pathogen-associated GUS activity was observed (upper panel). In two of the five inspected leaf discs GUS activity was detected in cell clusters, but these were independent of pathogen presence (lower panel). The numbers indicate leaves with GUS activity per total inspected leaves in this experiment. Red arrows indicate *H. arabidopsis* or *P. capsici* hyphae. Scale bars indicate 50 μ m.

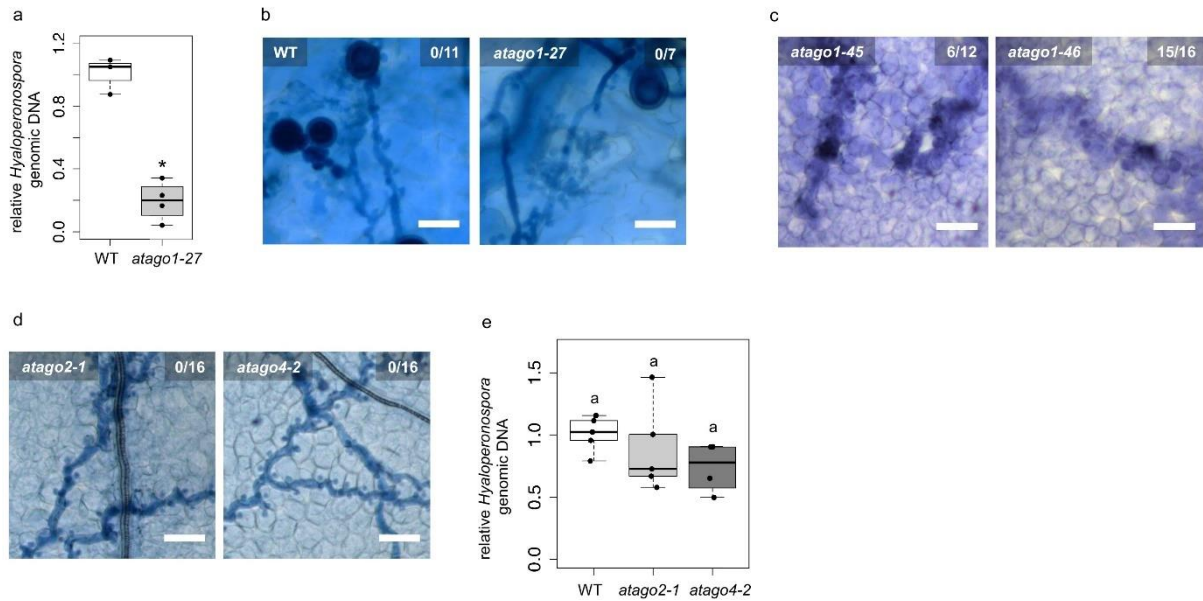


Figure 2 – figure supplement 1

Enhanced resistance against infection was restricted to *atago1* mutants.

(a) *H. arabidopsidis* genomic DNA content in cotyledons was lower in *atago1-27* compared to WT, as measured by qPCR relative to plant genomic DNA at 4 dpi with $n \geq$ three biological replicates. (b) Trypan Blue-stained microscopy images of *atago1-27* cotyledons did not show any necrosis at 7 dpi. (c) Trypan Blue-stained microscopy images of *atago1-45* and *atago1-46* revealed trailing necrosis at 7 dpi with *H. arabidopsidis*. (d) Trypan Blue-stained microscopy images presenting *H. arabidopsidis*-infected *atago2-1* and *atago4-2* seeding leaves at 7 dpi. (e) *H. arabidopsidis* genomic DNA was quantified in WT versus *atago2-1* and *atago4-2* by qPCR at 4 dpi relative to plant genomic DNA represented by $n \geq$ four biological replicates. Numbers in the micrographs represent observed leaves with necrosis per total inspected leaves. Asterisk indicates significant difference by one tailed Student's t-test with $p \leq 0.05$. Letters indicate groups of statistically significant difference by ANOVA followed by TukeyHSD with $p \leq 0.05$.

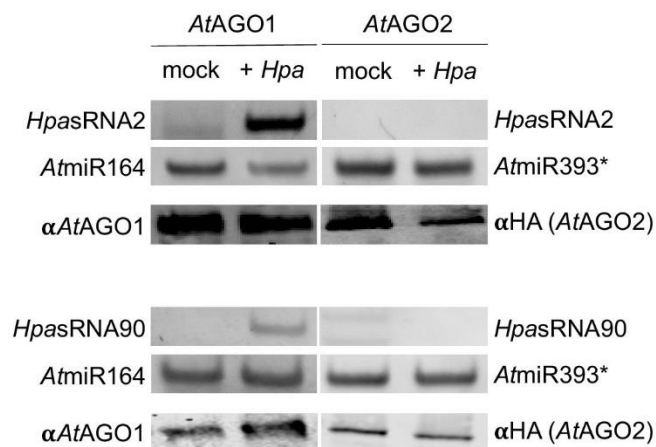


Figure 2 – figure supplement 2

Stem-loop RT-PCR of *HpasRNAs* from *AtAGO1*-IP or *AtAGO2*-IP of mock-treated or *H. arabidopsidis* infected leaf tissue.

AtmiRNA164 and *AtmiRNA393** were used as positive *AtAGO*-IP controls. Pull-down of *AtAGO1* was achieved with WT plants using an *AtAGO1* native antibody, and *AtAGO2* with HA-epitope tagged *AtAGO2*-expressing *A. thaliana* Col-0 using anti-HA antibody with the lower panel showing Western blot analysis.

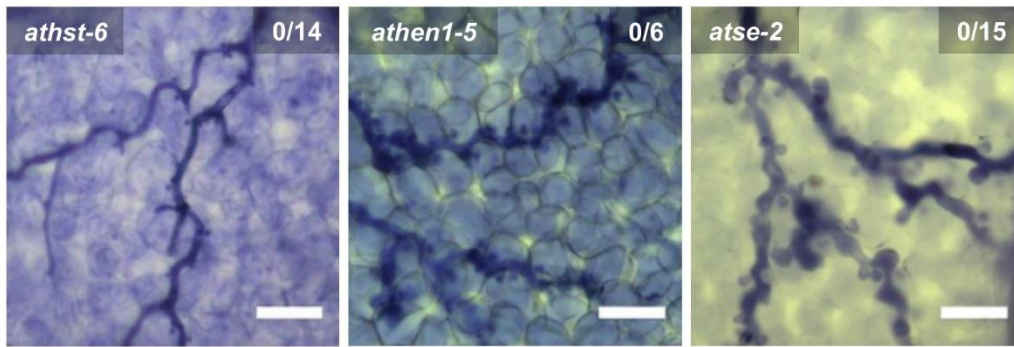


Figure 2 – figure supplement 3

Trypan Blue-stained microscopy images presenting the *At*miRNA biogenesis mutants *athst-6*, *athen1-5* and *atse-2* did not show any trailing necrosis at 7 dpi.

Scale bars in microscopy images indicate 50 μ m and numbers in the micrographs represent observed leaves with necrosis per total inspected leaves.

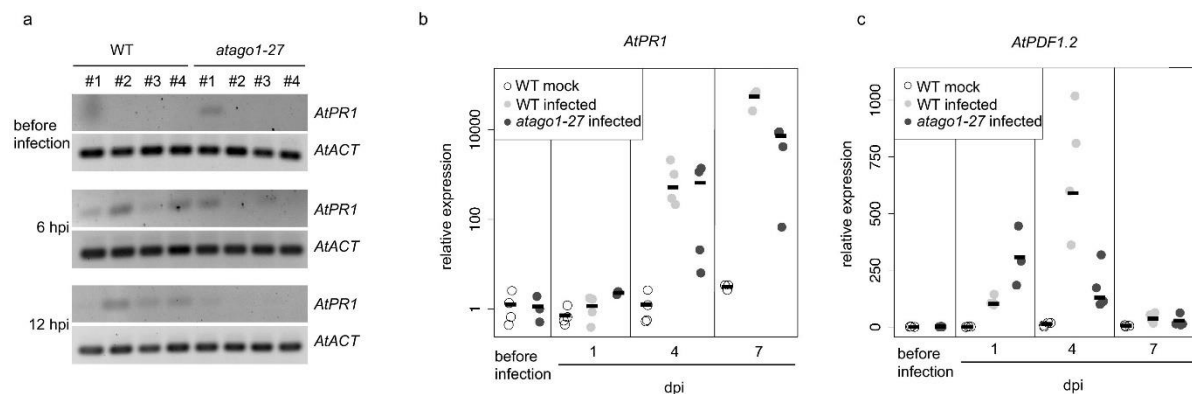


Figure 2 – figure supplement 4

Common defence-related marker gene induction was not enhanced in *atago1-27* mutants.

(a) Expression analysis of *AtPR1* by RT-PCR in WT and *atago1-27* did not show obvious differences at 6 and 12 h post inoculation with *H. arabidopsidis*. *AtActin* was used as reference gene with four biological replicates. (b and c) Relative expression of *AtPR1* and *AtPDF1.2* determined by qRT-PCR using *AtActin* as reference. The bar represents the average of $n \geq$ three biological replicates, each comprising two technical replicates.

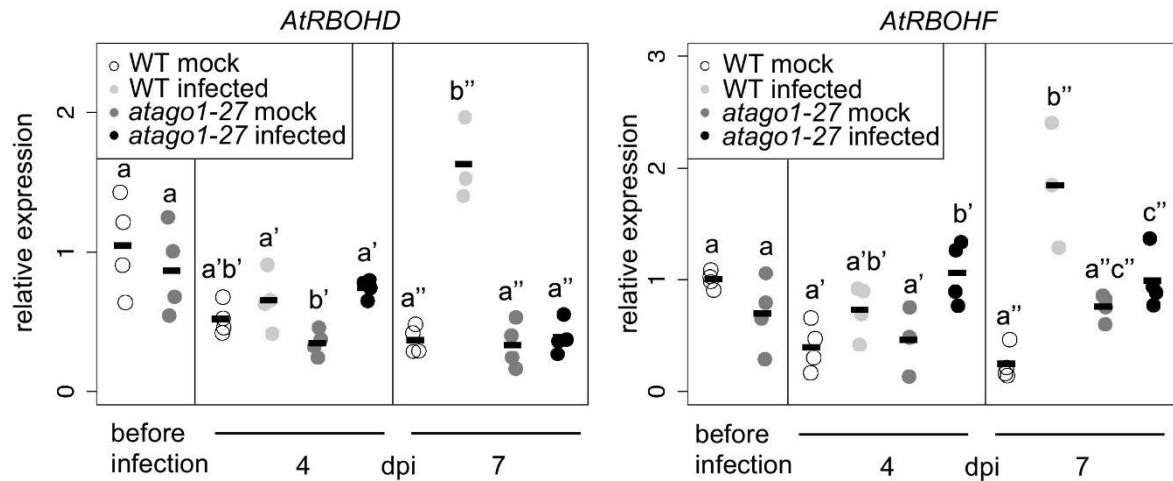


Figure 2 – figure supplement 5

Relative mRNA expression of *AtRBOHD* and *AtRBOHF* determined by qRT-PCR using *AtActin* as reference in WT and *atago1-27* in *H. arabidopsidis* and mock treated plants.

The bars represent the average of $n \geq$ three biological replicates, each comprising two technical replicates. Letters indicate groups of statistically significant difference within one time point by ANOVA followed by TukeyHSD with $p \leq 0.05$.

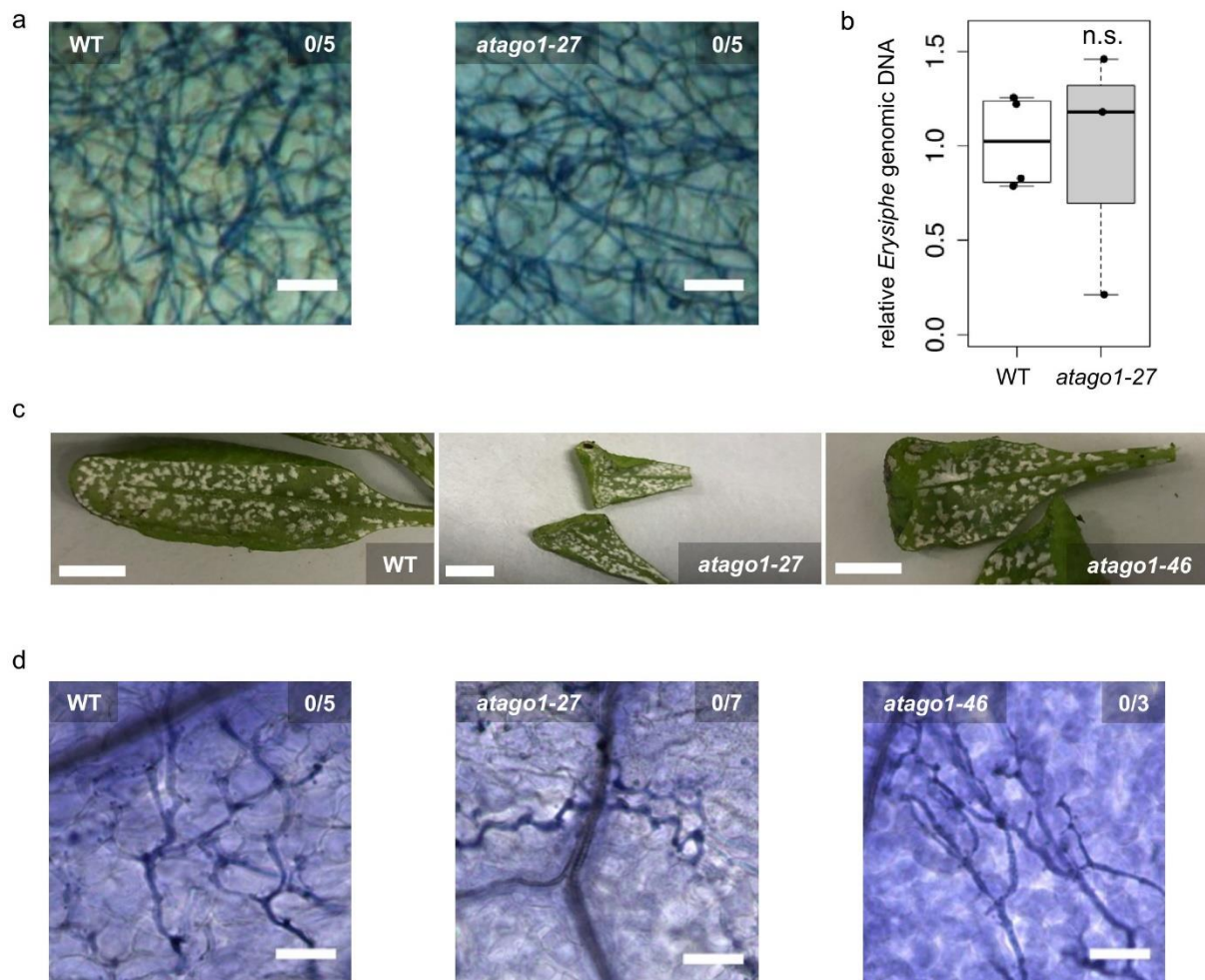


Figure 2 – figure supplement 6

Susceptibility of *atago1* mutants to infection with the biotrophic fungus *E. cruciferarum* and the oomycete *A. laibachii* remained unaltered.

(a) Trypan Blue-stained microscopy images of WT or *atago1-27* leaves infected with *Erysiphe cruciferarum* did not show necrosis at 8 dpi. Scale bars in microscopy images indicate 50 μ m and numbers represent observed leaves with necrosis per total inspected leaves. (b) *E. cruciferarum* genomic DNA content in WT and *atago1-27* was not significantly different at 4 dpi relative to plant genomic DNA as measured by qPCR in $n \geq$ three biological replicates. (c) Macroscopic infection phenotype of the white rust *Albugo laibachii* remained unaltered in *atago1-27* and *atago1-46* mutants at 3 weeks post inoculation. (d) Trypan Blue-stained microscopy images of WT, *atago1-27* or *atago1-46* leaves infected with *A. laibachii* did not show necrosis at 7 dpi. Scale bars in microscopy images indicate 50 μ m and numbers represent observed leaves with necrosis per total inspected leaves. Scale bars in the total leaf pictures indicate 50 mm. Significance was determined by one tailed Student's t-test with $p \leq 0.05$.

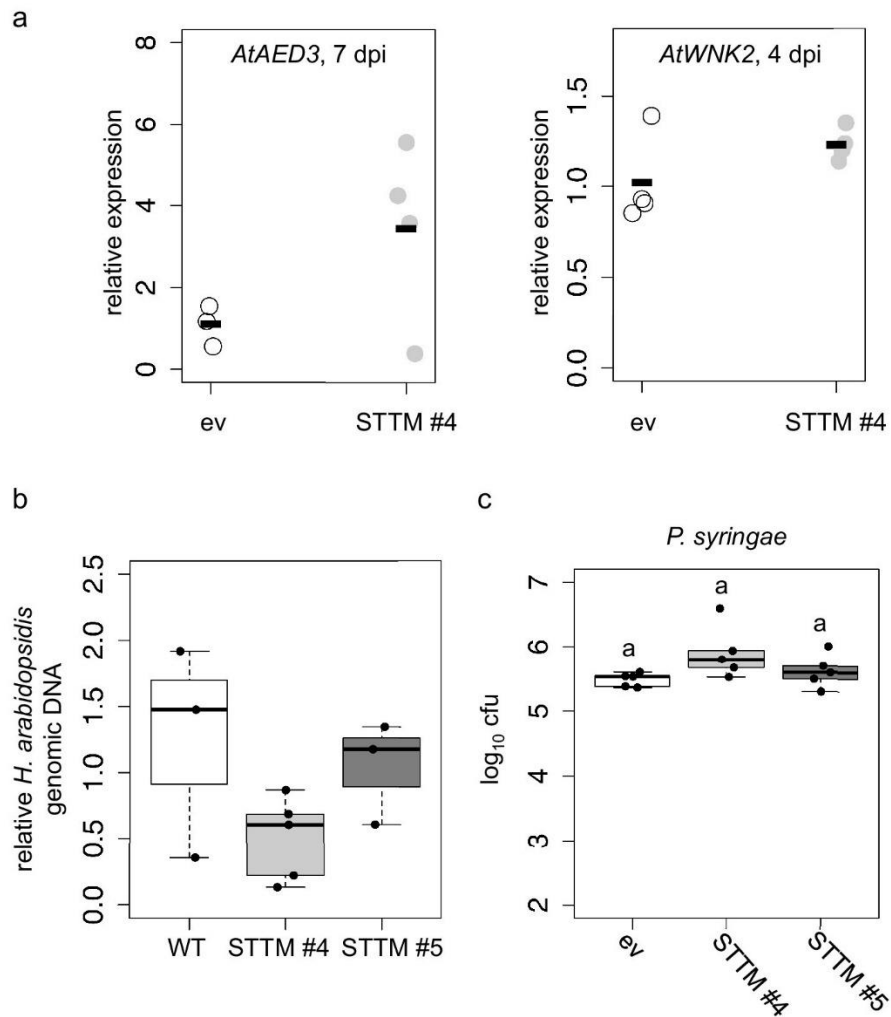


Figure 3 – figure supplement 1

STTM plants revealed higher expression of target genes and lower *H. arabidopsidis* abundance.

(a) Relative expression of *AtAED3* at 7 dpi and *AtWNK2* at 4 dpi was determined for STTM or empty vector (ev) expressing plants upon *H. arabidopsidis* inoculation at 7 and 4 dpi, respectively, by qRT-PCR. One biological replicate represented three leaves, the bars represent the average of $n \geq$ three biological replicates. The differences of the average were not statistically significant as determined by Student's t-test. (b) *H. arabidopsidis* genomic DNA content in leaves was increased in STTM #4 and STTM #5 plants compared to empty vector (ev) expressing WT plants at 4 dpi with $n \geq$ three biological replicates. The differences were not statistically significant as determined by ANOVA followed by TukeyHSD. (c) STTM-expressing Arabidopsis plants did not exhibit increased resistance against bacterial infection. The bacterial growth was determined by counting colony-forming units (cfu) at 3 days post inoculation. One biological replicate represents bacteria from three leaf discs. Letters in c) indicate significant difference ($p \leq 0.05$) according to one site ANOVA followed by TukeyHSD including three biological replicates.

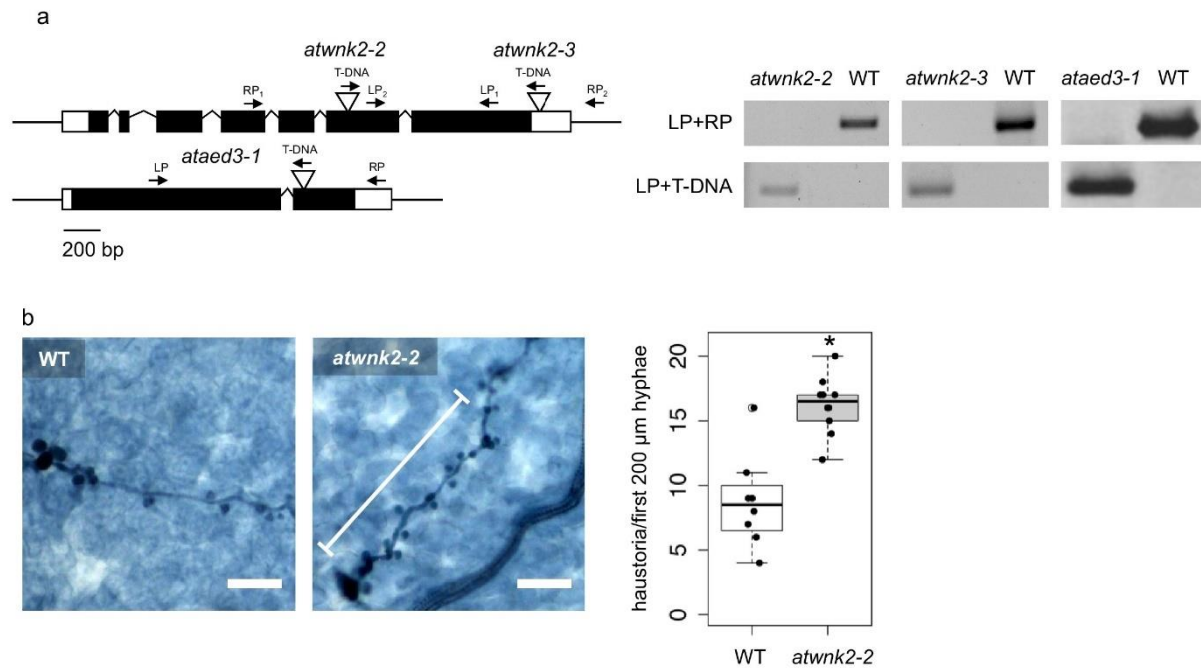


Figure 4 – figure supplement 1

Further details on sRNA target gene mutants.

(a) Gene models of *AtWNK2* and *AtAED3*. The insertion site of the T-DNA is marked by the triangles and the genotyping primer binding sites are shown with arrows. T-DNA insertion of *HpasRNA* target gene mutant lines *atwnk2-2*, *atwnk2-3* and *ataed3-1* were verified by genomic DNA PCR. (b) Trypan Blue-stained microscopy images revealed a higher number of haustoria in the first 200 µm of hyphae (indicated by white bar alongside the hyphae) from the spore germination site in *atwnk2-2* compared to WT with $n \geq$ eight leaves. Asterisk indicates significant difference by one tailed Student's t-test with $p \leq 0.05$. Similar results were obtained in two independent experiments.



Figure 4 – figure supplement 2

Target sequence-resistant versions of *AtAED3* (*AtAED3r*) and *AtWNK2* (*AtWNK2r*) were created by introducing synonymous nucleotide substitutions indicated by red letters.



Figure 4 – figure supplement 3

Transgenic *A. thaliana atwnk2-2* was complemented with *proWNK2:WNK2* or *proWNK2:WNK2r* that resulted in a WT-like flowering time point, while empty vector (ev) exhibited early flowering phenotype, as reported for *atwnk2-2* (Wang et al., 2008).

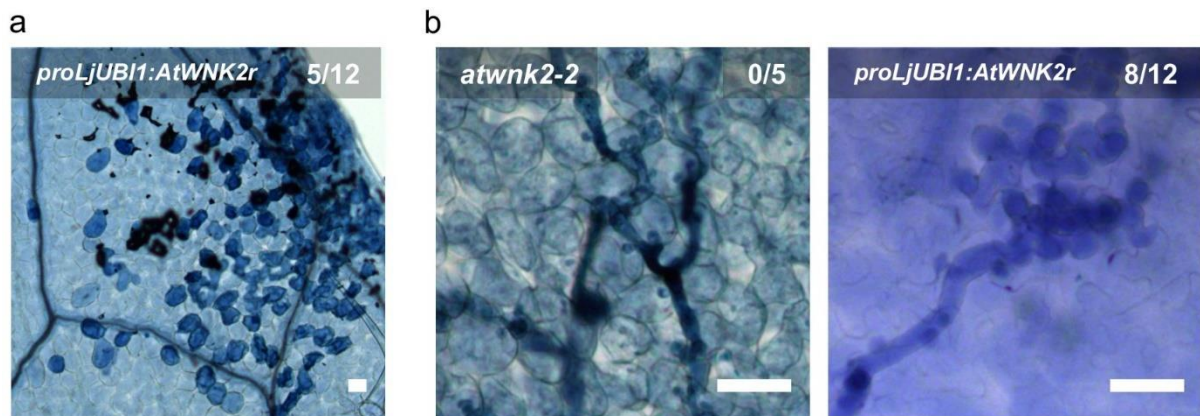


Figure 4 – figure supplement 4

A. thaliana plants overexpressing *proLjUBI1:AtWNK2r* in the *atwnk2-2* background revealed local necrosis without pathogen infection (a) and aberrant hyphae and haustoria swellings (b).

Scale bars in microscopy images indicate 50 μ m and the numbers represent observed leaves with necrosis or swellings respectively per total inspected leaves.

a

	Noco2	Cala2	Emoy2
<i>HpasRNA77</i>			
<i>HpasRNA88</i>			
<i>HpasRNA78</i>			
<i>HpasRNA75</i>			
<i>HpasRNA61</i>			
<i>HpasRNA2</i>			
<i>HpasRNA90</i>			
<i>HpasRNA76</i>			
<i>HpasRNA96</i>			
<i>HpasRNA85</i>			
<i>HpasRNA83</i>			
<i>HpasRNA53</i>			
<i>HpasRNA44</i>			
<i>HpasRNA4</i>			
<i>HpasRNA74</i>			
<i>HpasRNA30</i>			
<i>HpasRNA54</i>			
<i>HpasRNA39</i>			
<i>HpasRNA51</i>			
<i>HpasRNA47</i>			
<i>HpasRNA36</i>			
<i>HpasRNA92</i>			
<i>HpasRNA28</i>			
<i>HpasRNA38</i>			
<i>HpasRNA69</i>			
<i>HpasRNA57</i>			
<i>HpasRNA82</i>			
<i>HpasRNA12</i>			
<i>HpasRNA14</i>			
<i>HpasRNA52</i>			
<i>HpasRNA20</i>			
<i>HpasRNA55</i>			
<i>HpasRNA43</i>			
<i>HpasRNA99</i>			

■ identical □ allelic variation

b

<i>HpasRNA</i>	Target gene	Locus	Mutation location/ consequence			Number of <i>A. thaliana</i> accessions with mutation
			Bulge	10/11	Seed region	
<i>HpasRNA2</i>	With no lysine (K) kinase 2	CDS		Synony.		1
<i>HpasRNA12</i>	AAR2 protein family	3' UTR				3
<i>HpasRNA28</i>	E3 ubiquitin ligase	5' UTR				4
<i>HpasRNA28</i>	BTB/POZ domain-containing protein	CDS		Missense		1
<i>HpasRNA30</i>	Polymerase gamma 2	CDS			Synony.	339
<i>HpasRNA39</i>	Heat stress transcription factor A-1d	CDS			Missense	409
<i>HpasRNA47</i>	Transcription factor ORG2	CDS			Synony.	122
<i>HpasRNA52</i>	Stress response NST1-like protein	3' UTR				17
<i>HpasRNA53</i>	Polyadenylate-binding protein	CDS		Missense		8
<i>HpasRNA53</i>	Beta-1,6-N-acetylglucosaminyltransferase	3' UTR				2
<i>HpasRNA54</i>	NIMA-related kinase 4	5' UTR				2
<i>HpasRNA57</i>	Monocopper oxidase-like protein	CDS		Missense	Missense	1/1
<i>HpasRNA57</i>	AIAPC7	5' UTR				2/2
<i>HpasRNA57</i>	Disease resistance/LRR family protein	CDS	Frameshift		Missense	1/20
<i>HpasRNA69</i>	Tonoplast dicarboxylate transporter	CDS			Synony.	6
<i>HpasRNA74</i>	Transmembrane protein	CDS			Synony.	1
<i>HpasRNA82</i>	ABI2	CDS		Missense	Synony.	12/1
<i>HpasRNA90</i>	F-box protein	CDS	Frameshift			3

■ prevents predicted targeting ■ prevents predicted cleavage by AGO/RISC ■ weakens predicted targeting

Figure 4 – figure supplement 5

Sequence diversity of *HpasRNAs* and their predicted *Arabidopsis* target mRNAs.

(a) *HpasRNAs* were conserved among the three *H. arabidopsidis* isolates, Noco2, Cala2, Emoy2. (b) Sequence variations were found in the predicted *Arabidopsis* mRNAs analysing 1135 *A. thaliana* accessions. Three categories (colour coded) were considered to possibly prevent target silencing: indels causing bulges that block the *HpasRNA/AtmRNA* base pairing (red), SNPs at the position 10/11 interfering with RISC-mediated cleavage (orange), and SNPs in the *HpasRNA* seed region (account to RNA nucleotide positions from 2 to 12) losing *HpasRNA/AtmRNA* base pairing (green).

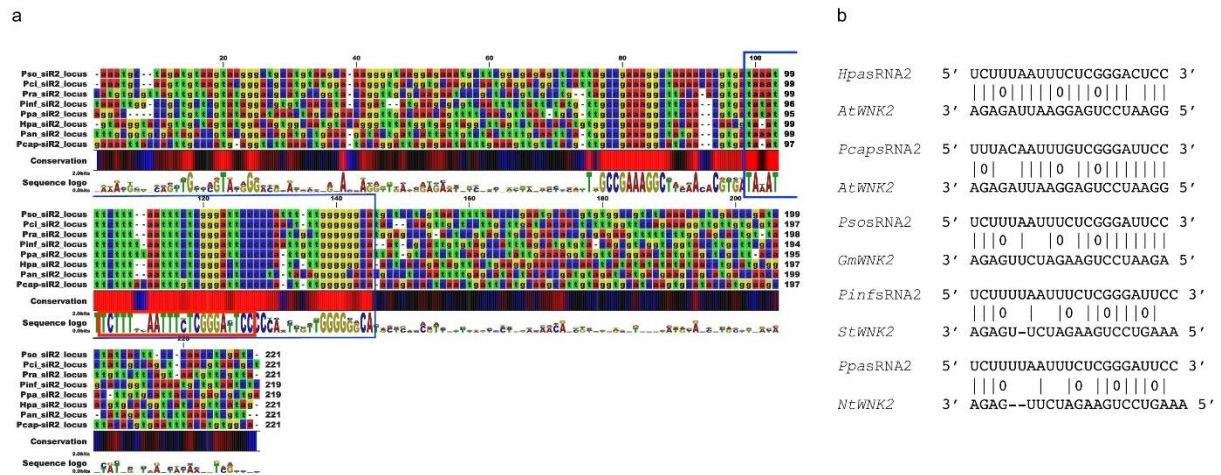


Figure 4 – figure supplement 6

The pathogen sRNA2 and its target are conserved across different plant pathogenic oomycetes and hosts.

(a) Oomycete *SRNA2* genomic loci are conserved among different plant pathogenic oomycete species of the genera *Hyaloperonospora*, *Phytophthora*, and *Pythium* (Hpa = *Hyaloperonospora arabidopsidis*, Pcap = *Phytophthora capsici*, Pso = *Phytophthora sojae*, Pan = *Pythium aphanidermatum*, Pinf = *Phytophthora infestans*, Ppa = *Phytophthora parasitica*). Blue box at the consensus sequence indicates the region of sRNA transcription as identified by sRNA-seq analysis and red box marks the consensus of the mature 21 nt *HpasRNA2* region. (b) Target prediction alignment of *sRNA2* homologs from different oomycete species with the target sequences of homolog *WNK2*s from respective host plant species (At = *Arabidopsis thaliana*, Gm = *Glycine max*, St = *Solanum tuberosum*, Nt = *Nicotiana tabacum*).

Supplemental file 1
sRNA read numbers.

	reads total number	mapping to 100 % to <i>A. thaliana</i> (TAIR10)	mapping to 100% to <i>H. arabidopsidis</i> and <i>A. thaliana</i>	mapping to 100% only to <i>H. arabidopsidis</i> (master genome)	unmapped reads
4 dpi, mock	32666246 (100%)	24070919 (73.68%)	12164538 (37.24%)	173233 (0.53%)	8422094 (25.78%)
4 dpi, <i>Hyaloperonospora</i> <i>-infected</i>	51300261 (100%)	27277198 (53.17%)	14069872 (27.43%)	4475759 (8.72%)	19547304 (38.10%)
7 dpi, mock	65214950 (100%)	49384100 (75.72%)	26990855 (41.39%)	227576 (0.35%)	15603274 (23.92%)
7 dpi, <i>Hyaloperonospora</i> <i>-infected</i>	87671980 (100%)	36159870 (41.24%)	19845298 (22.64%)	18766796 (21.41%)	32745314 (37.35%)
AGO1-IP 3 dpi					
	12908869 1 (100%)	109247735 (84.63%)	2834932 (2.19%)	26145 (0.02%)	19814811 (15.35%)
AGO1-IP 4 dpi					
	47889809 (100%)	35297292 (73.71%)	878152 (1.83%)	333374 (0.69%)	12259143 (25.59%)
AGO2-IP 4 dpi					
	14720448 (100%)	11405460 (77.48%)	6645388 (45.14%)	127292 (0.86%)	3187696 (21.65%)

Supplemental file 2

Predicted *A. thaliana* target genes of *HpasRNAs*.

(Author note: Due to space limitations the original table was split in three separate tables.)

	<i>HpasRNA</i>	genomic origin	total sRNAs 4 dpi		total sRNAs 7 dpi		<i>AtAGO1</i> 3 dpi		<i>AtAGO1</i> 4 dpi		<i>AtAGO2</i> 4 dpi	
			RAW	RPM	RAW	RPM	RAW	RPM	RAW	RPM	RAW	RPM
1	<i>HpasRNA4</i>	non-annotated region	19	4	396	34	1	38	26	82	5	68
2	<i>HpasRNA12</i>	non-annotated region	23	5	234	20	1	38	3	9	0	0
3	<i>HpasRNA14</i>	non-annotated region	22	5	226	19	0	0	29	91	3	41
4	<i>HpasRNA20</i>	non-annotated region	31	7	182	15	1	38	10	31	2	27
5	<i>HpasRNA75</i>	non-annotated region	10	2	236	20	0	0	1	3	0	0
6	<i>HpasRNA39</i>	non-annotated region	38	8	127	12	0	0	19	60	1	14
7	<i>HpasRNA38</i>	non-annotated region	24	5	128	12	0	0	3	9	0	0
8	<i>HpasRNA2</i>	non-annotated region	24	5	138	12	2	76	24	76	1	14
9	<i>HpasRNA36</i>	non-annotated region	22	5	132	11	1	38	7	22	0	0
10	<i>HpasRNA28</i>	non-annotated region	14	3	149	12	0	0	10	31	0	0
11	<i>HpasRNA51</i>	non-annotated region	26	6	111	9	0	0	7	22	1	14
12	<i>HpasRNA52</i>	non-annotated region	25	6	109	9	0	0	1	3	0	0
13	<i>HpasRNA44</i>	non-annotated region	13	3	121	11	0	0	4	13	0	0
14	<i>HpasRNA47</i>	non-annotated region	18	4	115	10	0	0	3	9	0	0
15	<i>HpasRNA43</i>	non-annotated region	11	2	122	11	1	38	5	16	0	0
16	<i>HpasRNA76</i>	non-annotated region	28	6	77	6	1	38	0	0	2	27
17	<i>HpasRNA30</i>	non-annotated region	3	1	140	12	0	0	11	35	0	0
18	<i>HpasRNA54</i>	non-annotated region	13	3	105	9	1	38	8	25	0	0
19	<i>HpasRNA53</i>	non-annotated region	12	3	107	9	0	0	9	28	0	0
20	<i>HpasRNA61</i>	non-annotated region	15	3	93	8	3	115	1	3	1	14
21	<i>HpasRNA55</i>	non-annotated region	11	2	102	9	0	0	4	13	0	0

22	HpasRNA83	non-annotated region	21	5	71	6	1	38	1	3	1	14
23	HpasRNA69	non-annotated region	11	2	85	7	0	0	60	189	2	27
24	HpasRNA85	non-annotated region	15	3	69	6	0	0	4	13	3	41
25	HpasRNA74	non-annotated region	11	2	79	7	2	76	11	35	0	0
26	HpasRNA87	non-annotated region	13	3	67	6	0	0	3	9	0	0
27	HpasRNA57	non-annotated region	1	0	96	8	0	0	73	230	4	55
28	HpasRNA77	non-annotated region	5	1	77	6	1	38	25	79	3	41
29	HpasRNA90	non-annotated region	8	2	67	6	0	0	1	3	1	14
30	HpasRNA96	non-annotated region	9	2	62	5	0	0	1	3	1	14
31	HpasRNA99	non-annotated region	9	2	62	5	3	115	9	28	0	0
32	HpasRNA78	non-annotated region	0	0	77	6	1	38	0	0	0	0
33	HpasRNA82	non-annotated region	2	0	71	6	2	76	2	6	0	0
34	HpasRNA92	annotated protein-coding gene	3	1	65	5	2	76	0	0	0	0

HpasRNA	TAPIR target prediction					
	score	alignment		ATG code	putative function	target site location
HpasRNA4	2,5	miRNA_3'	GGTAACGAGTTATGACAATGT			
		aln	o o o			
		target_5'	TCATTGCTCGATGCTGTTACA	At1g16840	putative transcription factor	5UTR
HpasRNA12	4	miRNA_3'	TCTGAGCGCTCGTGTAGGAAC			
		aln	o o o			
		target_5'	AGACTTGTGAGCAGATTCTTG	AT1G66510	AAR2 protein family	3UTR
HpasRNA14	4	miRNA_3'	TCTGCTGAGTTCTAGATGCGT			
		aln	o o o			
		target_5'	GGCCGATGCAAGATCTGCGCA	AT4G26940	Hexosyltransferase	Exon
HpasRNA20	4	miRNA_3'	TTGGTAAATCTAGGAGTCAGA			
		aln	o			

		target_5'	AACCATTTTGATCTTCAATCT	AT3G47990	E3 ubiquitin-protein ligase SIS3	5UTR
HpasRNA75	1	miRNA_3'	ATTGGTCTGCTGATTCGGTTA			
		aln				
		target_5'	TAACCATACGACTAAGCCAAT	AT1G73810	Core-2/l-branching beta-1,6-N-acetylglucosaminyltransferase-like protein	3UTR
	4	miRNA_3'	ATTGGTCTGCTGATTCGGTTA			
		aln	o o o			
		target_5'	CGATCCGACGACTGAGCCAAT	AT1G03780	Protein TPX2	exon
HpasRNA39	4	miRNA_3'	GTGCAAAGTCGTCGTAGGCTT			
		aln	o o			
		target_5'	AATGTTTCGGCAGCATCAGAA	AT1G32330	Heat stress transcription factor A-1d	exon
HpasRNA38	3	miRNA_3'	TAAGGGGAAGTGTGCAGCTTC			
		aln	o o oo			
		target_5'	GTTTCCCTTTGCACGTCGAAG	AT3G05380	DIRP ;Myb-like DNA-binding domain	exon
HpasRNA2	3,5	miRNA_3'	CCTCAGGGCTCTTTAATTCT			
		aln	o o o			
		target_5'	GGAATCCTGAGGAATTAGAGA	AT3G22420	With no lysine (K) kinase 2	exon
HpasRNA36	4	miRNA_3'	GTTCGAGAGGAGCTACAGGTT			
		aln	ooo o o			
		target_5'	TGGGCTCATCTTGATGTCCAA	AT1G55320	AAE18	exon
HpasRNA28	3	miRNA_3'	TAAGGCAGAAGGCGGCGGTAC			
		aln	oo o			
		target_5'	ATTTTCTCTTTCGCCGCCATG	AT5g19430	C3HC4-type RING finger E3 ubiquitin ligase	5UTR
	3	miRNA_3'	TAAGGCAGAAGGCGGCGGTAC			
		aln	o o			
		target_5'	GTTTCTCTTCCGCCGCCATC	AT5G66560	BTB/POZ domain-containing protein	exon

	3,5	miRNA_3'	TAAGGCAGAAGGCGGCGGTAC			
		aln	o o			
		target_5'	CTTCCGGTTTCCGCCCGCGTG	AT1G15390	Peptide deformylase	exon
HpasRNA51	3,5	miRNA_3'	GTTAGTCATTACAGTTTCAGC			
		aln	o			
		target_5'	CAATCAGTGATGTCAATGTCT	AT4G27220	NB-ARC domain-containing disease resistance protein	exon
	4	miRNA_3'	GTTAGTCATTACAGTTTCAGC			
		aln	o			
		target_5'	CTATCAGTAGTGTCAAATTCG	At3g15900	homoserine O-acetyltransferase	exon
HpasRNA52	4	miRNA_3'	TGTGCAGAAGACTTAGGGGAA			
		aln	o o o o			
		target_5'	AGATGTTTTCTGAATTCTCTT	AT4G25690	stress response NST1-like protein	3UTR
HpasRNA44	4	miRNA_3'	GGCAGTGAACCAGAAGCTTAC			
		aln	o o o			
		target_5'	TGGTTACTCGGTTTTCGAATG	AT3G19830	Calcium-dependent lipid-binding (CaLB domain) family protein	exon
HpasRNA47	3	miRNA_3'	G TTCAGATTGGCAGGTTCTAC			
		aln	o			
		target_5'	CAAGTCTCATCGTCCAAGATT	AT3G56970	Transcription factor ORG2	exon
	4	miRNA_3'	G TTCAGATTGGCAGGTTCTAC			
		aln	o			
		target_5'	CAAATCTCATCGTCCAAGATT	AT3G56980	Transcription factor ORG3	exon
HpasRNA43	3,5	miRNA_3'	TTGTCATTTAAAGTCAGCAGT			
		aln	o o			

		target_5'	AATAGTAAATCTCAGTTGTCA	AT3G47910	Ubiquitin carboxyl-terminal hydrolase-related protein	exon
HpasRNA76	3	miRNA_3'	CGGTCTGACGAGGTAGGGCGC			
		aln	o			
		target_5'	GCAAAACTGCTCCATCCTGCG	AT2G26440	Probable pectinesterase/pectinesterase inhibitor 12	exon
HpasRNA30	2,5	miRNA_3'	GTCTCAAATCCTTACCTTTAA			
		aln	o o			
		target_5'	CAGGTTTTAGGAATGGAAGTT	AT3G51630	Probable serine/threonine-protein kinase WNK5	exon
	3,5	miRNA_3'	GTCTCAAATCCTTACCTTTAA			
		aln	oo . o o			
		target_5'	TGGATTTTGGGAATGGAGATT	AT4G34410	Ethylene-responsive transcription factor ERF109	exon
	3,5	miRNA_3'	GTCTCAAATCCTTACCTTTAA			
		aln	o			
		target_5'	CAGATTTTGGGAATGGAAAAT	AT1G50840	polymerase gamma 2	exon
	4	miRNA_3'	GTCTCAAATCCTTACCTTTAA			
		aln	o o o			
		target_5'	TAGAGTTAGGGGATGGAAATG	AT2G19430	THO complex subunit 6	exon
HpasRNA54	3,5	miRNA_3'	GTGAGGTGGTGTACCGCCAT			
		aln	o o o			
		target_5'	CTCTTCACCACGGTGTCTGGTA	AT3G63280	NIMA-related kinase 4	5UTR
HpasRNA53	4	miRNA_3'	GATTGGTCTGCTGATTCGGTT			
		aln	o o			
		target_5'	TTAACGGGACGACTATGCCAA	AT1G47490	Polyadenylate-binding protein RBP47C	exon

	2	miRNA_3'	GATTGGTCTGCTGATTCGGTT			
		aln				
		target_5'	ATAACCATACGACTAAGCCAA	AT1G73810	Core-2/l-branching beta-1,6-N-acetylglucosaminyltransferase family protein	3UTR
HpasRNA61	2	miRNA_3'	CAGGTAGTCTAGACCACTCTT			
		aln	oo			
		target_5'	TTCCATTGGATCTGGTGAGAA	AT3G55640	Ca-dependent solute carrier-like protein	exon
HpasRNA55	4	miRNA_3'	TTGTATCTCTTCTGCGGCAT			
		aln	o o o			
		target_5'	AAGATGCAGAAAGATGCCGTG	AT3G24460	Serinc-domain containing serine and sphingolipid biosynthesis protein	exon
HpasRNA83	3,5	miRNA_3'	CTTGTTTAAGTACTGTCTAGT			
		aln	o o o			
		target_5'	GAACAAGGTTATGATAGATCA	AT5G09450	Pentatricopeptide repeat-containing protein	exon
HpasRNA69	4	miRNA_3'	TACGTCATCACAAGCTGCCAT			
		aln	o o			
		target_5'	ATGTTGTAGTGTTTCGACGGCG	AT5G47560	Tonoplast dicarboxylate transporter	exon
HpasRNA85	3,5	miRNA_3'	CTTCTGCAAGTCGTCGTGGCA			
		aln	o			
		target_5'	GGAGACGATCATCAGCACCGT	At2g39950	flocculation protein	exon
HpasRNA74	4	miRNA_3'	GGTTTGCAGTGTCTGGCGCAA			
		aln	o			
		target_5'	ACAAACGTCACTGACTGCGTT	AT5G07730	transmembrane protein	exon
HpasRNA87	3,5	miRNA_3'	ACTCGTCAGACAGGTCTAGTA			
		aln	o o o			
		target_5'	TGAGCAGCTTGTCCGATTAT	AT3G60830	Actin-related protein 7	exon

HpasRNA57	4	miRNA_3'	TAGGAAAGGAAGTAGTGACGA			
		aln				
		target_5'	ACCCTCTCCTACATCACTGCT	AT5G51480	Monocopper oxidase-like protein SKS2	exon
	2,5	miRNA_3'	TAGGAAAGGAAGTAGTGACGA			
		aln	o o			
		target_5'	ATCTTTTACTTCATCGCTGCT	AT2G39090	AtAPC7	5UTR
	3,5	miRNA_3'	TAGGAAAGGAAGTAGTGACGA			
		aln	o o o			
		target_5'	ACCTTTTCCTTTATCATTGCT	AT3G23010	Disease resistance family protein/LRR family protein	exon
HpasRNA77	3	miRNA_3'	AACGAGTTATGACAATGTCAA			
		aln				
		target_5'	TTGCTCTATACTATTACAGTT	AT5G49030	Isoleucyl-tRNA synthetase	3UTR
	4	miRNA_3'	AACGAGTTATGACAATGTCAA			
		aln	oo o			
		target_5'	TTGCCTGAAGCTGTTACAGTT	AT5G50170	C2 and GRAM domain-containing protein	exon
	3,5	miRNA_3'	AACGAGTTATGACAATGTCAA			
		aln	o o			
		target_5'	TTGCTCGATGCTGTTACAGGT	At1g16840	unknown protein	3UTR
HpasRNA90	3,5	miRNA_3'	CGATCACAAGTACTAGTATTT			
		aln	o o			
		target_5'	TCTGGTGATCGTGATCATAAA	AT2G23160	F-box protein	exon
	4	miRNA_3'	CGATCACAAGTACTAGTATTT			

		aln	o o o			
		target_5'	GCTAATGTTTCATGGTCGTAGA	AT1G09750	Aspartyl protease AED3	exon
HpasRNA96	4	miRNA_3'	CGTTTGAAGTCGTTAGAGCCT			
		aln	o o			
		target_5'	GCTGCCTGCAGCAATCTCGGG	AT2G42005	Amino acid transporter ANTL1	exon
HpasRNA99	4	miRNA_3'	GCGTGAGTCTACTGCTGCTTT			
		aln	o o o			
		target_5'	AGGATTCAGATGACGATGAAG	AT2G34170	unknown protein	exon
HpasRNA78	4	miRNA_3'	AGAAGGTGCATCGAACGGATC			
		aln	o o			
		target_5'	TTTTCCTTGAAGCTTGCCTAG	AT2G38820	Protein of unknown function	5UTR
	3	miRNA_3'	AGAAGGTGCATCGAACGGATC			
		aln	o			
		target_5'	TCTTCAACTTAGCTTGTCTAG	AT3G21250	Multidrug resistance-associated protein 6	Exon
HpasRNA82	3	miRNA_3'	TCCAAGACGGTCAAGCAACGA			
		aln	o			
		target_5'	AGTTTCTTCTAGTTCGTTGCT	AT5G57050	AtABI2	Exon
HpasRNA92	4	miRNA_3'	TAAGGAGTCCAGAGTATTAGA			
		aln	o o o o			
		target_5'	GTTCTTACGTTTCATGATCT	AT1G49210	E3 ubiquitin-protein ligase ATL76	Exon

HpasRNA		level of target site conservation
	ATG code	types and numbers (in brackets) of target site polymorphisms found in 1135 <i>A. thaliana</i> genomes
HpasRNA4	AT1G16840	SNPs (2), deletions (0), insertions (0)
HpasRNA12	AT1G66510	SNPs (4), deletions (2), insertions (0)
HpasRNA14	AT4G26940	SNPs (0), deletions (0), insertions (0)
HpasRNA20	AT3G47990	SNPs (3), deletions (0), insertions (0)

HpasRNA75	AT1G73810	SNPs (1), deletions (0), insertions (0)
	AT1G03780	SNPs (2), deletions (0), insertions (0)
HpasRNA39	AT1G32330	SNPs (5), deletions (0), insertions (0)
HpasRNA38	AT3G05380	SNPs (1), deletions (0), insertions (0)
HpasRNA2	AT3G22420	SNPs (1), deletions (0), insertions (0)
HpasRNA36	AT1G55320	SNPs (2), deletions (0), insertions (0)
HpasRNA28	AT5g19430	SNPs (3), deletions (0), insertions (0)
	AT5G66560	SNPs (1), deletions (0), insertions (0)
	AT1G15390	SNPs (2), deletions (0), insertions (0)
HpasRNA51	AT4G27220	SNPs (2), deletions (0), insertions (0)
	At3g15900	SNPs (0), deletions (0), insertions (0)
HpasRNA52	AT4G25690	SNPs (2), deletions (0), insertions (0)
HpasRNA44	AT3G19830	SNPs (2), deletions (0), insertions (0)
HpasRNA47	AT3G56970	SNPs (3), deletions (0), insertions (0)
	AT3G56980	SNPs (0), deletions (0), insertions (0)
HpasRNA43	AT3G47910	SNPs (0), deletions (0), insertions (0)
HpasRNA76	AT2G26440	SNPs (0), deletions (0), insertions (0)
HpasRNA30	AT3G51630	SNPs (0), deletions (0), insertions (0)
	AT4G34410	SNPs (1), deletions (0), insertions (0)
	AT1G50840	SNPs (2), deletions (0), insertions (0)
	AT2G19430	SNPs (1), deletions (0), insertions (0)
HpasRNA54	AT3G63280	SNPs (3), deletions (0), insertions (0)
HpasRNA53	AT1G47490	SNPs (4), deletions (0), insertions (0)
	AT1G73810	SNPs (2), deletions (0), insertions (0)
HpasRNA61	AT3G55640	SNPs (0), deletions (0), insertions (0)
HpasRNA55	AT3G24460	SNPs (0), deletions (0), insertions (0)
HpasRNA83	AT5G09450	SNPs (0), deletions (0), insertions (0)
HpasRNA69	AT5G47560	SNPs (1), deletions (0), insertions (0)

HpasRNA85	At2g39950	SNPs (0), deletions (0), insertions (0)
HpasRNA74	AT5G07730	SNPs (1), deletions (0), insertions (0)
HpasRNA87	AT3G60830	SNPs (0), deletions (0), insertions (0)
HpasRNA57	AT5G51480	SNPs (3), deletions (0), insertions (0)
	AT2G39090	SNPs (2), deletions (0), insertions (1)
	AT3G23010	SNPs (2), deletions (0), insertions (1)
HpasRNA77	AT5G49030	SNPs (2), deletions (0), insertions (0)
	AT5G50170	SNPs (0), deletions (0), insertions (0)
	AT1G16840	SNPs (2), deletions (0), insertions (0)
HpasRNA90	AT2G23160	SNPs (1), deletions (1), insertions (0)
	AT1G09750	SNPs (0), deletions (0), insertions (0)
HpasRNA96	AT2G42005	SNPs (3), deletions (0), insertions (0)
HpasRNA99	AT2G34170	SNPs (0), deletions (0), insertions (0)
HpasRNA78	AT2G38820	SNPs (1), deletions (0), insertions (0)
	AT3G21250	SNPs (0), deletions (0), insertions (0)
HpasRNA82	AT5G57050	SNPs (4), deletions (0), insertions (0)
HpasRNA92	AT1G49210	SNPs (2), deletions (0), insertions (0)

Supplemental file 3

List of oligonucleotides used in this study.

Primer name	Sequence	Purpose
Hpa_siR2_RT	GTCGTATCCAGTGCAGGGTCCGAGGTATTCGCACTGGATACGACGGAGTC	Stemloop RT
Hpa_siR2_fwd	GCGGCGGTTCTTTAATTTCTCG	PCR
Hpa_siR30_RT	GTCGTATCCAGTGCAGGGTCCGAGGTATTCGCACTGGATACGACAGAGT	Stemloop RT
Hpa_siR30_fwd	GCGGCGAATTTCCATTCCTA	PCR
Hpa_siR90_RT	GTCGTATCCAGTGCAGGGTCCGAGGTATTCGCACTGGATACGAGCTAGT	Stemloop RT

Hpa_siR90_fwd	GCGGCGGCGGGATGGAGCA	PCR
At_miR164_SL	GTCGTATCCAGTGCAGGGTCCGAGGTATTCGCACTGGATACGACGCACG	Stemloop RT
At_miR164_fwd	GCGGCGTGGAGAAGCAGGGC	PCR
At_miR393*_SL	GTCGTATCCAGTGCAGGGTCCGAGGTATTCGCACTGGATACGACAATCCA	Stemloop RT
At_miR393*_fwd	CTCGCTATCATGCGATCTCT	PCR
univ_stemloop_PCR_r ev	GTATCCAGTGCAGGGTCCGAGGT	PCR
Hpa_ACT_fwd	GTGTCGCACACTGTACCCATTTAT	PCR for pathogen biomass
Hpa_ACT_rev	ATCTTCATCATGTAGTCGGTCAAGT	PCR for pathogen biomass
Ath_iASK_fwd	CTTATCGGATTTCTCTATGTTTGGC	PCR for pathogen biomass (from Gachon & Saindrenan 2004)
Ah_iASK_rev	GAGCTCCTGTTTATTTAACTTGTACATACC	PCR for pathogen biomass (from Gachon & Saindrenan 2004)
Ec_TUB_fwd	TGACAGCCCGGAATGAGT	PCR for pathogen biomass (Engelsdorf et al., 2015)

Ec_TUB_rev	TTGTCTTCGTTTCCCAGGTC	PCR for pathogen biomass (Engelsdorf et al., 2015)
At_PR1_fwd	CTCGGAGCTACGCAGAACAA	qRT-PCR
At_PR1_rev	GCCTTCTCGCTAACCCACAT	qRT-PCR
At_PDF1.2_fwd	CTTGTTCTCTTTGCTGCTTTTCGAC	qRT-PCR
At_PDF1.2_rev	TAGTTGCATGATCCATGTTTG	qRT-PCR
At_RPP4_fwd	GAAGGCACTCAAGGCCTCATT	qRT-PCR
At_RPP4_rev	GACAATAATCCCACCATAGCCTTT	qRT-PCR
At_SNC1_fwd	GCCGGATATGATCTTCGGAA	qRT-PCR
At_SNC1_rev	CGGCAAGCTCTTCAATCATG	qRT-PCR
At_WNK2_fwd	CTTGGA CTGCTGCGATTC	qRT-PCR
At_WNK2_rev	GATTTGTGCCGGGTGAGTACAT	qRT-PCR
At_AED3_fwd	AGAGACGAGTTTAGGAAGCA	qRT-PCR
At_AED3_rev	AAAAAGAGAGGGAGAGAGAGA	qRT-PCR
At_RBOHD_fwd	CGAATGGCATCCTTTCTCAATC	qRT-PCR (from Morales et al. 2016)
At_RBOHD_rev	GTCACCGAGAGTGCGGATATG	qRT-PCR (from Morales et al. 2016)
At_RBOHF_fwd	CTTGGCATTGGTGCAACTCC	qRT-PCR (from Morales et al. 2016)

At_RBOHF_rev	TCTTTCGTCTTGGCGTGTCA	qRT-PCR (from Morales et al. 2016)
At_ACT_fwd	CAGTGGTCGTACAACCGGTATT	qRT-PCR
At_ACT_rev	GTCTCTTACAATTTCCCGCTCT	qRT-PCR
T-DNA_SALK	ATTTTGCCGATTTTCGGAAC	Genotyping PCR
T-DNA SAIL	TAGCATCTGAATTTTCATAACCAATCTCGATACAC	Genotyping PCR
SALK_121042 (wnk2-2) LP	CTCGTCTCATCTCATTCTCCG	Genotyping PCR
SALK_121042 (wnk2-2) RP	TTGCGTTGGTACTTCAAACC	Genotyping PCR
SALK_206118 (wnk2-3) LP	TCGATCTTTTCGCTAACGATG	Genotyping PCR
SALK_206118 (wnk2-3) RP	TTCCCCACTATTTGTGTGCTC	Genotyping PCR
SAIL_722_G02C1 (aed3-1) LP	CCTCATCCACTTACTCAACCG	Genotyping PCR
SAIL_722_G02C1 (aed3-1) RP	CGCTGAAGCAAGAGATGAAAC	Genotyping PCR
STTM siR2	AGGTCTCTCACCGGAGTCCCGAGctaAAATTAAGAgttgttgttattggtctaatttaaataatg	Full length STTM
	gtctaaagaagaagaatGGAGTCCCGAGctaAAATTAAGAAAGGTGAGACCA	
STTM siR30	AGGTCTCTCACCCAGAGTTTLAGGctaAATGGAAATTggttgttgttattggtctaatttaaataatg	Full length STTM
	gtctaaagaagaagaatCAGAGTTTLAGGctaAATGGAAATTAAGGTGAGACCA	

STTM siR90	AGGTCTCTCACCGCTAGTGTTCAActaTGATCATAAAggtgtgtgtgtatggctaatttaaatatg gtctaaagaagaagaatGCTAGTGTTCAActaTGATCATAAAAAGGTGAGACCA	Full length STTM
STTM rRNA	AGGTCTCTCACAGTCAGACGAAActaCGATTTGCAggtgtgtgtgtatggctaatttaaatatg gtctaaagaagaagaatAGTCAGACGAAActaCGATTTGCAAAGGTGAGACCA	Full length STTM
STTM scrambledRNA	AGGTCTCTCACCTCTCTAATTCCctaTCAGGATTCCggtgtgtgtgtatggctaatttaaatatg gtctaaagaagaagaatTCTAGGACCATctaGAACATTAGCAAGGTGAGACCA	Full length STTM
Outer_WNK2_fwd	ATGAAGACATTACGGGTCTCACACCATGAATGGTGAAGAAAGCTT	WNK2r cloning
Outer_WNK2_rev	ATGAAGACATCAGAGGTCTCACCTTCATATCCACGGCATCCACAG	WNK2r cloning
Bsal_WNK2_fwd	ATGAAGACATGAGGCCTATTGACTACTACAAT	WNK2r cloning
Bsal_WNK2_rev	ATGAAGACATCCTCATAACAAATCCATCCA	WNK2r cloning
Bpil_WNK2_fwd	ATGAAGACATAGGACAAGAGCTGTTCTTC	WNK2r cloning
Bpil_WNK2_rev	ATGAAGACATTCTCAGAACTATCGAACTCAT	WNK2r cloning
target_site_mut_fwd	ATGAAGACATAAACCTGAAGAGCTGGAAAAGTTTTTCAGAGAGTTC	WNK2r cloning
target_site_mut_rev	ATGAAGACATTTCCAGCTCTTCAGGGTTTCTTGTGAAATTTTGAAGC	WNK2r cloning
Outer_AED3_fwd	ATGAAGACATTACGGGTCTCACACCATGGCCTCCTCAAGTCTCCATT	AED3r cloning
Outer_AED3_rev	ATGAAGACATCAGAGGTCTCACCTTGTTGCAGGGCTCAGGAGCAATTC	AED3r cloning
Bsal(1)_AED3_fwd	ATGAAGACATATCTCAAACACTACGTCGCTTTAC	AED3r cloning
Bsal(1)_AED3_rev	ATGAAGACATAGATACCAATGACATAGGCC	AED3r cloning
Bsal(2)_AED3_fwd	ATGAAGACATATTGGGTCAACCCAAATCCATC	AED3r cloning
Bsal(2)_AED3_rev	ATGAAGACATCAATAGACCCAGTTTCAACGAC	AED3r cloning
target_site_mut_fwd	ATGAAGACATACTGATGTTTATGGTACTCGACACAAGTAACGACGCCGTTTG	AED3r cloning
target_site_mut_rev	ATGAAGACATCAGTTGTGGAGGAGTGCCGAGTTTG	AED3r cloning

Outer_proWNK2_fwd	ATGAAGACATTACGGGTCTCAGCGGCATTCTTATAATTTCTTATGG	WNK2 promoter cloning
Outer_proWNK2_rev	ATGAAGACATCAGAGGTCTCACAGAGCGTTCGGTTTACTAAACCGG	WNK2 promoter cloning
Outer_proAED3_fwd	ATGAAGACATTACGGGTCTCAGCGGATCTCTGCTCAACCACCAAG	AED3 promoter cloning
Outer_proAED3_rev	ATGAAGACATCAGAGGTCTCACAGAGGTTTTGGCTAATGTGATTG	AED3 promoter cloning
Bsal(1)_proAED3_fwd	ATGAAGACATCGCGTGAACGAACAATGAGAG	AED3 promoter cloning
Bsal(1)_proAED3_rev	ATGAAGACATCGCGACCTCTGAAATACTTAC	AED3 promoter cloning
GUS_fwd	CGGGTCTCACACCATGTTACGTCC	Silencing reporter cloning
GUS_rev	AGAGGTCTCTCCTTTTGTGGCC	Silencing reporter cloning
Csy4 binding site full length	ATGGTCTCATCTGAACAATGGTTCACCTGCCGTATAGGCAGCTAAGAAAGGCACCAGAGACC AT	Silencing reporter cloning
siR2/siR90 target site upstream	ATGGTCTCATCTGAACAATGGGAATCCTGAGGAATTAGAGAGCTAATGTTTCATGGTCCTAGA GGCACCAGAGACCAT	Silencing reporter cloning
siR2/siR90 target site downstream	ATGGTCTCAAAGGCAGGAATCCTGAGGAATTAGAGAGCTAATGTTTCATGGTCCTAGATGGAA TCAGAGACCAT	Silencing reporter cloning

miR164a target site upstream	ATGGTCTCATCTGAACAATGAGCACGTGTCCTGTTTCTCCAGGCACCAGAGACCAT	Silencing reporter cloning
miR164a target site downstream	ATGGTCTCAAAGGCAAGCACGTGTCCTGTTTCTCCATGGAATCAGAGACCAT	Silencing reporter cloning
scrambled target site upstream	ATGGTCTCATCTGAACAATGATGCTGCATTTGCACTCTCCGGCACCAGAGACCAT	Silencing reporter cloning
scrambled target site downstream	ATGGTCTCAAAGGCAATCATCATCATCATCATCTGGAATCAGAGACCAT	Silencing reporter cloning
AED3_RT	CACATTCACCTGCTTCCTAAAC	5' RACE
AED3_PCR_primer	ATAGTAAAGTGATGGACGGCG	5' RACE
AED3_nested_PCR_p rimer	AAGCTAGGGAGGCAGTATGAG	5' RACE
WNK2_RT	CATCATCACCGTTTCTCTTCCC	5' RACE
WNK2_PCR_primer	TCTCAACAAACTCACGAACCTC	5' RACE
WNK2_nested_PCR_ primer	GTAACCATCTCCAACACACAC	5' RACE

II: Plant ARGONAUTE protein immunopurification for pathogen cross kingdom small RNA analysis.

**Plant ARGONAUTE Protein Immunopurification
for Pathogen Cross Kingdom Small RNA Analysis**
 Florian Dunker[#], Bernhard Lederer[#] and Arne Weiberg^{*}

Faculty of Biology, Genetics, Biocenter Martinsried, LMU Munich, Großhaderner Str. 2-4, 82152 Planegg-Martinsried, Germany

*For correspondence: a.weiberg@lmu.de

[#]Contributed equally to this work

[Abstract] Over the last decade, it has been noticed that microbial pathogens and pests deliver small RNA (sRNA) effectors into their host plants to manipulate plant physiology and immunity for infection, known as cross kingdom RNA interference. In this process, fungal and oomycete parasite sRNAs hijack the plant ARGONAUTE (AGO)/RNA-induced silencing complex to post-transcriptionally silence host target genes. We hereby describe the methodological details of how we recovered cross kingdom sRNA effectors of the oomycete pathogen *Hyaloperonospora arabidopsidis* during infection of its host plant *Arabidopsis thaliana*. This Bio-protocol contains two parts: first, a detailed description on the procedure of plant AGO/sRNA co-immunopurification and sRNA recovery for Illumina high throughput sequencing analysis. Second, we explain how to perform bioinformatics analysis of sRNA sequence reads using a Galaxy server. In principle, this protocol is suitable to investigate AGO-bound sRNAs from diverse host plants and plant-interacting (micro)organisms.

Keywords: Cross kingdom RNA interference, ARGONAUTE co-immunopurification, Small RNA, Plant-microbe interactions, *Arabidopsis thaliana*, *Hyaloperonospora arabidopsidis*, Downy mildew disease

[Background] Small RNAs (sRNAs) can serve as pathogen effectors that hijack the plant ARGONAUTE (AGO)/RNA-induced silencing complex (RISC) and silence host mRNAs for infection, a virulence mechanism termed cross kingdom RNA interference (Weiberg *et al.*, 2015; Zeng *et al.*, 2019). Profiling the repertoire of sRNAs bound to the plant AGO during infection is the method of choice, to gain a global overview on plant-invasive pathogen sRNAs that might function through the host AGO/RISC. Antibody-based, co-immunopurification (co-IP) of plant AGO/sRNAs, the functional components of a RISC, coupled to sRNA high throughput sequencing is the gold standard to quantify silencing sRNAs in plants (Mi *et al.*, 2008; Montgomery *et al.*, 2008; Carbonell *et al.*, 2012). Such approaches have led to the discovery of specifications for the binding of sRNAs to distinct members of the plant AGO protein family (Mi *et al.*, 2008; Montgomery *et al.*, 2008) and revealed characteristic changes of AGO-bound sRNA profiles according to plant environmental and stress responses (Zhang *et al.*, 2011). In this context, protocols have been published describing how to co-immunopurify plant AGO/sRNAs in order to study AGO-bound, endogenous plant sRNAs under various conditions (Qi and Mi, 2009; Zhao *et al.*, 2012; Carbonell, 2017).

In this bio-protocol, we provide a detailed description of *A. thaliana* AGO1/sRNAs co-IP isolated from *H. arabidopsidis*-infected seedlings and the recovery of both plant and pathogen AGO1-bound sRNAs for high throughput sequencing analysis. By this method, we discovered several novel pathogen sRNA effectors as well as plant silencing sRNAs that were responsive to *H. arabidopsidis* infection (Dunker *et al.*, 2020). Applying this protocol allowed us to investigate sRNAs bound to other members of the plant AGO family, as well. For instance, we successfully co-immunopurified *A. thaliana* AGO2/sRNAs using a *proAGO2:HA-AGO2* transgenic *A. thaliana* line (Montgomery *et al.*, 2008) in combination with commercial anti-Human influenza hemagglutinin (HA) antibody, and could identify several AGO2-bound *H. arabidopsidis* sRNAs (Dunker *et al.*, 2020). Although experimentally validated in the *A. thaliana* system, we propose this protocol being suitable for AGO/sRNAs co-IP and analysis of silencing sRNAs in various plant species and plant-interacting (micro)organisms, given a suitable antibody for AGO co-IP is available and host and microbe genome sequences are known.

Materials and Reagents

Materials

1. Blotting paper (Ahlstrom Munksjö, catalog number: BF4)
2. DNA LoBind® 1.5 ml reaction tubes (Eppendorf, catalog number: 0030108051)
3. Falcon tubes 50 ml and 15 ml (Greiner Bio-One, catalog numbers: 227261 and 188271)
4. Glass pipettes (10 ml)
5. Miracloth (Merck Millipore, catalog number: 475855)
6. Propagation soil substrate (Stender, catalog number: A210)
7. Reaction tubes 1.5 and 2 ml (Sarstedt, catalog numbers: 72.690 and 72.691)
8. 14-day-old *Arabidopsis thaliana* seedlings (ecotype Col-0)
9. *Hyaloperonospora arabidopsidis* spores (strain Noco2)

Reagents

Note: If this protocol refers to water, it always implies de-ionized, ultrapure water.

1. Liquid nitrogen
2. Acrylamide/bis-acrylamide solution (Rotiphorese Gel A, Carl Roth, catalog number: 3037)
3. Anti-AGO1 polyclonal antibody (Agrisera, catalog number: AS09 527)
4. Ammonium persulfate (APS) p.a. (Carl Roth, catalog number: 9592)
5. Bromophenol blue Dye (Carl Roth, catalog number: A512)
6. cOmplete® protease inhibitor cocktail (Roche, ordered via Sigma-Aldrich, catalog number: 04693116001)
7. Diethyl pyrocarbonate (DEPC, Carl Roth, catalog number: K028)
8. 1,4-Dithiothreitol p.a. (DTT, Carl Roth, catalog number: 6908)
9. Desoxyribonucleotide mix (dNTP, 10 mM each nucleotide type) for molecular biology (New England Biolabs, catalog number: N0447)

10. 96% Ethanol Ph. Eur. (VWR chemicals, catalog number: 20905.296)
11. Ethylenediamine tetraacetic acid (EDTA) disodium salt dehydrate (Gerbu Biotechnik GmbH, catalog number: 1034)
12. Glacial acetic acid (Carl Roth, catalog number: 3738)
13. Glycerol Ph. Eur. (Carl Roth, catalog number: 6967)
14. Glycine p.a. (PanReac/AppliChem, catalog number: 131340)
15. Glycogen RNA grade (Thermo Fisher Scientific, catalog number: R0551)
16. GoTaq® G2 DNA Polymerase (Promega, catalog number: M7841)
17. IRDye® 800CW Goat anti-Rabbit IgG Secondary Antibody (LI-COR, catalog number: 926-32211)
18. Magnesium chloride (25 mM; for molecular biology) (New England Biolabs, catalog number: B9021)
19. NEBNext® Multiplex Small RNA Library Prep Set for Illumina (New England Biolabs, catalog number: E7300)
20. Nonidet P-40 (NP-40, no longer available, the replacement product is IGEPAL CA-630 Sigma-Aldrich, catalog number: I8896)
21. 10 bp O'RangeRuler DNA ladder (Thermo Fisher Scientific, catalog number: SM1313)
22. Potassium chloride (KCl) molecular biology grade (Merck Millipore, catalog number: 529552)
23. Potassium dihydrogen phosphate (KH₂PO₄) p.a. (Carl Roth, catalog number 3904)
24. Protein A agarose (Roche, ordered via Sigma-Aldrich, catalog number: PROTAA-RO)
25. Proteinase K (Thermo Fisher Scientific, catalog number: EO0491)
26. RiboLock® RNase inhibitor (Thermo Fisher Scientific, catalog number: EO0381)
27. ROTI C/I (Chloroform/Isoamyl alcohol mixture, Carl Roth, catalog number: X984)
28. ROTI-Phenol (Carl Roth, catalog number: 0038)
29. ROTI-Phenol/Chloroform/Isoamyl alcohol (Carl Roth, catalog number: A156)
30. Sodium chloride (NaCl) p.a. (Carl Roth, catalog number: 3957)
31. Sodium dodecyl sulfate (SDS) ultrapure (Carl Roth, catalog number: 2326)
32. SuperScript® III (Thermo Fisher Scientific, catalog number: 18080093)
33. Disodium hydrogen phosphate (Na₂HPO₄) p.a. (Carl Roth, T876)
34. Tetramethylethylenediamine (TEMED) for electrophoresis (Carl Roth, catalog number: 2367)
35. 1 M Tris-HCl pH 6.8 stock solution (made from Tris ultrapure, PanReac/AppliChem, catalog number: A1086, pH adjusted with HCl, Carl Roth, catalog number: X896)
36. 1 M Tris-HCl pH 7.5 stock solution (made from Tris ultrapure, PanReac/AppliChem, catalog number: A1086, pH adjusted with HCl, Carl Roth, catalog number: X896)
37. 1 M Tris-HCl pH 8.0 stock solution (made from Tris ultrapure, PanReac/AppliChem, catalog number: A1086, pH adjusted with HCl, Carl Roth, catalog number: X896)
38. 1.5 M Tris-HCl pH 8.8 stock solution (made from Tris ultrapure, PanReac/AppliChem, catalog number: A1086, pH adjusted with HCl, Carl Roth, catalog number: X896)
39. Tris ultrapure (PanReac/AppliChem, catalog number: A1086)
40. Triton X-100 (Carl Roth, catalog number: 6683)

41. Tween 20 (Sigma-Aldrich, catalog number: P9416)
42. 5× Protein SDS loading buffer (see Recipes)
43. 10× Protein SDS running buffer (see Recipes)
44. 10× Protein transfer buffer (see Recipes)
45. 10× PBS pH 7.4 (see Recipes)
46. 50× TAE buffer (see Recipes)
47. DEPC-treated water (see Recipes)
48. IP extraction buffer (see Recipes)
49. IP washing buffer (see Recipes)
50. RNA release buffer (see Recipes)
51. 6% 0.5× TAE gel (see Recipes)
52. 10% 0.5× TAE gel (see Recipes)
53. 8% SDS resolution gel (see Recipes)
54. SDS stacking gel (see Recipes)

Equipment

1. Falcon cooling centrifuge with 15 ml and 50 ml adapters (Eppendorf, model: 5810R, catalog number: 5811000325)
2. Funnel (e.g., Plastic funnel, Carl Roth, catalog number: 2041)
3. Growth chamber
4. Hemocytometer (Neubauer counting chamber, Carl Roth, catalog number: PC73.1)
5. Mortar and pestle
6. PAGE electrophoresis system (Mighty small II system, Hoefer Inc., catalog number: SE250)
7. PCR cycler (FlexCycler, Analytik Jena, succession product is Biometra TOne, Analytik Jena)
8. Standard pipettes of 100-1000 µl, 20-200 µl, 2-20 µl and 1-10 µl (Gilson, catalog numbers: F123602, F123601, F123600, F144802)
9. Pipette controller (Integra Biosciences, ordered via VWR, catalog number: 612-0927)
10. Rolling shaker (TRM 50, IDL GmbH, catalog number: 5200330100)
11. Rotator (AG, FINEPCR, no order number found)
12. Small scissors
13. Spatula
14. Spray unit (Carl Roth, catalog number: YC44.1)
15. Tabletop centrifuge for micro tubes (Eppendorf, model: 5424R, catalog number: 5404000410)
16. Table top mixer (Scientific Industries, model: Vortex Genie 2, catalog number: SI-0236)
17. Thermo shaker with 1.5 ml reaction tube adapter (Eppendorf, model: Thermomixer C, catalog number: 5382000015, can be also used as heat block)
18. Wet blot tank system (Mighty small transfer tank, Hoefer Inc., catalog number: TE22)

Software

Software, bioinformatics tools, and databases:

1. Galaxy server (release 19.01)
2. Illumina Demultiplex (Galaxy Version 1.0.0) (alternative tool for demultiplexing: bcl2fastqc https://support.illumina.com/sequencing/sequencing_software/bcl2fastq-conversion-software.html)
3. Clip adaptor sequence (Galaxy Version 1.0.0) (alternative tool for adapter trimming: Trimmomatic [Bolger *et al.*, 2014])
4. Filter FASTQ reads by quality score and length (Galaxy Version 1.0.0)
5. FastQC Read Quality reports (Galaxy Version 0.72)
6. Map with Bowtie for Illumina (Galaxy Version 1.1.0)
7. SAM to FASTQ creates a FASTQ file (Galaxy Version 1.56.1)
8. Filter with SortMeRNA of ribosomal RNAs in metatranscriptomic data (Galaxy Version 2.1b.6)
9. Collapse FASTA sequences (Galaxy Version 1.0.0)
10. TAPIR: target prediction for plant microRNAs (Bonnet *et al.*, 2010)
11. *A. thaliana* TAIR10.0 genome sequence, cDNA sequences
12. *H. arabidopsidis* Noks1 (PRJNA298674), Noks1 is a single spore isolate from a Noco2 sample (Bailey *et al.*, 2011)

Procedure

Note: Figure 1 provides an overview scheme of the protocol wet-lab part for your consideration. Plant AGO/sRNA co-immunopurification does not require in vivo cross-linking. Before starting, we suggest carefully read the entire protocol. During the procedure, work as quickly as possible, on ice and in a 4 °C cold room, when possible, in order to prevent RNA or protein degradation.

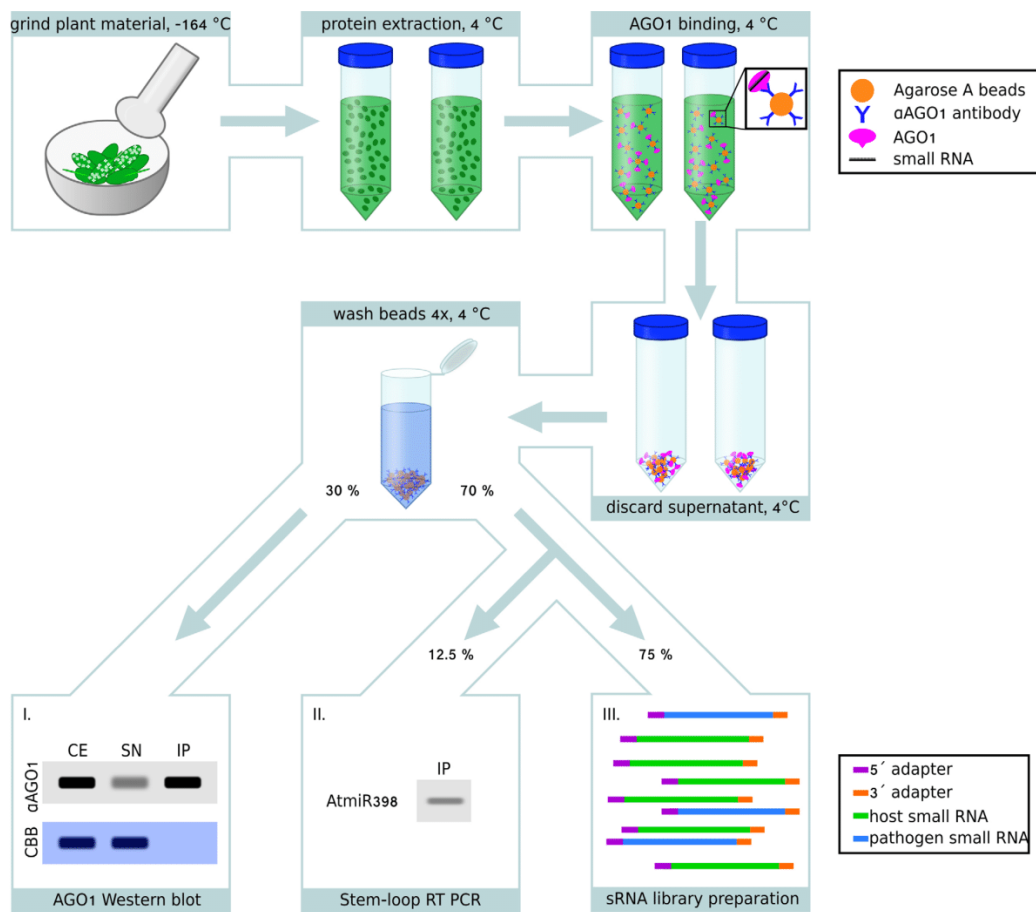


Figure 1. Schematic workflow of plant AGO co-IP for sRNA analysis. *A. thaliana* seedling leaves infected with *H. arabidopsidis* were ground under liquid nitrogen with pestle and mortar. After adding the IP extraction buffer to the ground leaf material, *A. thaliana* AGO1 proteins were immunopurified (IP) using an AGO1-specific antibody and Protein A agarose beads. After washing the beads, IP samples were used for Western blot analysis and small RNA extraction in a sample volume ratio of 30%/70%, respectively. As a quality control for successful IP, AGO1 was tested in the crude extract (CE), in the supernatant (SN), and in the IP fractions by the Western blot analysis, using total protein reference stained by Coomassie Brilliant Blue (CBB) as a loading control (I.), refer to Figure 2 for a Western blot example. As a quality control for successful co-IP and sRNA extraction, an aliquot (12.5%) of the extracted RNA was used for stem-loop RT PCR amplifying the *A. thaliana* miR398 (AtmiR398) known to bind AGO1 (II.), refer to Figure 3 for a stem-loop RT PCR example. Upon positive results of protein and RNA quality control experiments, the sRNA library was prepared for Illumina-based sequencing (III.).

A. *A. thaliana* seedling inoculation with *H. arabidopsidis*

Note: We normally perform dual co-IP experiment of a mock-treated and a pathogen-inoculated sample. However, if more samples are to be prepared, we suggest to process them sequentially in

order to prevent protein or RNA degradation. The following inoculation procedure was adapted from Asai et al. (2015).

1. Use 14-day-old *A. thaliana* Col-0 seedlings grown under long-day condition (16 h light/8 h dark) at 22 °C and 60% relative humidity in propagation soil substrate. Prepare 10 squared pots (7 × 8 cm) of seedlings per AGO co-IP experiment to obtain enough leaf material.
2. Collect conidiospores of *H. arabidopsidis* strain Noco2 from *A. thaliana* Col-0 infected seedlings at 7 days post inoculation using small scissors. Pool collected leaves in a 50 ml Falcon tube avoiding any soil particles.
3. Harvested approximately 2 g of infected fresh leaf material and add 10 ml water to wash off the conidiospores from infected leaves by vigorously shaking the Falcon tube. Filter the conidiospore suspension through a Miracloth and estimate conidiospore concentration by counting conidiospores with a hemocytometer using a light microscope. Adjust the conidiospore suspension to a concentration of 2.5×10^4 spores/ml.
4. Evenly spray 10 ml of 2.5×10^4 spores/ml suspension (or water as mock treatment) on top of *A. thaliana* seedlings using a spray unit.
5. Cover the inoculated or mock-treated seedlings with a transparent lid and seal it, for instance with adhesive tape, to keep high humidity for infection. Incubate the seedlings under long-day conditions (16 h light/8 h dark) at 18 °C for 4-7 days.

B. Plant AGO/sRNA co-immunopurification

1. Harvest 5 grams of fresh leaf material at a given time point (in this protocol, we refer to 4 and 7 days post inoculation) with a small pair of scissors and directly transfer leaf material into a pre-cooled mortar containing liquid nitrogen. Grind the leaves into a fine powder with a pre-cooled pestle. Avoid carrying over any soil particles.
2. Once the entire leaf material is powdered, pre-cool a 50 ml Falcon tube and a spatula tip using liquid nitrogen. Transfer the powdered leaf material from the mortar into the Falcon tube using the pre-cooled spatula. Optionally, use a pre-cooled funnel for the transfer. Double-check that all liquid nitrogen has been evaporated before closing the Falcon tube with the plastic lid to avoid explosion of the tube. Place the closed Falcon tube back into liquid nitrogen.
3. Place the Falcon tube from the liquid nitrogen into an ice box and add immediately 20 ml of immunopurification (IP) extraction buffer per 5 grams leaf fresh weight. Due to low temperature of the sample, the IP extraction buffer might freeze at this step. Close the Falcon tube again and thoroughly mix the leaf material in the buffer by placing it on a rolling shaker in a 4 °C cold room to let it thaw. Thawing might take up to 50 min.
4. Double-check that thawing is complete, before proceeding.
5. From this step onwards, always keep the sample placed on ice. Spin-down the leaf debris at $3,200 \times g$ for 15 min using a pre-cooled (4 °C) centrifuge.
6. In a 4 °C cold room, filter the supernatant through a two-layered Miracloth into a new Falcon tube with the help of a glass pipette to remove the cell debris. At this point, split a sample into

two aliquots of 10 ml each. Set aside a 200 μ l aliquot from this filtered crude extract (CE = input sample) for Western blot analysis. Mix the Western blot sample with 50 μ l 5 \times protein SDS loading buffer and boil it for 5 min at 95 $^{\circ}$ C in a thermo shaker. Store the Western blot sample at -20 $^{\circ}$ C until further use.

7. To continue with AGO co-immunopurification, add 5 μ g anti-AGO1 antibody per 5 g original leaf tissue weight as well as 200 μ l of protein A agarose beads to the crude extract. Incubate the sample on a rotation wheel for 2 h in a 4 $^{\circ}$ C cold room.

Note: The Protein A agarose beads in the Materials list are provided being pre-equilibrated and ready to use by the manufacturers. Read carefully the manufacturers' manual on how to use this product.

8. Spin-down the sample in a pre-cooled centrifuge at 200 \times g and 4 $^{\circ}$ C for 30 s. Take a 200 μ l aliquot from the supernatant (SN = unbound fraction) for Western blot analysis. Mix the Western blot sample with 50 μ l 5 \times protein SDS loading buffer and boil it for 5 min at 95 $^{\circ}$ C. Store the Western blot sample at -20 $^{\circ}$ C until further use.
9. To continue with AGO co-IP, discard the rest of the supernatant. Add 1 ml of ice-cold IP wash buffer to the pelleted beads of the sample, carefully resuspend the beads by pipetting up and down and unify the two sample aliquots into a single 2 ml micro tube.
10. Spin down the sample in a pre-cooled centrifuge at 200 \times g and 4 $^{\circ}$ C for 30 s. Remove the supernatant and wash the pelleted beads with 1 ml freshly prepared, ice-cold IP wash buffer by pipetting up and down.
11. Repeat the washing step of the pelleted beads 3 more times.
12. Resuspend the pelleted beads in 1 ml wash buffer and transfer 300 μ l (30% of the sample volume) into a new micro tube for Western blot analysis (IP = immunopurified fraction), keeping the remaining 700 μ l (70% of the sample volume) for RNA extraction. Spin-down both sample aliquots and discard the supernatant.
13. Add 50 μ l of 1 \times protein SDS loading buffer (prepared from 5 \times protein SDS loading buffer by diluting with IP wash buffer) to the pelleted beads of the Western blot sample. Boil the beads with the loading buffer for 5 min at 95 $^{\circ}$ C. Store the Western blot sample at -20 $^{\circ}$ C until further use.

C. sRNA recovery from co-immunopurified AGO1 bound to Protein-A agarose beads

Note: Adequate personal protection is mandatory during this part of the protocol since toxic chemicals such as Proteinase K, SDS, phenol, and chloroform are used. Dispose all toxic chemicals according to local legislation.

1. Add 300 μ l of IP wash buffer and resuspend the pelleted beads by pipetting up and down. Add 150 μ l of RNA release buffer. Incubate the sample in a thermo shaker at 300 rpm and 65 $^{\circ}$ C for 15 min.
2. Add 450 μ l water-saturated phenol and mix the samples using a vortexer for 2 min.

3. Separate the phenol-water phases by centrifugation at 10,000 × g at room temperature for 8 min, and transfer the upper aqueous phase including the RNA into a new micro tube.
4. Add 450 µl of Phenol/Chloroform/Isoamylalcohol (PCI) mixture (25:24:1) to the RNA sample, invert the sample 10 times and separate the PCI-water phases by centrifugation at 10,000 × g and room temperature for 8 min, and transfer the upper aqueous phase containing the RNA into a new micro tube.
5. Repeat the Step C4 two additional times, using Chloroform/Isoamylalcohol mixture (24:1) instead of the PCI. Take great care to avoid carry-over of any traces of the organic phase before starting RNA precipitation. Optionally from this step on, DNA/RNA LoBind® plastic ware can be used to reduce RNA loss.
6. Precipitate the RNA of the sample by adding in the given order 0.1× volume 3 M sodium acetate, 2.5× volume 96% ethanol, and 20 µg Glycogen (RNA grade). Upon mixing, place the sample at -20 °C for a minimum of 1 h for RNA precipitation.
Note: This is a safe stopping point. RNA samples can be stored in 80% ethanol at -20 °C.
7. Pellet the RNA by centrifugation at 20,000 × g and 4 °C for 30 min, and wash the RNA pellet with 500 µl 80% ethanol diluted in DEPC-treated water.
8. Pellet the RNA by centrifugation at 20,000 × g and 4 °C for 20 min, remove all liquids and air-dry the RNA pellet until ethanol is completely evaporated.
Note: Optionally, the RNA pellet can be dried faster in an open-cap micro tube at 37 °C. However, avoid "over-drying" the RNA pellet.
9. Resuspend the RNA pellet in 8 µl DEPC-treated water. Completely resolve the RNA pellet by incubating the sample for 5 min at 65 °C.
10. Store the remaining RNA for the library preparation at -80 °C for up to 3 months.
Note: Optionally, we recommend to perform stem-loop reverse transcription PCR to detect A. thaliana microRNA(s) of choice in the AGO co-IP sample as a quality control on the successful recovery of sRNAs before starting the sRNA library cloning (see Figure 3).

D. Western blot analysis for AGO1 co-immunopurification quality control

Note: The following steps guide through standard Western blot to analyze the three sample types collected throughout the AGO co-immunopurification procedure (crude extract, supernatant, immunopurification). This analysis is essential to confirm efficient AGO purification. In this protocol, Western blots results were visualized on an LI-COR Odyssey detection system. However, any standard protocol for protein identification by Western blot can be used as well.

1. Assemble a protein gel electrophoresis chamber and fill it with protein running buffer. Load 20 µl per sample of the crude extract from Step B6 (CE), the supernatant (SN) after agarose bead collection from Step B8, and of the AGO co-IP (IP) from Step B13 on an 8% polyacrylamide gel. Load 3 µl of a pre-stained protein size marker on the same gel.

Note: For standard protein SDS polyacrylamide gel electrophoresis (PAGE), we used a Rotiphorese acrylamide/bis-acrylamide solution, APS, and TEMED to prepare a discontinuous gel consisting of a 2 ml collection gel at pH 6.8 and a 7 ml separation gel at pH 8.8.

2. Initiate the SDS-PAGE run for 30 min at ~10 V/cm, then increase the voltage to ~17.5 V/cm and let the PAGE run until the 50 kilo-Dalton (kDa) band of the protein size marker reaches the edge of the gel (electrophoresis run takes approximately 90 min).
3. Disassemble the PAGE gel from the electrophoresis chamber and measure the gel size dimensions. Prepare two blotting papers and a PVDF blotting membrane of the measured gel size. Equilibrate the blotting papers and two sponges in the protein transfer buffer for 5 min. Activate the blotting membrane by submerging in 96% ethanol for 1 min and quickly wash-off the ethanol with water. Equilibrate the blotting membrane in the protein transfer buffer until use.

Note: Use a PVDF membrane that is compatible with the Odyssey detection method.

4. Assemble the blotting sandwich in the following order: i) cathode, ii) sponge, iii) blotting paper, iv) polyacrylamide gel, v) PVDF membrane, vi) blotting paper, vii) sponge, viii) anode. Fill the complete blotting tank with protein transfer buffer. Set the amperage to 1 mA cm⁻² of blotting membrane surface and perform blotting of the proteins overnight in a 4 °C cold room.
5. On the following day, increase the amperage to 2 mA cm⁻² for 30 min. This step might increase the focus of protein bands.
6. Disassemble the blotting sandwich and roll the membrane with the blotted site to the inside to fit in a 50 ml Falcon tube. Add 10 ml of 5% (v/v) skim fat milk in 1× PBS. Block the membrane for 1 h in a 4 °C cold room on a rolling shaker.
7. Discard the blocking solution and quickly wash the blotting membrane with 1× PBS. Add 4 ml of primary antibody solution (anti AtAGO1 1 µg/µl diluted 1:4,000 in 1% milk in a 0.1% PBST buffer) and incubate on a rolling shaker overnight in a 4 °C cold room.
8. Wash the blotting membrane 4 times each for 5 min on a rolling shaker in a 4 °C cold room with 10 ml of 0.2% PBST buffer.
9. Remove the PBST washing buffer and add 5 ml of secondary antibody solution (anti-rabbit IRdye800 (1 µg/µl) diluted 1:3,000 in 1% milk in a 0.1% PBST with 0.02% SDS). Incubate on a rolling shaker for 1-2 h at room temperature.
10. Wash the blot 4 times each for 10 min on a rolling shaker in a 4 °C cold room with 10 ml of 0.2% PBST.
11. Take the membrane out of the Falcon tube and rinse the blotting membrane for 1 min with water and let it dry between two blotting papers. Scan the membrane using an LI-COR Odyssey Scanning device. The band of AGO1 appears at ~130 kDa.

Note: A representative example of a Western blot analysis is displayed in Figure 2. Samples with low AGO signal intensity might still be valid for sRNA library cloning and high throughput sequencing.

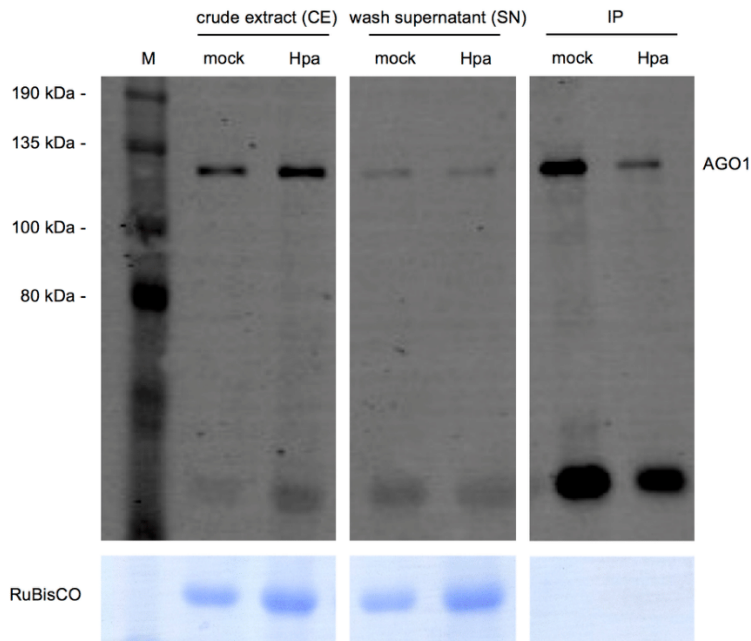


Figure 2. Quality control of AGO1 immunopurification by Western blotting. Three sample fractions of the AGO1 co-IP experiment were analyzed: crude extract (CE), supernatant (SN), and the IP fraction. These three fractions were analyzed in an *A. thaliana* mock-treated and in an *H. arabidopsidis*-infected (Hpa) sample. The top figure shows the detection of *A. thaliana* AGO1 using an AGO1-specific antibody at the expected size of ~130 kDa. Note that AGO1 signals were stronger in IP fractions than in SN. The bottom figure displays the ribulose-1,5-bisphosphate carboxylase/-oxygenase (RuBisCO) signal from a Coomassie Brilliant Blue total protein staining of the Western blot membrane. Note that RuBisCO signals disappeared in the IP fraction. The broad range pre-stained protein marker was used as a protein size marker (M).

E. *A. thaliana* miRNA stem-loop reverse transcription (RT) PCR for AGO/sRNA co-immunopurification quality control

Note: Before proceeding with library preparation, it is recommended to validate successful RNA co-immunopurification by stem-loop RT PCR. We use the Arabidopsis miR398 known to bind AGO1. The protocol directly follows the stem-loop RT PCR protocol as previously described (Varkonyi-Gasic et al., 2007).

1. Use 1 μ l of your eluted RNA (12.5% sample volume) for this quality control assay and pipet it into a PCR micro tube. Add the following components to your RNA sample:
 - 1 μ l of AtmiR398-specific stem-loop RT primer (1 μ M), for the sequence design of stem-loop RT primers, refer to Varkonyi-Gasic et al. (2007)
 - 0.5 μ l of dNTP mix (10 mM each)
 - 8 μ l DEPC-treated water

Heat the sample to 65 °C for 5 min in a PCR cyclor. Cool it down on ice for 1 min.

Add the following components per sample:

- 4 μ l 5 \times first strand SuperScript III reaction buffer
- 2 μ l DTT (0.1M)
- 4 μ l MgCl₂ (25 mM)
- 0.25 μ l SuperScript III[®] reverse transcriptase
- 0.25 μ l RiboLock

2. Run the following thermo cycler protocol:

- step 1 16 °C 30 min
- step 2 30 °C 30 s
- step 3 42 °C 20 s
- step 4 50 °C 1 s; back to step 2 (60x)
- step 5 85 °C 10 min
- step 6 End

Note: The final end-point PCR can be performed with any standard Taq-Polymerase. Below, a protocol using the GoTaq[®] Polymerase is described.

3. Amplify the reverse transcribed miRNA by end-point PCR. Dilute your stem-loop RT product 1:10 with water as a PCR template.

4. Pipet the following components into a PCR micro tube:

- 3 μ l 5 \times Green GoTaq[®] reaction buffer
- 0.3 μ l dNTP mix (10 mM each)
- 0.5 μ l miR398 forward primer (10 μ M), for the sequence design of sRNA forward primer, see Varkonyi-Gasic *et al.* (2007).
- 0.5 μ l universal stem-loop reverse primer (10 μ M), primer sequence according to Varkonyi-Gasic *et al.* (2007).
- 9.5 μ l water
- 0.2 μ l GoTaq[®] G2 Polymerase
- 1 μ l stem-loop RT product (1:10 diluted in water)

5. Perform the following thermo cycler protocol:

- step 1 94 °C 2 min
- step 2 94 °C 30 s
- step 3 60 °C 30 s
- step 4 72 °C 20 s; back to step 2 (36 \times)
- step 5 72 °C 2 min
- step 6 End

6. Prepare a 10% 0.5 \times TAE polyacrylamide gel. Assemble a gel electrophoresis running system. Fill it with 0.5 \times TAE running buffer.

7. Load 7 μ l of each sample in a pocket of the polyacrylamide gel. Pipet 2 μ l of 10 bp O'RangeRuler as size marker on the same gel.

8. Run the gel at ~18 V/cm for 90 min to separate PCR products.

- Disassemble the running chamber and stain the gel with ethidium bromide or any other substitutive DNA dye (e.g., SYBR Gold) for 3 min. If the AGO/sRNA co-immunopurification was successful, you should obtain a PCR band at the size of 69 bp. As an example, a stem-loop RT PCR result of AtmiR398 from an AGO1 co-IP sample is shown in Figure 3.

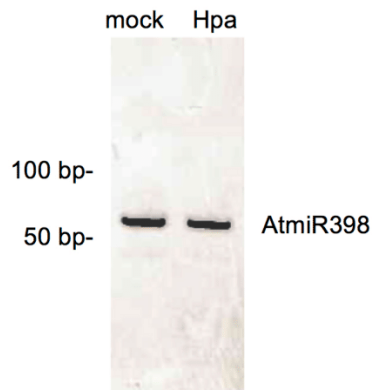


Figure 3. Quality control of sRNAs extracted from AGO1 co-IP samples. For both mock-treated and *H. arabidopsidis*-infected (Hpa) AGO1-co-IP RNA samples, stem-loop RT PCR was performed to detect the AGO1-bound *A. thaliana* AtmiR398. A PCR band of the expected size of 69 base pairs (bp) was visible for both samples. A 10 bp O'RangeRuler DNA ruler was used as a size marker. Depicted samples represent *A. thaliana* leaf materials harvested at 4 days post treatment.

F. sRNA library cloning for Illumina next generation sequencing

Note: We used the NEBNext® Multiplex Small RNA Library Prep Set for Illumina to perform library preparation that is suitable for non-modified as well as modified sRNAs, such as 3' terminal 2'-O-methylation. The protocol is a reprint of the original manufacturer's protocol with slight modifications we applied for AGO co-IP sRNA library cloning. In case library kit protocols are updated by the manufacturer, we recommend to consider the updated instructions.

- Dilute the required amount of 3' SR adaptor (supplied by NEB kit) 1:2 in nuclease-free water. Mix the following per sample in a 1.5 ml LoBind® reaction tube:
6 µl RNA from the AGO co-IP (75% of the eluted RNA sample volume)
1 µl diluted 3' SR adaptor
- Incubate the tube for 2 min at 70 °C in a thermo block.
- Add the following:
10 µl 3' Ligation reaction buffer (2×) (supplied by NEB kit)
3 µl 3' Ligation enzyme mix (supplied by NEB kit)
- Incubate the sample reaction for 18 h at 16 °C.

Note: This prolonged reaction time is recommended to increase the ligation efficiency of methylated sRNAs.

5. Dilute the SR RT primer (supplied by NEB kit) 1:2 in nuclease-free water.
6. Add the following components to the 3'-adaptor/RNA ligation mix (Step F4):
 - 4.5 μ l nuclease-free water
 - 1 μ l diluted SR RT primer
7. Incubate the mixture for 5 min at 75 °C. Transfer the tube to 37 °C for 15 min, then to 25 °C for 15 min.
8. In the meantime, resuspend the lyophilized 5' SR adaptor (supplied by NEB kit) in 120 μ l of nuclease-free water. Store 20 μ l aliquots of the adaptor solution at -80 °C.
9. Mix the required amount of 5' SR adaptor (supplied by NEB kit) in a 1:1:1 ratio with nuclease-free water and 10 mM ATP in a 200 μ l PCR tube. Store remaining adaptor solution at -80 °C.
10. Incubate the 5' SR adaptor mix (Step F9) in a thermo cycler for 2 min at 70 °C, and place the mix on ice immediately. Use the denatured adaptor mix for the following ligation reaction within 30 min.
11. Add the following components to the reaction tube from Step F7:
 - 1 μ l 5' SR adaptor mix (Step F10)
 - 1 μ l 10 \times 5' ligation reaction buffer (supplied by NEB kit)
 - 2.5 μ l 5' ligation enzyme mix (supplied by NEB kit)
12. Incubate reaction mix for 1 h at 25 °C in a heat block.
13. After this incubation step, add the following components to the reaction and mix well:
 - 8 μ l first strand synthesis reaction buffer (supplied by NEB kit)
 - 1 μ l murine RNase inhibitor (supplied by NEB kit)
 - 1 μ l ProtoScript II reverse transcriptase (supplied by NEB kit)
14. Incubate for 60 min at 50 °C. Stop RT reaction at 70 °C for 15 min.
15. Add the following components to the cDNA and mix well:
 - 50 μ l LongAmp Taq 2 \times master mix
 - 2.5 μ l SR primer for Illumina
 - 2.5 μ l Index primer (use a distinct Index primer for each treatment)

Note: As PCR performs better in small reaction volumes, we run 20 μ l reaction volumes. After the PCR run was completed, samples were pooled before further procedure.
16. Amplify the library using the following PCR protocol:
 - step 1 94 °C 30 s
 - step 2 94 °C 15 s
 - step 3 62 °C 30 s
 - step 4 70 °C 15 s; back to step 2 (18-22 \times)
 - step 5 70 °C 5 min
 - step 6 End

Note: The expected size of a PCR product representing cloned 21 nucleotides sRNAs is ~140 base pairs. Nevertheless, the PCR product sometimes appears smeary at this point.

G. Purification of the sRNA library for Illumina sequencing

1. Add 0.1× volume 3 M sodium acetate in DEPC-treated water to the PCR reaction in a 1.5 ml LoBind® reaction tube followed by 2.5× volume of ethanol (96%) and 20 µg glycogen. After mixing the solution, incubate the sample for a minimum of 1 hour at -20 °C.
2. Prepare a 6% 0.5× TAE polyacrylamide gel.
3. Pellet the sRNA library DNA by centrifugation at 20,000 × g and 4 °C for 30 min. Remove the supernatant and add 500 µl of 80% ethanol diluted in DEPC-treated water.
4. Repeat pelleting the sRNA library DNA by centrifugation at 20,000 × g and 4 °C for 20 min, remove all liquid from the sample and air-dry the pellet until the ethanol completely evaporated.
Note: Optionally, the DNA pellet can be dried faster in an open-cap micro tube at 37 °C, however, avoid "over-drying" the DNA pellet.
5. Resuspend the DNA pellet in 25 µl DEPC-treated water. Incubate the sample for 5 min at 65 °C, if you encounter problems with bringing DNA pellet in solution.
6. Mix the eluted library DNA sample with 5 µl of 6× gel loading dye (supplied by NEB kit). Mix the 6× gel loading dye well prior usage.
7. Assemble a gel electrophoresis running system. Fill the electrophoresis tank with 0.5× TAE running buffer.
8. Load 5 µl of the Quick-load pBR322 DNA-MspI digest size marker (supplied by NEB kit) on the same polyacrylamide gel.
9. Use two gel slots per sample by loading 15 µl per well to avoid overloading of the gel lane.
10. Perform gel electrophoresis run with 15 ~V/cm for 60 min; after this running time, the bromophenol blue dye of the loading buffer typically reaches the bottom edge of the gel.
11. Disassemble the gel cast and stain the polyacrylamide gel with ethidium bromide or any other substitutive DNA dye (e.g., SYBR Gold) for 3 min. Under a UV documentation station, cut out the DNA band of the gel at the size of 140-150 base pairs. Avoid any DNA band at ~120 base pairs, as this size usually represents adaptor dimers.
12. Place the gel piece into a new 1.5 ml DNA LoBind® reaction tube. Use a blue pipette tip to crush the gel piece. Add 250 µl of 1× gel elution buffer (supplied by NEB kit).
13. Elute the sRNA library DNA from the crushed gel pieces by rotating the sample for 2 h at room temperature or overnight in a 4 °C cold room.
14. Spin the sample at 10,000 × g and room temperature for 10 min, and transfer the supernatant into a new 1.5 ml DNA LoBind® reaction tube. Try to collect all liquids from the reaction tube.
15. Repeat spinning the sample at 10,000 × g at room temperature for 10 min, and transfer the supernatant into a new 1.5 ml DNA LoBind® reaction tube. At this step, avoid transferring any remaining gel pieces.
16. Add 0.1× volume 3 M sodium acetate in DEPC-treated water, 2.5× volume of 96% ethanol, and 20 µg of glycogen. For DNA precipitation, mix the solution and incubate the sample for a minimum of 30 min at -80 °C.
17. Prepare a 6% 0.5× TAE polyacrylamide gel.

18. Pellet library DNA by centrifugation at 20,000 × *g* and 4 °C for 30 min. Discard the supernatant and add 500 µl of 80% ethanol diluted in DEPC-treated water.
19. Pellet the DNA by centrifugation at 20,000 × *g* and 4 °C for 20 min, remove all liquids and air-dry the DNA pellet until ethanol is completely evaporated.
Note: Optionally, the DNA pellet can be dried faster in an open-cap micro tube at 37 °C, however, avoid “over-drying” the DNA pellet.
20. Resuspend the DNA pellet in 25 µl DEPC-treated water. Incubate the DNA pellet for 5 min at 65 °C, if encounter problems with bringing the pellet in solution.
21. Repeat the gel clean-up of library DNA, following the Steps G6-G18.
22. Store purified library DNA in 80% ethanol at -20 °C, until sequencing.
Note: Storage of library DNA is valid for up to 12 months.
23. To proceed with sequencing, precipitate the library DNA by centrifugation at 20,000 × *g* and 4 °C for 20 min, remove all liquids and air-dry the pellet until ethanol is completely evaporated.
Note: In this last step, do not use DEPC-treated water for DNA pellet resuspension as it can interfere with Illumina sequencing; instead use nuclease free water (supplied by the NEB kit).
24. Resuspend the sample in nuclease free water for Illumina HiSeq run.
Note: For sRNA library sequencing, we used an Illumina HiSeq1500 platform in single-end mode with 50 base read length. To obtain sufficient read numbers of pathogen sRNAs collected from infected plant tissue, we recommend to sequence minimum at a depth of 50 million reads per library.

H. sRNA Illumina sequencing analysis

*Note: An overview workflow of the bioinformatics part of this Bio-protocol is shown in Figure 4. sRNA sequencing data were analyzed using a Galaxy Server (Giardine et al., 2005). All tools of the analysis pipeline are also freely available as stand-alone versions, except the Illumina demultiplexing package and the Clip adapter script. As an adequate substitution of these steps, the Illumina bcl2fastqc tool and Trimmomatic can be used, respectively. In the following, a step-by-step description of the bioinformatics pipeline is given for the recovery and identification of *H. arabidopsidis* sRNA sequences bound to *A. thaliana* AGO1 during infection, including a target prediction of *A. thaliana* mRNAs using identified *H. arabidopsidis* AGO1-bound sRNA sequences. As indicated in Figure 4, a similar analysis can be run to predict plant mRNA targets of endogenous *A. thaliana* small RNAs.*

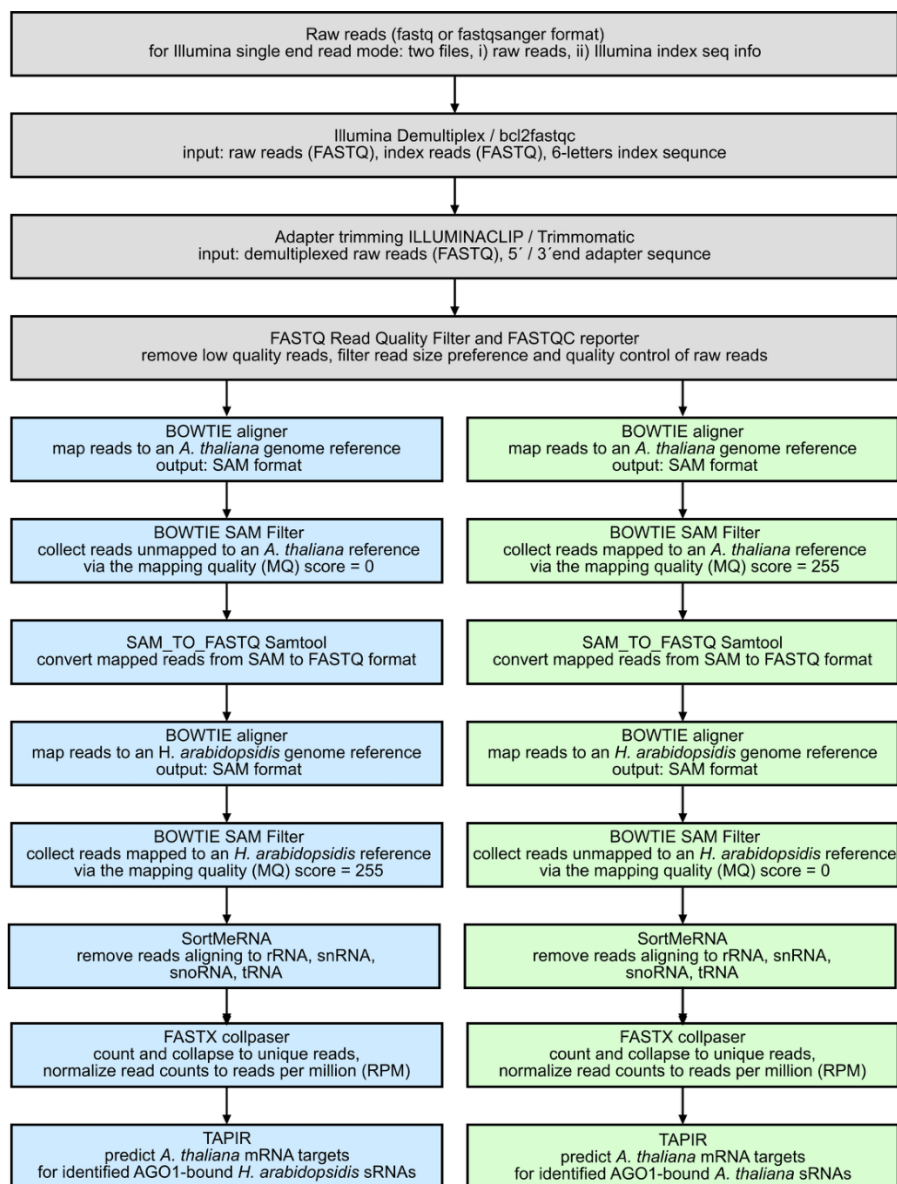


Figure 4. Bioinformatics workflow to analyze AGO1 co-IP sRNA NGS data. After standard processing of sRNA raw reads, sequences can be grouped into pathogen-derived sRNAs (*H. arabidopsidis*) and host plant-derived (*A. thaliana*) sRNAs for further analysis.

1. If applicable; demultiplex sRNA libraries using the Illumina Demultiplex or the bcl2fastqc tool by giving the library sequence indices.
2. Remove 3'-end adapter sequences from sRNA reads using Clip adapter or the ILLUMINA CLIP function of Trimmomatic (Bolger *et al.*, 2014).
3. Remove low quality reads by setting a minimum Phred quality score of 30.0 and a size range from 19-30 nucleotides using the FASTQ Filter tool (Blankenberg *et al.*, 2010). The FASTQ_filter command is also available as part of the USEARCH package

(<https://drive5.com/usearch/features.html>).

Note: Optionally, useful information on sRNA sequencing quality can be found by consulting the FastQC reporter tool at any step of the bioinformatics analysis.

4. To remove *A. thaliana* sRNA reads from the dataset, align the raw reads to the *A. thaliana* reference genome (e.g., TAIR10 for ecotype Col-0) using the Bowtie aligner (Langmead *et al.*, 2009). We recommend allowing one mismatch (-v 1) to map reads to the *A. thaliana* reference genome. By this step, a mapping quality score (MQ) is attributed to individual reads with a score of 255 (aligned) or 0 (unaligned) given in a SAM format output file.
5. Collect reads with MQ = 0, as these reads do not align to the *A. thaliana* reference genome using the Filter_tool (Galaxy Version 1.1.0).
6. Convert the SAM file (unaligned to *A. thaliana*) into a FASTQ file format using the SAM_to_FASTQ tool with SAMtools (Li *et al.*, 2009).
7. Use the Bowtie aligner to align reads from Step H6 to an *H. arabidopsidis* Noks1 reference genome (PRJNA298674), allowing zero mismatch (-v 0).
8. Collect reads with MQ = 255, as these read aligned to the *H. arabidopsidis* reference genome, using the Filter_tool (Galaxy Version 1.1.0).

Note: We do not recommend to use the Bowtie2 short-read aligner, as this version does not allow binary mapping scores (aligned or unaligned), rather attributes low MQ values to reads with multiple alignment events. Many pathogen sRNAs that we found being loaded into plant AGOs are derived from repetitive DNA, thus such sequences could be easily lost through Bowtie2 quality aware mapping.

9. As a quality control for the successful *A. thaliana* AGO1-co-IP sRNA sequencing, display read counts aligning to the *A. thaliana* reference genome (go back to Step H5 and collect reads with MQ = 255), by read length and 5'-prime nucleotide distribution. *A. thaliana* AGO1 preferentially binds 21 nt sRNAs with 5' prime uracil. This analysis can be run by the FastQC tool, as shown in Figure 5.

*Optionally, remove reads from your dataset (Step H8) that align to ribosomal RNA (rRNA), transfer RNA (tRNA), or small nuclear/nucleolar RNA (snRNA, snoRNA) sequences using the SortMeRNA tool (Kopylova *et al.*, 2012). In particular, rRNA-derived sRNA reads often occur in high abundance in sRNA library sequencing data, if no riboRNA-depletion was performed prior to RNA cloning.*

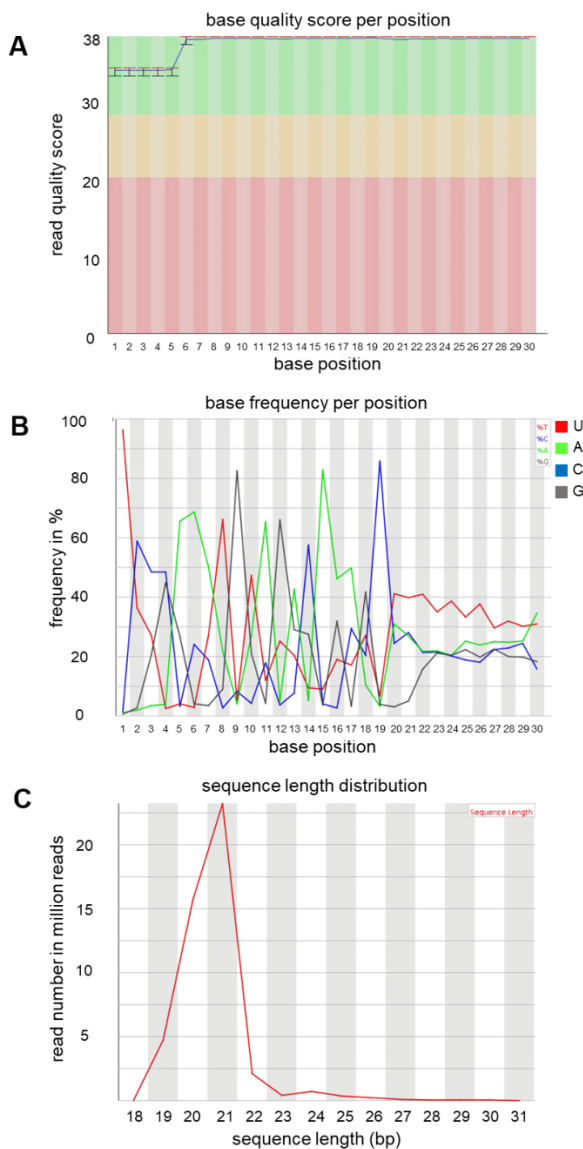


Figure 5. FastQC report of AGO1 co-IP sRNA NGS data. As plant AGOs are typically associated to distinct sRNA classes, AGO1 co-IP sRNA NGS data reflect some unique features that can be used as a quality control in such experiments. High quality (> 30 Phred score) sRNA reads of the size range of 19-30 bases were collected (A). AGO1-associated sRNAs showed preference to 5' prime Uracil U – in sRNA sequencing data Thymine T (B), and to a size of 21 nucleotides (C). Graphs shown here represent an AGO1 co-IP sample collected from *H. arabidopsidis*-infected *A. thaliana* at 4 days post inoculation. The total read number of this sRNA library was 51,089,216.

- Count and unify sRNA reads to unique sequence tags using a collapse tool, e.g., the FASTX-toolkit (http://hannonlab.cshl.edu/fastx_toolkit/index.html).

11. Transform read numbers of unique sRNA sequences into reads per million (rpm) by normalizing to the total library read numbers (referring to the organism of interest, here *H. arabidopsidis*).
Note: Before starting mRNA target prediction, it can be useful to apply an abundancy filter of small RNA reads.
12. For predicting mRNA targets of candidate sRNAs, several target prediction tools were implemented. We have used the TAPIR tool (Bonnet *et al.*, 2010) to predict *A. thaliana* mRNA targets of *H. arabidopsidis* sRNA candidates using an *A. thaliana* cDNA dataset. For target prediction, a maximal score of 4.5 penalizing mismatches in the mRNA/sRNA base pairing, and a maximal free energy ratio of 0.7 were set as thresholds.

Recipes

A. Buffers

1. 5× Protein SDS loading buffer
 - 225 mM Tris-HCl (pH 6.8)
 - 5% (w/v) SDS
 - 50% (v/v) glycerol
 - 0.05% (w/v) bromophenol blue dye
 - 455 mM DTT (added directly before use)
2. 10× Protein SDS running buffer
 - 30 g Tris ultrapure
 - 144 g glycine
 - 10 g SDS
 - Fill up to 1 L with ultrapure water and stir until salts are dissolved
 - The pH does not need to be adjusted
3. 10× Protein transfer buffer
 - 30 g Tris ultrapure
 - 144 g glycine
 - Fill up to 900 ml with ultrapure water and stir until salts are dissolved
 - Adjust the pH to 8.3 with HCl
 - Fill up to 1 L with ultrapure water
4. 10× PBS pH 7.4
 - 80 g NaCl
 - 2 g KCl
 - 14.4 g Na₂HPO₄
 - 2.4 g KH₂PO₄
 - Fill up to 900 ml with ultrapure water
 - Adjust the pH to 7.4 with HCl
 - Fill up to 1 l with ultrapure water

For PBST 0.1% and 0.2% add the respective amount of Tween 20

5. 50× TAE buffer
 - 242 g Tris ultrapure
 - 18.6 g EDTA
 - a. Dissolve in 950 ml of water
 - b. Adjust the pH to 8.0 with glacial acetic acid
 - c. Fill up to 1 L with water
6. DEPC-treated water
 - Add 1 ml DEPC to 1 L of ultrapure water
 - Let it stir overnight
 - Autoclave for 20 min at 121 °C
7. IP extraction buffer
 - 20 mM Tris-HCl (pH 7.5)
 - 300 mM NaCl
 - 5 mM MgCl₂
 - 0.5% (v/v) NP-40
 - 5 mM DTT (add directly before use)
 - 1 tablet protease inhibitor/50 ml sample volume (add directly before use)
 - 5 µl RNase inhibitor (40 U)/50 ml sample volume (add directly before use)
 - Make up to 50 ml with DEPC-treated water
8. IP washing buffer
 - 20 mM Tris-HCl (pH 7.5)
 - 300 mM NaCl
 - 5 mM MgCl₂
 - 0.5% (v/v) Triton X-100
 - 5 mM DTT (add directly before use)
 - 1 tablet protease inhibitor/50 ml sample volume (add directly before use),
 - Fill up to 50 ml with DEPC-treated water
9. RNA release buffer
 - 100 mM Tris-HCl (prepare from 1 M Tris-HCl pH 7.5)
 - 10 mM EDTA (prepare from 0.5 M EDTA pH 8.0)
 - 300 mM NaCl
 - 2% SDS
 - 1 µg/µl Proteinase K (add directly before use).

B. Polyacrylamide gel recipes (for 10 ml gel volume)

Nucleic acid polyacrylamide gel recipes:

1. 6% 0.5× TAE gel

- 7.8 ml H₂O
- 2.0 ml 30% acrylamide/bis-acrylamide solution
- 0.1 ml 50× TAE buffer
- 0.1 ml 10% APS
- 0.008 ml TEMED
- 2. 10% 0.5× TAE gel
 - 6.5 ml H₂O
 - 3.3 ml 30% acrylamide/bis-acrylamide solution
 - 0.1 ml 10% APS
 - 0.1 ml 50× TAE buffer
 - 0.004 ml TEMED

SDS-protein PAGE gel recipes:

1. 8% SDS resolution gel
 - 4.6 ml H₂O
 - 2.7 ml 30% acrylamide/bis-acrylamide solution
 - 2.5 ml 1.5 M Tris-HCl (pH 8.8)
 - 0.1 ml 10% SDS
 - 0.1 ml 10% APS
 - 0.006 ml TEMED
2. SDS stacking gel
 - 2.1 ml H₂O
 - 0.5 ml 30% acrylamide/bis-acrylamide solution
 - 0.38 ml 1.0 M Tris-HCl (pH 6.8)
 - 0.03 ml 10% SDS
 - 0.03 ml 10% APS
 - 0.003 ml TEMED

Acknowledgments

This protocol has been developed to identify *H. arabidopsidis* small RNAs that bind to the *A. thaliana* AGO/RISC during plant infection (Dunker *et al.*, 2020). The authors wish to thank New England Biolabs® for their permission to include the library preparation kit protocol within this protocol. This work was supported by a grant from the Deutsche Forschungsgemeinschaft DFG (WE 5707/1-1) to AW. The funders had no role in the study design, data collection, interpretation, or the decision to publish.

Competing interests

The authors declare no competing interests.

References

1. Asai, S., Shirasu, K. and Jones, J. D. (2015). [Hyaloperonospora arabidopsidis \(Downy Mildew\) infection assay in Arabidopsis](#). *Bio-protocol* 5(20): e1627.
2. Bailey, K., Cevik, V., Holton, N., Byrne-Richardson, J., Sohn, K. H., Coates, M., Woods-Tor, A., Aksoy, H. M., Hughes, L., Baxter, L., Jones, J. D., Beynon, J., Holub, E. B. and Tor, M. (2011). [Molecular cloning of ATR5^{Emoy2} from Hyaloperonospora arabidopsidis, an avirulence determinant that triggers RPP5-mediated defense in Arabidopsis](#). *Mol Plant Microbe Interact* 24(7): 827-838.
3. Blankenberg, D., Gordon, A., Von Kuster, G., Coraor, N., Taylor, J., Nekrutenko, A. and Galaxy, T. (2010). [Manipulation of FASTQ data with Galaxy](#). *Bioinformatics* 26(14): 1783-1785.
4. Bolger, A. M., Lohse, M. and Usadel, B. (2014). [Trimmomatic: a flexible trimmer for Illumina sequence data](#). *Bioinformatics* 30(15): 2114-2120.
5. Bonnet, E., He, Y., Billiau, K. and Van de Peer, Y. (2010). [TAPIR, a web server for the prediction of plant microRNA targets, including target mimics](#). *Bioinformatics* 26(12): 1566-1568.
6. Carbonell, A. (2017). [Immunoprecipitation and high-throughput sequencing of ARGONAUTE-bound target RNAs from plants](#). *Methods Mol Biol* 1640: 93-112.
7. Carbonell, A., Fahlgren, N., Garcia-Ruiz, H., Gilbert, K. B., Montgomery, T. A., Nguyen, T., Cuperus, J. T. and Carrington, J. C. (2012). [Functional analysis of three Arabidopsis ARGONAUTES using slicer-defective mutants](#). *Plant Cell* 24(9): 3613-3629.
8. Dunker, F., Trutzenberg, A., Rothenpieler, J. S., Kuhn, S., Pröls, R., Schreiber, T., Tissier, A., Kemen, A., Kemen, E., Huckelhoven, R. and Weiberg, A. (2020). [Oomycete small RNAs bind to the plant RNA-induced silencing complex for virulence](#). *Elife* 9: e56096.
9. Giardine, B., Riemer, C., Hardison, R. C., Burhans, R., Elnitski, L., Shah, P., Zhang, Y., Blankenberg, D., Albert, I., Taylor, J., Miller, W., Kent, W. J. and Nekrutenko, A. (2005). [Galaxy: a platform for interactive large-scale genome analysis](#). *Genome Res* 15(10): 1451-1455.
10. Kopylova, E., Noé, L. and Touzet, H. (2012). [SortMeRNA: fast and accurate filtering of ribosomal RNAs in metatranscriptomic data](#). *Bioinformatics* 28(24): 3211-3217.
11. Langmead, B., Trapnell, C., Pop, M. and Salzberg, S. L. (2009). [Ultrafast and memory-efficient alignment of short DNA sequences to the human genome](#). *Genome Biology* 10(3): R25.
12. Li, H., Handsaker, B., Wysoker, A., Fennell, T., Ruan, J., Homer, N., Marth, G., Abecasis, G., Durbin, R. and Genome Project Data Processing, S. (2009). [The Sequence Alignment/Map format and SAMtools](#). *Bioinformatics* 25(16): 2078-2079.
13. Mi, S., Cai, T., Hu, Y., Chen, Y., Hodges, E., Ni, F., Wu, L., Li, S., Zhou, H., Long, C., Chen, S., Hannon, G. J. and Qi, Y. (2008). [Sorting of small RNAs into Arabidopsis argonaute complexes](#)

- is directed by the 5' terminal nucleotide. *Cell* 133(1): 116-127.
14. Montgomery, T. A., Howell, M. D., Cuperus, J. T., Li, D., Hansen, J. E., Alexander, A. L., Chapman, E. J., Fahlgren, N., Allen, E. and Carrington, J. C. (2008). [Specificity of ARGONAUTE7-miR390 interaction and dual functionality in TAS3 trans-acting siRNA formation.](#) *Cell* 133(1): 128-141.
 15. Qi, Y. and Mi, S. (2010). [Purification of *Arabidopsis* argonaute complexes and associated small RNAs.](#) *Methods Mol Biol* 592: 243-254.
 16. Varkonyi-Gasic, E., Wu, R., Wood, M., Walton, E. F. and Hellens, R. P. (2007). [Protocol: a highly sensitive RT-PCR method for detection and quantification of microRNAs.](#) *Plant Methods* 3: 12.
 17. Weiberg, A., Bellinger, M. and Jin, H. (2015). [Conversations between kingdoms: small RNAs.](#) *Curr Opin Biotechnol* 32: 207-215.
 18. Zeng, J., Gupta, V. K., Jiang, Y., Yang, B., Gong, L. and Zhu, H. (2019). [Cross-kingdom small RNAs among animals, plants and microbes.](#) *Cells* 8(4): 371.
 19. Zhang, X., Zhao, H., Gao, S., Wang, W. C., Katiyar-Agarwal, S., Huang, H. D., Raikhel, N. and Jin, H. (2011). [Arabidopsis Argonaute 2 regulates innate immunity via miRNA393*-mediated silencing of a Golgi-localized SNARE gene, MEMB12.](#) *Mol Cell* 42(3): 356-366.
 20. Zhao, H., Lii, Y., Zhu, P. and Jin, H. (2012). [Isolation and profiling of protein-associated small RNAs.](#) *Methods Mol Biol* 883: 165-176.

III: An *Arabidopsis* downy mildew non-RxLR effector suppresses induced plant cell death to promote biotroph infection.



RESEARCH PAPER

An Arabidopsis downy mildew non-RxLR effector suppresses induced plant cell death to promote biotroph infection

Florian Dunker*, Lorenz Oberkofler*, Bernhard Lederer, Adriana Trutzenberg and Arne Weiberg†^{ID}

Faculty of Biology, Genetics, Biocenter Martinsried, LMU Munich, Großhaderner Str. 2–4, 82152 Planegg-Martinsried, Germany

* These authors contributed equally to this work.

† Correspondence: a.weiberg@lmu.de

Received 6 July 2020; Editorial decision 5 October 2020; Accepted 13 October 2020

Editor: Peter Bozhkov, Swedish University of Agricultural Sciences, Sweden

Abstract

Our understanding of obligate biotrophic pathogens is limited by lack of knowledge concerning the molecular function of virulence factors. We established Arabidopsis host-induced gene silencing (HIGS) to explore gene functions of *Hyaloperonospora arabidopsidis*, including *CYSTEINE-RICH PROTEIN (HaCR)1*, a potential secreted effector gene of this obligate biotrophic pathogen. *HaCR1* HIGS resulted in *H. arabidopsidis*-induced local plant cell death and reduced pathogen reproduction. We functionally characterized *HaCR1* by ectopic expression in *Nicotiana benthamiana*. *HaCR1* was capable of inhibiting effector-triggered plant cell death. Consistent with this, *HaCR1* expression in *N. benthamiana* led to stronger disease symptoms caused by the hemibiotrophic oomycete pathogen *Phytophthora capsici*, but reduced disease symptoms caused by the necrotrophic fungal pathogen *Botrytis cinerea*. Expressing *HaCR1* in transgenic Arabidopsis confirmed higher susceptibility to *H. arabidopsidis* and to the bacterial hemibiotrophic pathogen *Pseudomonas syringae*. Increased *H. arabidopsidis* infection was in accordance with reduced *PATHOGENESIS RELATED (PR)1* induction. Expression of full-length *HaCR1* was required for its function, which was lost if the signal peptide was deleted, suggesting its site of action in the plant apoplast. This study provides phytopathological and molecular evidence for the importance of this widespread, but largely unexplored class of non-RxLR effectors in biotrophic oomycetes.

Keywords: *Arabidopsis thaliana*, downy mildew, host-induced gene silencing (HIGS), *Hyaloperonospora arabidopsidis*, non-RxLR cysteine-rich protein effectors (CRs), obligate biotrophic plant parasite.

Introduction

Oomycetes include some notorious plant pathogens that severely reduce global crop yield and cause enormous economic loss every year. To date, oomycete pest management relies on inbreeding of *RESISTANCE (R)* genes and chemical plant protection. In this context, the occurrence of new virulent pathogen genotypes that overcome *R* gene-mediated resistance or chemical crop protection jeopardizes food security (Fry, 2008; Cohen *et al.*, 2015; Delmas *et al.*, 2017). Thus, there

is an urgent need for developing innovative, sustainable strategies to control oomycete pests. However, a lack of understanding of pathogen virulence at the molecular level restricts this goal.

In oomycetes, classical forward or reverse genetics approaches remain challenging due to di- or polyploidy, and due to the fact that many oomycetes are obligate biotrophs, like the downy mildew pathogen *Hyaloperonospora*

Abbreviations: CFP, cyan fluorescent protein; CR, cysteine-rich; dpi, days post-inoculation; FITC, fluorescein isothiocyanate; GFP, green fluorescent protein; HIGS, host-induced gene silencing; NLR, nucleotide-binding oligomerization domain-like receptor; *R* gene, resistance gene; RNAi, RNA interference; qRT-PCR, quantitative reverse transcription–polymerase chain reaction; Pst, *Pseudomonas syringae* pv *tomato*; SA, salicylic acid; SP, signal peptide; WT, wild type; YFP, yellow fluorescent protein.

© The Author(s) 2020. Published by Oxford University Press on behalf of the Society for Experimental Biology.

This is an Open Access article distributed under the terms of the Creative Commons Attribution License (<http://creativecommons.org/licenses/by/4.0/>), which permits unrestricted reuse, distribution, and reproduction in any medium, provided the original work is properly cited.

arabidopsidis infecting the model plant *Arabidopsis* (Coates and Beynon, 2010). Obligate biotrophs are impossible to grow in axenic culture despite numerous attempts (McDowell, 2014), and thus genetic transformation of these organisms is not achievable. Alternative approaches to investigating the function of pathogen effectors and other types of virulence genes in obligate biotrophs, which do not rely on pathogen transformation, are therefore highly appreciated. *Hyaloperonospora arabidopsidis* is one of the most used model pathogens to investigate *Arabidopsis* innate immune response to obligate biotrophs and was ranked the second most important oomycete pathogen by researchers in terms of scientific and economic relevance (Kamoun et al., 2015). It is highly adapted and specialized to its sole natural host plant, *Arabidopsis*, and infection frequently occurs in wild *Arabidopsis* plants (McDowell, 2014; Agler et al., 2016).

Genome sequencing of *H. arabidopsidis* uncovered a large repertoire of over 100 putative effector genes suggesting an extensive resource to suppress plant immunity (Baxter et al., 2010) and to enable host cell reprogramming for pathogen accommodation and propagation (Thordal-Christensen et al., 2018). Oomycete effectors are typically classified by sequence features into RxLRs, Crinklers, necrosis-inducing like proteins, elicitors, and if no further sequence homology is apparent, cysteine-rich (CR) proteins (Cabral et al., 2011). Current research in oomycete effectors focuses on RxLRs that are typically translocated into host cells and are relatively easy to predict *in silico* (Anderson et al., 2015). *Hyaloperonospora arabidopsidis* probably employs RxLRs to modulate plant immunity, too (Fabro et al., 2011; Pel et al., 2014). Nevertheless, a defined molecular function of only just a few oomycete effectors has been reported, mainly through ectopic expression *in planta* (Caillaud et al., 2013; Wirthmueller et al., 2018). In addition, non-RxLR effectors presumably contribute to virulence, as well. Nevertheless, *H. arabidopsidis* non-RxLR CR protein effectors remain functionally uncharacterized, despite the fact that they comprise some of the most highly expressed *H. arabidopsidis* genes during infection (Cabral et al., 2011; Asai et al., 2014).

Artificial expression of double-stranded RNA (dsRNA) in host plants can lead to silencing of complementary genes in their pathogens and pests, a strategy known as host-induced gene silencing (HIGS) (Baum et al., 2007; Mao et al., 2007; Koch and Kogel, 2014). Indeed, HIGS is a powerful method of choice for reverse genetics in plant-associated organisms with no transformation protocols available, such as root knot nematodes, mycorrhizal fungi and biotrophic pathogens, like powdery mildew and rust fungi (Nowara et al., 2010; Helber et al., 2011; Pliego et al., 2013; Dinh et al., 2014; Yin and Hulbert, 2018). Regarding oomycetes, an initial HIGS approach in *Arabidopsis* failed to knockdown gene expression of *Phytophthora parasitica* although HIGS small interfering RNA accumulated in the plant (Zhang et al., 2011). Nevertheless, HIGS was successfully introduced in *Solanum tuberosum* (potato) against the hemibiotrophic pathogen *Phytophthora infestans* and in lettuce against the downy mildew pathogen *Bremia lactucae*, conferring plant disease resistance (Govindarajulu et al., 2015; Jahan et al., 2015). Conversely, silencing of the RxLR-type avirulence

gene *Avr3a1* by HIGS allowed infection of resistant tobacco by *Phytophthora capsici* (Vega-Arreguín et al., 2014), highlighting the power of HIGS to enable functional gene studies in plant-oomycete interactions. Recently, HIGS was suggested to induce gene suppression of infecting fungal and oomycete pathogens by plant endogenous small RNAs in *Arabidopsis* and in cotton, proposing a novel RNA-based plant defence mechanism (Zhang et al., 2016; Cai et al., 2018; Hou et al., 2019; Hou and Ma, 2020). In this report, we used *Arabidopsis* HIGS for targeted gene knockdown of the *H. arabidopsidis* *CYSTEINE-RICH (HaCR) 1* and ectopic plant expression of *HaCR1* to explore the function of this non-RxLR CR effector protein in plant-pathogen interactions.

Material and methods

Plant materials and cultivation

Arabidopsis wild type (WT) Col-0, HIGS construct transformants and *Hyaloperonospora arabidopsidis* *HaCR1* overexpression lines were cultivated under long day conditions in a growth chamber (16 h light: 8 h dark, 22 °C and 150 $\mu\text{mol m}^{-2} \text{s}^{-1}$ photon flux density). Fourteen-day-old seedlings were used for *H. arabidopsidis* inoculation.

Arabidopsis effector overexpression lines were cultivated under short day conditions in a walk-in growth chamber (8 h light: 16 h dark, 22 °C and 150 $\mu\text{mol m}^{-2} \text{s}^{-1}$ photon flux density). Five- to six-week-old plants were used for bacterial inoculation.

Wild tobacco (*Nicotiana benthamiana* Domin) plants were grown in a walk-in growth chamber under long day conditions (16 h light: 8 h dark, 22 °C and 275 $\mu\text{mol m}^{-2} \text{s}^{-1}$ photon flux density) for 4 weeks prior to *Agrobacterium tumefaciens*-mediated transformation.

Microorganism cultivation

Hyaloperonospora arabidopsidis Güm. strain Noco2 was maintained on *Arabidopsis* Col-0 seedlings and used for plant inoculation at a concentration of $2\text{--}2.5 \times 10^4$ spores ml^{-1} , as described previously (Ried et al., 2019). *Phytophthora capsici* Leonian strain LT263 (Hurtado-Gonzales and Lamour, 2009) was cultured on rye agar plates (Caten and Jinks, 1968) for 3 d at room temperature before plant inoculation. *Botrytis cinerea* Pers. strain B05.10 was cultured on HA agar plates for 2 d prior to plant inoculation. *Pseudomonas syringae* pv. *tomato* Van Hall (Pst) DC3000 and Pst DC3000 *hrcC*⁻ mutant were cultured on LB agar plates with rifampicin.

Plasmid construction

For HIGS constructs targeting *HaCR1*, *HaACTA*, *HaA1E*, or *HaDCL1*, target gene fragments of 334, 311, 267, and 256 bp length, respectively, were amplified from cDNA using home-made Phusion DNA polymerase. The DNA stretches were tested for off-targets in *Arabidopsis* and *H. arabidopsidis* cDNAs using the Si-Fi2.1 tool (<http://labtools.ipk-gatersleben.de/index.html>) and have a maximum of two off-target small RNAs, as opposed to hundreds of effective on-target small RNAs.

RNA hairpins were cloned under the control of the strong *proLjUBI* promoter using the previously described and validated Golden Gate based RNAi plasmid assembly kit, containing the *Arabidopsis AtWRKY33* intron 1 and the 35S terminator (Binder et al., 2014). Yellow fluorescent protein (YFP; mCherry for green fluorescent protein (GFP)-RNAi hairpin) was used in the final expression vector as an *in planta* transformation marker, and *Agrobacterium tumefaciens* AGL1 was transformed with completed vector constructs via electroporation.

Plasmid constructs for *in planta* expression were also made using the plant Golden Gate plasmid assembly kit (Binder et al., 2014). The coding sequence of *HaCR1* was obtained by PCR amplification of *H. arabidopsidis* cDNA with Phusion High-Fidelity Polymerase (New

England Biolabs, Frankfurt, Germany). The *HaCR1* coding sequence lacking the signal peptide was amplified with home-made Taq DNA polymerase, as Phusion polymerase did not result in any amplification. Taq amplicons were blunted using Phusion DNA polymerase. All PCR products were validated by Sanger sequencing (LMU Genomics service unit, Planegg, Germany) before expression vector assembly.

The binary expression vector was assembled by ligation of the C-terminal GFP-tagged full-length or signal peptide-deleted *HaCR1* sequences under the control of the *proLjUBI* promoter. As a control, a vector expressing only GFP was constructed. A list of primers used for the construction of plasmids is provided in Supplementary Table S1 at JXB online.

Arabidopsis transformation

Arabidopsis Col-0 plants were transformed by the floral dip method with *A. tumefaciens* strain AGL1, as described previously (Clough and Bent, 1998). Transformants from effector overexpression experiments were selected by kanamycin resistance on ½ MS agar plates with 1% sucrose and 50 mg l⁻¹ kanamycin, as described previously (Harrison *et al.*, 2006). Transformants expressing HIGS constructs were selected at the seedling stage by YFP fluorescence using a fluorescence stereo microscope. All experiments were performed on transgenic *Arabidopsis* plants in the T₂ generation.

Trypan Blue staining

Infected leaves were stained to visualize oomycete infection structures with Trypan Blue (Sigma-Aldrich, Steinheim, Germany), as previously described (Koch and Slusarenko, 1990). Leaves were de-stained with saturated chloralhydrate (Sigma-Aldrich) and imaged on a CTR 6000 microscope (Leica Microsystems, Wetzlar, Germany) with a DFC450 CCD-Camera (Leica).

RNA isolation, cDNA synthesis, and quantitative PCR

For DNA or RNA analysis, five *Arabidopsis* leaves from infected plants were pooled into one biological replicate, frozen in liquid nitrogen, and ground to powder using steel beads and a bead mill (MM400, Retsch, Haan, Germany). RNA was isolated using a modified cetyltrimethylammonium bromide-based protocol (Bemm *et al.*, 2016). DNA digestion was performed on 1 µg total RNA using RNase-free DNase I (Thermo Fisher Scientific, Vilnius, Lithuania) after the manufacturer's instructions. For cDNA synthesis, SuperScript III (Thermo Fisher Scientific) and oligo-dT primers (50 µM) were used, following the manufacturer's instructions. Gene expression was determined by quantitative PCR (qPCR) using the EvaGreen master mix (Metabion, Planegg, Germany) or primaQUANT SYBRGreen Mastermix (Steinbrenner Laborsysteme, Wiesenbach, Germany) and a qPCR cyclor (QuantStudio5, Thermo Fisher Scientific). For normalization of quantification values, *H. arabidopsidis* *ELONGATION FACTOR 1a* (*HaEF1a*) was validated as a reference gene using *40S ribosomal protein S3A* (*HaWS021*) and β -*TUBULIN* (*HaTUB*) genes (Yan and Liou, 2006) (see Supplementary Fig. S1). For expression analysis of *Arabidopsis* genes, *AtACTIN2* (*AtACT2*) was used as reference gene (An *et al.*, 1996). Stable expression of *AtACT2* was validated by correlating with the expression of *AtTUBULIN* (*AtTUB*). *AtTUB* was used in combination with *AtUBQ10* as reference genes when was *AtACT2* subjected for gene expression analysis itself. Differential expression was calculated using the 2^{- $\Delta\Delta C_t$} method (Livak and Schmittgen, 2001) and the reference gene(s) used for normalization are detailed in the figure legends. All primers with annealing temperature are listed in Supplementary Table S1.

Phylogenetic analysis

Conserved protein domains and motifs were analysed with InterPro (<https://www.ebi.ac.uk/interpro/>). Sequences of group I and II CR proteins from *H. arabidopsidis* were obtained from the NCBI GenBank (accession numbers JF800102–JF800110). The draft genome sequence of the

Noco2 single spore isolate Noks1 was obtained from NCBI GenBank (accession number PRJNA298674). A phylogenetic tree and sequence alignment were constructed with CLC Main Workbench 7.6.4 (<https://digitalinsights.qiagen.com/>), with default settings for the alignment, and the tree was constructed using neighbour joining and Jukes–Cantor distance measurement. A cysteine-rich protein from *Phytophthora parasitica* (PpCR; F443_03861) was used to root the tree.

Transient Nicotiana benthamiana transformation

Agrobacterium tumefaciens strain AGL1 was grown for 2 d at 28 °C in LB medium with appropriate antibiotics. Bacteria were harvested by centrifugation at 4000 g and incubated in induction buffer (10 mM MES–KOH pH 5.6, 10 mM MgCl₂, 150 µM acetosyringone) for 1–2 h. The OD₆₀₀ was adjusted to 0.5 for each construct to perform pathogen assays and 0.25 for protein localization experiments. Leaves were infiltrated using needleless syringes and plants were replaced in the growth chamber under the same conditions.

Phytophthora/Botrytis pathogen assay

Two days after *A. tumefaciens* infiltration, *N. benthamiana* plants were inoculated with the respective pathogen by adding two Ø 0.5 cm agar plugs with mycelium per leaf. Images were taken with a camera and lesion sizes were measured with Fiji/ImageJ software (<https://imagej.net/Fiji>).

Cell death suppression assay

HaCR1-GFP, Δ *SP-HaCR1-GFP*, or *GFP* plasmids were co-transformed with the effector *AvrE1* cloned from *Pseudomonas syringae* pv. *tomato* that elicits cell death in *N. benthamiana* (Badel *et al.*, 2006). *Agrobacterium tumefaciens* cell concentration of all constructs was equally adjusted to a final OD₆₀₀ of 1.0. Infiltration was performed on 4-week-old *N. benthamiana* plants. Each individual construct was injected into the same leaf at separate areas (1.5 cm²). Pictures of the leaves were taken 5 d post-infiltration and analysed by mean grey value counts using the Fiji/ImageJ software (<https://imagej.net/Fiji>).

Epifluorescence and confocal microscopy

Overview pictures of *N. benthamiana* leaves were taken using a M165 FC epifluorescence stereomicroscope (Leica microsystems) with a GFP/DsRED filter. Confocal laser-scanning microscopy of *N. benthamiana* leaves was performed with an upright SP5 confocal laser scanning microscope (Leica Microsystems) and imaged using an HCX IRAPO L256/0.95W objective (Leica Microsystems). For image acquisition, the resolution was set to 1024×1024 pixels and the frame average to 4. Fluorescent tags were excited using an argon laser at 20% power. GFP was excited with a 488 nm laser line and detected at 500–530 nm, cyan fluorescent protein (CFP) was excited with a 458 nm laser line and detected at 465–505 nm.

Collection of apoplastic wash fluid and apoplastic protein isolation

Six-week-old *N. benthamiana* plants were transformed with *A. tumefaciens*, as described above. To isolate apoplastic wash fluids we adapted and modified a published protocol for the isolation of apoplastic fluids and vesicles from *Arabidopsis* (Rutter *et al.*, 2017), describing here the modifications. Two days after infiltration, the leaves were detached and the leaf surface was gently washed with ultrapure water. The leaflet was cut along the midrib and damaged areas were excised. The leaf stripes were washed in ultrapure water for 5 min to remove cytoplasm contamination from the cut surface. The leaf pieces were vacuum infiltrated with apoplastic wash buffer (20 mM MES, 2 mM CaCl₂, 0.1 M NaCl, pH 6.0 with NaOH) for 4 min with a desiccator and the vacuum slowly removed within 4 min. The apoplastic fluid was then collected via centrifugation for 15 min at 250 g and 4°C. The isolated apoplastic wash fluid was split and one

part directly used for apoplastic protease activity measurement. The other part was used for total apoplastic protein extraction. Therefore, proteins were collected by trichloroacetic acid and acetone precipitation and dissolved in 5× protein loading dye (225 mM Tris–HCl pH 6.8, 450 mM dithiothreitol (DTT), 5% SDS, 50% glycerol, 0.05% Bromphenol Blue).

Total protein extraction and western blot analysis

Proteins were extracted from *N. benthamiana* leaf discs, as described previously (Cerri et al., 2017). Protein extracts were supplemented with 5× loading dye (225 mM Tris–HCl pH 6.8, 450 mM DTT, 5% SDS, 50% glycerol, 0.05% Bromphenol Blue), boiled for 5 min at 95 °C, and separated via SDS–PAGE. Transgene constructs were detected via western blot using α-GFP antibody (Clones 7.1 and 13.1; Roche Diagnostics, Mannheim, Germany) and by secondary antibody α-mouse IRDye800 (Li-Cor, Bad Homburg, Germany). The membrane was scanned with the Odyssey imaging system (Li-Cor). To visualize total protein content, either the polyacrylamide gel was stained using silver nitrate (Roti-Black P, Carl Roth, Karlsruhe, Germany) or the membrane after blotting was stained with staining solution (0.1% Coomassie Brilliant Blue G250 (Serva, Heidelberg, Germany), 10% acetic acid, 40% ethanol in water) and de-stained with a solution of 10% acetic acid–30% ethanol.

Plant protease activity assay

Plant protease activity of isolated apoplastic wash fluid was determined using the Pierce fluorescent protease assay kit (Thermo Fisher Scientific) following the manufacturer's instructions for samples with low pH. Fluorescence was determined using a microplate reader (Tecan, Männedorf, Switzerland) with excitation and emission wavelengths of 485 nm and 538 nm, respectively. Protease activity was normalized on total protein content determined by Coomassie Brilliant Blue staining and quantified using Fiji/ImageJ (<https://imagej.net/Fiji>) as previously described (Miller, 2010).

Pseudomonas syringae pathogen assay

Liquid LB medium with rifampicin was inoculated with a single colony of *Pst* DC3000 and *Pst* DC3000 *hrcC*[−] and incubated overnight at 28°C. The bacteria were collected by centrifugation and diluted with 10 mM MgCl₂ to a final OD₆₀₀ of 0.0006. Leaves of 5- to 6-week-old Arabidopsis plants grown under short day conditions were infiltrated with the bacterial suspension, covered with a transparent lid and incubated under long day conditions. Two to three days after inoculation, leaf chlorosis of infiltrated leaves became visible and three leaf discs per biological replicate were harvested with a cork borer (Ø 0.6 cm). Leaf discs were homogenized in 10 mM MgCl₂ using a bead mill (MM400, Retsch) and two steel beads. A dilution series was plated on LB plates with rifampicin, and colony forming units were counted using a stereomicroscope.

Results

HIGS is a powerful tool for functional gene studies in *H. arabidopsidis*

We used Arabidopsis HIGS in order to investigate the functional roles of genes in the obligate biotrophic plant pathogen *H. arabidopsidis*. As proof of concept, we chose four *H. arabidopsidis* candidate genes as HIGS targets, for which we presumed that gene knockdown would affect pathogen infection, namely the housekeeping gene *ACTIN A* (*HaACT*^{RNAi}), the *CYSTEINE-RICH1* protein gene (*HaCR1*^{RNAi}), an *ALDOSE-1-EPIMERASE* (*HaA1E*^{RNAi}) gene, and the type-III RNA endonuclease gene *DICER-LIKE1* (*HaDCL1*^{RNAi}). *HaACT A* (*HpaG807716*) is

constitutively expressed in *H. arabidopsidis* and other oomycetes, and is a crucial component of the cytoskeleton (Ketelaar et al., 2012). *HaCR1* (*HpaG806256*) and *HaA1E* (*HpaG814621*) are putative pathogenicity factors that are highly expressed in *H. arabidopsidis* during Arabidopsis infection (Asai et al., 2014). *HaDCL1* (*HpaG808216*) is likely involved in biogenesis of *H. arabidopsidis* small RNAs, which we recently found to play an important role in suppressing plant genes for host infection (Dunker et al., 2020). The fungal plant pathogen *Botrytis cinerea* uses small RNAs for Arabidopsis plant infection, too (Weiberg et al., 2013), and HIGS against *Botrytis DCLs* indeed conferred disease resistance (Wang et al., 2016). To clone HIGS RNA hairpin transgenes (Fig. 1A), we chose target gene fragments that we predicted to not induce any off-target silencing either in *H. arabidopsidis* or in Arabidopsis using the Si-Fi2.1 tool (Lück et al., 2019). We confirmed the overall efficiency of our generated hairpin constructs by transient expression of a GFP RNA hairpin in leaves of the *N. benthamiana* line 16c stably expressing GFP (Ruiz et al., 1998) by *A. tumefaciens* infiltration. Transgenic GFP expression was clearly suppressed at local *A. tumefaciens* infiltration zones, as previously described (Kościańska et al., 2005), and release of repression by infiltration of a construct to co-express the viral RNAi suppressor protein p19 (Silhavy et al., 2002) verified GFP silencing via RNAi (see Supplementary Fig. S2). Therefore, we concluded that our constructs would effectively confer RNA silencing. Hence, we generated stable transgenic Arabidopsis lines expressing HIGS RNA hairpins in the ecotype Col-0. T₂ plants were selected and inoculated with the *H. arabidopsidis* isolate Noco2, which is virulent on Arabidopsis Col-0. We inspected infection phenotypes of WT and HIGS plants at 4 and 7 d post-inoculation (dpi) by light microscopy using the Trypan Blue staining method. Pathogen hyphae and haustoria were visible in all plant lines at 4 dpi, confirming successful infection (Supplementary Fig. S3). At 7 dpi, local plant cell death was visible around the infecting hyphae in plants of a *HaACT*^{RNAi} and two independent *HaCR1*^{RNAi} lines (Fig. 1B). Such *H. arabidopsidis*-induced local plant cell death, known as trailing necrosis, is associated with enhanced disease resistance against *H. arabidopsidis* infection (Uknes et al., 1992). Trailing necrosis also occurred, albeit to a lesser extent, in *HaA1E*^{RNAi} plants (Supplementary Fig. S4A), but not in WT (Fig. 1C) or in *HaDCL1*^{RNAi} plants (Supplementary Fig. S4B). In *HaACT*^{RNAi} and *HaCR1*^{RNAi} plants, trailing necrosis was accompanied by a reduction of *H. arabidopsidis* oospore production (Fig. 1C; Supplementary Fig. S5). To examine the effect of HIGS on target gene expression, we determined transcript levels of *HaACT A* and *HaCR1* in WT and *HaACT*^{RNAi} or *HaCR1*^{RNAi} plants, respectively. We did not detect any target gene amplification by RT-PCR in non-inoculated HIGS plants, ensuring that the target gene-specific primers did not produce any signal derived from the HIGS hairpin construct (Supplementary Fig. S6). Stable expression of the reference gene *ELONGATION FACTOR 1α* (*HaEF1α*, *HpaG809424*) was validated by quantitative reverse transcription (qRT)-PCR correlating their C_t values with two other reference genes, *40S ribosomal*

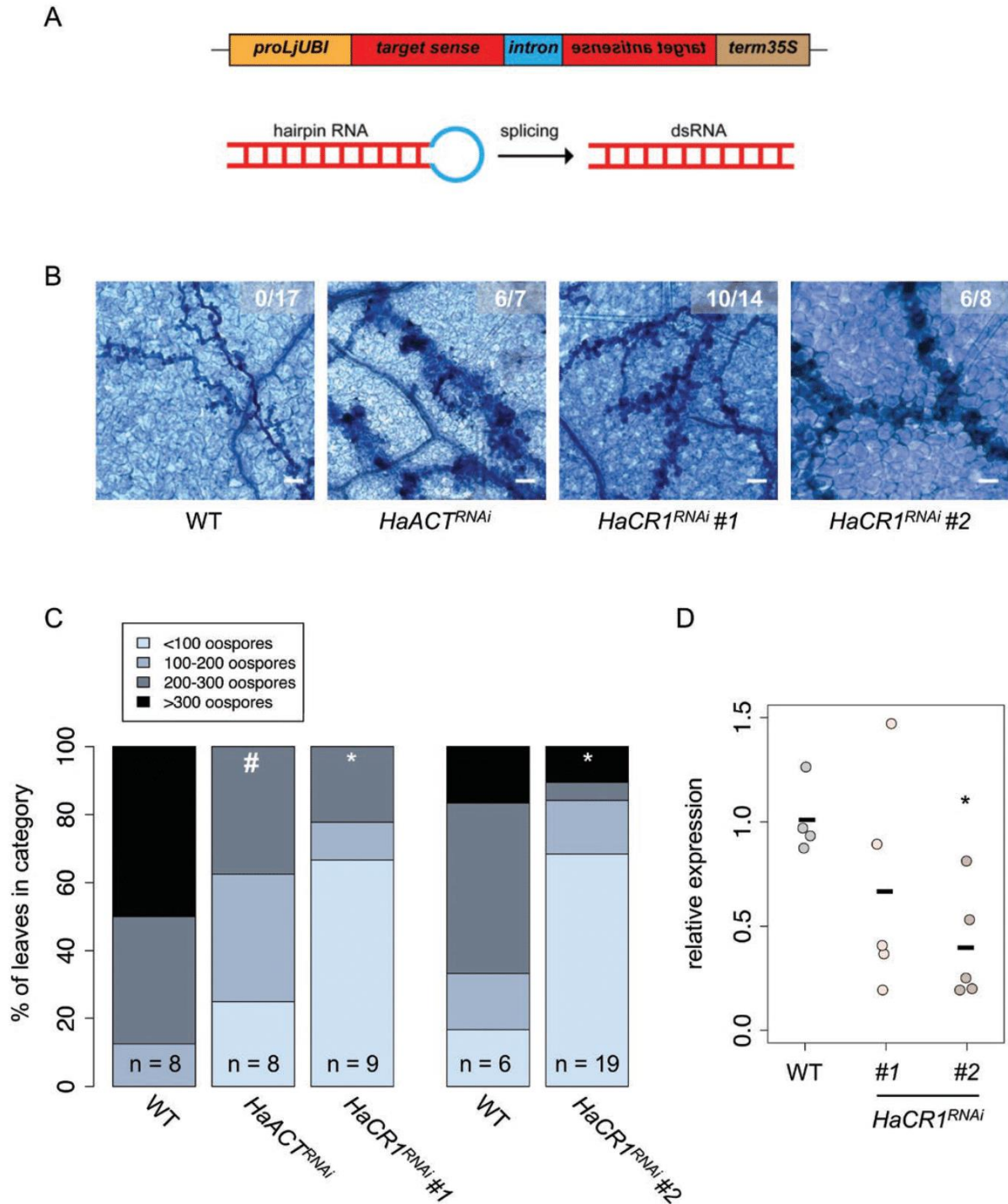


Fig. 1. Targeted gene knockdown of *HaCR1* and *HaACT A* via HIGS in Arabidopsis. (A) Representative scheme of HIGS constructs. (B) Trypan Blue staining of *H. arabidopsidis*-infected *HaACT^{RNAi}* and *HaCR1^{RNAi}* plants at 7 dpi revealed induced trailing necrosis around the pathogen hyphae. At minimum, seven leaves were inspected per genotype, from which a representative image is shown. Numbers in micrographs represent observed leaves with trailing necrosis per total inspected leaves. Scale bars represent 50 μ m. (C) *HaACT^{RNAi}* and *HaCR1^{RNAi}* plants allowed lower numbers of *H. arabidopsidis* oospore production compared with WT plants at 7 dpi. Oospore density (in categories) was counted with *n* representing the number of inspected leaves. * $P \leq 0.05$, # $P \leq 0.1$, significant difference by χ^2 test. (D) *HaCR1* gene knockdown in *H. arabidopsidis* was quantified by qRT-PCR in two independent *HaCR1^{RNAi}* lines upon infection at 4 dpi, with WT as control plants and *HaEF1 α* and *HaWS021* as reference genes. The bars indicate the average of at least three biological replicates each comprising six to eight plant leaves. * $P \leq 0.05$, significant difference by Student's *t*-test.

protein *S3A* (*HaWS021*, *HpaG810967*) and *HaTUB* (a β -tubulin, *HpaG814031*), and of *AtACT2* (*At3G18780*) by plotting the C_t values against *AtTUB* (*At5G62690*) (Supplementary Fig. S1A–D) according to the MIQE guidelines (Bustin et al., 2009). Gene silencing of *HaACT A* and *HaCR1* was evident at 4 dpi in a *HaACT^{RNAi}* line (Supplementary Fig. S7A) and in two independent HIGS lines of *HaCR1^{RNAi}* (Fig. 1D). Neither target gene was suppressed at 7 dpi. (Supplementary Fig. S7B). The *HaACT^{RNAi}* plants appeared smaller than WT plants (Supplementary Fig. S8A), and thus we assumed an off-target effect on Arabidopsis *ACTIN* by the *HaACT^{RNAi}* transgene. We determined the expression of the two Arabidopsis *ACTIN* genes, *AtACT2* (*At3G18780*) and *AtACT11* (*At3G12110*), showing the highest sequence similarity to *HaACT A*. The qRT-PCR analysis did not indicate any significant down-regulation of *AtACT2* or *AtACT11* upon *H. arabidopsidis* infection at 4 dpi (Supplementary Fig. S8B), rendering the connection between the HIGS construct and the plant growth phenotype unclear. We considered the possibility that such a growth phenotype in *HaACT^{RNAi}* plants could have influenced the infection outcome with *H. arabidopsidis*. The transgenic Arabidopsis *HaCR1^{RNAi}* plants did not display any obvious pleiotropic effects, and we concluded that pathogen-induced plant cell death and enhanced disease resistance were due to *HaCR1* silencing. With these data, we considered that *HaCR1* was an important virulence factor of *H. arabidopsidis* to infect Arabidopsis.

HaCR1 is a member of the *H. arabidopsidis* CR effector protein family

To seek the potential function of *HaCR1*, we performed *in silico* protein sequence analysis. The *HaCR1* 172-amino-acid sequence has a predicted 19-amino-acid secretion signal peptide, but no further predicted functional domains or motifs. Sixteen family members of the *HaCR* proteins were previously classified into group I and group II by their cysteine pattern, with *HaCR1* belonging to group I (Cabral et al., 2011). We accomplished phylogenetic analysis on the group I and II *HaCR* proteins using a *Phytophthora capsici* CR protein to root the phylogenetic tree. Phylogeny analysis suggested separate clades of *HaCR*s, with *HaCR1* forming one branch with its close homologues *HaCR3* (*HpaG813024*) and *HaCR4* (*HpaG806254*), and the second clade consisting in *HaCR5* (*HpaG814422*), *HaCR6* (Cabral et al., 2011), and *HaCR7* (*HpaG814216*). Further *HaCR* clades were not explicitly reliable due to overall low sequence conservation (see Supplementary Fig. S9A). We did not detect *HaCR2*, a *HaCR1* homologue that was previously reported in the *H. arabidopsidis* strain Waco9 (Cabral et al., 2011), in the genome sequence of Noks1, a single-spore isolate of Noco2 (Bailey et al., 2011). Waco9 *HaCR2* and Noks1 *HaCR1* share a 96.9% amino acid sequence identity and 98.4% sequence similarity, but *HaCR2* comprises an additional 89-amino-acid insertion in the middle part of the protein (Cabral et al., 2011). Consistent with the absence of *HaCR2* for the Noks1 genome sequence, we could not amplify a *HaCR2*

orthologue by RT-PCR. We therefore concluded that there is no *HaCR2* orthologue existing in the strain Noco2. *HaCR1* and its closest homologue *HaCR3* (BLASTp E-value 9×10^{-30}) share 53.4% sequence identity and 61.1% sequence similarity (Supplementary Fig. S9B) on the amino acid level. *HaCR1* is unique to the species of *H. arabidopsidis*, because we did not find any *HaCR1* homologue in another oomycete species by BLASTp search against the NCBI database (E-value cut-off ≤ 1). As *HaCR3* shared also 68.2% of transcript sequence identity to *HaCR1* (Supplementary Fig. S10A), we sought to examine co-suppression of *HaCR3* in *HaCR1^{RNAi}* plants upon *H. arabidopsidis* infection. We performed qRT-PCR for gene expression analysis and observed comparable *HaCR3* transcript accumulation in WT and *HaCR1^{RNAi}* plants at 4 dpi (Supplementary Fig. S10B), suggesting that *HaCR1^{RNAi}* was specific to knockdown *HaCR1*, but not *HaCR3*.

HaCR1 inhibits induced plant cell death and promotes infection by (hemi)biotrophs

In order to shed light on *HaCR1* function during plant infection, we performed transient expression assays using *N. benthamiana* leaves. We cloned a full-length *HaCR1* version and fused it with a C-terminal GFP tag (*HaCR1-GFP*), a C-terminal GFP-tagged *HaCR1* version without its predicted signal peptide (Δ SP-*HaCR1-GFP*), and GFP without any *HaCR1* sequence as a negative control (GFP) for expression in *N. benthamiana* leaves (Fig. 2A, B). Because *HaCR1* knockdown by HIGS resulted in plant trailing necrosis, we hypothesized that *HaCR1* might promote infection through suppressing plant cell death. To test this hypothesis, we co-expressed the *HaCR1-GFP* or the Δ SP-*HaCR1-GFP* construct together with the *P. syringae* effector *AvrE*, a known trigger of plant cell death in *N. benthamiana* (Badel et al., 2006). Only *HaCR1-GFP* was able to dampen *AvrE1*-induced plant cell death in contrast to both Δ SP-*HaCR1-GFP* and GFP (Fig. 2C). To further substantiate the role of *HaCR1* as a plant cell death inhibitor for plant infection, we inoculated *HaCR1-GFP*-infiltrated *N. benthamiana* leaves with the hemibiotrophic oomycete pathogen *P. capsici* or with the necrotrophic fungal pathogen *B. cinerea*. These two pathogens lack any homologous protein with sequence similarity to *HaCR1* (no BLASTp hit with E-value ≤ 5). *Phytophthora capsici* generated significantly larger lesions in *HaCR1-GFP* expressing leaves, compared with Δ SP-*HaCR1-GFP* or GFP expressing leaves (Fig. 2D). In contrast, *B. cinerea*, the infection of which is supported by induced plant cell death (Govrin and Levine, 2000), produced significantly smaller lesions in *HaCR1-GFP* expressing leaves than in Δ SP-*HaCR1-GFP* or in GFP expressing leaves (Fig. 2E). Since *HaCR1* does not contain any RxLR plant cell translocation motif, we postulated that it could be active in the plant apoplast. To inspect *HaCR1* intercellular localization in plants, we co-expressed a CFP-fused protein of the known plant plasma membrane marker *Lti6B* (Kurup et al., 2005) with *HaCR1-GFP*, Δ SP-*HaCR1-GFP*, or GFP in *N. benthamiana* leaves. Confocal microscopy studies revealed overlapping GFP and CFP signals for *HaCR1-GFP* indicating co-localization with *Lti6B* and the presence of *HaCR1* in both the plant

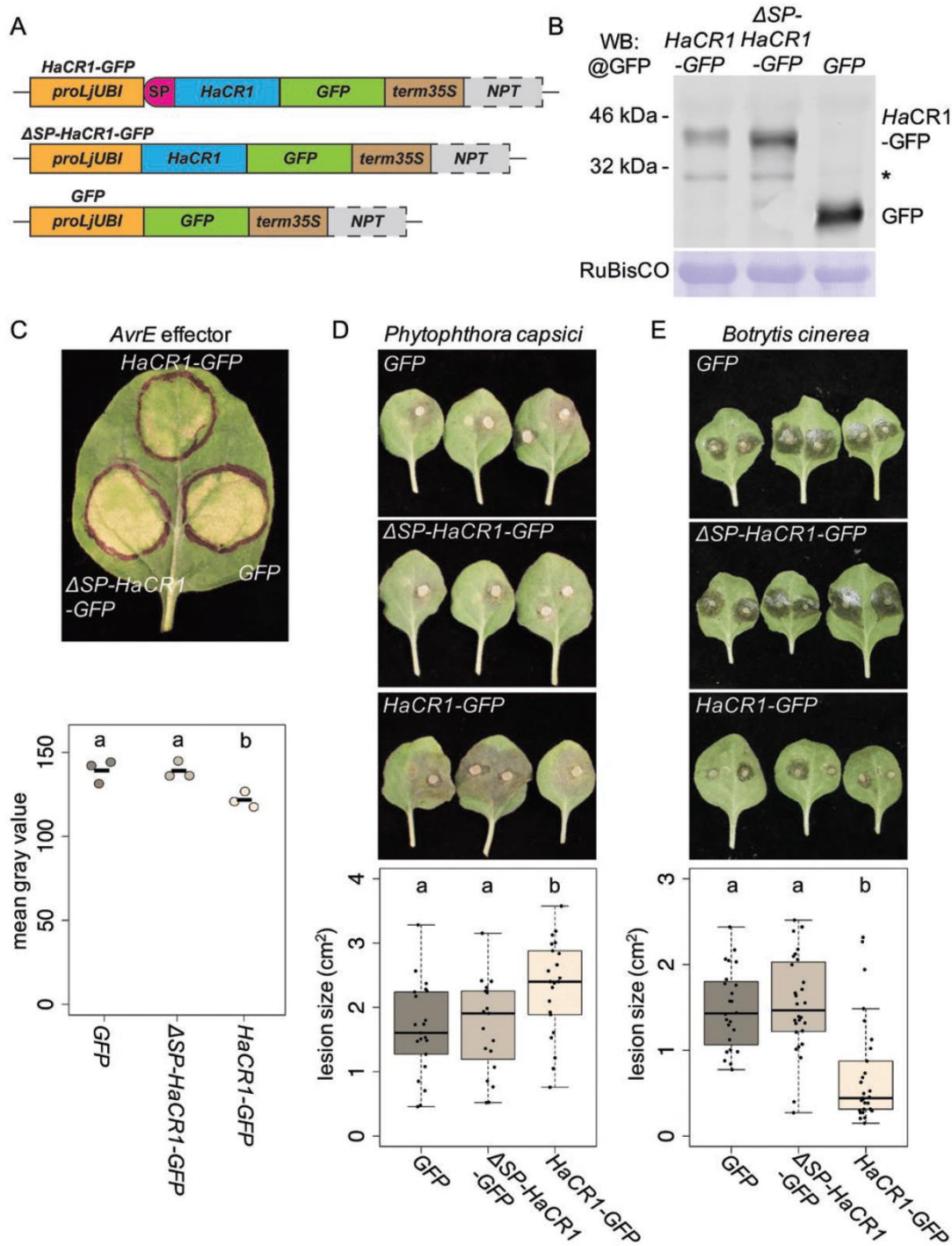


Fig. 2. Expression of full-length *HaCR1* in *N. benthamiana* suppresses effector-triggered plant cell death and promoted disease of *P. capsici* but reduced disease of *B. cinerea*. (A) Schematic overview of *HaCR1* expression cassettes: C-terminal *GFP* fused to full-length *HaCR1*, C-terminal *GFP* fused to a *HaCR1* version without signal peptide (Δ SP), and *GFP* without *HaCR1*. *ProLjUBI* is a *Lotus Ubiquitin* promoter, *SP* represents signal peptide, *term35S* is a S35 viral terminator, *NPT* is a *Neomycin-phosphotransferase* resistance gene (only included when transforming *Arabidopsis*). (B) Western blot analysis confirmed expression of *HaCR1*-*GFP*, Δ SP-*HaCR1*-*GFP* fusion proteins or *GFP* in *A. tumefaciens*-infiltrated tobacco leaves. The expected size of *HaCR1*-*GFP* was 40.6 kDa, of Δ SP-*HaCR1*-*GFP* was 38.7 kDa, and of free *GFP* was 26.9 kDa. Asterisk indicates a non-specific band. *RuBisCO* stained with Coomassie G250 was used as a loading control. (C) A representative picture of a tobacco leaf at 5 d after *A. tumefaciens* co-infiltration carrying either *HaCR1*-*GFP*, Δ SP-*HaCR1*-*GFP* or *GFP* together with a construct carrying the bacterial effector *AvrE* promoting cell death. This experiment was repeated three times with comparable results. Each experiment included three infiltrated leaves. Quantification of chlorosis symptoms was performed by measuring the mean gray value of the infiltrated area, with $n=3$. (D) *Agrobacterium tumefaciens*-infiltrated *N. benthamiana* leaves of *HaCR1*-*GFP*, Δ SP-*HaCR1*-*GFP* or *GFP* were inoculated with *P. capsici*, and pictures were taken at 2 dpi. Lesion size quantification on *N. benthamiana* leaves induced by *P. capsici* at 2 dpi, as determined by ImageJ with $n \geq 20$ lesions of $n \geq 10$ leaves. (E) *Agrobacterium tumefaciens*-infiltrated *N. benthamiana* leaves of

apoplast and the symplast, while $\Delta SP-HaCR1-GFP$ or GFP indicated signals separate from Lti6B and seemingly located only in the plant symplast (Fig. 3A). These results demonstrated that $HaCR1$ was functional in suppressing induced plant cell death, and its signal peptide was crucial for this function.

HaCR1 might act as an apoplastic protease inhibitor to support infection

A previously described role of fungal CR proteins is the inhibition of apoplastic plant protease (Rooney et al., 2005). Therefore, we hypothesized that $HaCR1$ might function as a decoy to inhibit plant apoplastic proteases, too. To challenge this hypothesis, we measured the capacity of $HaCR1$ to interfere with the apoplastic plant protease activity *in vitro*. We collected apoplastic wash fluids from *N. benthamiana* leaves expressing either $HaCR1-GFP$ or $\Delta SP-HaCR1-GFP$. Comparative analysis of the total leaf versus the apoplastic proteins by SDS-PAGE and silver staining displayed a reduction of the intracellular protein ribulose-1,5-bisphosphate carboxylase/oxygenase (RuBisCO) in the apoplast fraction indicating successful enrichment of apoplastic proteins, even though we could not entirely prevent cytoplasmic protein contamination, as RuBisCO and $\Delta SP-HaCR1-GFP$ were still detectable in apoplast samples (Fig. 3B). Indeed, the apoplastic wash collected from *N. benthamiana* leaves expressing $HaCR1-GFP$ exhibited a significant reduction of plant protease activity determined by fluorescein isothiocyanate (FITC)-casein compared with $\Delta SP-HaCR1-GFP$ (Fig. 3C, D). This result further supported a function of $HaCR1$ in the plant apoplast.

To investigate the suppressive effect of $HaCR1$ on plant immunity in the native host Arabidopsis during *H. arabidopsidis* infection, we generated transgenic Arabidopsis plants expressing $HaCR1-GFP$ or $\Delta SP-HaCR1-GFP$ under the strong constitutive *Lotus Ubiquitin* promoter (Maekawa et al., 2008). We recovered three independent Arabidopsis T₂ lines for $HaCR1-GFP$ and two independent lines for $\Delta SP-HaCR1-GFP$ and verified ectopic expression of fusion proteins in seedlings by fluorescence microscopy and western blot analysis (see Supplementary Fig. S11A, B). None of the transgenic lines exhibited any obvious growth or morphological change (Fig. 4A). We pooled and germinated seeds of the corresponding transgenic lines and challenged seedlings with the virulent *H. arabidopsidis* Noco2. Disease progression was estimated by *H. arabidopsidis* housekeeping gene expression of *HaACT A* relative to plant *AtACT 2* at 4 and 7 dpi. Moderate but significantly increased pathogen quantity was evident in $HaCR1-GFP$ expressing seedlings, compared with $\Delta SP-HaCR1-GFP$ (Fig. 4B). Moreover, expression of the Arabidopsis salicylic acid (SA)-dependent immunity marker gene *AtPR1* was significantly less induced in seedlings expressing $HaCR1-GFP$ compared with $\Delta SP-HaCR1-GFP$ upon *H. arabidopsidis* infection (Fig. 4C). This finding supported a role of the full-length $HaCR1$ in plant immune suppression. The jasmonic

acid-dependent immunity marker gene *AtPDF1.2* did not exhibit any difference between $HaCR1-GFP$ and $\Delta SP-HaCR1-GFP$ upon *H. arabidopsidis* infection (Supplementary Fig. S12). To further explore if the $HaCR1$ -suppressive effect on SA-dependent immunity played a role during infection, we inoculated transgenic Arabidopsis lines either with the virulent bacterial hemibiotrophic pathogen *Pseudomonas syringae* pv. *tomato* (*Pst*) strain DC3000 or the avirulent mutant *Pst* DC3000 *hrcC*⁻ lacking a functional type-III secretion system (Roine et al., 1997). Bacterial growth of DC3000 was significantly enhanced in $HaCR1-GFP$ expressing Arabidopsis, compared with $\Delta SP-HaCR1-GFP$. In contrast, bacterial population of *hrcC*⁻ remained unaltered between the two different transgenic plant lines (Fig. 4D). These results further supported that $HaCR1$ is an apoplastic effector that impairs plant immunity against diverse biotrophic and hemibiotrophic plant pathogens.

Discussion

In this study, we used Arabidopsis HIGS for functional gene studies in the obligate biotrophic pathogen *H. arabidopsidis*. The short lifecycle, available cloning tools, and easy transformation of the host plant Arabidopsis enables the conducting of HIGS experiments in a relatively short time period. We applied HIGS to knockdown *HaACT A*, *HaDCL1*, *HaCR1*, and *HaA1E* in order to survey functional roles of these pathogen genes during host plant colonization. The $HaCR1^{RNAi}$, $HaACT^{RNAi}$ plants, and to a lesser extent $HaA1E^{RNAi}$, exhibited trailing necrosis at *H. arabidopsidis* infection sites. In addition, $HaCR1^{RNAi}$ and $HaACT^{RNAi}$ plants allowed reduced proliferation of oospores (Fig. 1A–C; Supplementary Fig. S4A), the sexual reproductive structure of oomycetes (Slusarenko and Schlaich, 2003). Both infection phenotypes are related to reduced disease, as comparable trailing necrosis symptoms had been observed when Arabidopsis was primed for immunity, or connected to Arabidopsis ecotypes infected with sub-compatible *H. arabidopsidis* strains (Uknes et al., 1992; Krasileva et al., 2011). The resistance response in $HaACT^{RNAi}$ plants also suggested that down-regulation of *HaACT A* was not compensated through functional redundancy by the paralogue *HaACT B* (*HpaG809873*), despite considerable sequence homology with the $HaACT^{RNAi}$ HIGS construct (see Supplementary Fig. S13A). The attenuated disease development in $HaACT^{RNAi}$, $HaCR1^{RNAi}$, and $HaA1E^{RNAi}$ plants was not due to plant transformation or due to expression of non-self dsRNA in Arabidopsis, because $HaDCL1^{RNAi}$ did not reveal any higher plant resistance or suppressed pathogen virulence (Supplementary Fig. S4B). Why $HaDCL1^{RNAi}$ plants did not reveal higher resistance despite the important role of pathogen small RNAs during infection (Dunker et al., 2020) remains to be investigated. One possible explanation might be functional redundancy of the two *HaDCLs* identified in the genome of *H. arabidopsidis* (Bollmann et al., 2016). Similarly,

HaCR1-GFP, $\Delta SP-HaCR1-GFP$, or *GFP* were inoculated with *B. cinerea*, and pictures were taken at 3 dpi. Lesion size quantification on *N. benthamiana* leaves induced by *B. cinerea* at 3 dpi, as determined by ImageJ with $n \geq 20$ lesions of $n \geq 10$ leaves. Letters in (C–E) indicate groups of statistically significant difference by ANOVA followed by Tukey's HSD test with $P \leq 0.05$.

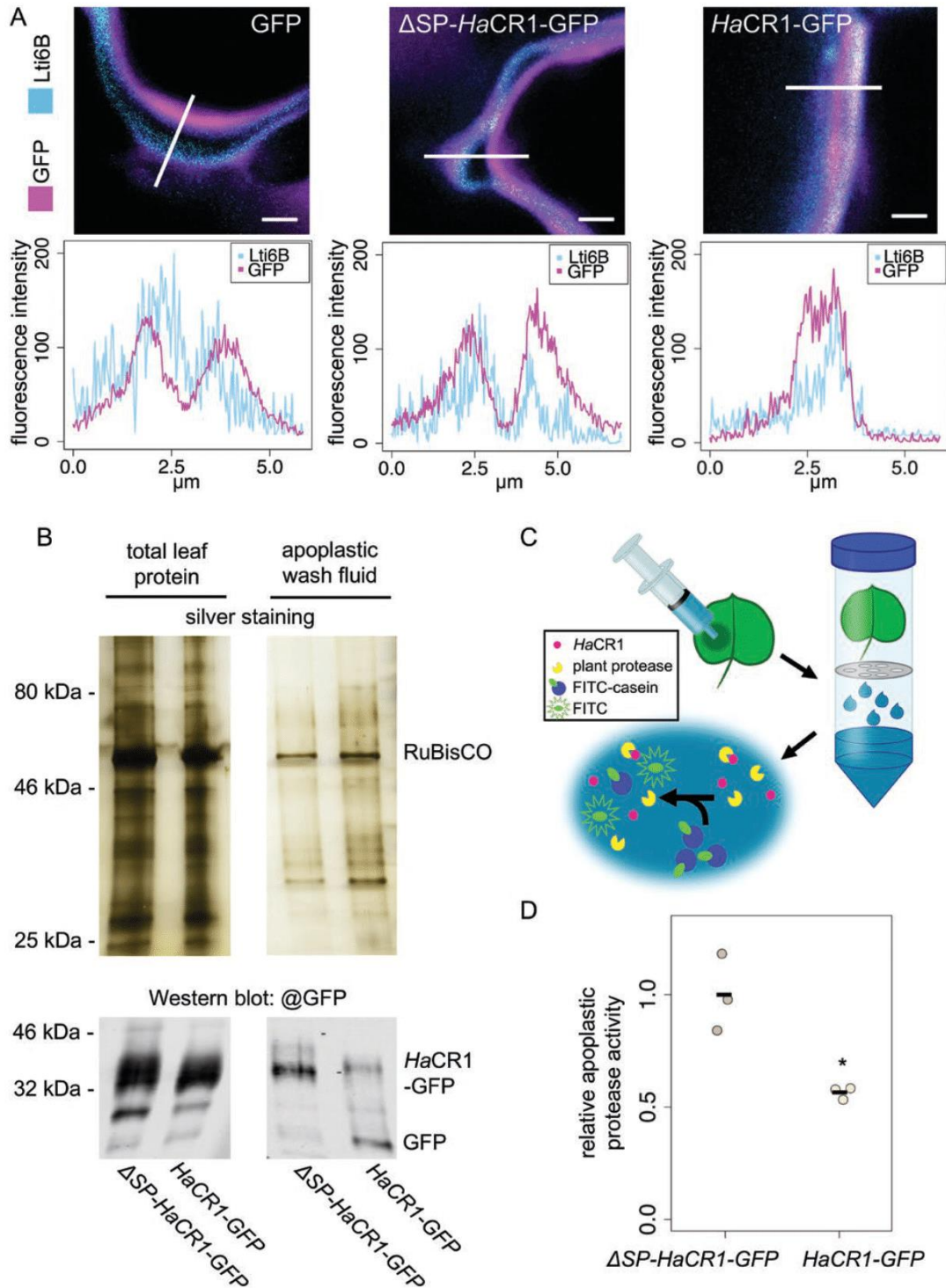


Fig. 3. *HaCR1* localizes to the plant apoplast and is capable of inhibiting apoplastic plant protease activity. (A) Confocal laser scanning microscopy was used to inspect intercellular localization of *HaCR1*-GFP, Δ SP-*HaCR1*-GFP, or GFP alone. The plasma membrane (PM) was visualized by the PM marker LTI6B fused with CFP. Six independent events of co-localization were evaluated per construct. Scale bars represent 100 μ m. The upper panel displays overlaid LTI6B-CFP and *HaCR1*-GFP, Δ SP-*HaCR1*-GFP, or GFP fluorescence signal intensities alongside the bar, as indicated in the fluorescence microscopy images (lower panel). (B) Total leaf protein and apoplastic wash fluid fraction visualized via a silver-stained SDS-PAGE indicated depletion of cytoplasmic proteins, such as RuBisCO, from the apoplastic wash fluid. Western blot shows detection of *HaCR1* and free GFP in total leaf and apoplastic wash fluid from the same experiment. (C) Schematic overview of the apoplastic protease activity assay. *Nicotiana benthamiana* leaves were transformed by *A. tumefaciens* infiltration, apoplastic wash fluid was collected by centrifugation, and endogenous protease activity was determined by addition of FITC-casein. Upon protease activity, casein is hydrolysed and quenching of FITC fluorescence is released. (D) Protease activity in the apoplastic wash fluid was measured and compared with apoplastic proteins collected from *N. benthamiana* leaves expressing *HaCR1*-GFP or Δ SP-*HaCR1*-GFP. Protease activity was normalized to total protein quantities of apoplastic fluid samples. Each data point represents an independent experiment using eight leaves. * $P < 0.05$, significant difference by Student's *t*-test.

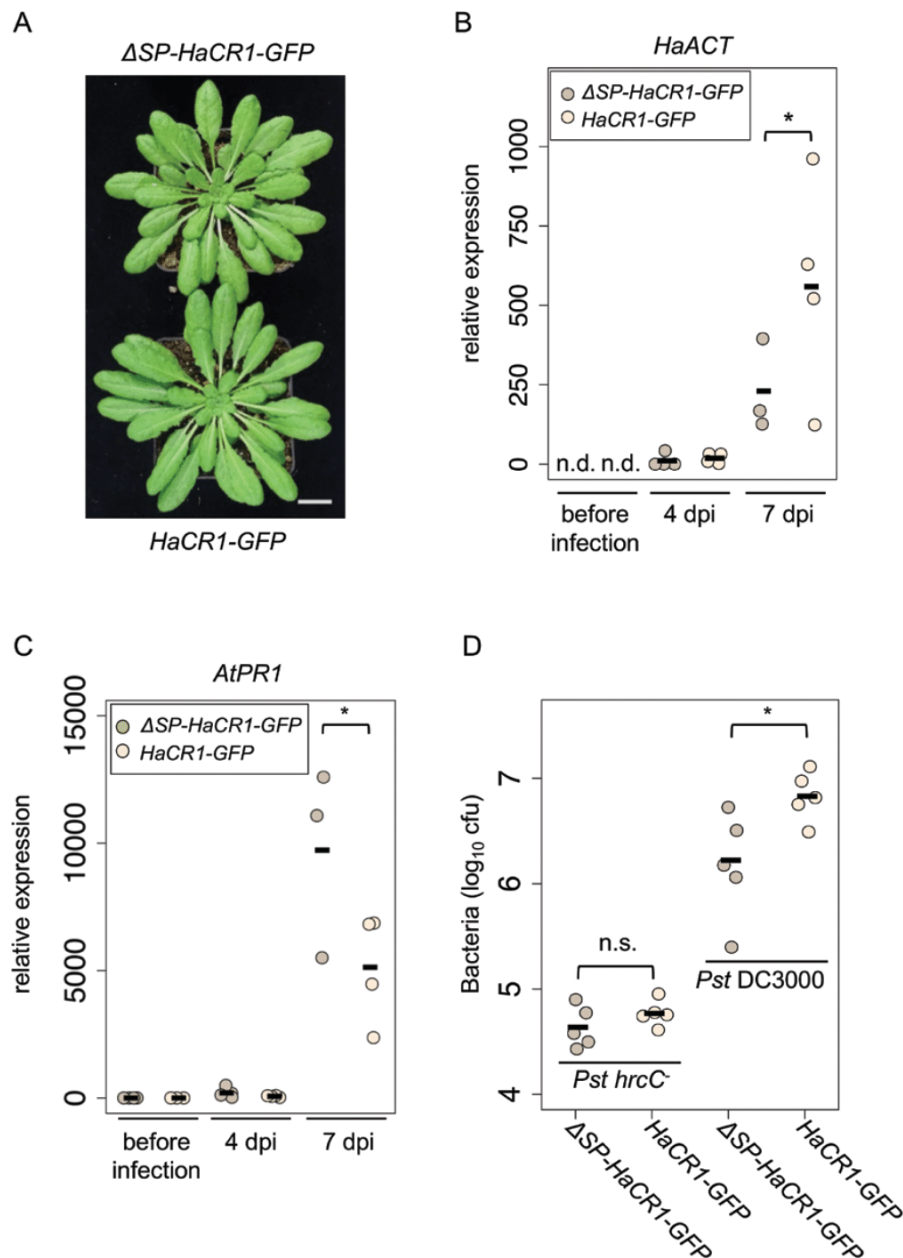


Fig. 4. Ectopic expression of *HaCR1* in Arabidopsis enhances susceptibility to *H. arabidopsidis* and bacterial infection and compromises plant immunity. (A) Growth of Arabidopsis plants overexpressing either $\Delta SP-HaCR1-GFP$ or $HaCR1-GFP$. The scale bar represents 2 cm. (B) *H. arabidopsidis* biomass was determined by *HaACT* expression relative to plant *AtACT* in $HaCR1-GFP$ expressing Arabidopsis, compared with $\Delta SP-HaCR1-GFP$ at 4 and 7 dpi. *HaACT* expression was not detected (n.d.) before infection. (C) *AtPR1* was quantified by qRT-PCR using *AtACT2* and *AtTUB* as reference genes, and relative transcript levels were compared between Arabidopsis expressing *HaCR1-GFP* or $\Delta SP-HaCR1-GFP$ at 4 and 7 dpi with *H. arabidopsidis*. (D) Arabidopsis susceptibility to the virulent *Pst* DC3000 or the avirulent *Pst* DC3000 *hrcC*⁻ was evaluated by counting colony forming units (cfu) at 3 dpi. Each data point represents cfu derived from three infected leaf discs. For (B, C), each experiment was performed at least with three biological replicates, and each biological replicate represented two technical repeats. For (B–D) * $P < 0.05$, significant difference by one-tailed Student's *t*-test.

the mild phenotype expressed in the Arabidopsis *HaA1E*^{RNAi} line might be explained by the presence of two paralogous and potentially functionally redundant genes: *HaA1E-LIKE* (*HaA1EL*, *HpaG807738*) and *HaA1E-LIKE2* (*HaA1EL2*, *HpaG807727*). *HaA1EL* shares 66.3% amino acid identity and 79.6% amino acid similarity, while *HaA1EL2* shares 86.6% amino acid identity and 90.3% amino acid similarity

with *HaA1E*. *HaA1EL* and *HaA1EL2* showed also 79.4% and 89.9% coding sequence identity, respectively. In addition, they revealed a considerable DNA sequence homology with our *HaA1E*^{RNAi} HIGS construct (Supplementary Fig. S13B). However, *HaA1EL2* lacks an annotated open reading frame with a signal peptide and displayed very weak expression during infection. In contrast *HaA1E* and *HaA1EL* both

comprise a predicted signal peptide and were previously found to be strongly expressed in *H. arabidopsidis* infecting Arabidopsis (Asai *et al.*, 2014).

At the molecular level, target gene suppression of *HaACT* and *HaCR1* by HIGS was evident at 4 dpi, but not at 7 dpi (Fig. 1D; Supplementary Fig. S7). At this later time point, *H. arabidopsidis* had induced trailing necrosis of plant cells at the infection sites of HIGS plants. We suggest that plant cell death would lead to a collapsed haustoria–plant cell interface, which likely stopped the transport of RNAs from plants into the pathogen (Hudzik *et al.*, 2020). Transgenic *HaACT*^{RNAi} expressing Arabidopsis displayed pleiotropic effects, for instance slower plant growth, although we did not predict any Arabidopsis *ACTIN* as off-target of the *HaACT*^{RNAi} construct *in silico*, and the two closest orthologues of *HpaACT A*, *AtACT2* and *AtACT11*, were not suppressed in the Arabidopsis HIGS line (Supplementary Fig. S8). Tracing back off-target effects would require plant RNA degradome analysis (Casacuberta *et al.*, 2015), and was not further investigated as it would go beyond the scope of our study. With this experience, we propose to omit pathogen house-keeping genes as targets in HIGS studies although successful silencing would likely promote plant disease resistance. Since pathogen effector genes are unique and homologues do not exist in the host plant, HIGS against *HaCR1* did not encounter any off-target problem. An interesting alternative to HIGS for targeted gene knock-down in *H. arabidopsidis* that is based on exogenous application of 5' capped small interfering RNAs has been recently reported (Bilir *et al.*, 2019). Applying *Cellulose synthase A3* antisense RNAs to *H. arabidopsidis* conidia suspension inhibited spore germination on the leaf surface. Both, transgenic HIGS and external RNA treatment are innovative strategies to further explore gene functions of this pathogen.

To further investigate the role of *HaCR1* during plant infection, we expressed *HaCR1* in *N. benthamiana* and Arabidopsis. One obvious disease symptom in transgenic *HaCR1*^{RNAi} plants was the induction of local plant cell death suggesting that *HaCR1* might be involved in cell death suppression. Such a function of *HaCR1* was supported by the inhibitory activity on bacterial effector AvrE-induced plant cell death in *N. benthamiana* leaves (Fig. 2C). Of note, full-length *HaCR1*, but not a signal peptide-deleted version, was capable of suppressing plant cell death in this assay. AvrE expressed in *N. benthamiana* leaves was previously described to be localized at the cell plasma membrane (Xin *et al.*, 2015), a possible contact compartment of *in planta*-expressed full length *HaCR1* with AvrE. However, the molecular mechanism of AvrE-induced cell death repression by *HaCR1* is not clear, and needs to be further explored by identifying the molecular interactors of *HaCR1*. On the one hand, *HaCR1* promoted disease caused by the oomycete hemibiotrophic pathogen *P. capsici* (Fig. 2D). We suggest that *P. capsici* profits from *HaCR1*-repressed plant cell death during the early biotrophic phase. This is in line with Avr1b from *Phytophthora sojae* that impaired plant cell death and promoted lesion formation of this hemibiotrophic pathogen (Dou *et al.*, 2008). On the other

hand, *HaCR1* expression limited disease symptoms caused by the necrotrophic fungal pathogen *B. cinerea* (Fig. 2E), because this pathogen exploits and promotes plant apoptosis for infection (Veloso and van Kan, 2018). In this context, reduced *Botrytis* virulence was reported in plants expressing animal cell death suppressors (Dickman *et al.*, 2001). Consistent with plant cell death suppressive activity, *HaCR1* also promoted disease progression caused by other (hemi)biotrophic pathogens, *P. syringae* DC3000 and *H. arabidopsidis* itself (Fig. 4B, E). *HaCR1* overexpression in Arabidopsis moderately promoted *H. arabidopsidis* disease, which might be explained by the high expression of endogenous *HaCR1* in *H. arabidopsidis* during infection. Similarly, a previous study on *HaRxLR* effectors could detect only small positive effects on *H. arabidopsidis* infection suggesting a combined action of effectors to effectively suppress plant immunity (Pel *et al.*, 2014).

To better understand the molecular function of *HaCR1*, we explored its peptide composition. *HaCR1* contains a predicted secretion signal peptide but no further plant cell translocation domain indicating its function in the plant apoplast. In accordance, only full-length *HaCR1* expression in plants suppressed induced plant cell death and promoted infection of (hemi)biotrophs, while a secretion signal peptide-truncated *HaCR1* version expressed in plants lost these activities. This is in agreement with other apoplastic effectors found in fungal pathogens, such as *Zymoseptoria tritici* and *Magnaporthe oryzae* (Kim *et al.*, 2013; Kettles *et al.*, 2017). A conserved class of apoplastic effectors in fungi are the LysMs. These effectors act as decoys that prevent microbe-associated molecular pattern (MAMP)-triggered plant immunity, for instance by binding chitin oligomers and thereby hampering chitin recognition by plant pattern receptors (Kombrink and Thomma, 2013; Zeng *et al.*, 2020). However, *HaCR1*, like all other members of the *HaCR* family, does not contain any predicted protein domain or motif, making a specific ligand binding rather unlikely. Instead, we found evidence that plant-expressed *HaCR1* can interfere with apoplastic plant protease activity *in vitro* (Fig. 3D), similar to fungal CR proteins exhibiting protease inhibition activity (Rooney *et al.*, 2005). The strict dependency of *HaCR1* function on the presence of a signal peptide, and thereby its apoplastic localization, suggests a link between the cell death inhibition function and plant protease inhibition. In this context, several apoplastic plant proteases are crucial regulatory components of plant programmed cell death, and protease inhibitory effectors of fungi and oomycetes have been associated with inhibition of plant programmed cell death (Dickman and Fluhr, 2013; Salguero-Linares and Coll, 2019).

In general, small, apoplastic CR peptides containing no further sequence-conserved domains have been described in high numbers for oomycete and fungal pathogens suggesting a functional conservation in a wide range of pathogens (Sperschneider *et al.*, 2018). Pathogen-secreted protease inhibitors or decoys prevent degradation of pathogen effectors or the release of MAMPs produced by plant proteases (Jiang and Tyler, 2012). Such a function of *HaCR1* is supported by our results, because Arabidopsis overexpressing *HaCR1* exhibited reduced *AtPR1* induction upon *H. arabidopsidis* infection

(Fig. 4C), and *HaCR1* expression in plants promoted infection of (hemi)biotrophic pathogens *H. arabidopsidis*, *P. capsici*, and *P. syringae*.

Our data revealed an important role of a CR effector protein in host infection by the obligate biotrophic pathogen *H. arabidopsidis*. A next crucial step to understand the molecular mechanism of how *HaCR1* suppresses pathogen-induced plant cell death will be to uncover its molecular interactors, which are likely to include plant apoplastic proteases or receptor-like proteins. This knowledge would be crucial to completely elucidate whether the dual function of *HaCR1* in plant protease inhibition and cell death inhibition is directly or indirectly linked, or is independent.

Supplementary data

Supplementary data are available at *JXB* online.

Fig. S1. Expression correlation analysis of *H. arabidopsidis* and Arabidopsis reference genes by qRT-PCR.

Fig. S2. Expression of *GFP^{RNAi}* by *A. tumefaciens* infiltration led to *GFP* silencing in the *N. benthamiana* line 16c stably expressing *GFP*.

Fig. S3. Arabidopsis *HaACT^{RNAi}* and *HaCR1^{RNAi}* plants displayed no obviously altered infection phenotype at 4 dpi.

Fig. S4. Infection phenotype of the Arabidopsis *HaA1E^{RNAi}* and the *HaDCL1^{RNAi}* lines.

Fig. S5. Representative leaves used for *H. arabidopsidis* oospore quantification.

Fig. S6. Validation of RT-PCR primers to assess *H. arabidopsidis* target gene expression in Arabidopsis HIGS plants.

Fig. S7. *H. arabidopsidis* target gene expression when infecting Arabidopsis HIGS plants.

Fig. S8. Growth phenotype of 14-day-old Arabidopsis WT, *HaCR1^{RNAi}* or *HaACT^{RNAi}* seedlings.

Fig. S9. The *HaCR* family in the *H. arabidopsidis* strain Noco2.

Fig. S10. *HaCR3* expression was not suppressed during infection of *HaCR1^{RNAi}* plants.

Fig. S11. Arabidopsis seedlings of individual transformation lines expressing *HaCR1-GFP* or Δ *SP-HaCR1-GFP*.

Fig. S12. Expression of *AiPDF1.2* was not different when comparing Δ *SP-HaCR1-GFP* or *HaCR1-GFP* expressing Arabidopsis seedlings upon *H. arabidopsidis* infection.

Fig. S13. Sequence alignment of RNAi constructs with the target gene and the closest homologues.

Table S1. Primers used in this study.

Acknowledgements

The authors thank Adriana Hörmann for her help with *H. arabidopsidis* and plant cultivation. We thank Dr Dagmar Hann for providing *A. tumefaciens* GV3101 carrying pGWB314 to express AvrE, and *Pst* DC3000 as well as Dr David Chiasson for sharing a Golden Gate plasmid to express LTI6b-CFP in *N. benthamiana*. We further thank Dr Silke Robatzek and Dr Martin Janda for providing the *Pst* DC3000 *hrcC⁻* mutant. The *P. capsici* strain LT263 was kindly provided by Dr Francine Govers. We want to thank Chloé Cathebras for help with confocal microscopy. We would like to thank Duncan Crosbie for

proofreading as a native English speaker. This work was supported by a grant from the Deutsche Forschungsgemeinschaft (DFG) to Dr Arne Weiberg (Grant-ID WE 5707/1-1). The authors declare no conflict of interest.

Author contributions

FD: conceptualization, formal analysis, investigation, methodology, validation, visualization, writing—original draft preparation, writing—review and editing; LO: formal analysis, investigation, methodology, validation, visualization; BL: investigation, methodology, validation, writing—review and editing; AT: resources; AW: conceptualization, funding acquisition, supervision, writing—original draft preparation, writing—review and editing.

Data availability

All data supporting the findings of this study are available within the paper and within its [Supplementary data](#) published online. All plasmids and transgenic plant lines created during this study are available from the corresponding author (AW) upon reasonable request.

References

- Aglar MT, Ruhe J, Kroll S, Morhenn C, Kim ST, Weigel D, Kemen EM. 2016. Microbial hub taxa link host and abiotic factors to plant microbiome variation. *PLoS Biology* **14**, e1002352.
- An Y-Q, McDowell JM, Huang S, McKinney EC, Chambliss S, Meagher RB. 1996. Strong, constitutive expression of the *Arabidopsis* *ACT2/ACT8 actin* subclass in vegetative tissues. *The Plant Journal* **10**, 107–121.
- Anderson RG, Deb D, Fedkenheuer K, McDowell JM. 2015. Recent progress in RXLR effector research. *Molecular Plant-Microbe Interactions* **28**, 1063–1072.
- Asai S, Rallapalli G, Piquerez SJ, Caillaud MC, Furzer OJ, Ishaque N, Wirthmueller L, Fabro G, Shirasu K, Jones JD. 2014. Expression profiling during Arabidopsis/downy mildew interaction reveals a highly-expressed effector that attenuates responses to salicylic acid. *PLoS Pathogens* **10**, e1004443.
- Badel JL, Shimizu R, Oh HS, Collmer A. 2006. A *Pseudomonas syringae* pv. *tomato avrE1/hopM1* mutant is severely reduced in growth and lesion formation in tomato. *Molecular Plant-Microbe Interactions* **19**, 99–111.
- Bailey K, Çevik V, Holton N, *et al.* 2011. Molecular cloning of ATR5Emoy2 from *Hyaloperonospora arabidopsidis*, an avirulence determinant that triggers RPP5-mediated defense in Arabidopsis. *Molecular Plant-Microbe Interactions* **24**, 827–838.
- Baum JA, Bogaert T, Clinton W, *et al.* 2007. Control of coleopteran insect pests through RNA interference. *Nature Biotechnology* **25**, 1322–1326.
- Baxter L, Tripathy S, Ishaque N, *et al.* 2010. Signatures of adaptation to obligate biotrophy in the *Hyaloperonospora arabidopsidis* genome. *Science* **330**, 1549–1551.
- Bemm F, Becker D, Larisch C, *et al.* 2016. Venus flytrap carnivorous lifestyle builds on herbivore defense strategies. *Genome Research* **26**, 812–825.
- Bilir Ö, Telli O, Norman C, Budak H, Hong Y, Tör M. 2019. Small RNA inhibits infection by downy mildew pathogen *Hyaloperonospora arabidopsidis*. *Molecular Plant Pathology* **20**, 1523–1534.
- Binder A, Lambert J, Morbitzer R, Popp C, Ott T, Lahaye T, Parniske M. 2014. A modular plasmid assembly kit for multigene expression, gene silencing and silencing rescue in plants. *PLoS One* **9**, e88218.
- Bollmann SR, Fang Y, Press CM, Tyler BM, Grünwald NJ. 2016. Diverse evolutionary trajectories for small RNA biogenesis genes in the oomycete genus *Phytophthora*. *Frontiers in Plant Science* **7**, 284.
- Bustin SA, Benes V, Garson JA, *et al.* 2009. The MIQE guidelines: minimum information for publication of quantitative real-time PCR experiments. *Clinical Chemistry* **55**, 611–622.

- Cabral A, Stassen JH, Seidl MF, Bautor J, Parker JE, Van den Ackerveken G.** 2011. Identification of *Hyaloperonospora arabidopsidis* transcript sequences expressed during infection reveals isolate-specific effectors. *PLoS One* **6**, e19328.
- Cai Q, Qiao L, Wang M, He B, Lin F-M, Palmquist J, Huang S-D, Jin H.** 2018. Plants send small RNAs in extracellular vesicles to fungal pathogen to silence virulence genes. *Science* **360**, 1126–1129.
- Caillaud MC, Asai S, Rallapalli G, Piquerez S, Fabro G, Jones JD.** 2013. A downy mildew effector attenuates salicylic acid-triggered immunity in *Arabidopsis* by interacting with the host mediator complex. *PLoS Biology* **11**, e1001732.
- Casacuberta JM, Devos Y, du Jardin P, Ramon M, Vaucheret H, Nogué F.** 2015. Biotechnological uses of RNAi in plants: risk assessment considerations. *Trends in Biotechnology* **33**, 145–147.
- Caten CE, Jinks JL.** 1968. Spontaneous variability of single isolates of *Phytophthora infestans*. I. Cultural variation. *Canadian Journal of Botany* **46**, 329–348.
- Cerri MR, Wang Q, Stolz P, et al.** 2017. The ERN1 transcription factor gene is a target of the CCaMK/CYCLOPS complex and controls rhizobial infection in *Lotus japonicus*. *New Phytologist* **215**, 323–337.
- Clough SJ, Bent AF.** 1998. Floral dip: a simplified method for *Agrobacterium*-mediated transformation of *Arabidopsis thaliana*. *The Plant Journal* **16**, 735–743.
- Coates ME, Beynon JL.** 2010. *Hyaloperonospora arabidopsidis* as a pathogen model. *Annual Review of Phytopathology* **48**, 329–345.
- Cohen Y, Van den Langenberg KM, Wehner TC, Ojiambo PS, Hausbeck M, Quesada-Ocampo LM, Lebeda A, Sierotzki H, Gisi U.** 2015. Resurgence of *Pseudoperonospora cubensis*: the causal agent of cucurbit downy mildew. *Phytopathology* **105**, 998–1012.
- Delmas CE, Dussert Y, Delière L, Couture C, Mazet ID, Richart Cervera S, Delmotte F.** 2017. Soft selective sweeps in fungicide resistance evolution: recurrent mutations without fitness costs in grapevine downy mildew. *Molecular Ecology* **26**, 1936–1951.
- Dickman MB, Fluhr R.** 2013. Centrality of host cell death in plant-microbe interactions. *Annual Review of Phytopathology* **51**, 543–570.
- Dickman MB, Park YK, Oltersdorf T, Li W, Clemente T, French R.** 2001. Abrogation of disease development in plants expressing animal antiapoptotic genes. *Proceedings of the National Academy of Sciences, USA* **98**, 6957–6962.
- Dinh PT, Brown CR, Elling AA.** 2014. RNA interference of effector gene *Mc16D10L* confers resistance against *Meloidogyne chitwoodi* in *Arabidopsis* and potato. *Phytopathology* **104**, 1098–1106.
- Dou D, Kale SD, Wang X, et al.** 2008. Conserved C-terminal motifs required for avirulence and suppression of cell death by *Phytophthora sojae* effector Avr1b. *The Plant Cell* **20**, 1118–1133.
- Dunker F, Trutzenberg A, Rothenpieler JS, et al.** 2020. Oomycete small RNAs bind to the plant RNA-induced silencing complex for virulence. *eLife* **9**, e56096.
- Fabro G, Steinbrenner J, Coates M, et al.** 2011. Multiple candidate effectors from the oomycete pathogen *Hyaloperonospora arabidopsidis* suppress host plant immunity. *PLoS Pathogens* **7**, e1002348.
- Fry W.** 2008. *Phytophthora infestans*: the plant (and R gene) destroyer. *Molecular Plant Pathology* **9**, 385–402.
- Govindarajulu M, Epstein L, Wroblewski T, Michelmore RW.** 2015. Host-induced gene silencing inhibits the biotrophic pathogen causing downy mildew of lettuce. *Plant Biotechnology Journal* **13**, 875–883.
- Govrin EM, Levine A.** 2000. The hypersensitive response facilitates plant infection by the necrotrophic pathogen *Botrytis cinerea*. *Current Biology* **10**, 751–757.
- Harrison SJ, Mott EK, Parsley K, Aspinall S, Gray JC, Cottage A.** 2006. A rapid and robust method of identifying transformed *Arabidopsis thaliana* seedlings following floral dip transformation. *Plant Methods* **2**, 19.
- Helber N, Wippel K, Sauer N, Schaarschmidt S, Hause B, Requena N.** 2011. A versatile monosaccharide transporter that operates in the arbuscular mycorrhizal fungus *Glomus* sp is crucial for the symbiotic relationship with plants. *The Plant Cell* **23**, 3812–3823.
- Hou Y, Ma W.** 2020. Natural host-induced gene silencing offers new opportunities to engineer disease resistance. *Trends in Microbiology* **28**, 109–117.
- Hou Y, Zhai Y, Feng L, et al.** 2019. A *Phytophthora* effector suppresses trans-kingdom RNAi to promote disease susceptibility. *Cell Host & Microbe* **25**, 153–165.e5.
- Hudzik C, Hou Y, Ma W, Axtell MJ.** 2020. Exchange of small regulatory RNAs between plants and their pests. *Plant Physiology* **182**, 51–62.
- Hurtado-Gonzales OP, Lamour KH.** 2009. Evidence for inbreeding and apomixis in close crosses of *Phytophthora capsici*. *Plant Pathology* **58**, 715–722.
- Jahan SN, Åsman AK, Corcoran P, Fogelqvist J, Vetukuri RR, Dixelius C.** 2015. Plant-mediated gene silencing restricts growth of the potato late blight pathogen *Phytophthora infestans*. *Journal of Experimental Botany* **66**, 2785–2794.
- Jiang RH, Tyler BM.** 2012. Mechanisms and evolution of virulence in oomycetes. *Annual Review of Phytopathology* **50**, 295–318.
- Kamoun S, Furzer O, Jones JD, et al.** 2015. The Top 10 oomycete pathogens in molecular plant pathology. *Molecular plant pathology* **16**, 413–434.
- Ketelaar T, Meijer HJ, Spiekerman M, Weide R, Govers F.** 2012. Effects of latrunculin B on the actin cytoskeleton and hyphal growth in *Phytophthora infestans*. *Fungal Genetics and Biology* **49**, 1014–1022.
- Kettles GJ, Bayon C, Canning G, Rudd JJ, Kanyuka K.** 2017. Apoplastic recognition of multiple candidate effectors from the wheat pathogen *Zymoseptoria tritici* in the nonhost plant *Nicotiana benthamiana*. *New Phytologist* **213**, 338–350.
- Kim SG, Wang Y, Lee KH, et al.** 2013. In-depth insight into in vivo apoplastic secretome of rice-*Magnaporthe oryzae* interaction. *Journal of Proteomics* **78**, 58–71.
- Koch A, Kogel KH.** 2014. New wind in the sails: improving the agronomic value of crop plants through RNAi-mediated gene silencing. *Plant Biotechnology Journal* **12**, 821–831.
- Koch E, Slusarenko A.** 1990. *Arabidopsis* is susceptible to infection by a downy mildew fungus. *The Plant Cell* **2**, 437–445.
- Kombrink A, Thomma BP.** 2013. LysM effectors: secreted proteins supporting fungal life. *PLoS Pathogens* **9**, e1003769.
- Kościańska E, Kalantidis K, Wypijewski K, Sadowski J, Tabler M.** 2005. Analysis of RNA silencing in agroinfiltrated leaves of *Nicotiana benthamiana* and *Nicotiana tabacum*. *Plant Molecular Biology* **59**, 647–661.
- Krasileva KV, Zheng C, Leonelli L, Goritschnig S, Dahlbeck D, Staskawicz BJ.** 2011. Global analysis of *Arabidopsis*/downy mildew interactions reveals prevalence of incomplete resistance and rapid evolution of pathogen recognition. *PLoS One* **6**, e28765.
- Kurup S, Runions J, Köhler U, Laplaze L, Hodge S, Haseloff J.** 2005. Marking cell lineages in living tissues. *The Plant Journal* **42**, 444–453.
- Livak KJ, Schmittgen TD.** 2001. Analysis of relative gene expression data using real-time quantitative PCR and the $2^{-\Delta\Delta C_T}$ method. *Methods* **25**, 402–408.
- Lück S, Kreszies T, Strickert M, Schweizer P, Kuhlmann M, Douchkov D.** 2019. siRNA-finder (si-Fi) software for RNAi-target design and off-target prediction. *Frontiers in Plant Science* **10**, 1023.
- Maekawa T, Kusakabe M, Shimoda Y, Sato S, Tabata S, Murooka Y, Hayashi M.** 2008. Polyubiquitin promoter-based binary vectors for overexpression and gene silencing in *Lotus japonicus*. *Molecular Plant-Microbe Interactions* **21**, 375–382.
- Mao YB, Cai WJ, Wang JW, Hong GJ, Tao XY, Wang LJ, Huang YP, Chen XY.** 2007. Silencing a cotton bollworm P450 monooxygenase gene by plant-mediated RNAi impairs larval tolerance of gossypol. *Nature Biotechnology* **25**, 1307–1313.
- McDowell JM.** 2014. *Hyaloperonospora arabidopsidis*: a model pathogen of *Arabidopsis*. In: Dean RA, Lichens-Park A, Kole C, eds. *Genomics of plant-associated fungi and oomycetes: Dicot pathogens*. Berlin, Heidelberg: Springer, 209–234.
- Miller L.** 2010. Analyzing gels and western blots with ImageJ. lukemiller.org.
- Nowara D, Gay A, Lacomme C, Shaw J, Ridout C, Douchkov D, Hensel G, Kumlehn J, Schweizer P.** 2010. HIGS: host-induced gene silencing in the obligate biotrophic fungal pathogen *Blumeria graminis*. *The Plant Cell* **22**, 3130–3141.

- Pel MJ, Wintermans PC, Cabral A, Robroek BJ, Seidl MF, Bautor J, Parker JE, Van den Ackerveken G, Pieterse CM. 2014. Functional analysis of *Hyaloperonospora arabidopsidis* RXLR effectors. *PLoS One* **9**, e110624.
- Pliogo C, Nowara D, Bonciani G, *et al.* 2013. Host-induced gene silencing in barley powdery mildew reveals a class of ribonuclease-like effectors. *Molecular Plant-Microbe Interactions* **26**, 633–642.
- Ried MK, Banhara A, Hwu FY, Binder A, Gust AA, Höfle C, Hückelhoven R, Nürnberger T, Parniske M. 2019. A set of Arabidopsis genes involved in the accommodation of the downy mildew pathogen *Hyaloperonospora arabidopsidis*. *PLoS Pathogens* **15**, e1007747.
- Roine E, Wei W, Yuan J, Nurmiaho-Lassila E-L, Kalkkinen N, Romantschuk M, He SY. 1997. Hrp pilus: An *hrp*-dependent bacterial surface appendage produced by *Pseudomonas syringae* pv. *tomato* DC3000. *Proceedings of the National Academy of Sciences, USA* **94**, 3459–3464.
- Rooney HCE, Van't Klooster JW, van der Hoorn RAL, Joosten MHAJ, Jones JDG, de Wit PJGM. 2005. *Cladosporium Avr2* inhibits tomato Rcr3 protease required for Cf-2-dependent disease resistance. *Science* **308**, 1783–1786.
- Ruiz MT, Voinnet O, Baulcombe DC. 1998. Initiation and maintenance of virus-induced gene silencing. *The Plant Cell* **10**, 937–946.
- Rutter B, Rutter K, Innes R. 2017. Isolation and quantification of plant extracellular vesicles. *Bio-Protocol* **7**, doi: 10.21769/BioProtoc.2533.
- Salguero-Linares J, Coll NS. 2019. Plant proteases in the control of the hypersensitive response. *Journal of Experimental Botany* **70**, 2087–2095.
- Silhavy D, Molnár A, Lucioli A, Szittya G, Hornyik C, Tavazza M, Burgyán J. 2002. A viral protein suppresses RNA silencing and binds silencing-generated, 21- to 25-nucleotide double-stranded RNAs. *The EMBO Journal* **21**, 3070–3080.
- Slusarenko AJ, Schlaich NL. 2003. Downy mildew of *Arabidopsis thaliana* caused by *Hyaloperonospora parasitica* (formerly *Peronospora parasitica*). *Molecular Plant Pathology* **4**, 159–170.
- Sperschneider J, Dodds PN, Singh KB, Taylor JM. 2018. ApoplastP: prediction of effectors and plant proteins in the apoplast using machine learning. *New Phytologist* **217**, 1764–1778.
- Thordal-Christensen H, Birch PRJ, Spanu PD, Panstruga R. 2018. Why did filamentous plant pathogens evolve the potential to secrete hundreds of effectors to enable disease? *Molecular Plant Pathology* **19**, 781–785.
- Uknes S, Mauch-Mani B, Moyer M, Potter S, Williams S, Dincher S, Chandler D, Slusarenko A, Ward E, Ryals J. 1992. Acquired resistance in *Arabidopsis*. *The Plant Cell* **4**, 645–656.
- Vega-Arreguín JC, Jalloh A, Bos JI, Moffett P. 2014. Recognition of an Avr3a homologue plays a major role in mediating nonhost resistance to *Phytophthora capsici* in *Nicotiana* species. *Molecular Plant-Microbe Interactions* **27**, 770–780.
- Veloso J, van Kan JAL. 2018. Many shades of grey in *Botrytis*-host plant interactions. *Trends in Plant Science* **23**, 613–622.
- Wang M, Weiberg A, Lin FM, Thomma BP, Huang HD, Jin H. 2016. Bidirectional cross-kingdom RNAi and fungal uptake of external RNAs confer plant protection. *Nature Plants* **2**, 16151.
- Weiberg A, Wang M, Lin F-M, Zhao H, Zhang Z, Kaloshian I, Huang H-D, Jin H. 2013. Fungal small RNAs suppress plant immunity by hijacking host RNA interference pathways. *Science* **342**, 118–123.
- Wirthmueller L, Asai S, Rallapalli G, *et al.* 2018. Arabidopsis downy mildew effector HaRxL106 suppresses plant immunity by binding to RADICAL-INDUCED CELL DEATH1. *New Phytologist* **220**, 232–248.
- Xin X-F, Nomura K, Ding X, *et al.* 2015. *Pseudomonas syringae* effector avirulence protein E localizes to the host plasma membrane and down-regulates the expression of the NONRACE-SPECIFIC DISEASE RESISTANCE1/HARPIN-INDUCED1-LIKE13 gene required for antibacterial immunity in Arabidopsis. *Plant Physiology* **169**, 793–802.
- Yan HZ, Liou RF. 2006. Selection of internal control genes for real-time quantitative RT-PCR assays in the oomycete plant pathogen *Phytophthora parasitica*. *Fungal Genetics and Biology* **43**, 430–438.
- Yin C, Hulbert SH. 2018. Host-induced gene silencing (HIGS) for elucidating *Puccinia* gene function in wheat. *Methods in Molecular Biology* **1848**, 139–150.
- Zeng T, Rodriguez-Moreno L, Mansurkhodzhaev A, *et al.* 2020. A lysin motif effector subverts chitin-triggered immunity to facilitate arbuscular mycorrhizal symbiosis. *New Phytologist* **225**, 448–460.
- Zhang M, Wang Q, Xu K, Meng Y, Quan J, Shan W. 2011. Production of dsRNA sequences in the host plant is not sufficient to initiate gene silencing in the colonizing oomycete pathogen *Phytophthora parasitica*. *PLoS One* **6**, e28114.
- Zhang T, Zhao YL, Zhao JH, Wang S, Jin Y, Chen ZQ, Fang YY, Hua CL, Ding SW, Guo HS. 2016. Cotton plants export microRNAs to inhibit virulence gene expression in a fungal pathogen. *Nature Plants* **2**, 16153.

Supplementary data:

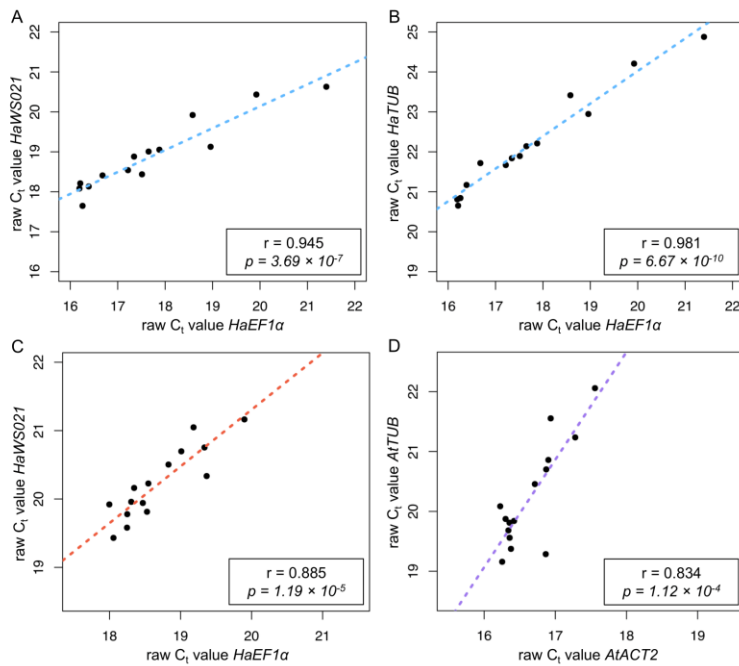


Figure S1: Expression correlation analysis of *H. arabidopsidis* and *A. thaliana* reference genes by qRT-PCR. Raw C_t values of three *H. arabidopsidis* reference genes and two *A. thaliana* reference genes were recorded in infected *A. thaliana* plants. A) Correlation plot of C_t values between A) *HaEF1 α* and *HaWS021*, B) *HaEF1 α* and *HaTUB* and C) *HaEF1 α* and *HaWS021* are displayed. C_t values in A) and B) were measured at 4 dpi and in C) at 7 dpi. Despite considerable variation in the C_t values between samples reflecting the variation of the *H. arabidopsidis* infection strength, expression of the three genes was highly correlated, validating their stable expression. D) C_t values of the two *A. thaliana* reference genes *AtACT2* and *AtTUB* displayed correlated expression. Data were recorded from expression resembling pooled samples at 4 and 7 dpi. The boxes in A) - D) display the Pearson's correlation coefficient r and p -value of correlation for each correlation analysis.

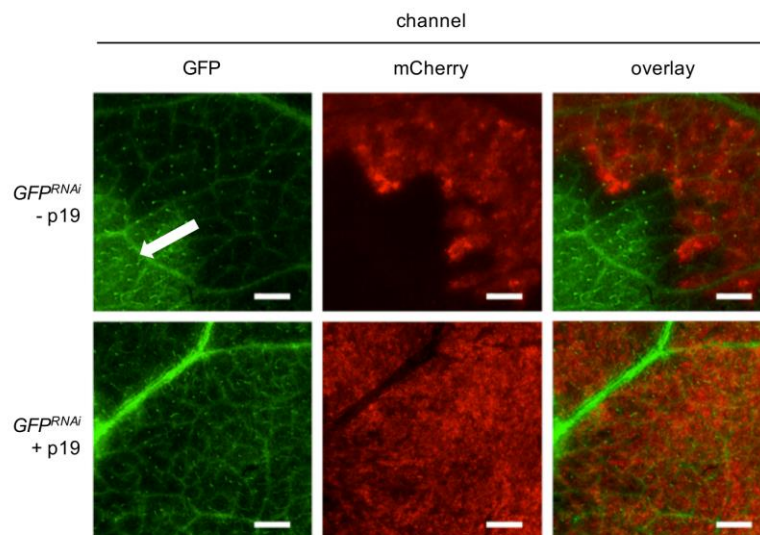


Figure S2: Expression of *GFP^{RNAi}* by *A. tumefaciens* infiltration led to *GFP* silencing in the *N. benthamiana* line 16c stably expressing *GFP*. Epifluorescence pictures were taken 2 days post infiltration, mCherry was used as a transformation marker. The arrow displays the endogenous GFP fluorescence of line 16c in the untransformed region. Co-expression of the viral RNAi suppressor p19 was used to validate RNAi-dependent gene silencing. The scale bars indicates 1 mm.

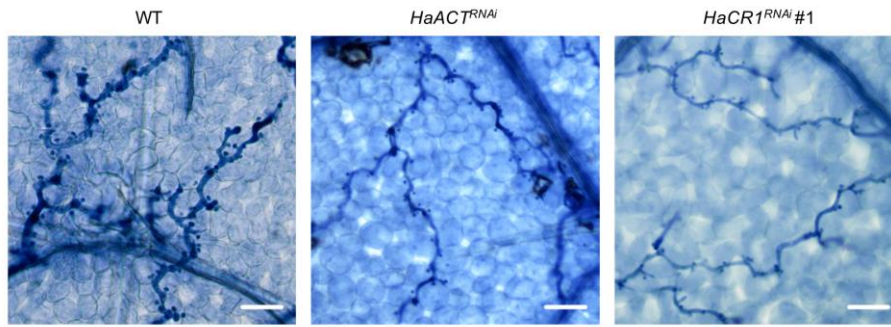


Figure S3: *A. thaliana* *HaACT*^{RNAi} and *HaCR1*^{RNAi} plants displayed no obviously altered infection phenotype at 4 dpi. A minimum of five leaves was inspected per genotype. Scale bars represent 50 μm.

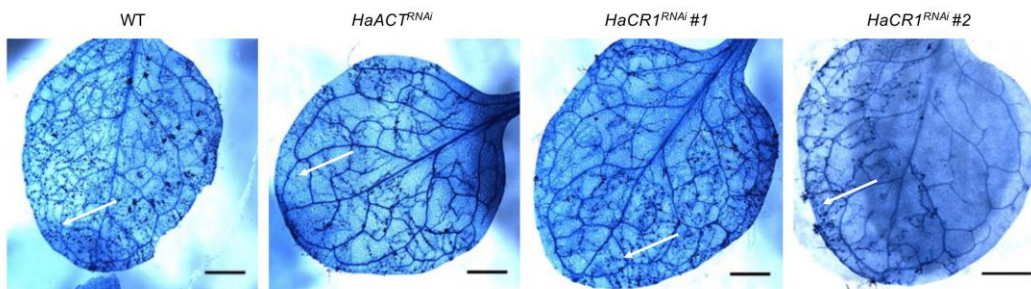


Figure S5: Representative leaves used for *H. arabidopsidis* oospore quantification. *A. thaliana* *HaACT*^{RNAi} and both *HaCR1*^{RNAi} lines allowed reduced oospore production. The white arrow indicates an oospore. Leaves were inspected at 7 dpi. Scale bars indicate 2 mm.

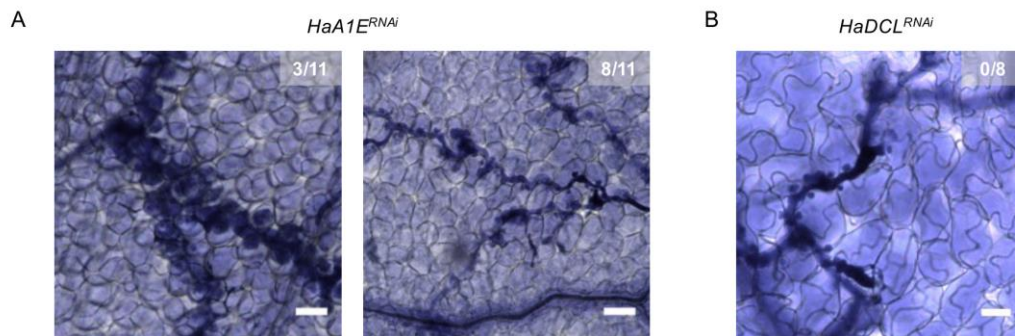


Figure S4: Infection phenotype of the *A. thaliana* *HaA1E*^{RNAi} and the *HaDCL1*^{RNAi} lines. A) The *A1E*^{RNAi} line exhibited moderate resistance against *H. arabidopsidis*. At 7 dpi, trailing necrosis was detected in three out of eleven infected seedling leaves, while eight out of eleven leaves displayed no trailing necrosis. B) *HaDCL1*^{RNAi} plants did not display trailing necrosis upon infection with *H. arabidopsidis*. Scale bars represent 50 μm.

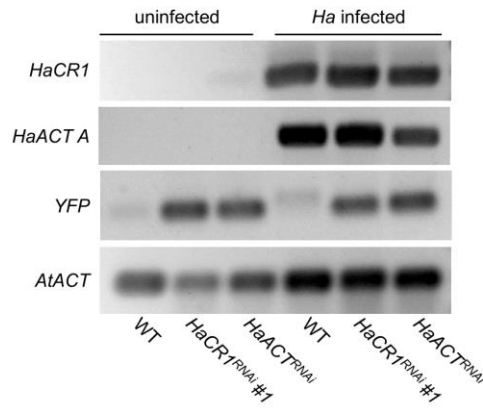


Figure S6: Validation of RT-PCR primers to assess *H. arabidopsidis* target gene expression in *A. thaliana* HIGS plants. RT-PCR of *H. arabidopsidis* *HaACT A* and *HaCR1* in mock-treated and *H. arabidopsidis*-infected *A. thaliana* WT and HIGS plants at 4 dpi. The HIGS construct did not generate any detectable PCR products with the *H. arabidopsidis*-specific target gene primers for *HaACT A* and *HaCR1* in non-infected plant samples. *YFP* expression was used as control for transgene expression in HIGS plants. *AtACT* was used to validate cDNA synthesis.

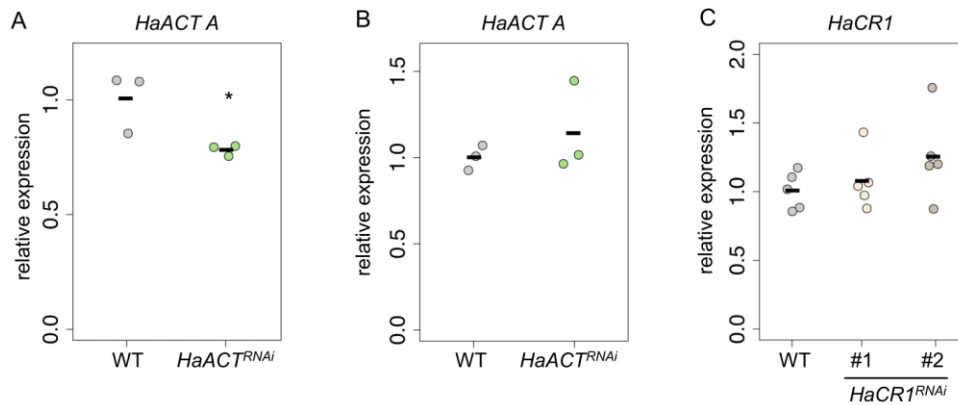


Figure S7: *H. arabidopsidis* target gene expression when infecting *A. thaliana* HIGS plants. A) Quantitative RT-PCR of *HaACT A* in *H. arabidopsidis*-infected *A. thaliana* WT and *HaACT^{RNAi}* plants at 4 dpi using *HaEF1 α* as a reference genes. B) Quantitative RT-PCR of *HaACT A* in *H. arabidopsidis*-infected WT and corresponding HIGS plants at 7 dpi using *HaEF1 α* as a reference gene. C) Quantitative RT-PCR of *HaCR1* in *H. arabidopsidis*-infected WT and two independent HIGS lines (#1, #2) at 7 dpi using *HaEF1 α* and *HaWS021* as reference genes. The bars indicate the average of three biological replicates each comprising six to eight leaves. Asterisks indicate significant difference by student's t-test with $p \leq 0.05$.

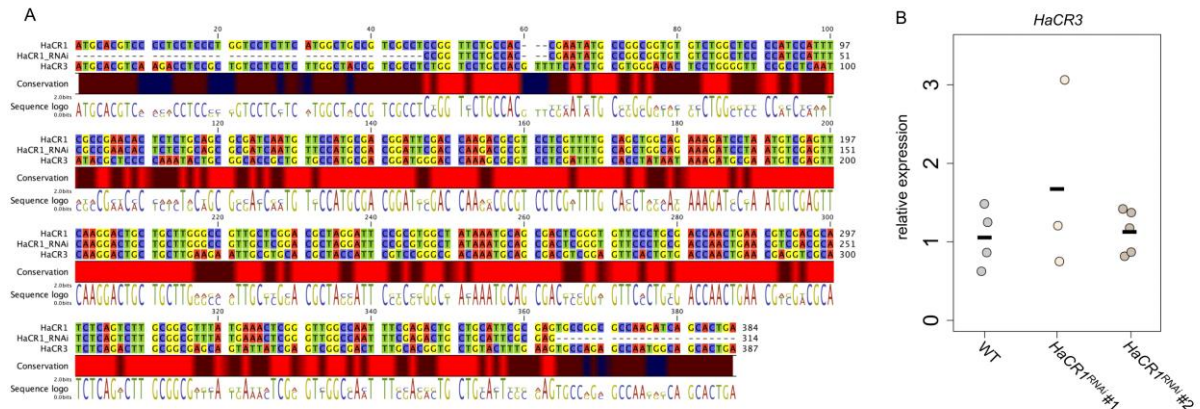


Figure S10: *HaCR3* expression was not suppressed during infection of *HaCR1*^{RNAi} plants. A) DNA Sequence alignment of the coding sequences of *HaCR1* and *HaCR3* with the sequence of the *HaCR1*^{RNAi} construct. B) Quantitative RT-PCR of *HaCR3* in *A. thaliana* WT and *HaCR1*^{RNAi} plants at 4 dpi using \geq three biological replicates. *HaEF1 α* and *HaWS021* were used as reference genes.

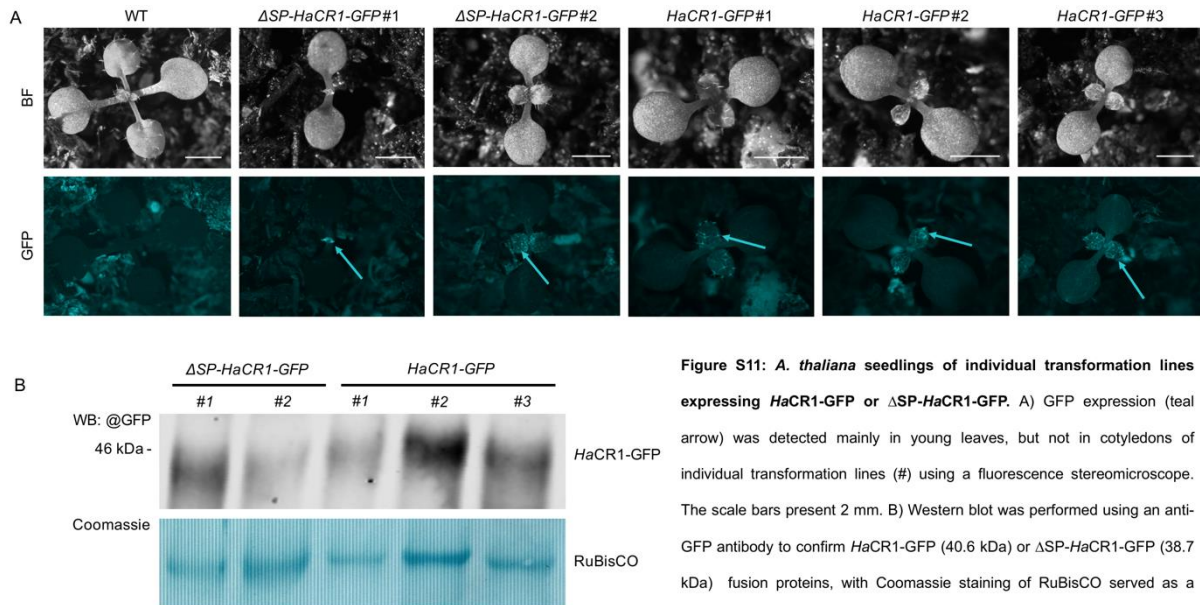


Figure S11: *A. thaliana* seedlings of individual transformation lines expressing *HaCR1*-GFP or Δ SP-*HaCR1*-GFP. A) GFP expression (teal arrow) was detected mainly in young leaves, but not in cotyledons of individual transformation lines (#) using a fluorescence stereomicroscope. The scale bars present 2 mm. B) Western blot was performed using an anti-GFP antibody to confirm *HaCR1*-GFP (40.6 kDa) or Δ SP-*HaCR1*-GFP (38.7 kDa) fusion proteins, with Coomassie staining of RuBisCO served as a loading control.

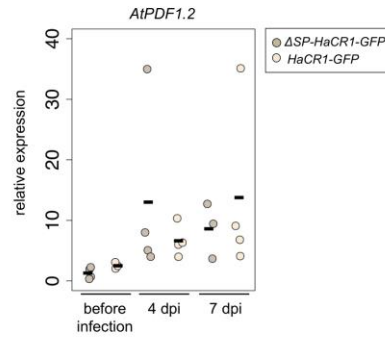


Figure S12: Expression of *AtPDF1.2* was not different when comparing ΔSP -*HaCR1-GFP* or *HaCR1-GFP* expressing *A. thaliana* seedlings upon *H. arabidopsis* infection. *AtPDF1.2* expression was determined by qRT-PCR using *AtACT2* and *AtTUB* as reference genes.

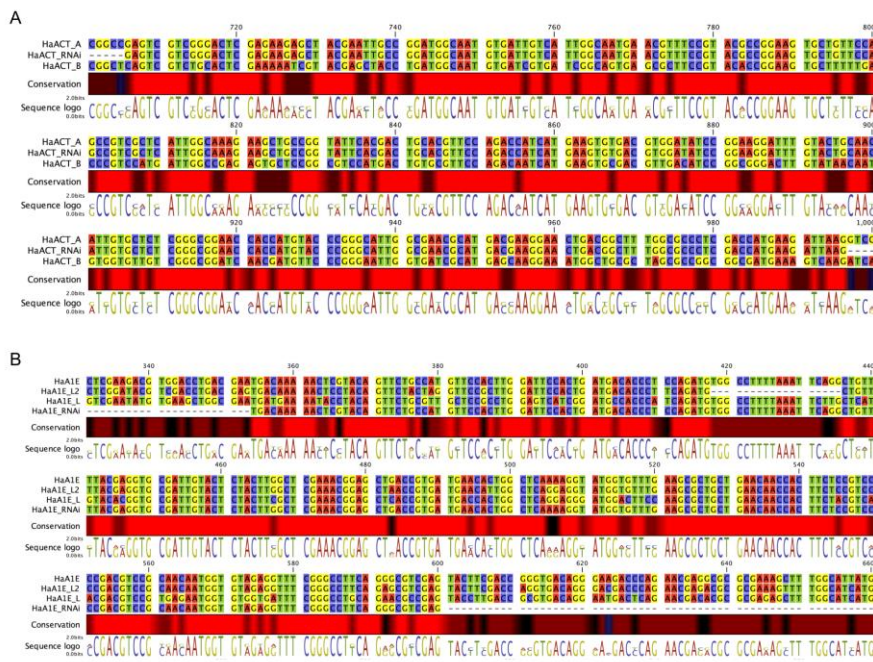


Figure S13: DNA sequence alignment of the target gene and closest paralogs at the HIGS target site. A) Sequence alignment of *HaACT A* with *HaACT B*. B) Sequence alignment of *HaA1E* with the two paralogs *HaA1EL* and *HaA1EL2*. The numbers above the alignments in A) and B) are showing the position in the target transcript.

Table S: 1: List of primers used in this study			
Name	Sequence	Annealing Temperature	Purpose
HaCR1_RNAi_fwd	ggtctcacaccCCGTTCTGCCACCGAATAT		RNAi construct cloning
HaCR1_RNAi_rev	ggtctcaccttCTCGGAATGCAGCAGTCTC		RNAi construct cloning
HaACT_RNAi_fwd	ggtctcacaccGAGTCGTCGGGACTCGAGAA		RNAi construct cloning
HaACT_RNAi_rev	ggtctcaccttCTTAATCTTCATGGTCGAGG		RNAi construct cloning
HaDCL1_RNAi_fwd	ggtctcacaccTACCCGCGGCTCTTTGCCAC		RNAi construct cloning
HaDCL1_RNAi_rev	ggtctcaccttTACTATTTGCGCCAAGCAG		RNAi construct cloning
HaA1E_RNAi_fwd	ggtctcacaccTGACAAAACTCGTACAGTT		RNAi construct cloning
HaA1E_RNAi_rev	ggtctcaccttCTCGACGCCCTGAAGGCCCG		RNAi construct cloning
GFP_RNAi_fwd	ggtctcacaccAGTGGAGAGGGTGAAGGTGA		RNAi construct cloning
GFP_RNAi_rev	ggtctcaccttAAAGGGCAGATTGTGTGGAC		RNAi construct cloning
HaCR1_fwd	TAGGTCTCACACCATGCACGTCCCCTCCTCCCTG		HaCR1 for <i>in planta</i> expression
HaCR1_rev	TAGGTCTCACCTTGTGCTGATCTTGGCGCCGGCAC		HaCR1 for <i>in planta</i> expression
HaCR1_noSP_fwd	ATGGTCTCACACCATGACCGAATATGCCGGCGGTGTG		HaCR1 for <i>in planta</i> expression
HaCR1_RT_fwd	CTCCCTGGTCCTTTCAT	52 °C	qPCR
HaCR1_RT_rev	CCTCAACTGAAAAGCTCA	52 °C	qPCR
HaAct_RT_fwd	CGTGCGCGACATTAAGAGA	52 °C	qPCR
HaAct_RT_rev	GAGCCACCAATCCACACCGA	52 °C	qPCR
HaEF1 α _RT_fwd	TTGGTGGTTGCTTCGGGTGT	52 °C	qPCR
HaEF1 α _RT_rev	TTGGGCGGGTTCAGGTTGT	52 °C	qPCR

HaTUB_fwd	TTGGTGTGTGCTGCTATGTCT	52 °C	qPCR
HaTUB_rev	CTCATCCACCTCCTTCGTA	52 °C	qPCR
HaWS021_fwd	CACAAAGAAGCGTCCAAACCA	52 °C	qPCR
HaWS021_rev	CCGGGACGAACTTCAAAAACA	52 °C	qPCR
HaCR3_fwd	GTCCTCCTCTTGGCTACCGTC	52 °C	qPCR
HaCR3_rev	GTGCTGCCATTGGCTCTGGCA	52 °C	qPCR
AtACT2_RT_fwd	CAGTGGTCGTACAACCGGTATT	52-60 °C	qPCR
AtACT2_RT_rev	GTCTCTTACAATTTCCCGCTCT	52-60 °C	qPCR
AtACT11_fwd	AACTTTCAACTCCTGCCATG	56 °C	qPCR
AtACT11_rev	CTGCAAGGTCCAAACGCAGA	56 °C	qPCR
AtPR1_RT_fwd	CTCGGAGCTACGCAGAACAA	60 °C	qPCR
AtPR1_RT_rev	GCCTTCTCGCTAACCCACAT	60 °C	qPCR
AtPDF1.2_RT_fwd	CTTGTTCTCTTTGCTGCTTTGAC	60 °C	qPCR
AtPDF1.2_RT_rev	TAGTTGCATGATCCATGTTTG	60 °C	qPCR
AtTUB_fwd	TGTTCAAGGCGAGTGAGTGAG	56 °C	qPCR
AtTUB_rev	ATGTTGCTCTCCGCTTCTGT	56 °C	qPCR
AtUBQ10_rev	GGTTTGTGTTTTGGGGCCTTG	56 °C	qPCR
AtUBQ10_fwd	CGAAGCGATGATAAAGAAGAAGTTCG	56 °C	qPCR

Discussion

Hyaloperonospora arabidopsidis as a new cross-kingdom RNAi model

At the outset of this thesis there was only one reported, unambiguous event of natural cross-kingdom RNAi: sRNAs of the necrotrophic fungus *Botrytis cinerea* silencing targets in its hosts *Arabidopsis* and tomato (*Solanum lycopersicum*) (Weiberg et al., 2013). Thus, it was unclear how widespread cross-kingdom RNAi is and whether it extends to distinct plant pathogens (Chaloner et al., 2016). Thus, the first aim of this project was to clarify if the oomycete pathogen *H. arabidopsidis* uses sRNAs to promote virulence. In the first part of this thesis, I provide conclusive evidence that *H. arabidopsidis* uses sRNA effectors to achieve plant colonization and virulence. I applied co-immunopurification coupled to next generation sRNA sequencing and identified 133 *H. arabidopsidis* sRNAs associated with the host *AtAGO1* RISC which were predicted to target 49 *Arabidopsis* genes. *AtAGO1* associated sRNAs mimicked in size, and 5' nucleotide plant miRNAs and were distinct from *AtAGO2* immunopurified sRNA profiles, which clearly suggests a specific loading *in vivo*. In contrast, one wouldn't expect unspecific binding of sRNAs to the PAZ domain (named after the three proteins P-element induced wimpy testis (PIWI), ARGONAUTE, and ZWILLE (Vaucheret, 2008)) of AGO proteins during sample preparation to reveal specific sRNA characteristics and RISC preference.

I also provided a detailed protocol of our analysis of *AtAGO*-associated *H. arabidopsidis* sRNAs to foster the application of this method in cross-kingdom RNAi research. This protocol describes not only the experimental part, but also the bioinformatic analysis pipeline of the sequencing results, especially how to discriminate invasive pathogen sRNAs from endogenous plant sRNAs *in silico*.

I expected the *AtAGO*-bound *H. arabidopsidis* sRNAs to silence predicted plant target genes. Accordingly, I measured a moderate, but consistent repression of the sRNA target genes in infected plants. I however suspected that target gene silencing only occurred in host cells in direct contact with *H. arabidopsidis*, and was therefore partially masked by a strong dilution effect of uninfected leaf cells with unaltered expression.

In line with this, induction of the plant defense gene *AtPRI* was efficiently inhibited by *H. arabidopsidis* effectors in haustoria-containing host cells with direct pathogen contact. This inhibition was only visible through an *in situ proPRI:GUS* reporter and not by transcriptional analysis via qRT-PCR as high induction of *AtPRI* in uninfected cells masked the local repression by *H. arabidopsidis* (Caillaud et al., 2013).

Using a novel *in situ* silencing reporter designed by me together with Dr. Arne Weiberg, I observed highly localized, but very efficient silencing of plant target transcripts. This effect was independent of pathogenesis and sequence specific, as a scrambled, random target sequence, did not result in reporter activation. I observed reporter activation only adjacent to the pathogen hyphae within a maximum range of two cell layers. Notably, this is overall spatially congruent with prevention of *AtPR1* transcription (Caillaud et al., 2013). As I used the native target gene promoter and the native transcript fragment as target sequence, I provide, in my opinion, the most direct and strongest evidence of efficient target gene silencing under natural conditions so far.

My reporter bears significant advantages over previous reporter systems that are based on direct silencing of a target sequence tagged reporter transcript, leading to repression of a fluorescent protein or GUS (B. Wang et al., 2017; Weiberg et al., 2013). I employed the sequence specific RNA endonuclease Csy4 (Haurwitz et al., 2010) in a plant codon optimized version designed by Dr. Tom Schreiber to completely repress reporter gene expression in absence of silencing sRNAs. As I turned Csy4, instead of the reporter gene, into a sRNA target by adding the native *HasRNA* target sequence, I designed a reporter that becomes activated upon silencing. Therefore, the readout is displayed as a highly localized, qualitative signal appearance instead of a potentially rather small signal reduction that is frequently difficult to quantify in a reproducible manner.

In spite of the clear silencing effect of *HpasRNAs* and slicer activity of AtAGO1, 5' RACE-PCR analysis did not support mRNA cleavage of target mRNAs. I did not detect any enrichment of transcripts ends at the position opposite of the 10/11th nucleotide of the pathogen sRNA, as expected after AGO1 slicing activity (Mallory and Bouché, 2008). Even when thousands of cDNA fragments were sequenced by next generation sequencing, I could not directly verify the action of *H. arabidopsidis* sRNA effectors. I however detected a massive number of shorter transcripts, indicating rapid mRNA degradation. Therefore, repeating the experiment with an *atxrn4* exoribonuclease mutant, impaired in sRNA guided cleavage remnant decay, will potentially help to detect the direct slicing product (Schon et al., 2018; Souret et al., 2004). Alternatively, a holistic view of sRNA induced mRNA cleavage in both Arabidopsis and *H. arabidopsidis* can be obtained by degradome-seq as performed for the *Cuscuta*-Arabidopsis interaction (Johnson et al., 2019).

After I validated functional silencing of Arabidopsis genes by *H. arabidopsidis* sRNAs, I wondered about the importance of this process for overall pathogen virulence. A key role of sRNAs effectors is implicated by the markedly increased resistance and the occurrence of

trailing necrosis, when plants with impaired RISC activity like *atago1-27*, *atago1-45* and *atago1-46* were inoculated with *H. arabidopsidis*. Still, these results have to be taken with caution, as the loss of endogenous gene regulation in *atago1-27* and other *atago1* mutants leads to highly pleiotropic effects in development and physiology (Morel et al., 2002).

Nonetheless, I suggest that large parts of the *atago1-27* infection resistance are linked to the activity of *H. arabidopsidis* sRNAs, as the miRNA biogenesis mutant *atdcl1-11*, the siRNA pathway mutants *atdcl2dcl3dcl4* and *atrd6-15*, and further miRNA pathway mutants all did not display markedly increased disease resistance. This provides evidence that endogenous host RNAi perturbations are rather unlikely the cause for the observed resistance. As cross-kingdom sRNAs mimicked plant miRNAs by their molecular features, only *atago1* mutants but not *atago2* or *atago4* mutants displayed increased resistance.

Furthermore, increased plant disease resistance was observed when pathogen sRNA effectors were scavenged with a short tandem target mimic (STTM) (Yan et al., 2012), providing an independent line of evidence for the crucial role of *H. arabidopsidis* sRNA effectors. This is remarkable, because preventing the action of only three *Hpas*sRNA effectors was sufficient to observe markedly decreased pathogen virulence and released target gene repression, despite dozens of translocated sRNAs. Potentially, not all translocated sRNAs are functional alone but they act synergistically to interfere with entire plant pathways. Thereby, loss of single sRNAs might be sufficient to allow the plant at least partial re-activation of entire immune pathways giving rise to the strong resistance phenotype.

As STTM stacking, i.e., the combination of multiple STTMs in one crop plant, potentially results in broad band resistance against various pathogens performing cross-kingdom RNAi, STTMs are also a focal point of interest for future applied, agricultural research. As pest resistance against this control strategy will most likely involve single nucleotide polymorphisms (SNPs) in the target site, it could be relatively easily countered with complementary mutations of the STTM. However, more thorough research is obligatory to enable translation of this technology into crops and agricultural ecosystems.

I anticipated that host genes targeted by *H. arabidopsidis* sRNAs contribute to host immunity against this pathogen. The two verified cross-kingdom RNAi target genes *AtAED3* and *AtWNK2* however have not been previously attributed to plant immunity (Breitenbach et al., 2014; Wang et al., 2008). Nevertheless, infection assays using Arabidopsis knock-out mutants demonstrated quantitative contribution to defense against *H. arabidopsidis* and *AtWNK2* overexpression lines revealed clear signs of auto-immunity like spontaneous cell death (Chakraborty et al., 2018). I thereby suggest that analysis of cross-kingdom RNAi targets can

lead to the identification of unknown immunity factors that were overlooked in forward genetics screens (M. Wang et al., 2017b).

Taken these results together, I provide compelling evidence that *H. arabidopsidis* induces cross-kingdom RNAi via the host AGO1/RISC demonstrating for the first time sRNA effectors in an oomycete plant pathogen. Moreover, cross-kingdom RNAi in an oomycete plant pathogen interaction is suggested in *Phytophthora infestans* during potato infection in a preprint report. The authors propose a dual function of the *P. infestans* miR8788 to regulate both endogenous targets as well as the potato *LIPASE-LIKE (StLL)* 1 gene required for anti-oomycete defense (Hu et al., 2020).

B. cinerea and *H. arabidopsidis*: two complementary cross-kingdom RNAi model systems

H. arabidopsidis is in most aspects highly divergent from the first established model system *B. cinerea*. While *B. cinerea* displays a very wide host range of over 1000 plant species (Velo and van Kan, 2018), the host range of the downy mildew pathogen *H. arabidopsidis* is restricted to a single species, the model plant *Arabidopsis* (McDowell, 2014). *B. cinerea* has a necrotrophic life style, killing plant tissue and obtaining nutrients from the debris (van Kan, 2006). In contrast, *H. arabidopsidis*, an obligate biotroph, entirely depends on nutrient acquisition from living host cells via haustoria (Coates and Beynon, 2010). On the phylogenetic level oomycetes are highly distinct from *Botrytis cinerea*, a true fungus from the phylum of ascomycetes. These two major eukaryotic lineages diverged around 1.7 billion years ago, meaning this separation occurred 500 million years earlier than between animals and fungi (Parfrey et al., 2011).

Despite all these differences, I discovered striking similarities in the employment of sRNA effectors to silence host immunity genes. sRNA effectors resembled plant miRNAs in important sequence features like length and 5' U preference, enabling the misuse of the host RNAi machinery. The strong dependency of sRNA effectors on the host AGO1 protein is displayed by the increased infection resistance by *atago1-27* mutants towards both pathogens. This is particularly noteworthy, as many other *Arabidopsis* immunity factor mutants display increased susceptibility towards necrotrophs like *B. cinerea*, but reduced susceptibility to biotrophs like *H. arabidopsidis*, or *vice versa* (Mosher et al., 2013; Murmu et al., 2014; Spoel and Dong, 2008; von Saint Paul et al., 2011). Our results, together with other recently discovered cross-kingdom RNAi events in fungi, plants and even bacteria, imply that sRNA exchange between organisms is a general virulence/defense strategy in organismal interactions (Maizel et al., 2020; Zeng et al., 2019).

Having established cross-kingdom RNAi in the *H. arabidopsidis*/Arabidopsis pathosystem, researchers have now a new model system at hand that bears several advantages to complement the relatively well-established model *B. cinerea*:

H. arabidopsidis has a very long interaction phase of up to one week without host cell death. This enables the clear separation of host gene repression by silencing or host cell death, but also application of activatable silencing reporters. The reporter is provided sufficient time to get switched on, without the risk of artifacts due to cell death. This is especially relevant as high autofluorescence is a known artifact of dying or dead cells, and GUS staining may be ectopically activated by high peroxidase activity as found in cells undergoing PCD (Dixit et al., 2006; Guivarc'h et al., 1996; Van Baarlen et al., 2007).

An additional advantage of *H. arabidopsidis* is the highly quantitative disease resistance phenotype, which can be determined in relatively high throughput by microscopic analysis after trypan blue staining, sporangiophore or conidiospore counting and quantitative PCR of genomic DNA (Anderson and McDowell, 2015; Furci et al., 2019).

On the other hand, *H. arabidopsidis* also displays some disadvantages: above all, it can't be transformed and genetically modified (McDowell, 2014). Also, the very narrow host range can be detrimental rendering, for example, infection assays on transiently transformed *N. benthamiana* impossible. These shortcomings can be compensated by the use of *Botrytis*, that can be transformed relatively easy and has a wide host range of virtually all dicot plants (Velo and van Kan, 2018). Therefore, *H. arabidopsidis* and *B. cinerea* represent truly complementary cross-kingdom RNAi model systems.

Cross-kingdom RNAi: childhood friend or recurrent affair of life?

With an ever-increasing number of model systems for cross-kingdom RNAi it becomes evident that functional sRNA exchange is a common, widespread feature of plant microbe interactions (Maizel et al., 2020; Zeng et al., 2019). Thus, it can be concluded that sRNA-based communication either arose early during eukaryote evolution or multiple times independently. An argument for an ancient origin of cross-kingdom RNAi are some shared features: both *H. arabidopsidis* and *B. cinerea* seem to rely mainly on the host AGO1 protein as a hub for the sRNA arsenal (Dunker et al., 2020; Weiberg et al., 2013). This suggests that their sRNA effectors are not transported to the host together with a corresponding pathogen Argonaute as “ready to use” RISC complexes.

In contrast, nematode sRNAs were found in vesicles together with one specific AGO protein. Nematodes are known to encode for dozens of Argonaute proteins, including a large number of so called worm-specific AGOs (WAGOs). Thereby, a specialization of one of them for

selection, transport of sRNAs or catalyzing RNAi in the host cell appears more likely (Chow et al., 2019). However, in comparison the *H. arabidopsidis* genome encodes for only two AGO proteins and the *B. cinerea* genome for four (Bollmann et al., 2018; Breiting, 2016).

Notably, three of the best described cross-kingdom RNAi models *B. cinerea*, *H. arabidopsidis* and *C. campestris* were all found to target different host kinases (Dunker et al., 2020; Shahid et al., 2018; M. Wang et al., 2017b; Weiberg et al., 2013), suggesting a potential, common weak point of plant defense exploited by sRNA effectors. This is even more striking as otherwise the three pathogens have very little in common, and encounter substantially different host immune responses (Glazebrook, 2005). However, as kinases are frequently regulators, their action can be largely defined by their phosphorylation targets and the three pathogens do not target a particular common protease family, but mitogen-activated protein kinases, with no lysine kinases and a receptor-like kinase, respectively.

Besides these shared features there are also some remarkable differences among described sRNA effectors. First and foremost, the sRNA effectors of distinct plant pathogens such as *B. cinerea*, *H. arabidopsidis* and *Cuscuta* target vastly different transcript sets (Dunker et al., 2020; Johnson et al., 2019; Weiberg et al., 2013). Out of in total 258 predicted target genes only a single target gene was shared by *B. cinerea* and *Cuscuta* and not a single target of *H. arabidopsidis* was shared. The sole common target (AT4G28300) encodes for a proline-rich, cell wall localized, but otherwise undescribed protein. This finding might highlight the distinct evolution of sRNA effectors and their targets as it is in contrast to protein effectors which converged on common hubs (Mukhtar et al., 2011; Weßling et al., 2014).

The vast majority of *B. cinerea* sRNA effectors derive from LTR-retrotransposon sequences (Weiberg et al., 2013), while most *H. arabidopsidis* sRNA effectors were encoded by non-annotated, non-transposon regions. Even if the genome annotation of retrotransposons in *H. arabidopsidis* is probably incomplete, it still remains highly unlikely that transposons play a comparably dominant role for cross-kingdom sRNA production. In this line, cross-kingdom sRNAs in the parasitic plant genus *Cuscuta* were derived from miRNAs, the cereal fungal pathogen *P. striiformis* f. sp. *tritici* uses a miRNA-like RNA (milRNA) and plant defensive sRNAs comprised miRNAs as well as phased siRNAs (Cai et al., 2018b; Hou et al., 2019; Shahid et al., 2018; B. Wang et al., 2017; Zhang et al., 2016). These distinct loci encoding for cross-kingdom sRNAs imply convergent evolution of sRNA recruitment in attack or defense, rather than common evolution.

An intriguing speculation is the acquisition of core components of the sRNA exchange machinery via horizontal gene transfer from fungi to plant pathogenic oomycetes. Along this

line, *H. arabidopsidis* has potentially acquired 3.16% of its entire secreted proteome, including a plethora of its effectors, from fungi. This highlights the crucial role of massive horizontal gene transfer for plant pathogenic oomycete evolution (Richards et al., 2011; Savory et al., 2015). To shed light on the evolutionary origin of cross-kingdom RNAi remains one of the greatest challenges for future research.

Host-induced gene silencing as a tool for functional gene studies in *H. arabidopsidis*

The earliest studies on functional sRNA transport between organisms were reporting host-induced gene silencing by ectopic dsRNA expression. Besides the potential of HIGS to revolutionize crop protection as detailed in the introduction, it also provides a tool to study gene function in organisms without established transformation methods. Accordingly, HIGS has been successfully applied in a wide range of obligate biotrophic organisms like powdery mildews, rust fungi, root-knot nematodes and arbuscular mycorrhiza fungi (Helber et al., 2011; Huang et al., 2006; Nowara et al., 2010; Qi et al., 2018). While HIGS was already reported for crop protection against the lettuce downy mildew *Bremia lactuae* (Govindarajulu et al., 2015), it was not yet established for the important model pathogen *H. arabidopsidis*. Despite its negligible economic impact, it was elected as the second most important plant pathogenic oomycete because of its ability to efficiently infect the model plant (Kamoun et al., 2015).

During this study, me and my colleagues achieved HIGS of *H. arabidopsidis* genes and employed it for functional gene studies. We however also encountered a prevalent problem of HIGS as our transgenic plants targeting the *HaACT A* displayed increased resistance, but also obvious off-target effects in the plant itself (Auer and Frederick, 2009). These off-target effects weren't induced by silencing of one of the two most similar Arabidopsis Actin transcripts, highlighting the difficulty to pin-point the cause of off-target effects. It should be noted that the off-target prediction software Si-Fi (Lück et al., 2019) did not report a high probability off-target in Arabidopsis, illustrating the challenges to avoid off-target with *in silico* prediction software. The best possibility to trace down off-targets comprehensively is degradome-seq of HIGS lines compared with WT or empty vector control plants (Casacuberta et al., 2015), which is however laborious and costly.

To minimize the risk of off-targets I recommend to focus on effectors as targets rather than highly conserved housekeeping genes. Effector genes normally have very low conservation, are absent from the host genome, and despite their collaborative function a single effector gene knockdown can result in impaired virulence (Thordal-Christensen et al., 2018). Thus, I observed both reduced pathogen virulence and an unaltered plant growth phenotype in our *HaCRI^{RNAi}* lines.

Despite the relatively large number of successful HIGS applications, the insights into the molecular mechanisms governing HIGS remain limited. While for insect herbivores it is generally accepted that only long (>60 nt) dsRNAs lead to efficient silencing (Bolognesi et al., 2012; Zhang et al., 2015), the fundamental question whether long dsRNAs or the processed sRNAs are the active agents of HIGS has not been clarified in plant/fungal and plant/oomycete interactions. First insights from *Botrytis cinerea* point to ready, sRNAs as the mobile RNA providing efficient silencing. This conclusion was based on the observation that sRNAs accumulated in the pathogen cells upon infection of a HIGS plant, even when the pathogen *DCL* genes were knocked out (Wang et al., 2016). Similarly, according to a preprint study, efficient host-induced gene silencing of *Pseudomonas syringae* genes was only mediated by “ready”, sRNAs. There, in a cross between the HIGS line and an *atdcl2dcl3dcl4* triple mutant target transcript repression was completely abolished (Singla-Rastogi et al., 2019). This highlighted obligatory plant dicing of the long dsRNA precursor, however as bacteria miss Dicer homologs (Shabalina and Koonin, 2008), it is difficult to transfer this knowledge directly to eukaryotic organisms.

Where do we go from here? Future directions of cross-kingdom RNAi research

Several pathosystems, like the *Arabidopsis/Botrytis* and the *Arabidopsis/Verticillium* interaction have been suggested to reveal bidirectional sRNA exchange (Cai et al., 2019). This thesis provides evidence for a bidirectional cross-kingdom RNA cross-talk in the *Arabidopsis/H. arabidopsidis* model system. Although I did not investigate natural host-induced gene silencing, the integration of a hairpin cassette targeting *HaCRI* resulted in silencing of the target gene and increased plant resistance. These findings together with the inhibition of spore germination by exogenous application by sRNAs targeting *Cellulose synthase 3A* (Bilir et al., 2019), clearly suggest a functional RNA uptake machinery in *H. arabidopsidis*. While it seems likely that introduction of dsRNAs in the HIGS lines exploits an already existing plant sRNA defense machinery, more direct evidence is necessary to validate bidirectional exchange of sRNAs under natural conditions in this particular plant microbe interaction.

With an increasing number of model systems of cross-kingdom RNAi, the elucidation of the evolutionary processes shaping cross-kingdom sRNA arsenals becomes feasible. In general, two main hypotheses for this process exist that may vary from species to species:

On the one hand, sRNAs and their targets are shaped by an evolutionary arms race between host and pathogen, comparable to protein effectors and *R* genes. This would result in an additional, extremely fast layer of evolution and it would be expected that both sRNAs and their

target sites are under strong positive selection. This hypothesis would imply that co-evolution of sRNAs and targets leads to higher complementarity and silencing potential in host than in non-host species. Specific evolution is most likely occurring in strongly adapted pathogens with narrow host ranges, as downy mildews, as loss of silencing capacity by host mutations could deprive the pathogen of its sole nutrient source leading to extinction.

The complementary sequence changes observed in several *Cuscuta* species can be regarded as a strong indication for rapid evolution of cross-kingdom sRNA encoding loci and their host targets. As sRNA target sites in the host are encoding highly conserved amino acid stretches, target sequence polymorphisms between hosts are largely restricted to the wobble position of the codons. These SNPs are however counter-acted by complementary changes in the miRNA effector superfamilies of *Cuscuta*. Thereby, *Cuscuta* species achieve durable targeting and additionally infection of a wider host range (Johnson et al., 2019).

On the other hand, the frequently so-called “shot gun strategy” is a completely different evolutionary approach to enable silencing of a wide range of diverse target sequences, like for example defending against a wide range of pathogens. This describes that a large number of random sRNAs are secreted and some of them will, by chance, lead to a detrimental pathogen gene mis-regulation. However, it is also likely that broad host pathogens like *Botrytis* employ a similar strategy, as a specific evolution of adapted sRNAs for hundreds of hosts seems unfeasible (Veloso and van Kan, 2018). In this scenario, there wouldn't be any specific selection pressure on the cross-kingdom sRNAs. A potential example are the PRR derived pha-siRNAs by *Arabidopsis*, used to defend against *P. capsici*, a pathogen that was never observed infecting Brassicaceae under natural conditions (Hausbeck and Lamour, 2004; Hou et al., 2019). Therefore, it is suggested that PPR-derived siRNAs represent a diverse, neutrally evolving sequence resource, that by chance will target attacking pathogen transcripts (Hudzik et al., 2020).

Another major open question remains the translocation of the sRNAs, as they have to cross various cellular boundaries. As the plant cell wall, as a major barrier, is removed at the site of haustoria (Bozkurt and Kamoun, 2020), they are prime suspects to provide the hub for delivery of sRNA effectors, as reported for protein effectors (S. Wang et al., 2017). Ultrastructure analysis by electron microscopy revealed a large number of membrane enclosed particles in the extrahaustorial matrix between the oomycete haustorium and the plant cell (Mims et al., 2004). These extracellular vesicles (EVs) have recently drawn a lot of attention and many researchers implicated them in cargo transfer between host and pathogen (Cai et al., 2019; Huang et al., 2019; Kwon et al., 2020). The direct evidence for sRNA transfer is, in comparison, surprisingly

limited and future research on transfer has to keep an open mind for alternative hypotheses (Rutter and Innes, 2020). Interestingly, both fungi like *Botrytis* and oomycetes like *H. arabidopsidis* have the capacity to take up naked sRNAs (Bilir et al., 2019; Wang et al., 2016), but the uptake mechanism and its relevance in natural systems remains nebulous. To date, the only well understood RNA uptake mechanism remains the Systemic RNAi defective (SID) 1/2 system of the nematode *C. elegans* (McEwan et al., 2012), but no SID sequence homologues have been detected in plants, fungi or oomycetes (M. Wang et al., 2017a).

As for natural sRNA exchange, the transport mechanisms for HIGS sRNAs are largely unknown. In a pre-print report EVs were also suggested to confer transport of such transgene derived sRNAs, as the authors detected HIGS hairpin derived sRNAs in EVs enriched by ultracentrifugation, and mutants of the plant ESCRT II complex were hampered in efficient HIGS (Koch et al., 2020). Another preprint study suggested silencing activity of EVs containing anti-bacterial sRNAs, determined by inhibition of coronatin-dependent stomata re-opening (Singla-Rastogi et al., 2019). More thorough purification and analysis of EV content and functional data providing direct evidence for translocation and uptake of functional RNAs are however needed to validate EV mediated transport of HIGS sRNAs.

Cysteine-rich proteins: the abandoned child of oomycete effector research

Defensive sRNAs and sRNA effectors represent a relatively new field in molecular plant pathology and were found to complement the arms race of plant disease resistance genes and pathogen protein effectors. The effector research in oomycetes is largely dominated by RxLR effectors as they comprise the vast majority of known avirulence genes and are translocated into the host cell. It is generally accepted that RxLRs play crucial virulence roles in the genus *Phytophthora* and downy mildew pathogens like *Hyaloperonospora arabidopsidis* (Anderson et al., 2015). However, the first contact between pathogen and host is principally made in the apoplast, which consequently represents the first and often already decisive battleground (Rocafort et al., 2020).

In this thesis, we provide first insights into the function of an apoplastic effector of *H. arabidopsidis* that belongs to the class of cysteine-rich proteins, the most prevalent effector class during infection (Asai et al., 2014; Cabral et al., 2011). Several lines of evidence suggest that this effector is involved in PCD inhibition. Gene knockdown by HIGS resulted in trailing necrosis of host cells around the hyphae, the expression of *HaCR1* in *N. benthamiana* could suppress AvrE effector-induced cell death and repressed growth of the fungal necrotroph *B. cinerea*. Accordingly, it was shown before that expression of animal anti apoptotic proteins can repress *B. cinerea* lesion formation as well (Dickman et al., 2001). In contrast, the enhanced

lesion formation of *P. capsici* seems at first contradictory to a role in host cell death inhibition. However, as *P. capsici* has a biotrophic phase, impairment of cell death during this phase putatively increases the ability for lesion formation after the switch to necrotrophy. Likewise, the RxLR effector Avr1b from *P. sojae* prevented induced cell death and still induced longer root lesions in soy bean (Dou et al., 2008). Upon expression in transgenic Arabidopsis, the effector weakened the induction of the salicylic acid responsive marker gene *AtPRI*. This gene encodes for a secreted sterol binding protein that has been shown to be especially effective against sterol auxotrophs from the genera *Phytophthora* and *Peronospora* (Alexander et al., 1993; Gamir et al., 2017).

The effector function was clearly dependent on the presence of the signal peptide and, together with my colleagues, I validated that the effector localized at least partially to the apoplast determined by confocal microscopy and western blot on isolated apoplastic wash fluid. As *HaCR1* is lacking any annotated domains or motifs, a specific binding of MAMPs to prevent immunity, like for LysM effectors, seems unlikely (Kombrink and Thomma, 2013). Instead, we collected evidence that *HaCR1* could inhibit host extracellular proteases, a common trait for apoplastic effectors of filamentous plant pathogens (Jashni et al., 2015). For example, the cysteine rich effector Avr2 of the fungal pathogen *Cladosporium fulvum* exhibits multiple disulfide bridges that ensure effector function in host protease inhibition. The last 6 amino acids display a cysteine-cysteine-3 other amino acids-cysteine pattern, which forms one disulfide bridge and were found to be crucial to inhibit target protease function (Van't Klooster et al., 2011). Interestingly, this pattern is observed in the cysteine arrays of *H. arabidopsidis* cysteine-rich proteins including *HaCR1* (Cabral et al., 2011), however the exact formation of disulfide bridges remains to be determined experimentally.

It becomes increasingly evident that various families of secreted host proteases are essential regulators of the plant immunity response and in particular PCD (Balakireva and Zamyatnin, 2018; Misas-Villamil et al., 2016; Salguero-Linares and Coll, 2019). This aspect is strikingly similar to animals, where the regulation of apoptosis and cell autonomous immunity is performed by a family of cysteine proteases, so called caspases (Man and Kanneganti, 2016). The control of PCD by extracellular proteases also provides a link between the two observed functions of *HaCR1*, even though a final confirmation of this hypothesis is lacking and requires identification of the plant interactors.

Despite their prevalence, to the author's knowledge, only two previous reports investigated the role of any oomycete cysteine-rich protein during infection. The small cysteine-rich effector SCR96 from *Phytophthora cactorum* was induced during infection and triggered cell death

upon transient expression in *Nicotiana benthamiana*. Moreover, transgenic *SCR96^{RNAi}* oomycete lines with reduced expression of *SCR96* failed to resist oxidative stress, however if these two functions are linked or independent remains to be determined (Chen et al., 2016). Even less is known about the small cysteine-rich peptide SCR82 from *P. capsici*, that did neither induce cell death in *Arabidopsis* nor in *N. benthamiana*, but could trigger defense gene induction (Zhang et al., 2019).

One of the greatest challenges in effector research is the extremely high diversity and fast evolution of effector repertoires. Most of the effectors can be only found in a single pathogen species, some even only in one isolate. Thus, if the role of an effector is elucidated in a pathogen model species like *H. arabidopsidis*, it is frequently difficult to transfer this knowledge to closely related, economically relevant crop pathogens like for example the sunflower downy mildew *Plasmopara halstedii*. In a comparison of the effector repertoires, only six sequence homologs out of over one hundred effectors were detected (Sharma et al., 2015) and none of the CR proteins had a high-confidence homolog in other oomycetes (Cabral et al., 2011). However, as the general function of the plant immunity and physiology is highly conserved, there is potentially high functional conservation, despite lack of sequence identity. Accordingly, it was shown that highly diverse protein effector repertoires from bacteria, fungi and oomycetes converge on relatively few common host targets (Mukhtar et al., 2011; Weßling et al., 2014). Therefore, breeding efforts on effector targets is suggested as a complementary approach to inbreeding of *R* genes to obtain more durable broad range resistance (Gawehns et al., 2013).

Who am I? And if so, how many? Comparison of protein and sRNA effectors

The coevolution of plants and pathogens is driven by constant pressure to counteract each other only to maintain a stable interaction level, also described as “red queen hypothesis” (Clay and Kover, 1996). This leads to permanent evolution of novel virulence strategies by pathogens followed by novel defense strategies by host plants, as described by the zig-zag-model (Hein et al., 2009; Jones and Dangl, 2006). Therefore, both effectors and *R* genes are rapidly evolving proteins displaying extremely high degrees of sequence variation and abundance among individual populations. To increase the plasticity and mutation speed, pathogen effector loci are frequently organized in repeat arrays and linked to transposon regions (Dong et al., 2015).

In this line, sRNA effectors would provide an even faster level of evolution as every sequence variation in a given sRNA immediately impacts the complementarity, and thereby potentially the silencing capacity and interaction outcome. Most sRNA effectors from *H. arabidopsidis* and *B. cinerea* arise from non-coding, repetitive regions and are thought to be virtually free

from purifying selection. This, in theory, will result in high amounts of polymorphisms, high mutation rates, and low sequence conservation.

In contrast, mutations in the protein coding host target genes can lead to detrimental amino acid changes and are therefore counter selected. This puts evolutionary pressure on the host to accumulate synonymous mutations impairing silencing without changing the amino acid sequence. However, and intriguingly, such synonymous mutations of the wobble position were found to be compensated by corresponding polymorphisms in the miRNA families of various *Cuscuta* species, providing fascinating insights into plant/parasite coevolution (Johnson et al., 2019). Interestingly, we also found several sequence polymorphisms in the sRNA target sites in the sequenced accessions from the 1001 genome project (1001 Genomes Consortium, 2016). It however remains to be clarified if these are enriched compared to non-targeted parts of the transcriptome.

Surprisingly, I did not detect high variability in the sRNA encoding loci in the three sequenced *H. arabidopsidis* strains, which is in contrast to the higher sequence variation of *H. arabidopsidis* protein effectors. Among cysteine-rich protein effectors, 62.5% displayed sequence polymorphisms and two were even isolate specific (Cabral et al., 2011). However, a direct comparison is difficult, as protein effector sequences with several hundred nucleotides are much longer than sRNAs of 21 nucleotides, making SNPs more likely. Still, current data do not indicate any presence of larger sRNA families with complementary sequence variations in *H. arabidopsidis* as identified in the parasitic plant genus *Cuscuta* (Johnson et al., 2019). The high conservation of sRNA effectors might be a result from the very narrow host range of *H. arabidopsidis*, while the protein effectors must retain higher plasticity to avoid recognition by host *R* genes. At the moment, there is no indication that sRNAs can be used by the host to induce immunity, therefore sRNAs can be at worst neutral, but not highly detrimental for the pathogen (Niehl et al., 2016). This might lead to a reduced selection pressure compared to protein effectors. Finally, it should be noted that commonly used, genome sequenced, *H. arabidopsidis* strains like Noco2, Emoy2, and Cala2 were all collected in a relatively small region in England, compared to more than thousand sequenced Arabidopsis accessions from all over the Northern hemisphere (1001 Genomes Consortium, 2016). Therefore, *H. arabidopsidis* total sRNA and protein effector variance might still be underestimated.

Interestingly, both *HaCR1* and *HasRNA90* target extracellular proteases, however on different regulation levels. While *HasRNA90* repressed the expression of the apoplastic aspartyl protease *AtAED3*, *HaCR1* repressed the activity of extracellular protease proteins. As detailed above, proteases are crucial components of the immune response and in particular PCD signaling. It

will be intriguing to explore the detailed role of *AtAED3* in anti-oomycete immunity and whether *HaCR1* can even directly interact with this particular protease. Such a direct connection between cross-kingdom sRNAs and effector function is illustrated by the oomycete effector PSR2 that represses the formation of PPR derived siRNAs in Arabidopsis, which were suggested to repress *P. capsici* genes (Hou et al., 2019). Therefore, together sRNAs and proteinaceous effectors provide a more robust way to reprogram host physiology and prevent immunity (Figure 2). As the host has to counteract an attack on completely distinct levels to gain full resistance, this might provide selection pressure for the parallel usage of sRNA and protein effectors in *H. arabidopsidis*.

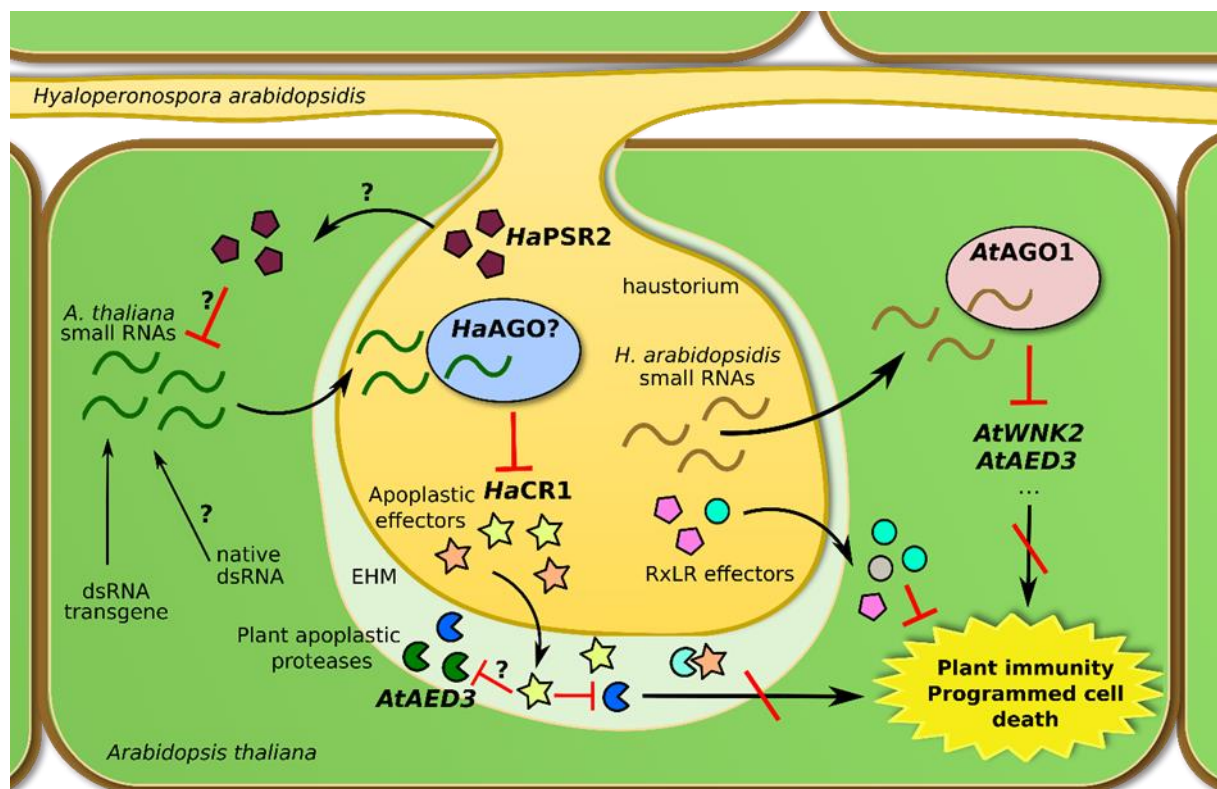


Figure 2: *H. arabidopsidis* uses both protein and sRNA effectors to achieve host infection. *H. arabidopsidis* sRNAs hijack the Arabidopsis AGO1 protein to silence immunity factors suppressing host immunity. Together with host translocated RxLR effectors, apoplastic effectors like *HaCR1* prevent the induction of programmed cell death (PCD). I suggest that the main role of *HaCR1* is the inhibition of extracellular proteases in the extrahaustorial matrix (EHM), which are well-described promoters of PCD. An intriguing speculation is that one inhibited protease is *AtAED3*, which would thereby be targeted by *H. arabidopsidis* on two independent levels: post-transcriptionally and protein activity. The model also illustrates the suppression of *HaCR1* in transgenic *HaCR1^{RNAi}* lines by host sRNAs, that probably exploit a natural defense mechanism. Potentially, the *H. arabidopsidis* homolog of PSR2 can interfere with host sRNA production and host-induced gene silencing, however its function hasn't yet been elucidated. This model implies the haustorium as the central hub for signal exchange as reported for RxLR effectors.

While an increasing number of pathosystems provides evidence for cross-kingdom RNAi, no such evidence has been found in the fungal pathogen *Zymospetoria tritici* (Kettles et al., 2019; X. Ma et al., 2020). Furthermore, other fungal pathogens, like *Ustilago maydis*, have even lost the entire canonical RNAi machinery (Laurie et al., 2008). Conversely, protein effectors *sensu stricto*, interacting with defined host proteins impairing plant immunity and retooling host physiology functions are largely absent from the necrotrophic *Botrytis cinerea*. Besides hydrolytic enzymes and PCD elicitors, sometimes also referred to as effectors, early interaction with the host immune system might be largely governed by sRNAs (Veloso and van Kan, 2018). It will be an enticing task of future research to unravel which evolutionary forces work in favor and against cross-kingdom RNAi.

On a holistic level, the relative contribution of protein and sRNA effectors to pathogen virulence remains one of the most exciting open questions. One of the greatest challenges elucidating this is the collaborative nature of effectors, where the effect of each individual effector is usually relatively minor (Cunnac et al., 2011). As components in effector delivery, like the type III secretion system of bacteria, are still unknown in eukaryotes, it is difficult to estimate the combined effect of all effectors by mutation of single or a few genes like in the *hrcC* mutant of *Pseudomonas* (Collmer et al., 2000; Petre and Kamoun, 2014). On the other hand, it is likely that certain transport mechanisms, like extracellular vesicles, are used by both effector proteins and sRNAs (Boevink, 2017; Boevink et al., 2020). In some aspect, the collaborative effect of the sRNAs can be assessed by the analysis of plant *ago* mutants. In the case of *H. arabidopsidis*, a fully compatible interaction of strain Noco2 with Arabidopsis ecotype Col-0 was rendered partially incompatible, displaying trailing necrosis and strongly reduced pathogen biomass and sporulation. This suggests, that the collaborative impact of sRNA effectors might be as crucial as the joint impact of protein effectors.

In this work, I provided initial insights into two poorly characterized classes of oomycete molecular weapons: sRNAs and cysteine-rich proteins. This thesis implies crucial roles for both of them and highlights the necessity for holistic research on oomycete virulence factors, not only focusing on RxLR effectors. With the introduction of *H. arabidopsidis* as a model system to study both sRNAs and cysteine-rich proteins, I am convinced that, based on this, future research can continue to unravel their modes of action and the evolutionary forces shaping them. This will potentially clear the central hurdle to start durable disarming of notorious oomycete crop pathogens challenging food supply for the world.

References

- 1001 Genomes Consortium, 2016. 1,135 genomes reveal the global pattern of polymorphism in *Arabidopsis thaliana*. *Cell* **166**, 481–491.
- Agler, M.T., Ruhe, J., Kroll, S., Morhenn, C., Kim, S.-T., Weigel, D., Kemen, E.M., 2016. Microbial hub taxa link host and abiotic factors to plant microbiome variation. *PLoS Biol.* **14**, e1002352.
- Alberts, B., 2015. Molecular biology of the cell, Sixth edition. ed. *Garland Science, Taylor and Francis Group*, New York, NY, USA.
- Alexander, D., Goodman, R.M., Gut-Rella, M., Glascock, C., Weymann, K., Friedrich, L., Maddox, D., Ahl-Goy, P., Luntz, T., Ward, E., 1993. Increased tolerance to two oomycete pathogens in transgenic tobacco expressing pathogenesis-related protein 1a. *Proc. Natl. Acad. Sci.* **90**, 7327–7331.
- Anderson, R.G., Casady, M.S., Fee, R.A., Vaughan, M.M., Deb, D., Fedkenheuer, K., Huffaker, A., Schmelz, E.A., Tyler, B.M., McDowell, J.M., 2012. Homologous RXLR effectors from *Hyaloperonospora arabidopsidis* and *Phytophthora sojae* suppress immunity in distantly related plants. *Plant J.* **72**, 882–893.
- Anderson, R.G., Deb, D., Fedkenheuer, K., McDowell, J.M., 2015. Recent progress in RXLR effector research. *Mol. Plant. Microbe Interact.* **28**, 1063–1072.
- Anderson, R.G., McDowell, J.M., 2015. A PCR assay for the quantification of growth of the oomycete pathogen *Hyaloperonospora arabidopsidis* in *Arabidopsis thaliana*. *Mol. Plant Pathol.* **16**, 893–898.
- Asai, S., Furzer, O.J., Cevik, V., Kim, D.S., Ishaque, N., Goritschnig, S., Staskawicz, B.J., Shirasu, K., Jones, J.D.G., 2018. A downy mildew effector evades recognition by polymorphism of expression and subcellular localization. *Nat. Commun.* **9**, 5192.
- Asai, S., Rallapalli, G., Piquerez, S.J.M., Caillaud, M.-C., Furzer, O.J., Ishaque, N., Wirthmueller, L., Fabro, G., Shirasu, K., Jones, J.D.G., 2014. Expression profiling during *Arabidopsis*/ downy mildew interaction reveals a highly-expressed effector that attenuates responses to salicylic acid. *PLoS Pathog.* **10**, e1004443.
- Åsman, A.K.M., Fogelqvist, J., Vetukuri, R.R., Dixelius, C., 2016. *Phytophthora infestans* Argonaute 1 binds microRNA and small RNAs from effector genes and transposable elements. *New Phytol.* **211**, 993–1007.
- Auer, C., Frederick, R., 2009. Crop improvement using small RNAs: applications and predictive ecological risk assessments. *Trends Biotechnol.* **27**, 644–651.

- Bailey, K., Çevik, V., Holton, N., Byrne-Richardson, J., Sohn, K.H., Coates, M., Woods-Tör, A., Aksoy, H.M., Hughes, L., Baxter, L., Jones, J.D.G., Beynon, J., Holub, E.B., Tör, M., 2011. Molecular cloning of ATR5^{Emoy2} from *Hyaloperonospora arabidopsidis*, an avirulence determinant that triggers RPP5-mediated defense in *Arabidopsis*. *Mol. Plant. Microbe Interact.* **24**, 827–838.
- Balakireva, A., Zamyatnin, A., 2018. Indispensable role of proteases in plant innate immunity. *Int. J. Mol. Sci.* **19**, 629.
- Baum, J.A., Bogaert, T., Clinton, W., Heck, G.R., Feldmann, P., Ilagan, O., Johnson, S., Plaetinck, G., Munyikwa, T., Pleau, M., Vaughn, T., Roberts, J., 2007. Control of coleopteran insect pests through RNA interference. *Nat. Biotechnol.* **25**, 1322–1326.
- Baumberger, N., Baulcombe, D.C., 2005. Arabidopsis ARGONAUTE1 is an RNA Slicer that selectively recruits microRNAs and short interfering RNAs. *Proc. Natl. Acad. Sci.* **102**, 11928–11933.
- Baxter, L., Tripathy, S., Ishaque, N., Boot, N., Cabral, A., Kemen, E., Thines, M., Ah-Fong, A., Anderson, R., Badejoko, W., Bittner-Eddy, P., Boore, J.L., Chibucos, M.C., Coates, M., Dehal, P., Delehaunty, K., Dong, S., Downton, P., Dumas, B., Fabro, G., Fronick, C., Fuerstenberg, S.I., Fulton, L., Gaulin, E., Govers, F., Hughes, L., Humphray, S., Jiang, R.H.Y., Judelson, H., Kamoun, S., Kyung, K., Meijer, H., Minx, P., Morris, P., Nelson, J., Phuntumart, V., Qutob, D., Rehmany, A., Rougon-Cardoso, A., Ryden, P., Torto-Alalibo, T., Studholme, D., Wang, Y., Win, J., Wood, J., Clifton, S.W., Rogers, J., Van den Ackerveken, G., Jones, J.D.G., McDowell, J.M., Beynon, J., Tyler, B.M., 2010. Signatures of adaptation to obligate biotrophy in the *Hyaloperonospora arabidopsidis* genome. *Science* **330**, 1549–1551.
- Bilir, Ö., Telli, O., Norman, C., Budak, H., Hong, Y., Tör, M., 2019. Small RNA inhibits infection by downy mildew pathogen *Hyaloperonospora arabidopsidis*. *Mol. Plant Pathol.* **20**, 1523–1534.
- Bittner-Eddy, P.D., Allen, R.L., Rehmany, A.P., Birch, P., Beynon, J.L., 2003. Use of suppression subtractive hybridization to identify downy mildew genes expressed during infection of *Arabidopsis thaliana*. *Mol. Plant Pathol.* **4**, 501–507.
- Boevink, P.C., 2017. Exchanging missives and missiles: the roles of extracellular vesicles in plant-pathogen interactions. *J. Exp. Bot.* **68**, 5411–5414.
- Boevink, P.C., Birch, P.R.J., Turnbull, D., Whisson, S.C., 2020. Devastating intimacy: the cell biology of plant–*Phytophthora* interactions. *New Phytol.* **228**, 445–458.

- Bollmann, S.R., Fang, Y., Press, C.M., Tyler, B.M., Grünwald, N.J., 2016. Diverse evolutionary trajectories for small RNA biogenesis genes in the oomycete genus *Phytophthora*. *Front. Plant Sci.* **7**, 284.
- Bollmann, S.R., Press, C.M., Tyler, B.M., Grünwald, N.J., 2018. Expansion and divergence of Argonaute genes in the oomycete genus *Phytophthora*. *Front. Microbiol.* **9**, 2841.
- Bologna, N.G., Voinnet, O., 2014. The diversity, biogenesis, and activities of endogenous silencing small RNAs in Arabidopsis. *Annu. Rev. Plant Biol.* **65**, 473–503.
- Bolognesi, R., Ramaseshadri, P., Anderson, J., Bachman, P., Clinton, W., Flannagan, R., Ilagan, O., Lawrence, C., Levine, S., Moar, W., Mueller, G., Tan, J., Uffman, J., Wiggins, E., Heck, G., Segers, G., 2012. Characterizing the mechanism of action of double-stranded RNA activity against western corn rootworm (*Diabrotica virgifera virgifera* LeConte). *PLoS ONE* **7**, e47534.
- Bozkurt, T.O., Kamoun, S., 2020. The plant-pathogen haustorial interface at a glance. *J. Cell Sci.* **133**.
- Breitenbach, H.H., Wenig, M., Wittek, F., Jordá, L., Maldonado-Alconada, A.M., Sarioglu, H., Colby, T., Knappe, C., Bichlmeier, M., Pabst, E., Mackey, D., Parker, J.E., Vlot, A.C., 2014. Contrasting roles of the apoplastic aspartyl protease APOPLASTIC, ENHANCED DISEASE SUSCEPTIBILITY1-DEPENDENT1 and LEGUME LECTIN-LIKE PROTEIN1 in Arabidopsis systemic acquired resistance. *Plant Physiol.* **165**, 791–809.
- Breitinger, T., 2016. RNAi in *Botrytis cinerea* – Characterization of AGO2 and small RNAs (Master thesis). Ludwig-Maximilians-Universität, München.
- Buck, A.H., Coakley, G., Simbari, F., McSorley, H.J., Quintana, J.F., Le Bihan, T., Kumar, S., Abreu-Goodger, C., Lear, M., Harcus, Y., Ceroni, A., Babayan, S.A., Blaxter, M., Ivens, A., Maizels, R.M., 2014. Exosomes secreted by nematode parasites transfer small RNAs to mammalian cells and modulate innate immunity. *Nat. Commun.* **5**, 5488.
- Cabral, A., Oome, S., Sander, N., Küfner, I., Nürnberger, T., Van den Ackerveken, G., 2012. Nontoxic Nep1-like proteins of the downy mildew pathogen *Hyaloperonospora arabidopsidis*: Repression of necrosis-inducing activity by a surface-exposed region. *Mol. Plant. Microbe Interact.* **25**, 697–708.
- Cabral, A., Stassen, J.H.M., Seidl, M.F., Bautor, J., Parker, J.E., Van den Ackerveken, G., 2011. Identification of *Hyaloperonospora arabidopsidis* transcript sequences expressed during infection reveals isolate-specific effectors. *PLoS ONE* **6**, e19328.

- Cahill, D.M., Rookes, J.E., Wilson, B.A., Gibson, L., McDougall, K.L., 2008. *Phytophthora cinnamomi* and Australia's biodiversity: impacts, predictions and progress towards control. *Aust. J. Bot.* **56**, 279.
- Cai, Q., He, B., Kogel, K.-H., Jin, H., 2018a. Cross-kingdom RNA trafficking and environmental RNAi — nature's blueprint for modern crop protection strategies. *Curr. Opin. Microbiol.* **46**, 58–64.
- Cai, Q., He, B., Weiberg, A., Buck, A.H., Jin, H., 2019. Small RNAs and extracellular vesicles: New mechanisms of cross-species communication and innovative tools for disease control. *PLoS Pathog.* **15**, e1008090.
- Cai, Q., Qiao, L., Wang, M., He, B., Lin, F.-M., Palmquist, J., Huang, S.-D., Jin, H., 2018b. Plants send small RNAs in extracellular vesicles to fungal pathogen to silence virulence genes. *Science* **360**, 1126–1129.
- Caillaud, M.-C., Asai, S., Rallapalli, G., Piquerez, S., Fabro, G., Jones, J.D.G., 2013. A downy mildew effector attenuates salicylic acid-triggered immunity in Arabidopsis by interacting with the host mediator complex. *PLoS Biol.* **11**, e1001732.
- Caillaud, M.-C., Wirthmueller, L., Sklenar, J., Findlay, K., Piquerez, S.J.M., Jones, A.M.E., Robatzek, S., Jones, J.D.G., Faulkner, C., 2014. The plasmodesmal protein PDL1 localises to haustoria-associated membranes during downy mildew infection and regulates callose deposition. *PLoS Pathog.* **10**, e1004496.
- Carbonell, A., 2017. Immunoprecipitation and high-throughput sequencing of ARGONAUTE-bound target RNAs from plants. *Methods Mol. Biol.* **1640**, 93–112.
- Casacuberta, J.M., Devos, Y., du Jardin, P., Ramon, M., Vaucheret, H., Nogué, F., 2015. Biotechnological uses of RNAi in plants: risk assessment considerations. *Trends Biotechnol.* **33**, 145–147.
- Chakraborty, J., Ghosh, P., Das, S., 2018. Autoimmunity in plants. *Planta* **248**, 751–767.
- Chaloner, T., van Kan, J.A.L., Grant-Downton, R.T., 2016. RNA 'information warfare' in pathogenic and mutualistic interactions. *Trends Plant Sci.* **21**, 738–748.
- Chen, X.-R., Li, Y.-P., Li, Q.-Y., Xing, Y.-P., Liu, B.-B., Tong, Y.-H., Xu, J.-Y., 2016. SCR96, a small cysteine-rich secretory protein of *Phytophthora cactorum*, can trigger cell death in the Solanaceae and is important for pathogenicity and oxidative stress tolerance. *Mol. Plant Pathol.* **17**, 577–587.
- Chow, F.W.-N., Koutsovoulos, G., Ovando-Vázquez, C., Neophytou, K., Bermúdez-Barrientos, J.R., Laetsch, D.R., Robertson, E., Kumar, S., Claycomb, J.M., Blaxter, M.,

- Abreu-Goodger, C., Buck, A.H., 2019. Secretion of an Argonaute protein by a parasitic nematode and the evolution of its siRNA guides. *Nucleic Acids Res.* **47**, 3594–3606.
- Clay, K., Kover, P.X., 1996. The Red Queen hypothesis and plant/pathogen interactions. *Annu. Rev. Phytopathol.* **34**, 29–50.
- Coates, M.E., Beynon, J.L., 2010. *Hyaloperonospora arabidopsidis* as a pathogen model. *Annu. Rev. Phytopathol.* **48**, 329–345.
- Collmer, A., Badel, J.L., Charkowski, A.O., Deng, W.L., Fouts, D.E., Ramos, A.R., Rehm, A.H., Anderson, D.M., Schneewind, O., van Dijk, K., Alfano, J.R., 2000. *Pseudomonas syringae* Hrp type III secretion system and effector proteins. *Proc. Natl. Acad. Sci.* **97**, 8770–8777.
- Cui, C., Wang, Y., Liu, J., Zhao, J., Sun, P., Wang, S., 2019. A fungal pathogen deploys a small silencing RNA that attenuates mosquito immunity and facilitates infection. *Nat. Commun.* **10**, 4298.
- Cunnac, S., Chakravarthy, S., Kvitko, B.H., Russell, A.B., Martin, G.B., Collmer, A., 2011. Genetic disassembly and combinatorial reassembly identify a minimal functional repertoire of type III effectors in *Pseudomonas syringae*. *Proc. Natl. Acad. Sci.* **108**, 2975–2980.
- Delmas, C.E.L., Dussert, Y., Delière, L., Couture, C., Mazet, I.D., Richart Cervera, S., Delmotte, F., 2017. Soft selective sweeps in fungicide resistance evolution: recurrent mutations without fitness costs in grapevine downy mildew. *Mol. Ecol.* **26**, 1936–1951.
- Derbyshire, M., Mbengue, M., Barascud, M., Navaud, O., Raffaele, S., 2019. Small RNAs from the plant pathogenic fungus *Sclerotinia sclerotiorum* highlight host candidate genes associated with quantitative disease resistance. *Mol. Plant Pathol.* **20**, 1279–1297.
- Derevnina, L., Petre, B., Kellner, R., Dagdas, Y.F., Sarowar, M.N., Giannakopoulou, A., De la Concepcion, J.C., Chaparro-Garcia, A., Pennington, H.G., van West, P., Kamoun, S., 2016. Emerging oomycete threats to plants and animals. *Philos. Trans. R. Soc. B Biol. Sci.* **371**, 20150459.
- Dickman, M.B., Park, Y.K., Oltersdorf, T., Li, W., Clemente, T., French, R., 2001. Abrogation of disease development in plants expressing animal antiapoptotic genes. *Proc. Natl. Acad. Sci.* **98**, 6957–6962.
- Dixit, R., Cyr, R., Gilroy, S., 2006. Using intrinsically fluorescent proteins for plant cell imaging. *Plant J.* **45**, 599–615.
- Dong, S., Raffaele, S., Kamoun, S., 2015. The two-speed genomes of filamentous pathogens: waltz with plants. *Curr. Opin. Genet. Dev.* **35**, 57–65.

- Dou, D., Kale, S.D., Wang, Xinle, Chen, Y., Wang, Q., Wang, Xia, Jiang, R.H.Y., Arredondo, F.D., Anderson, R.G., Thakur, P.B., McDowell, J.M., Wang, Y., Tyler, B.M., 2008. Conserved C-terminal motifs required for avirulence and suppression of cell death by *Phytophthora sojae* effector Avr1b. *Plant Cell* **20**, 1118–1133.
- Dunker, F., Trutzenberg, A., Rothenpieler, J.S., Kuhn, S., Pröls, R., Schreiber, T., Tissier, A., Kemen, A., Kemen, E., Hückelhoven, R., Weiberg, A., 2020. Oomycete small RNAs bind to the plant RNA-induced silencing complex for virulence. *eLife* **9**, e56096.
- Earle, G., Hintz, W., 2014. New approaches for controlling *Saprolegnia parasitica*, the causal agent of a devastating fish disease. *Trop. Life Sci. Res.* **25**, 101–109.
- Ellis, J.G., Dodds, P.N., 2011. Showdown at the RXLR motif: Serious differences of opinion in how effector proteins from filamentous eukaryotic pathogens enter plant cells. *Proc. Natl. Acad. Sci.* **108**, 14381–14382.
- Fabro, G., Steinbrenner, J., Coates, M., Ishaque, N., Baxter, L., Studholme, D.J., Körner, E., Allen, R.L., Piquerez, S.J.M., Rougon-Cardoso, A., Greenshields, D., Lei, R., Badel, J.L., Caillaud, M.-C., Sohn, K.-H., Van den Ackerveken, G., Parker, J.E., Beynon, J., Jones, J.D.G., 2011. Multiple candidate effectors from the oomycete pathogen *Hyaloperonospora arabidopsidis* suppress host plant immunity. *PLoS Pathog.* **7**, e1002348.
- Fahlgren, N., Bollmann, S.R., Kasschau, K.D., Cuperus, J.T., Press, C.M., Sullivan, C.M., Chapman, E.J., Hoyer, J.S., Gilbert, K.B., Grünwald, N.J., Carrington, J.C., 2013. *Phytophthora* have distinct endogenous small RNA populations that include short interfering and microRNAs. *PLoS ONE* **8**, e77181.
- Fang, X., Qi, Y., 2016. RNAi in plants: An Argonaute-centered view. *Plant Cell* **28**, 272–285.
- Flor, H.H., 1971. Current status of the gene-for-gene concept. *Annu. Rev. Phytopathol.* **9**, 275–296.
- Fry, W., 2008. *Phytophthora infestans*: the plant (and R gene) destroyer. *Mol. Plant Pathol.* **9**, 385–402.
- Furci, L., Jain, R., Stassen, J., Berkowitz, O., Whelan, J., Roquis, D., Baillet, V., Colot, V., Johannes, F., Ton, J., 2019. Identification and characterisation of hypomethylated DNA loci controlling quantitative resistance in *Arabidopsis*. *eLife* **8**, e40655.
- Gamir, J., Darwiche, R., van't Hof, P., Choudhary, V., Stumpe, M., Schneiter, R., Mauch, F., 2017. The sterol-binding activity of PATHOGENESIS-RELATED PROTEIN 1 reveals the mode of action of an antimicrobial protein. *Plant J.* **89**, 502–509.

- Gawehns, F., Cornelissen, B.J.C., Takken, F.L.W., 2013. The potential of effector-target genes in breeding for plant innate immunity. *Microb. Biotechnol.* **6**, 223–229.
- Glazebrook, J., 2005. Contrasting mechanisms of defense against biotrophic and necrotrophic pathogens. *Annu. Rev. Phytopathol.* **43**, 205–227.
- Govers, F., Bouwmeester, K., 2008. Effector trafficking: RXLR-dEER as extra gear for delivery into plant cells. *Plant Cell* **20**, 1728–1730.
- Govindarajulu, M., Epstein, L., Wroblewski, T., Michelmore, R.W., 2015. Host-induced gene silencing inhibits the biotrophic pathogen causing downy mildew of lettuce. *Plant Biotechnol. J.* **13**, 875–883.
- Grünwald, N.J., Goss, E.M., Press, C.M., 2008. *Phytophthora ramorum*: a pathogen with a remarkably wide host range causing sudden oak death on oaks and ramorum blight on woody ornamentals. *Mol. Plant Pathol.* **9**, 729–740.
- Guivarc'h, A., Caissard, J.C., Azmi, A., Elmayan, T., Chriqui, D., Tepfer, M., 1996. *In situ* detection of expression of the *gus* reporter gene in transgenic plants: ten years of blue genes. *Transgenic Res.* **5**, 281–288.
- Guo, X.-Y., Li, Y., Fan, J., Xiong, H., Xu, F.-X., Shi, J., Shi, Y., Zhao, J.-Q., Wang, Y.-F., Cao, X.-L., Wang, W.-M., 2019. Host-induced gene silencing of *MoAPI* confers broad-spectrum resistance to *Magnaporthe oryzae*. *Front. Plant Sci.* **10**, 433.
- Haas, B.J., Kamoun, S., Zody, M.C., Jiang, R.H.Y., Handsaker, R.E., Cano, L.M., Grabherr, M., Kodira, C.D., Raffaele, S., Torto-Alalibo, T., Bozkurt, T.O., Ah-Fong, A.M.V., Alvarado, L., Anderson, V.L., Armstrong, M.R., Avrova, A., Baxter, L., Beynon, J., Boevink, P.C., Bollmann, S.R., Bos, J.I.B., Bulone, V., Cai, G., Cakir, C., Carrington, J.C., Chawner, M., Conti, L., Costanzo, S., Ewan, R., Fahlgren, N., Fischbach, M.A., Fugelstad, J., Gilroy, E.M., Gnerre, S., Green, P.J., Grenville-Briggs, L.J., Griffith, J., Grünwald, N.J., Horn, K., Horner, N.R., Hu, C.-H., Huitema, E., Jeong, D.-H., Jones, A.M.E., Jones, J.D.G., Jones, R.W., Karlsson, E.K., Kunjeti, S.G., Lamour, K., Liu, Z., Ma, L., MacLean, D., Chibucos, M.C., McDonald, H., McWalters, J., Meijer, H.J.G., Morgan, W., Morris, P.F., Munro, C.A., O'Neill, K., Ospina-Giraldo, M., Pinzón, A., Pritchard, L., Ramsahoye, B., Ren, Q., Restrepo, S., Roy, S., Sadanandom, A., Savidor, A., Schornack, S., Schwartz, D.C., Schumann, U.D., Schwessinger, B., Seyer, L., Sharpe, T., Silvar, C., Song, J., Studholme, D.J., Sykes, S., Thines, M., van de Vondervoort, P.J.I., Phuntumart, V., Wawra, S., Weide, R., Win, J., Young, C., Zhou, S., Fry, W., Meyers, B.C., van West, P., Ristaino, J., Govers, F., Birch, P.R.J., Whisson,

- S.C., Judelson, H.S., Nusbaum, C., 2009. Genome sequence and analysis of the Irish potato famine pathogen *Phytophthora infestans*. *Nature* **461**, 393–398.
- Harvey, S., Kumari, P., Lapin, D., Griebel, T., Hickman, R., Guo, W., Zhang, R., Parker, J.E., Beynon, J., Denby, K., Steinbrenner, J., 2020. Downy mildew effector HaRxL21 interacts with the transcriptional repressor TOPLESS to promote pathogen susceptibility. *PLoS Pathog.* **16**, e1008835.
- Haurwitz, R.E., Jinek, M., Wiedenheft, B., Zhou, K., Doudna, J.A., 2010. Sequence- and structure-specific RNA processing by a CRISPR endonuclease. *Science* **329**, 1355–1358.
- Hausbeck, M.K., Lamour, K.H., 2004. *Phytophthora capsici* on vegetable crops: Research progress and management challenges. *Plant Dis.* **88**, 1292–1303.
- Head, G.P., Carroll, M.W., Evans, S.P., Rule, D.M., Willse, A.R., Clark, T.L., Storer, N.P., Flannagan, R.D., Samuel, L.W., Meinke, L.J., 2017. Evaluation of SmartStax and SmartStax PRO maize against western corn rootworm and northern corn rootworm: efficacy and resistance management. *Pest Manag. Sci.* **73**, 1883–1899.
- Hein, I., Gilroy, E.M., Armstrong, M.R., Birch, P.R.J., 2009. The zig-zag-zig in oomycete-plant interactions. *Mol. Plant Pathol.* **10**, 547–562.
- Helber, N., Wippel, K., Sauer, N., Schaarschmidt, S., Hause, B., Requena, N., 2011. A versatile monosaccharide transporter that operates in the arbuscular mycorrhizal fungus *Glomus* sp. is crucial for the symbiotic relationship with plants. *Plant Cell* **23**, 3812–3823.
- Hogenhout, S.A., Van der Hoorn, R.A.L., Terauchi, R., Kamoun, S., 2009. Emerging concepts in effector biology of plant-associated organisms. *Mol. Plant. Microbe Interact.* **22**, 115–122.
- Horsefield, S., Burdett, H., Zhang, X., Manik, M.K., Shi, Y., Chen, J., Qi, T., Gilley, J., Lai, J.-S., Rank, M.X., Casey, L.W., Gu, W., Ericsson, D.J., Foley, G., Hughes, R.O., Bosanac, T., von Itzstein, M., Rathjen, J.P., Nanson, J.D., Boden, M., Dry, I.B., Williams, S.J., Staskawicz, B.J., Coleman, M.P., Ve, T., Dodds, P.N., Kobe, B., 2019. NAD⁺ cleavage activity by animal and plant TIR domains in cell death pathways. *Science* **365**, 793–799.
- Hou, Y., Zhai, Y., Feng, L., Karimi, H.Z., Rutter, B.D., Zeng, L., Choi, D.S., Zhang, B., Gu, W., Chen, X., Ye, W., Innes, R.W., Zhai, J., Ma, W., 2019. A *Phytophthora* effector suppresses trans-kingdom RNAi to promote disease susceptibility. *Cell Host Microbe* **25**, 153–165.

- Hu, X., Persson Hodén, K., Liao, Z., Dörfors, F., Åsman, A., Dixelius, C., 2020. *Phytophthora infestans* Ago1-bound miRNA promotes potato late blight disease. *bioRxiv*.
- Huang, C.-Y., Wang, H., Hu, P., Hamby, R., Jin, H., 2019. Small RNAs – Big Players in Plant-Microbe Interactions. *Cell Host Microbe* **26**, 173–182.
- Huang, G., Allen, R., Davis, E.L., Baum, T.J., Hussey, R.S., 2006. Engineering broad root-knot resistance in transgenic plants by RNAi silencing of a conserved and essential root-knot nematode parasitism gene. *Proc. Natl. Acad. Sci.* **103**, 14302–14306.
- Hudzik, C., Hou, Y., Ma, W., Axtell, M.J., 2020. Exchange of small regulatory RNAs between plants and their pests. *Plant Physiol.* **182**, 51–62.
- Jahan, S.N., Åsman, A.K.M., Corcoran, P., Fogelqvist, J., Vetukuri, R.R., Dixelius, C., 2015. Plant-mediated gene silencing restricts growth of the potato late blight pathogen *Phytophthora infestans*. *J. Exp. Bot.* **66**, 2785–2794.
- Jashni, M.K., Mehrabi, R., Collemare, J., Mesarich, C.H., de Wit, P.J.G.M., 2015. The battle in the apoplast: further insights into the roles of proteases and their inhibitors in plant–pathogen interactions. *Front. Plant Sci.* **6**, 584.
- Jia, J., Lu, W., Zhong, C., Zhou, R., Xu, J., Liu, W., Gou, X., Wang, Q., Yin, J., Xu, C., Shan, W., 2017. The 25-26 nt small RNAs in *Phytophthora parasitica* are associated with efficient silencing of homologous endogenous genes. *Front. Microbiol.* **8**, 773.
- Jian, J., Liang, X., 2019. One small RNA of *Fusarium graminearum* targets and silences *CEBiP* gene in common wheat. *Microorganisms* **7**, 425.
- Johnson, N.R., dePamphilis, C.W., Axtell, M.J., 2019. Compensatory sequence variation between trans-species small RNAs and their target sites. *eLife* **8**, e49750.
- Jones, J.D.G., Dangl, J.L., 2006. The plant immune system. *Nature* **444**, 323–329.
- Judelson, H.S., Ah-Fong, A.M.V., 2019. Exchanges at the plant-oomycete interface that influence disease. *Plant Physiol.* **179**, 1198–1211.
- Kamoun, S., Furzer, O., Jones, J.D.G., Judelson, H.S., Ali, G.S., Dalio, R.J.D., Roy, S.G., Schena, L., Zambounis, A., Panabières, F., Cahill, D., Ruocco, M., Figueiredo, A., Chen, X.-R., Hulvey, J., Stam, R., Lamour, K., Gijzen, M., Tyler, B.M., Grünwald, N.J., Mukhtar, M.S., Tomé, D.F.A., Tör, M., Van Den Ackerveken, G., McDowell, J., Daayf, F., Fry, W.E., Lindqvist-Kreuzer, H., Meijer, H.J.G., Petre, B., Ristaino, J., Yoshida, K., Birch, P.R.J., Govers, F., 2015. The top 10 oomycete pathogens in molecular plant pathology. *Mol. Plant Pathol.* **16**, 413–434.
- Kanja, C., Hammond-Kosack, K.E., 2020. Proteinaceous effector discovery and characterization in filamentous plant pathogens. *Mol. Plant Pathol.* **21**, 1353–1376

- Kemen, E., Gardiner, A., Schultz-Larsen, T., Kemen, A.C., Balmuth, A.L., Robert-Seilaniantz, A., Bailey, K., Holub, E., Studholme, D.J., MacLean, D., Jones, J.D.G., 2011. Gene gain and loss during evolution of obligate parasitism in the white rust pathogen of *Arabidopsis thaliana*. *PLoS Biol.* **9**, e1001094.
- Kettles, G.J., Hofinger, B.J., Hu, P., Bayon, C., Rudd, J.J., Balmer, D., Courbot, M., Hammond-Kosack, K.E., Scalliet, G., Kanyuka, K., 2019. sRNA profiling combined with gene function analysis reveals a lack of evidence for cross-kingdom RNAi in the wheat – *Zymoseptoria tritici* pathosystem. *Front. Plant Sci.* **10**, 892.
- Khajuria, C., Ivashuta, S., Wiggins, E., Flagel, L., Moar, W., Pleau, M., Miller, K., Zhang, Y., Ramaseshadri, P., Jiang, C., Hodge, T., Jensen, P., Chen, M., Gowda, A., McNulty, B., Vazquez, C., Bolognesi, R., Haas, J., Head, G., Clark, T., 2018. Development and characterization of the first dsRNA-resistant insect population from western corn rootworm, *Diabrotica virgifera virgifera* LeConte. *PLoS ONE* **13**, e0197059.
- Khraiweh, B., Zhu, J.-K., Zhu, J., 2012. Role of miRNAs and siRNAs in biotic and abiotic stress responses of plants. *Biochim. Biophys. Acta BBA - Gene Regul. Mech.* **1819**, 137–148.
- Koch, A., Biedenkopf, D., Furch, A., Weber, L., Rossbach, O., Abdellatef, E., Linicus, L., Johannsmeier, J., Jelonek, L., Goesmann, A., Cardoza, V., McMillan, J., Mentzel, T., Kogel, K.-H., 2016. An RNAi-based control of *Fusarium graminearum* infections through spraying of long dsRNAs involves a plant passage and is controlled by the fungal silencing machinery. *PLoS Pathog.* **12**, e1005901.
- Koch, A., Kogel, K.-H., 2014. New wind in the sails: improving the agronomic value of crop plants through RNAi-mediated gene silencing. *Plant Biotechnol. J.* **12**, 821–831.
- Koch, A., Kumar, N., Weber, L., Keller, H., Imani, J., Kogel, K.-H., 2013. Host-induced gene silencing of cytochrome P450 lanosterol C14 -demethylase-encoding genes confers strong resistance to *Fusarium* species. *Proc. Natl. Acad. Sci.* **110**, 19324–19329.
- Koch, A., Schlemmer, T., Höfle, L., Werner, B., Preußner, C., Hardt, M., Möbus, A., Biedenkopf, D., Claar, M., Perlet, C., Jelonek, L., Goesmann, A., Garikapati, V., Spengler, B., Busche, T., Kalinowski, J., Kogel, K., 2020. Host-induced gene silencing involves transfer of dsRNA-derived siRNA via extracellular vesicles. *bioRxiv*.
- Koch, E., Slusarenko, A., 1990. Arabidopsis is susceptible to infection by a downy mildew fungus. *Plant Cell* **2**, 437–445.
- Kombrink, A., Thomma, B.P.H.J., 2013. LysM effectors: Secreted proteins supporting fungal life. *PLoS Pathog.* **9**, e1003769.

- Krasileva, K.V., Zheng, C., Leonelli, L., Goritschnig, S., Dahlbeck, D., Staskawicz, B.J., 2011. Global analysis of Arabidopsis/ downy mildew interactions reveals prevalence of incomplete resistance and rapid evolution of pathogen recognition. *PLoS ONE* **6**, e28765.
- Kusch, S., Frantzeskakis, L., Thieron, H., Panstruga, R., 2018. Small RNAs from cereal powdery mildew pathogens may target host plant genes. *Fungal Biol.* **122**, 1050–1063.
- Kwon, S., Tisserant, C., Tulinski, M., Weiberg, A., Feldbrügge, M., 2020. Inside-out: from endosomes to extracellular vesicles in fungal RNA transport. *Fungal Biol. Rev.* **34**, 89–99.
- Lai, Y., Eulgem, T., 2018. Transcript-level expression control of plant NLR genes. *Mol. Plant Pathol.* **19**, 1267–1281.
- Laurie, J.D., Linning, R., Bakkeren, G., 2008. Hallmarks of RNA silencing are found in the smut fungus *Ustilago hordei* but not in its close relative *Ustilago maydis*. *Curr. Genet.* **53**, 49–58.
- Lawton, K., Weymann, K., Friedrich, L., Vernooij, B., Uknes, S., Ryals, J., 1995. Systemic acquired resistance in Arabidopsis requires salicylic acid but not ethylene. *Mol. Plant-Microbe Interact.* **8**, 863–870.
- Lenarčič, T., Pirc, K., Hodnik, V., Albert, I., Borišek, J., Magistrato, A., Nürnberger, T., Podobnik, M., Anderluh, G., 2019. Molecular basis for functional diversity among microbial Nep1-like proteins. *PLoS Pathog.* **15**, e1007951.
- Li, F., Pignatta, D., Bendix, C., Brunkard, J.O., Cohn, M.M., Tung, J., Sun, H., Kumar, P., Baker, B., 2012. MicroRNA regulation of plant innate immune receptors. *Proc. Natl. Acad. Sci.* **109**, 1790–1795.
- López Sánchez, A., Stassen, J.H.M., Furci, L., Smith, L.M., Ton, J., 2016. The role of DNA (de)methylation in immune responsiveness of Arabidopsis. *Plant J.* **88**, 361–374.
- Lück, S., Kreszies, T., Strickert, M., Schweizer, P., Kuhlmann, M., Douchkov, D., 2019. siRNA-Finder (si-Fi) software for RNAi-target design and off-target prediction. *Front. Plant Sci.* **10**, 1023.
- Ma, S., Lapin, D., Liu, L., Sun, Y., Song, W., Zhang, X., Logemann, E., Yu, D., Wang, J., Jirschitzka, J., Han, Z., Schulze-Lefert, P., Parker, J.E., Chai, J., 2020. Direct pathogen-induced assembly of an NLR immune receptor complex to form a holoenzyme. *Science* **370**, eabe3069.
- Ma, X., Wiedmer, J., Palma-Guerrero, J., 2020. Small RNA bidirectional crosstalk during the interaction between wheat and *Zymoseptoria tritici*. *Front. Plant Sci.* **10**, 1669.

- Maizel, A., Markmann, K., Timmermans, M., Wachter, A., 2020. To move or not to move: roles and specificity of plant RNA mobility. *Curr. Opin. Plant Biol.* **57**, 52–60.
- Mallory, A.C., Bouché, N., 2008. MicroRNA-directed regulation: to cleave or not to cleave. *Trends Plant Sci.* **13**, 359–367.
- Man, S.M., Kanneganti, T.-D., 2016. Converging roles of caspases in inflammasome activation, cell death and innate immunity. *Nat. Rev. Immunol.* **16**, 7–21.
- Mao, Y.-B., Cai, W.-J., Wang, J.-W., Hong, G.-J., Tao, X.-Y., Wang, L.-J., Huang, Y.-P., Chen, X.-Y., 2007. Silencing a cotton bollworm P450 monooxygenase gene by plant-mediated RNAi impairs larval tolerance of gossypol. *Nat. Biotechnol.* **25**, 1307–1313.
- Masigol, H., Khodaparast, S.A., Woodhouse, J.N., Rojas-Jimenez, K., Fonvielle, J., Rezakhani, F., Mostowfizadeh-Ghahamfarsa, R., Neubauer, D., Goldhammer, T., Grossart, H., 2019. The contrasting roles of aquatic fungi and oomycetes in the degradation and transformation of polymeric organic matter. *Limnol. Oceanogr.* **64**, 2662–2678.
- McDowell, J.M., 2014. *Hyaloperonospora arabidopsidis*: A model pathogen of *Arabidopsis*. In: Dean, R.A., Lichens-Park, A., Kole, C. (Eds.), *Genomics of Plant-Associated Fungi and Oomycetes: Dicot Pathogens*. Springer, Berlin, Heidelberg, pp. 209–234.
- McEwan, D.L., Weisman, A.S., Hunter, C.P., 2012. Uptake of extracellular double-stranded RNA by SID-2. *Mol. Cell* **47**, 746–754.
- Mi, S., Cai, T., Hu, Y., Chen, Y., Hodges, E., Ni, F., Wu, L., Li, S., Zhou, H., Long, C., Chen, S., Hannon, G.J., Qi, Y., 2008. Sorting of small RNAs into Arabidopsis Argonaute complexes is directed by the 5' terminal nucleotide. *Cell* **133**, 116–127.
- Mims, C.W., Richardson, E.A., Holt III, B.F., Dangl, J.L., 2004. Ultrastructure of the hostpathogen interface in *Arabidopsis thaliana* leaves infected by the downy mildew *Hyaloperonospora parasitica*. *Can. J. Bot.* **82**, 1001–1008.
- Misas-Villamil, J.C., van der Hoorn, R.A.L., Doehlemann, G., 2016. Papain-like cysteine proteases as hubs in plant immunity. *New Phytol.* **212**, 902–907.
- Mitter, N., Worrall, E.A., Robinson, K.E., Li, P., Jain, R.G., Taochy, C., Fletcher, S.J., Carroll, B.J., Lu, G.Q., Xu, Z.P., 2017. Clay nanosheets for topical delivery of RNAi for sustained protection against plant viruses. *Nat. Plants* **3**, 16207.
- Montgomery, T.A., Howell, M.D., Cuperus, J.T., Li, D., Hansen, J.E., Alexander, A.L., Chapman, E.J., Fahlgren, N., Allen, E., Carrington, J.C., 2008. Specificity of ARGONAUTE7-miR390 interaction and dual functionality in TAS3 *trans*-acting siRNA formation. *Cell* **133**, 128–141.

- Morel, J.-B., Godon, C., Mourrain, P., Béclin, C., Boutet, S., Feuerbach, F., Proux, F., Vaucheret, H., 2002. Fertile hypomorphic ARGONAUTE (*ago1*) mutants impaired in post-transcriptional gene silencing and virus resistance. *Plant Cell* **14**, 629–639.
- Mosher, S., Seybold, H., Rodriguez, P., Stahl, M., Davies, K.A., Dayaratne, S., Morillo, S.A., Wierzbza, M., Favery, B., Keller, H., Tax, F.E., Kemmerling, B., 2013. The tyrosine-sulfated peptide receptors PSKR1 and PSY1R modify the immunity of Arabidopsis to biotrophic and necrotrophic pathogens in an antagonistic manner. *Plant J.* **73**, 469–482.
- Mukhtar, M.S., Carvunis, A.-R., Dreze, M., Epple, P., Steinbrenner, J., Moore, J., Tasan, M., Galli, M., Hao, T., Nishimura, M.T., Pevzner, S.J., Donovan, S.E., Ghamsari, L., Santhanam, B., Romero, V., Poulin, M.M., Gebreab, F., Gutierrez, B.J., Tam, S., Monachello, D., Boxem, M., Harbort, C.J., McDonald, N., Gai, L., Chen, H., He, Y., European Union Effectoromics Consortium, Vandenhoute, J., Roth, F.P., Hill, D.E., Ecker, J.R., Vidal, M., Beynon, J., Braun, P., Dangl, J.L., 2011. Independently evolved virulence effectors converge onto hubs in a plant immune system network. *Science* **333**, 596–601.
- Murmu, J., Wilton, M., Allard, G., Pandeya, R., Desveaux, D., Singh, J., Subramaniam, R., 2014. Arabidopsis GOLDEN2-LIKE (GLK) transcription factors activate jasmonic acid (JA)-dependent disease susceptibility to the biotrophic pathogen *Hyaloperonospora arabidopsidis*, as well as JA-independent plant immunity against the necrotrophic pathogen *Botrytis cinerea*. *Mol. Plant Pathol.* **15**, 174–184.
- Navarro, L., Dunoyer, P., Jay, F., Arnold, B., Dharmasiri, N., Estelle, M., Voinnet, O., Jones, J.D.G., 2006. A plant miRNA contributes to antibacterial resistance by repressing auxin signaling. *Science* **312**, 436–439.
- Nemri, A., Atwell, S., Tarone, A.M., Huang, Y.S., Zhao, K., Studholme, D.J., Nordborg, M., Jones, J.D.G., 2010. Genome-wide survey of Arabidopsis natural variation in downy mildew resistance using combined association and linkage mapping. *Proc. Natl. Acad. Sci.* **107**, 10302–10307.
- Niehl, A., Wyrsh, I., Boller, T., Heinlein, M., 2016. Double-stranded RNAs induce a pattern-triggered immune signaling pathway in plants. *New Phytol.* **211**, 1008–1019.
- Nowara, D., Gay, A., Lacomme, C., Shaw, J., Ridout, C., Douchkov, D., Hensel, G., Kumlehn, J., Schweizer, P., 2010. HIGS: Host-induced gene silencing in the obligate biotrophic fungal pathogen *Blumeria graminis*. *Plant Cell* **22**, 3130–3141.
- Oerke, E.-C., 2006. Crop losses to pests. *J. Agric. Sci.* **144**, 31–43.

- Parfrey, L.W., Lahr, D.J.G., Knoll, A.H., Katz, L.A., 2011. Estimating the timing of early eukaryotic diversification with multigene molecular clocks. *Proc. Natl. Acad. Sci.* **108**, 13624–13629.
- Pel, M.J.C., Wintermans, P.C.A., Cabral, A., Robroek, B.J.M., Seidl, M.F., Bautor, J., Parker, J.E., Van den Ackerveken, G., Pieterse, C.M.J., 2014. Functional analysis of *Hyaloperonospora arabidopsidis* RXLR effectors. *PLoS ONE* **9**, e110624.
- Petre, B., Kamoun, S., 2014. How do filamentous pathogens deliver effector proteins into plant cells? *PLoS Biol.* **12**, e1001801.
- Pliego, C., Nowara, D., Bonciani, G., Gheorghe, D.M., Xu, R., Surana, P., Whigham, E., Nettleton, D., Bogdanove, A.J., Wise, R.P., Schweizer, P., Bindschedler, L.V., Spanu, P.D., 2013. Host-induced gene silencing in barley powdery mildew reveals a class of ribonuclease-like effectors. *Mol. Plant. Microbe Interact.* **26**, 633–642.
- Qi, T., Zhu, X., Tan, C., Liu, P., Guo, J., Kang, Z., Guo, J., 2018. Host-induced gene silencing of an important pathogenicity factor *PsCPK1* in *Puccinia striiformis* f. sp. *tritici* enhances resistance of wheat to stripe rust. *Plant Biotechnol. J.* **16**, 797–807.
- Qiao, Y., Liu, L., Xiong, Q., Flores, C., Wong, J., Shi, J., Wang, X., Liu, X., Xiang, Q., Jiang, S., Zhang, F., Wang, Y., Judelson, H.S., Chen, X., Ma, W., 2013. Oomycete pathogens encode RNA silencing suppressors. *Nat. Genet.* **45**, 330–333.
- Qutob, D., Patrick Chapman, B., Gijzen, M., 2013. Transgenerational gene silencing causes gain of virulence in a plant pathogen. *Nat. Commun.* **4**, 1349.
- Rehmany, A.P., Gordon, A., Rose, L.E., Allen, R.L., Armstrong, M.R., Whisson, S.C., Kamoun, S., Tyler, B.M., Birch, P.R.J., Beynon, J.L., 2005. Differential recognition of highly divergent downy mildew avirulence gene alleles by *RPP1* resistance genes from two *Arabidopsis* lines. *Plant Cell* **17**, 1839–1850.
- Ren, B., Wang, X., Duan, J., Ma, J., 2019. Rhizobial tRNA-derived small RNAs are signal molecules regulating plant nodulation. *Science* **365**, 919–922.
- Richards, T.A., Soanes, D.M., Jones, M.D.M., Vasieva, O., Leonard, G., Paszkiewicz, K., Foster, P.G., Hall, N., Talbot, N.J., 2011. Horizontal gene transfer facilitated the evolution of plant parasitic mechanisms in the oomycetes. *Proc. Natl. Acad. Sci.* **108**, 15258–15263.
- Robinson, S.M., Bostock, R.M., 2014. β -glucans and eicosapolyenoic acids as MAMPs in plant-oomycete interactions: past and present. *Front. Plant Sci.* **5**, 797.
- Rocafort, M., Fudal, I., Mesarich, C.H., 2020. Apoplasmic effector proteins of plant-associated fungi and oomycetes. *Curr. Opin. Plant Biol.* **56**, 9–19.

- Rouxel, T., Balesdent, M.-H., 2010. Avirulence Genes. In: *Encyclopedia of Life Sciences*. John Wiley & Sons, Ltd, Chichester, UK.
- Rutter, B.D., Innes, R.W., 2020. Growing pains: addressing the pitfalls of plant extracellular vesicle research. *New Phytol.* **228**, 1505-1510.
- Salguero-Linares, J., Coll, N.S., 2019. Plant proteases in the control of the hypersensitive response. *J. Exp. Bot.* **70**, 2087–2095.
- Sang, H., Kim, J.-I., 2020. Advanced strategies to control plant pathogenic fungi by host-induced gene silencing (HIGS) and spray-induced gene silencing (SIGS). *Plant Biotechnol. Rep.* **14**, 1–8.
- Sanju, S., Siddappa, S., Thakur, A., Shukla, P.K., Srivastava, N., Pattanayak, D., Sharma, S., Singh, B.P., 2015. Host-mediated gene silencing of a single effector gene from the potato pathogen *Phytophthora infestans* imparts partial resistance to late blight disease. *Funct. Integr. Genomics* **15**, 697–706.
- Savary, S., Willocquet, L., Pethybridge, S.J., Esker, P., McRoberts, N., Nelson, A., 2019. The global burden of pathogens and pests on major food crops. *Nat. Ecol. Evol.* **3**, 430–439.
- Savory, F., Leonard, G., Richards, T.A., 2015. The role of horizontal gene transfer in the evolution of the oomycetes. *PLoS Pathog.* **11**, e1004805.
- Schon, M.A., Kellner, M.J., Plotnikova, A., Hofmann, F., Nodine, M.D., 2018. NanoPARE: parallel analysis of RNA 5' ends from low-input RNA. *Genome Res.* **28**, 1931–1942.
- Schornack, S., Huitema, E., Cano, L.M., Bozkurt, T.O., Oliva, R., Van Damme, M., Schwizer, S., Raffaele, S., Chaparro-Garcia, A., Farrer, R., Segretin, M.E., Bos, J., Haas, B.J., Zody, M.C., Nusbaum, C., Win, J., Thines, M., Kamoun, S., 2009. Ten things to know about oomycete effectors. *Mol. Plant Pathol.* **10**, 795–803.
- Shabalina, S.A., Koonin, E.V., 2008. Origins and evolution of eukaryotic RNA interference. *Trends Ecol. Evol.* **23**, 578–587.
- Shahid, S., Kim, G., Johnson, N.R., Wafula, E., Wang, F., Coruh, C., Bernal-Galeano, V., Phifer, T., dePamphilis, C.W., Westwood, J.H., Axtell, M.J., 2018. MicroRNAs from the parasitic plant *Cuscuta campestris* target host messenger RNAs. *Nature* **553**, 82–85.
- Sharma, R., Xia, X., Cano, L.M., Evangelisti, E., Kemen, E., Judelson, H., Oome, S., Sambles, C., van den Hoogen, D.J., Kitner, M., Klein, J., Meijer, H.J.G., Spring, O., Win, J., Zipper, R., Bode, H.B., Govers, F., Kamoun, S., Schornack, S., Studholme, D.J., Van den Ackerveken, G., Thines, M., 2015. Genome analyses of the sunflower pathogen *Plasmopara halstedii* provide insights into effector evolution in downy mildews and *Phytophthora*. *BMC Genomics* **16**, 741.

- Shivaprasad, P.V., Chen, H.-M., Patel, K., Bond, D.M., Santos, B.A.C.M., Baulcombe, D.C., 2012. A microRNA superfamily regulates nucleotide binding site-leucine-rich repeats and other mRNAs. *Plant Cell* **24**, 859–874.
- Silvestri, A., Fiorilli, V., Miozzi, L., Accotto, G.P., Turina, M., Lanfranco, L., 2019. In silico analysis of fungal small RNA accumulation reveals putative plant mRNA targets in the symbiosis between an arbuscular mycorrhizal fungus and its host plant. *BMC Genomics* **20**, 169.
- Silvestri, A., Turina, M., Fiorilli, V., Miozzi, L., Venice, F., Bonfante, P., Lanfranco, L., 2020. Different genetic sources contribute to the small RNA population in the arbuscular mycorrhizal fungus *Gigaspora margarita*. *Front. Microbiol.* **11**, 395.
- Singla-Rastogi, M., Charvin, M., Thiébeauld, O., Perez-Quintero, A.L., Ravet, A., Emidio-Fortunato, A., Mendu, V., Navarro, L., 2019. Plant small RNA species direct gene silencing in pathogenic bacteria as well as disease protection. *bioRxiv*.
- Slusarenko, A.J., Schlaich, N.L., 2003. Downy mildew of *Arabidopsis thaliana* caused by *Hyaloperonospora parasitica* (formerly *Peronospora parasitica*). *Mol. Plant Pathol.* **4**, 159–170.
- Souret, F.F., Kastenmayer, J.P., Green, P.J., 2004. AtXRN4 degrades mRNA in *Arabidopsis* and its substrates include selected miRNA targets. *Mol. Cell* **15**, 173–183.
- Spoel, S.H., Dong, X., 2008. Making sense of hormone crosstalk during plant immune responses. *Cell Host Microbe* **3**, 348–351.
- Spoel, S.H., Dong, X., 2012. How do plants achieve immunity? Defence without specialized immune cells. *Nat. Rev. Immunol.* **12**, 89–100.
- Svoboda, J., Mrugała, A., Kozubíková-Balcarová, E., Petrusek, A., 2017. Hosts and transmission of the crayfish plague pathogen *Aphanomyces astaci*: a review. *J. Fish Dis.* **40**, 127–140.
- Thines, M., 2014. Phylogeny and evolution of plant pathogenic oomycetes—a global overview. *Eur. J. Plant Pathol.* **138**, 431–447.
- Thines, M., Kamoun, S., 2010. Oomycete–plant coevolution: recent advances and future prospects. *Curr. Opin. Plant Biol.* **13**, 427–433.
- Thomma, B.P.H.J., Nürnberger, T., Joosten, M.H.A.J., 2011. Of PAMPs and effectors: The blurred PTI-ETI dichotomy. *Plant Cell* **23**, 4–15.
- Thordal-Christensen, H., Birch, P.R.J., Spanu, P.D., Panstruga, R., 2018. Why did filamentous plant pathogens evolve the potential to secrete hundreds of effectors to enable disease? *Mol. Plant Pathol.* **19**, 781–785.

- van Baarlen, P., Woltering, E.J., Staats, M., Van Kan, J.A.L., 2007. Histochemical and genetic analysis of host and non-host interactions of Arabidopsis with three *Botrytis* species: an important role for cell death control. *Mol. Plant Pathol.* **8**, 41–54.
- van Kan, J.A.L., 2006. Licensed to kill: the lifestyle of a necrotrophic plant pathogen. *Trends Plant Sci.* **11**, 247–253.
- van Niel, G., D'Angelo, G., Raposo, G., 2018. Shedding light on the cell biology of extracellular vesicles. *Nat. Rev. Mol. Cell Biol.* **19**, 213–228.
- van Schie, C.C.N., Takken, F.L.W., 2014. Susceptibility genes 101: How to be a good host. *Annu. Rev. Phytopathol.* **52**, 551–581.
- Van't Klooster, J.W., Van der Kamp, M.W., Vervoort, J., Beekwilder, J., Boeren, S., Joosten, M.H.A.J., Thomma, B.P.H.J., De Wit, P.J.G.M., 2011. Affinity of Avr2 for tomato cysteine protease Rcr3 correlates with the Avr2-triggered Cf-2-mediated hypersensitive response. *Mol. Plant Pathol.* **12**, 21–30.
- Vaucheret, H., 2008. Plant ARGONAUTES. *Trends Plant Sci.* **13**, 350–358.
- Vega-Arreguín, J.C., Jalloh, A., Bos, J.I., Moffett, P., 2014. Recognition of an Avr3a homologue plays a major role in mediating nonhost resistance to *Phytophthora capsici* in *Nicotiana* species. *Mol. Plant. Microbe Interact.* **27**, 770–780.
- Veloso, J., van Kan, J.A.L., 2018. Many shades of grey in *Botrytis*–host plant interactions. *Trends Plant Sci.* **23**, 613–622.
- Vetukuri, R.R., Asman, A.K., Jahan, S.N., Avrova, A.O., Whisson, S.C., Dixelius, C., 2013. Phenotypic diversification by gene silencing in *Phytophthora* plant pathogens. *Commun. Integr. Biol.* **6**, e25890.
- Vetukuri, R.R., Åsman, A.K.M., Tellgren-Roth, C., Jahan, S.N., Reimegård, J., Fogelqvist, J., Savenkov, E., Söderbom, F., Avrova, A.O., Whisson, S.C., Dixelius, C., 2012. Evidence for small RNAs homologous to effector-encoding genes and transposable elements in the oomycete *Phytophthora infestans*. *PLoS ONE* **7**, e51399.
- von Saint Paul, V., Zhang, W., Kanawati, B., Geist, B., Faus-Kessler, T., Schmitt-Kopplin, P., Schäffner, A.R., 2011. The Arabidopsis glucosyltransferase UGT76B1 conjugates isoleucic acid and modulates plant defense and senescence. *Plant Cell* **23**, 4124–4145.
- Wang, B., Sun, Y., Song, N., Zhao, M., Liu, R., Feng, H., Wang, X., Kang, Z., 2017. *Puccinia striiformis* f. sp. *tritici* microRNA-like RNA 1 (*Pst*-miR1), an important pathogenicity factor of *Pst*, impairs wheat resistance to *Pst* by suppressing the wheat pathogenesis-related 2 gene. *New Phytol.* **215**, 338–350.

- Wang, M., Thomas, N., Jin, H., 2017a. Cross-kingdom RNA trafficking and environmental RNAi for powerful innovative pre- and post-harvest plant protection. *Curr. Opin. Plant Biol.* **38**, 133–141.
- Wang, M., Weiberg, A., Dellota, E., Yamane, D., Jin, H., 2017b. Botrytis small RNA Bc-siR37 suppresses plant defense genes by cross-kingdom RNAi. *RNA Biol.* **14**, 421–428.
- Wang, M., Weiberg, A., Jin, H., 2015. Pathogen small RNAs: a new class of effectors for pathogen attacks. *Mol. Plant Pathol.* **16**, 219–223.
- Wang, M., Weiberg, A., Lin, F.-M., Thomma, B.P.H.J., Huang, H.-D., Jin, H., 2016. Bidirectional cross-kingdom RNAi and fungal uptake of external RNAs confer plant protection. *Nat. Plants* **2**, 16151.
- Wang, S., Boevink, P.C., Welsh, L., Zhang, R., Whisson, S.C., Birch, P.R.J., 2017. Delivery of cytoplasmic and apoplastic effectors from *Phytophthora infestans* haustoria by distinct secretion pathways. *New Phytol.* **216**, 205–215.
- Wang, Y., Liu, K., Liao, H., Zhuang, C., Ma, H., Yan, X., 2008. The plant WNK gene family and regulation of flowering time in Arabidopsis. *Plant Biol.* **10**, 548–562.
- Wang, Y., Tyler, B.M., Wang, Y., 2019. Defense and counterdefense during plant-pathogenic oomycete infection. *Annu. Rev. Microbiol.* **73**, 667–696.
- Wawra, S., Belmonte, R., Löbach, L., Saraiva, M., Willems, A., van West, P., 2012. Secretion, delivery and function of oomycete effector proteins. *Curr. Opin. Microbiol.* **15**, 685–691.
- Weiberg, A., Bellinger, M., Jin, H., 2015. Conversations between kingdoms: small RNAs. *Curr. Opin. Biotechnol.* **32**, 207–215.
- Weiberg, A., Wang, M., Bellinger, M., Jin, H., 2014. Small RNAs: A new paradigm in plant-microbe interactions. *Annu. Rev. Phytopathol.* **52**, 495–516.
- Weiberg, A., Wang, M., Lin, F.-M., Zhao, H., Zhang, Z., Kaloshian, I., Huang, H.-D., Jin, H., 2013. Fungal small RNAs suppress plant immunity by hijacking host RNA interference pathways. *Science* **342**, 118–123.
- Weßling, R., Epple, P., Altmann, S., He, Y., Yang, L., Henz, S.R., McDonald, N., Wiley, K., Bader, K.C., Gläßer, C., Mukhtar, M.S., Haigis, S., Ghamsari, L., Stephens, A.E., Ecker, J.R., Vidal, M., Jones, J.D.G., Mayer, K.F.X., Ver Loren van Themaat, E., Weigel, D., Schulze-Lefert, P., Dangl, J.L., Panstruga, R., Braun, P., 2014. Convergent Targeting of a Common Host protein-network by pathogen effectors from three kingdoms of life. *Cell Host Microbe* **16**, 364–375.

- Whisson, S., Vetukuri, R., Avrova, A., Dixelius, C., 2012. Can silencing of transposons contribute to variation in effector gene expression in *Phytophthora infestans*? *Mob. Genet. Elem.* **2**, 110–114.
- Whisson, S.C., Boevink, P.C., Moleleki, L., Avrova, A.O., Morales, J.G., Gilroy, E.M., Armstrong, M.R., Grouffaud, S., van West, P., Chapman, S., Hein, I., Toth, I.K., Pritchard, L., Birch, P.R.J., 2007. A translocation signal for delivery of oomycete effector proteins into host plant cells. *Nature* **450**, 115–118.
- Win, J., Krasileva, K.V., Kamoun, S., Shirasu, K., Staskawicz, B.J., Banfield, M.J., 2012. Sequence divergent RXLR effectors share a structural fold conserved across plant pathogenic oomycete species. *PLoS Pathog.* **8**, e1002400.
- Win, J., Morgan, W., Bos, J., Krasileva, K.V., Cano, L.M., Chaparro-Garcia, A., Ammar, R., Staskawicz, B.J., Kamoun, S., 2007. Adaptive evolution has targeted the C-terminal domain of the RXLR effectors of plant pathogenic oomycetes. *Plant Cell* **19**, 2349–2369.
- Wirthmueller, L., Asai, S., Rallapalli, G., Sklenar, J., Fabro, G., Kim, D.S., Lintermann, R., Jaspers, P., Wrzaczek, M., Kangasjärvi, J., MacLean, D., Menke, F.L.H., Banfield, M.J., Jones, J.D.G., 2018. Arabidopsis downy mildew effector HaRxL106 suppresses plant immunity by binding to RADICAL-INDUCED CELL DEATH1. *New Phytol.* **220**, 232–248.
- Woods-Tör, A., Studholme, D.J., Cevik, V., Telli, O., Holub, E.B., Tör, M., 2018. A suppressor/avirulence gene combination in *Hyaloperonospora arabidopsidis* determines race specificity in *Arabidopsis thaliana*. *Front. Plant Sci.* **9**, 265.
- Xiong, Q., Ye, W., Choi, D., Wong, J., Qiao, Y., Tao, K., Wang, Y., Ma, W., 2014. *Phytophthora* Suppressor of RNA silencing 2 is a conserved RxLR effector that promotes infection in soybean and *Arabidopsis thaliana*. *Mol. Plant. Microbe Interact.* **27**, 1379–1389.
- Yan, J., Gu, Y., Jia, X., Kang, W., Pan, S., Tang, X., Chen, X., Tang, G., 2012. Effective Small RNA destruction by the expression of a short tandem target mimic in *Arabidopsis*. *Plant Cell* **24**, 415–427.
- Zeng, J., Gupta, V.K., Jiang, Y., Yang, B., Gong, L., Zhu, H., 2019. Cross-Kingdom small RNAs among animals, plants and microbes. *Cells* **8**, 371.
- Zhang, J., Khan, S.A., Hasse, C., Ruf, S., Heckel, D.G., Bock, R., 2015. Full crop protection from an insect pest by expression of long double-stranded RNAs in plastids. *Science* **347**, 991–994.

- Zhang, M., Wang, Q., Xu, K., Meng, Y., Quan, J., Shan, W., 2011. Production of dsRNA sequences in the host plant is not sufficient to initiate gene silencing in the colonizing oomycete pathogen *Phytophthora parasitica*. *PLoS ONE* **6**, e28114.
- Zhang, T., Zhao, Y.-L., Zhao, J.-H., Wang, S., Jin, Y., Chen, Z.-Q., Fang, Y.-Y., Hua, C.-L., Ding, S.-W., Guo, H.-S., 2016. Cotton plants export microRNAs to inhibit virulence gene expression in a fungal pathogen. *Nat. Plants* **2**, 16153.
- Zhang, X., Zhao, H., Gao, S., Wang, W.-C., Katiyar-Agarwal, S., Huang, H.-D., Raikhel, N., Jin, H., 2011. *Arabidopsis* Argonaute 2 regulates innate immunity via miRNA393*-mediated silencing of a Golgi-localized SNARE gene, *MEMB12*. *Mol. Cell* **42**, 356–366.
- Zhang, Y., Li, X., 2019. Salicylic acid: biosynthesis, perception, and contributions to plant immunity. *Curr. Opin. Plant Biol.* **50**, 29–36.
- Zhang, Z., Huang, S., Tao, H., Zhang, Y., Zhao, Y., Ji, Z., Chen, X., 2019. Gene transcriptional pattern, prokaryotic expression and functional analysis of an apoplastic, hydrophobic and small effector SCR82 from *Phytophthora capsici*. *Acta Microbiologica Sin.* **59**, 1586–1599.
- Zhao, H., Lii, Y., Zhu, P., Jin, H., 2012. Isolation and profiling of protein-associated small RNAs. *Methods Mol. Biol.* **883**, 165–176.

Acknowledgement

Firstly, I want to thank my supervisor Dr. Arne Weiberg for giving me the opportunity to perform this study, his mental support and his dedication to science. It was a pleasure to work with you and I will always appreciate the freedom to pursue own ideas during my doctoral studies and shape the project together with you. You have been a great mentor and I have learned a lot during the five years in Munich that will be useful for my future career and beyond. I want to thank Prof. Dr. Martin Parniske for providing us with a fantastic lab environment and supporting us as a new, young group. I also want to thank him for the contributions to my project as one of my TAC members and being part of the evaluation committee.

I want to thank Prof. Dr. Kai Papenfort to complete my TAC and bring valuable suggestions at all phases of the project.

I am very thankful to Prof. Dr. Wolfgang Frank for his contribution of the second evaluation of my thesis and to Prof. Dr. Christof Osman to be part of the evaluation committee and the disputation. Finally, I want to thank Prof. Dr. Heinrich Jung and Prof. Dr. Silke Werth for their willingness to complete my evaluation committee.

I want to thank my fantastic students Jan, Adriana, Sarah, Lorenz, Alexandra and Berni. There was no part I loved as much about my job than discussing science and performing the projects together with you, and I hope I have been a good mentor to you. My publications would not have been possible without you, but even more important, I have met people in you that made my time in the lab and Munich so enjoyable.

A big thank goes to my lab mates Stanzi, Antoine, Berni, Lihong and An-Po from the AG Weiberg. After spending the first part of my project only with Arne, I was blessed to get such great colleagues as you have been. I would never want to miss your contributions to my project, the daily lab routine, and you have also become close friends of me. I still dream about our great hang-arounds on Antoine's roof terrace or Stanzi's garden, or our trips together with Arne and Amaryllis to Christmas markets around Munich.

I want to thank all other doctoral students and Post-Docs I have met during these 5 years in the Genetics. It would take pages to only describe a small part of the great impact you all had on my work, but also my life. You all make the Genetics a special place and I could not have been happier than to spend my time together with you. Juan, Yen-Yu, Chloé, Janet, Fang-Yu, Michi, Salar, Rafa, Anne, José, Kasia, Mattes, Martin B, David, Kathy, Max, Priya, Benjamin, Aline, and Samy: you're the best and I'll miss you, and I hope we'll see each other again!

I want to thank the LSM for all the support I received during my doctoral studies and the possibilities to educate myself. I want to thank especially Nadine and Francisca for their patience, so I could complete the curriculum in 5 years.

I want to thank our collaborators Reinhard Pröls and Ralph Hückelhoven (TU Munich), Ariane and Eric Kemen (University Tübingen) and Tom Schreiber (IPB) Halle for their contributions to my project.

I want to acknowledge the financial support I have received from the DFG, the SFB924 and LMU house positions kindly provided by Prof. Dr. Parniske and the travel grants from the DAAD enabling trips to conferences in Vienna and Glasgow.

I want to thank my family and my friends for providing me with the work/life balance necessary for such a project and the constant support. Special thanks for your patience during long explanations about the details of my project...

Finally, I want to thank you, Isabel. There is nothing in these five years, that comes close to the luck that I have met you. I love you ♥.